# Tests of Isothermal Soaking Procedures for Limiting Tube Denting in Nuclear Steam Generators

NP-1761
Research Project 623-2

Interim Report, April 1981

Prepared by

COMBUSTION ENGINEERING, INC.
Nuclear Power Systems
1000 Prospect Hill Road
Windsor, Connecticut 06095

Principal Investigator
T. A. Beineke

Other Authors
D. J. Morgan
J. F. Hall
K. E. Marugg
M. Wiatrowski

Prepared for

Steam Generator Owners Group

and

Electric Power Research Institute
3412 Hillview Avenue
Palo Alto, California 94304

EPRI Project Manager
R. G. Varsanik

Nuclear Power Division

## ORDERING INFORMATION

Requests for copies of this report should be directed to Research Reports Center (RRC), Box 50490, Palo Alto, CA 94303, (415) 965-4081. There is no charge for reports requested by EPRI member utilities and affiliates, contributing nonmembers, U.S. utility associations, U.S. government agencies (federal, state, and local), media, and foreign organizations with which EPRI has an information exchange agreement. On request, RRC will send a catalog of EPRI reports.



## NOTICE

This report was prepared by the organization(s) named below as an account of work sponsored by the Electric Power Research Institute, Inc. (EPRI) and the Steam Generator Owners Group. Neither EPRI, members of EPRI, the Steam Generator Owners Group, the organization(s) named below, nor any person acting on their behalf: (a) makes any warranty or representation, express or implied, with respect to the accuracy, completeness, or usefulness of the information contained in this report, or that the use of any information, apparatus, method, or process disclosed in this report may not infringe privately owned rights; or (b) assumes any liabilities with respect to the use of, or for damages resulting from the use of, any information, apparatus, method, or process disclosed in this report.

Prepared by
Combustion Engineering, Inc.
Windsor, Connecticut

# EPRI PERSPECTIVE

## PROJECT DESCRIPTION

RP623-2, Neutralization of Crevice Acids, is an experimental program sponsored by EPRI, under the management of the Steam Generator Project Office, to identify and apply chemical treatments to arrest steam generator denting corrosion. This interim report covers isothermal soaking with hydrazine-treated water and solutions of alkaline sodium phosphate. An evaluation of effectiveness was measured in isothermal denting tests (capsules) and in heat transfer denting tests (four tube pot boilers). This project is related to RPS112-1-2, RPS158, and RP699-1.

## PROJECT OBJECTIVES

This project is intended to identify chemicals and to develop procedures which can halt accelerated carbon steel corrosion in crevices and thereby arrest further dent progression either during operation or during shutdown. This report describes evaluation of hydrazine-treated water and alkaline phosphate solutions under isothermal and heat transfer conditions. These conditions are intended to simulate wet layup and hot standby conditions which would be encountered in an operating steam generator. The goal of these tests is to have no further denting occur upon reexposure to aggressive chemistry conditions.

## PROJECT RESULTS

The soak solutions evaluated in isothermal capsules were hydrazine-treated water (at 150°F and 565°F) and solutions of alkaline sodium phosphate (up to 1000 parts per million (ppm) $PO_4$ at 150°F and 3000 ppm at 565°F). Soaking times varied from one to seven days. Reductions in the rate of capsule

bulging were found to be more dependent upon the initial denting solution than on the conditions of the soaks. The pot boilers (refluxing autoclaves) were used to evaluate the effectiveness of halting denting with four-day isothermal soaks at 150°F. The soak solutions were hydrazine-treated water, 1000-ppm and 3000-ppm $PO_4$ solutions. None of the procedures were able to completely halt active denting. The maximum reduction in denting rate was 70%.

The soak solutions and procedures investigated are not effective in halting active denting. The limiting factors appear to be the slow rate of (1) chloride release from crevices and (2) diffusion of the neutralizer inward under isothermal conditions. Future studies should focus on techniques to enhance neutralizer penetration and on alternative neutralizer chemistry.

This information will be useful to plant operations and engineering staff who are considering using soaks to halt the progression of denting.

Richard G. Varsanik, Project Manager
Nuclear Power Division

## ABSTRACT

Capsule and pot boiler tests were conducted to develop and to evaluate shutdown soak solutions and procedures for limiting dent growth in nuclear steam generators. Testing was limited to isothermal soaking in the absence of boiling heat transfer. The effect of intermittent boiling produced by pressure or temperature cycling was not evaluated. Capsule tests of hydrazine-treated water and of alkaline phosphate solutions were conducted at 150°F and 565°F for soak times of 1, 4 and 7 days, and for phosphate concentrations ranging from 50 to 10000 ppm $PO_4$. Four day, low temperature soaks in wet layup, 1000 ppm $PO_4$ and 3000 ppm $PO_4$ were tested in pot boilers with active denting.

Although denting was not halted by any of the tested procedures, denting rates were reduced by as much as 70%. The inability to completely halt denting was attributed to the sluggish release of impurities as well as the limited uptake of neutralizers by crevices filled with magnetite. Isothermal soaks under the conditions tested will be of marginal benefit in limiting dent growth.

CONTENTS


| Section | | Page |
|---|---|---|
| 1 | INTRODUCTION | 1-1 |
| 2 | EXPERIMENTAL | 2-1 |
| | Capsule Testing | 2-1 |
| | Pot Boiler Testing | 2-11 |
| 3 | RESULTS | 3-1 |
| | Capsule Testing | 3-1 |
| | Bulging Rates | 3-1 |
| | Chemistry Data | 3-30 |
| | Capsule Destructive Examinations | 3-32 |
| | Pot Boiler Testing | 3-52 |
| | Overview | 3-52 |
| | Strain Gauge Response | 3-52 |
| | Eddy Current Examination | 3-62 |
| | Chemistry Data | 3-66 |
| | Deposit Examinations | 3-69 |
| | Corrosion Coupon Analysis | 3-78 |
| | Metallographic Examination | 3-79 |
| 4 | DISCUSSION | 4-1 |
| | Capsule Testing | 4-1 |
| | Pot Boiler Testing | 4-5 |
| | Destructive Examination | 4-10 |
| REFERENCES | | 4-13 |
| APPENDIX A | CAPSULE TESTING EXPERIMENTAL DETAILS | A-1 |
| APPENDIX B | CAPSULE METALLOGRAPHY | B-1 |
| APPENDIX C | POT BOILER TESTING EXPERIMENTAL DETAILS | C-1 |
| APPENDIX D | POT BOILER CORROSION COUPON ANALYSIS | D-1 |
| APPENDIX E | POT BOILER DENT METALLOGRAPHY | E-1 |

ILLUSTRATIONS


| Figure | | Page |
|---|---|---|
| 2-1 | Isothermal Capsule | 2-2 |
| 2-2 | Testing Sequence for Evaluating Isothermal Soaks | 2-4 |
| 2-3 | Schematic of Tube Bundle | 2-13 |
| 3-1 | Capsule Bulging Versus Furnace Time | 3-5 |
| 3-2 | Effectiveness of Water Soaks | 3-8 |
| 3-3 | Endurance of Water Soaks | 3-9 |
| 3-4 | Effectiveness of Water Soaks | 3-10 |
| 3-5 | Endurance of Water Soaks | 3-11 |
| 3-6 | Phosphate Soak at 150°F, Effectiveness | 3-13 |
| 3-7 | Phosphate Soak at 150°F, Endurance | 3-14 |
| 3-8 | Phosphate Soak at 565°F, Effectiveness | 3-15 |
| 3-9 | Phosphate Soak at 565°F, Endurance | 3-16 |
| 3-10 | Controls for Phosphate Soak Test | 3-17 |
| 3-11 | Phosphate Soak at 150°F, Effectiveness | 3-19 |
| 3-12 | Phosphate Soak at 150°F, Endurance | 3-20 |
| 3-13 | Phosphate Soak at 565°F, Effectiveness | 3-21 |
| 3-14 | Phosphate Soak at 565°F, Endurance | 3-22 |
| 3-15 | Controls for Phosphate Soak | 3-23 |
| 3-16 | Phosphate Soak at 150°F, Effectiveness | 3-27 |
| 3-17 | Phosphate Soak at 565°F, Effectiveness | 3-28 |
| 3-18 | Capsule AA-7. Transverse Section (4X). | 3-35 |
| 3-19 | Capsule DD-8. Transverse Section (4X). | 3-35 |
| 3-20 | Capsule AA-7. Transverse Section (75X). | 3-36 |
| 3-21 | Capsule AA-8. Transverse Section (75X). | 3-36 |
| 3-22 | Capsule DD-7. Transverse Section (75X). | 3-37 |
| 3-23 | Capsule DD-8. Transverse Section (75X). | 3-37 |
| 3-24 | SEM of Capsule AA-7 | 3-40 |
| 3-25 | SEM of Capsule DD-8 | 3-41 |
| 3-26 | SEM's of Octahedral Crystals - Capsule Y-1 | 3-42 |
| 3-27 | SEM of Capsule DD-8 | 3-45 |
| 3-28 | SEM of Capsule Y-10 | 3-46 |
| 3-29 | SEM of Capsule AA-8 | 3-47 |

| Figure | | Page |
|---|---|---|
| 3-30 | SEM's of the Longitudinal Section of Capsule DD-7 | 3-48 |
| 3-31 | SEM's of "Starfish-Like" Growths in Capsule DD-8 | 3-49 |
| 3-32 | SEM's of "Starfish-Like" Crystals in Capsule DD-8 | 3-50 |
| 3-33 | Pot 9 - Phase I Fault Operation Strain Gauge Response | 3-55 |
| 3-34 | Pot 11 - Phase I Fault Operation Strain Gauge Response | 3-56 |
| 3-35 | Pot 7E - Phase I Fault Operation Strain Gauge Response | 3-57 |
| 3-36 | Pot 9 - Phase 3 Volatile Operation Strain Gauge Response | 3-58 |
| 3-37 | Pot 11 - Phase 3 Volatile Operation Strain Gauge Response | 3-59 |
| 3-38 | Pot 7E - Phase 3 Volatile Operation Strain Gauge Response | 3-60 |
| 3-39 | SEM and P X-Ray Map of Specimen H-7E-4-K | 3-82 |
| 3-40 | SEM and $Cl^-$ X-Ray Map of Specimen H-7E-4-K | 3-83 |
| 4-1 | Capsule Bulging Rate versus Phosphate Concentration | 4-4 |
| 4-2 | Pot Boiler Correllation of Strain Gauge Data and Eddy Current Data | 4-8 |
| 4-3 | Denting Rate Reduction as a Function of Phosphate Concentration | 4-9 |

TABLES


| Table | | Page |
|---|---|---|
| 2-1 | Capsule Testing Matrix | 2-6 |
| 2-2 | Test Operation Summary | 2-14 |
| 2-3 | Volatile Chemistry Specifications Pot Boiler Testing | 2-15 |
| 3-1 | Summary of Capsule Bulging Rates During Dent Initiation | 3-4 |
| 3-2 | Effect of Water Soaks on Capsule Bulging Rates | 3-7 |
| 3-3 | W/EPRI Capsule Bulging Rate Data | 3-24 |
| 3-4 | 0.25 M $FeCl_2$ Capsule Bulging Rate Data | 3-29 |
| 3-5 | Pot Boiler Strain Rates | 3-61 |
| 3-6 | Pot 9 - Water Soak, Tube Denting Results | 3-63 |
| 3-7 | Pot 11 - Phosphate Soak - 1000 ppm, Tube Denting Results | 3-64 |
| 3-8 | Pot 7E - Phosphate Soak - 3000 ppm, Tube Denting Results | 3-65 |
| 3-9 | Estimated Chloride Removal | 3-68 |
| 3-10 | Pot Boiler 9, Post-Phase III Deposit Analysis | 3-70 |
| 3-11 | Pot Boiler 9, Post-Phase I Deposit Analysis | 3-71 |
| 3-12 | Pot Boiler 11, Final Examination Deposit Analysis | 3-72 |
| 3-13 | Pot Boiler 7E, Post Phase I Deposit Analysis | 3-74 |
| 3-14 | Pot Boiler 7E, Final Examination Deposit Analysis | 3-75 |
| 3-15 | X-Ray Diffraction Results Pot Boiler 9, 11, 7E Deposits | 3-77 |
| 3-16 | Average Corrosion Rates from Pot Boiler Tests | 3-78 |

4-1 Diametral Bulging Rates As a Function of Phosphate Concentration 4-3

4-2 Comparison of Strain Gauge and Eddy Current Data 4-7

# SUMMARY

## PURPOSE AND SCOPE

The goal of the joint C-E/EPRI Contract RP-623-2, Neutralization of Crevice Acids, was to provide operating PWR nuclear power plants with guidelines for field procedures to chemically control steam generator tube denting. This work evaluated isothermal soaking as a means of neutralizing acidity and removing impurities from crevice regions. Tests were conducted with hydrazine-treated water and with dilute solutions of alkaline sodium phosphates at both wet layup and hot standby conditions.

Two established experimental techniques for the production and evaluation of crevice magnetite and resulting tube denting were employed in this effort: 1) isothermal capsule testing and 2) heat transfer testing with four-tube pot boilers.

### Capsule Testing

A capsule is a small autoclave constructed of a length of steam generator tubing sealed at each end with swagelok caps. Contained within the capsule is a cylindrical slug made of support-plate material such that a crevice exists between the slug OD and the tube ID. Nonprotective magnetite can be formed within the crevice by placing an appropriate denting solution in the capsule and heating at 565$^{o}$F in a furnace for two to three weeks. After filling the crevice, the nonprotective magnetite continues to form, bulging the tubing at the elevation of the slug and producing a "reverse dent". The progress of corrosion can be followed by making accurate measurement of tubing OD at the elevation of the slug.

Capsule testing permitted screening of a large number of potential soak solutions within a short time. Reverse dents grown as described above were soaked in the various test solutions for specified times and temperatures. Capsules were then refilled and returned to the furnace. Periodic measurements of the bulge diameter were made to follow the progress of corrosion following the soak. Destructive examinations were performed on selected capsules to study magnetite morphology and to assess impurity removal, neutralizer penetration, and corrosion resulting from the soak.

The criteria for evaluating the results of these tests were as follows:

- A soak was effective if it caused bulging to stop when the capsule was refilled with unfaulted AVT subsequent to soaking.

- A soak was said to have endurance if it prevented additional bulging when the capsule was refilled with a denting solution. The time elapsed prior to reinitiation of bulging was a measure of the endurance of the treatment.

Four different denting solutions were employed in this study. Because of its continuity with the original studies of Potter and Mann [1], 0.1 M $FeCl_2$ (7000 ppm $Cl^-$) was used as a denting solution for a substantial portion of this work. This solution is also referred to as the "C-E reference denting solution" A more concentrated and perhaps more aggressive denting solution known as the "W/EPRI reference denting solution" was used in roughly half of this testing. This solution consisted of 0.1 M $NiCl_2$ + 0.1 M $CuCl_2$ in full strength seawater (total chloride 32000 ppm). Capsues bulged with these two solutions are referred to respectively as "C-E capsules" and "W/EPRI capsules". Additional denting solutions

included 0.25 M $FeCl_2$ (18000 ppm $Cl^-$) and 0.05 M $FeCl_2$ in full strength seawater (22000 ppm $Cl^-$).

The isothermal soak solutions evaluated in capsule testing were hydrazine-treated water (either simulating wet layup at 150°F or simulating volatile chemistry control at 565°F), and aqueous solutions of alkaline sodium phosphate in concentrations ranging up to 10000 ppm $PO_4$ at 150°F and 3000 ppm at 565°F. Soaking times varied between one day and seven days.

Pot Boiler Testing

Pot boilers are refluxing autoclaves used to evaluate tubing and support material corrosion at operating temperature under heat transfer conditions. They are heated from a high temperature, pressurized water test loop which circulates hot water on the ID of four widely-spaced inverted U-tubes. Steam generated on the secondary side is condensed and returned to the pot by gravity. Bare-tube heat fluxes are about an order of magnitude lower than in field units at 100% power. Crevice corrosion is studied by installing a support plate and/or concentrating rings on the tubing. These provide annular crevices similar to those in field units. With carbon steel, denting can be initiated in these crevices following pre-packing with corrosion products and operation under aggressive chemistry conditions. The course of denting is followed by instrumenting selected crevices with high temperature strain gauges. In addition, eddy current measurements of tube denting are made periodically during testing.

In this study, three pot boilers were used to evaluate four-day isothermal soaks at 150°F. The soak solutions were hydrazine-treated water, i.e. wet layup solution, 1000 ppm $PO_4$ and 3000 ppm $PO_4$. Following the soaks, the pots were

returned to operation under volatile chemistry control in order to determine the effectiveness of the procedure in reducing denting rates.

Upon the completion of testing, selected crevices were subjected to destructive examination. Magnetite morphology was observed by optical microscopy of both transverse and longitudinal crevice sections. Selected areas of magnetite were also examined via scanning electron microscopy (SEM) and energy dispersive spectroscopy (EDS) techniques. General corrosion was measured through the use of corrosion coupons.

## FINDINGS

None of the tested isothermal soak procedures were able to completely halt active denting in pot boiler testing. The maximum reduction in denting rates (post-soak to pre-soak) achieved was 70% following the four-day, low temperature soak with 3000 ppm $PO_4$.

A similar observation emerges from capsule testing; however, reductions in the rate of capsule bulging were observed to be far more dependent upon the initial denting environment than on any of the parameters of the various isothermal soaks. C-E capsules required a constant exposure to fault chemistry if bulging was to continue. Whenever the denting solution was removed and replaced with a solution free of chlorides, denting halted. In contrast, W/EPRI capsules continued to bulge when similarly treated. This suggests a relationship between the acid chloride concentration in the dent and the effectiveness of the soak procedure. W/EPRI capsules seem to be more representative of both pot boilers and field units in that bulging continues after recovery from fault chemistry. However, this comparison is extremely qualitative given that denting in field units is not understood as completely as laboratory-produced denting.

Corrosion in these W/EPRI capsules was not halted by any of the soak procedures utilizing alkaline sodium phosphates. No measureable reduction in bulging rates was observed at either 150°F or 565°F until the phosphate concentration exceeded 3000 ppm. Low temperature soaks at higher phosphate concentrations produced reductions in bulging rates by as much as 50%. These higher concentrations were not tested at 565°F.

Destructive examinations of both capsules and pot boilers revealed a striking relationship between post-soak denting rates and residual chloride within the crevices. C-E capsules in which corrosion stopped when the denting environment was removed, were found to be devoid of residual chloride. Pot boiler crevices along with all W/EPRI capsules and those C-E capsules which had been filled with fault chemistry subsequent to soaking, where corrosion continued, were found to contain residual chloride near the carbon steel interface. Apparently, none of the soak conditions tested were successful in leaching chloride impurities from crevice magnetite in W/EPRI capsules and in pot boilers. It is thought that this chloride, embedded within crevice magnetite, is the cause of continued corrosion and denting after chloride impurities have been removed from the bulk coolant. All of the soak conditions were apparently successful in removing chloride from crevice magnetite in C-E capsules.

In the destructive examination of capsules, no phosphate was found in the dented region of any of the specimens. However, one crevice from a pot boiler contained minor amounts of phosphate, but it was restricted to void areas and cracks in the periphery of the oxide, near the interface with the tubing. Corrosion coupon measurements gave no indication of abnormal corrosion associated with any of the soak procedures.

## CONCLUSIONS

Under the test conditions selected (150°F and 565°F for periods of up to 7 days) isothermal soaks with hydrazine-treated water and with aqueous solutions of phosphate did not halt denting. Reductions of as much as 70% in the rate of denting were observed in pot boiler testing after soaking with 3000 ppm $PO_4$. Rate-reduction data from capsule and pot boiler testing were extrapolated to estimate phosphate concentrations required to halt denting. Calculations based on W/EPRI capsule data predict that 20,000 ppm $PO_4$ would be required to halt denting. A similar treatment of pot boiler data indicates that denting would not be halted until the phosphate concentration is increased to 5000 ppm.

These predictions are tenuous due to the poor reproducibility of the capsule data and the limited data (three points) from pot boiler testing. Theoretically, there is no reason to expect the more concentrated phosphate solutions to leach chloride from crevice magnetite any more effectively than the more dilute solutions. The residual chloride would therefore be expected to reinitiate denting after soaking.

Short-term isothermal soaking, irrespective of the chemistry of the soak solution, is not an effective procedure for halting active denting in field units. The limiting factors appear to be the slow rates of release of chloride from crevices and of diffusion of neutralizer inward under isothermal conditions. Future studies should focus on techniques to enhance neutralizer penetration of crevice magnetite.

# Section 1

## INTRODUCTION

A major corrosion problem in nuclear steam generators arises from the accelerated corrosion of carbon steel tube support structures within crevices formed by intersections with the tubing. The oxide formed, a hard adherent non-protective magnetite, fills the crevice and exerts compressive forces on the tubing sufficient to produce local deformation. Cumulative stress in a support plate with a high incidence of denting can produce plate swelling and fracturing. Stress corrosion cracking of the tubing may result in regions of high stress at locally-deformed regions or in U-bends as a result of plate movement. This phenomenon, univerally known as "denting" is a major problem for seawater-sited plants, although it has also been observed in fresh water plants. This problem has been associated with condenser leakage and the subsequent concentration of impurities, particularly chlorides, in crevice areas.

Most investigators, beginning with Potter and Mann[1] agree that the breakdown of normally protective magnetite is due to the formation of an acidic chloride environment. In laboratory-produced dents, substantial quantities of chloride have been found near the carbon steel surface and deeply buried in the crevice under the non-protective magnetite. As a consequence, once initiated, denting does not generally require the continued presence of high levels of chlorides in the bulk water. Dented plants have experienced continued denting even after impurity ingress to the steam generators has been substantially reduced although laboratory testing indicates that the rate of denting is substantially lower when chloride concentrations are reduced.

The goal of the joint C-E/EPRI PR-623-2 program, Neutralization of Crevice Acids, is to provide operating plants with chemical procedures for removing or neutralizing acidic chlorides in crevices so as to stifle denting. Such procedures would be implemented at any of the following times:

- after the initial discovery of denting or after observed dent progression;
- as a corrective action after condenser leaks or after a given integrated chloride exposure;
- as a preventive action scheduled into refuelings or other major outages.

Isothermal soaks were considered first as near-term responses to denting which, if successful, could be rapidly developed for field application. The risk of deleterious side effects to field units due to exposure to the soak environment is small because of the short exposure time and the lack of a concentrating mechanism in crevices. However, isothermal soaks rely upon diffusion, a slow process, for the transport of impurities out of crevice regions and the movement of neutralizer in. Hence, prior to recommending such a procedure to the industry there was a need to experimentally establish soak parameters such as time required to be effective, the length of time effectiveness would be expected to last, and the conditions necessary to prolong effectiveness.

Only chemicals having a prior history of use in nuclear steam generators were selected for evaluation in soak environments. This was done to minimize both the risk of unknown side effects and the effort to qualify successful procedures for near-term field application. Soak environments included the following:

- dilute hydrazine solutions simulating cold wet layup and hot standby;

- alkaline solutions of sodium phosphates at both cold shutdown and hot standby.

The principal objective of this effort was to develop an isothermal soak procedure utilizing the above solution(s) for use by operating plants in limiting dent growth. Procedures were designed particularly for application in seawater plants in which copper alloys had been used in the feedtrain. Testing was conducted to determine the following properties for a given soak procedure:

- effectiveness, or ability to stifle active denting during subsequent operation without impurity ingress;

- endurance, or ability to retard the re-initiation of denting during subsequent operation with fresh impurity ingress;

- corrosivity, or the potential for corrosion of steam generator internals during soaking or from neutralizer residuals during subsequent operation.

A secondary objective of this study was to obtain data pertaining to the denting phenomenon, release of impurities and penetration of crevice magnetite by the active neutralizing agent.

The strategy for evaluating soak procedures was as follows:

- Denting was initiated in the test vehicle, after which chlorides were removed from the bulk environment. At this point, the test vehicle simulated a steam generator with active denting in which chlorides in

the bulk water had been reduced to nominal levels by blowdown and feed water clean-up.

- The soak procedure was applied, after which the neutralizing chemicals together with any eluted impurities were removed from the bulk environment.

- Effectiveness was determined by following the progress of denting in the test vehicle while at operating conditions with no impurity ingress. This simulated post-soak operation of a plant with a tight condenser.

- Endurance was determined by following the progress of denting with fresh impurity ingress, simulating renewed condenser leakage.

- Corrosivity was determined through destructive examination of the test vehicle and from corrosion coupons or specimens where appropriate.

- Mechanistic Information was obtained by studying the structure and chemical composition of the non-protective magnetite grown in the test vehicle.

Soak procedures were evaluated in two fundamentally different test vehicles - capsules and pot boilers. Capsules are small autoclaves made of steam generator tubing which are generally used for isothermal corrosion testing. In this study they were used to screen potential soak formulations and to optimize application parameters. Pot boilers are small refluxing autoclaves heated internally by the circulation of pressurized water ($600^{o}F$ at approximately 2000 psig) through inverted U-tubes. Steam produced on the secondary side is condensed at system pressure and returned to the pot by gravity. Pot boilers were used to evaluate promising soak procedures in an environment more representative of actual field units. This

environment includes boiling heat transfer on the tube, concentrating crevices, and actual tube denting induced by seawater and copper alloy feedtrain corrosion product ingress.

This report summarizes the testing performed, presents the results, and evaluates these results relative to the usefulness of isothermal soaking for field units.

Experimental test facilities, procedures and test conditions are described in Section 2. Results from both capsule and pot boiler testing are reported in Section 3. A discussion of pertinent results, evaluations and conclusions are found in Section 4. The appendixes contain more complete descriptions of the capsule and pot boiler testing, lengthy tabulations of test data, and all data generated by capsule and pot boiler destructive examinations.

Section 2

# EXPERIMENTAL

A general description of capsule and pot boiler testing is presented, together with a summary of testing conditions and a discussion of data evaluation. Detailed test procedures are presented in Appendixes A and B for capsule testing and Appendixes C, D, and E for pot boiler testing.

## CAPSULE TESTING

### Overview

Capsules are mini-autoclaves constructed of steam generator tubing, which are used for isothermal corrosion testing of tubing and support materials in aqueous solutions. External sources of heat such as constant temperature baths, standard autoclaves, and furnaces are utilized to establish test temperature. The overall design is shown in Figure 2-1. In denting studies, the support material is inserted as a close-fitting cylindrical slug. When non-protective magnetite is formed on the slug's OD, the crevice fills and the capsule bulges at the elevation of the slug. The occurrence, amount and rate of capsule bulging as a function of slug material, chemical environment, and temperature are the principal experimental observations. Additional information can be gained from the study of changes in solution chemistry and from destructive examinations.

The original objective of capsule testing was to determine how the effectiveness and endurance of isothermal soaking were related to soak conditions. Parameters evaluated included time, temperature, and for phosphate soaks, concentrations and sodium to phosphate molar ratio ($Na/PO_4$). These results were to be used to establish test conditions for water and phosphate

ISOTHERMAL CAPSULE DESIGN

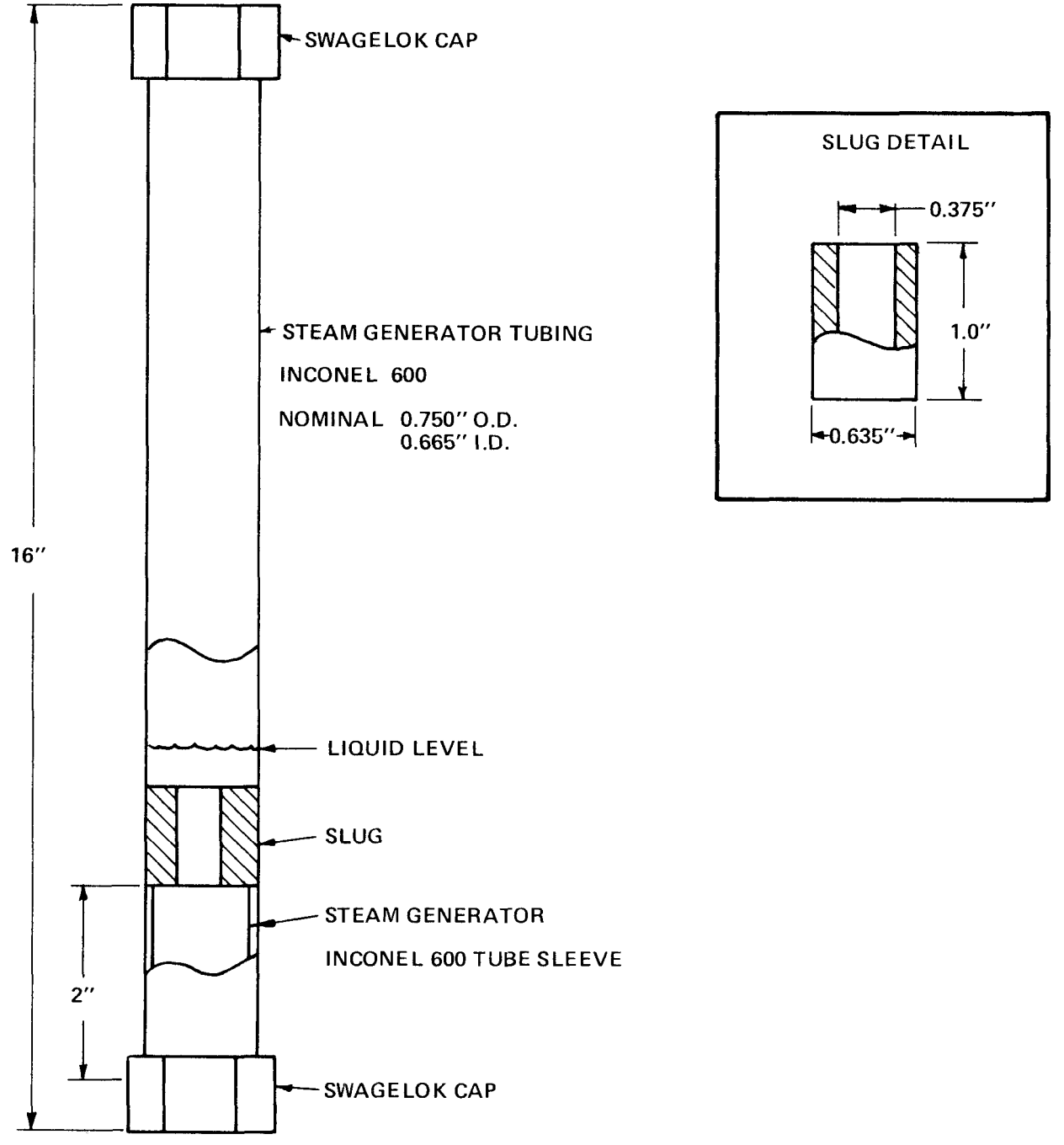


Figure 2-1

soak tests in pot boilers. As testing proceeded, two additional objectives were defined. First, testing was expanded to study the influence of different dent initiation environments on capsule bulging rates and soak test results. This followed early observations that soak effectiveness correlated more strongly with the denting chemistry used than with the soak application parameters. Secondly, additional efforts were made to extract information bearing on the mechanisms of denting, impurity elution, and neutralization.

The capsule testing matrix is presented in Table 2-1. Tests are grouped into the following three areas:

- Evaluation of water soaks.
- Evaluation of soaks in alkaline phosphate solutions.
- Evaluation of capsule denting environments.

A total of 97 capsule tests were conducted under this phase of the project.

Methodology

The testing sequence for evaluating isothermal soaks, shown in Figure 2-2, consisted of three phases: dent (or bulge) initiation, neutralizer/soak application, and post-soak testing.

Dent Initiation. Corrosion was initiated by filling the capsule with an appropriate denting solution and heating to 565$^{o}$F in an electric furnace. Generally 1 to 5 mils of diametral bulging could be produced in about three weeks. For most tests, one of the following solutions was used to initiate capsule bulging or "inverse denting".

Figure 2-2

CAPSULE TESTING SEQUENCE

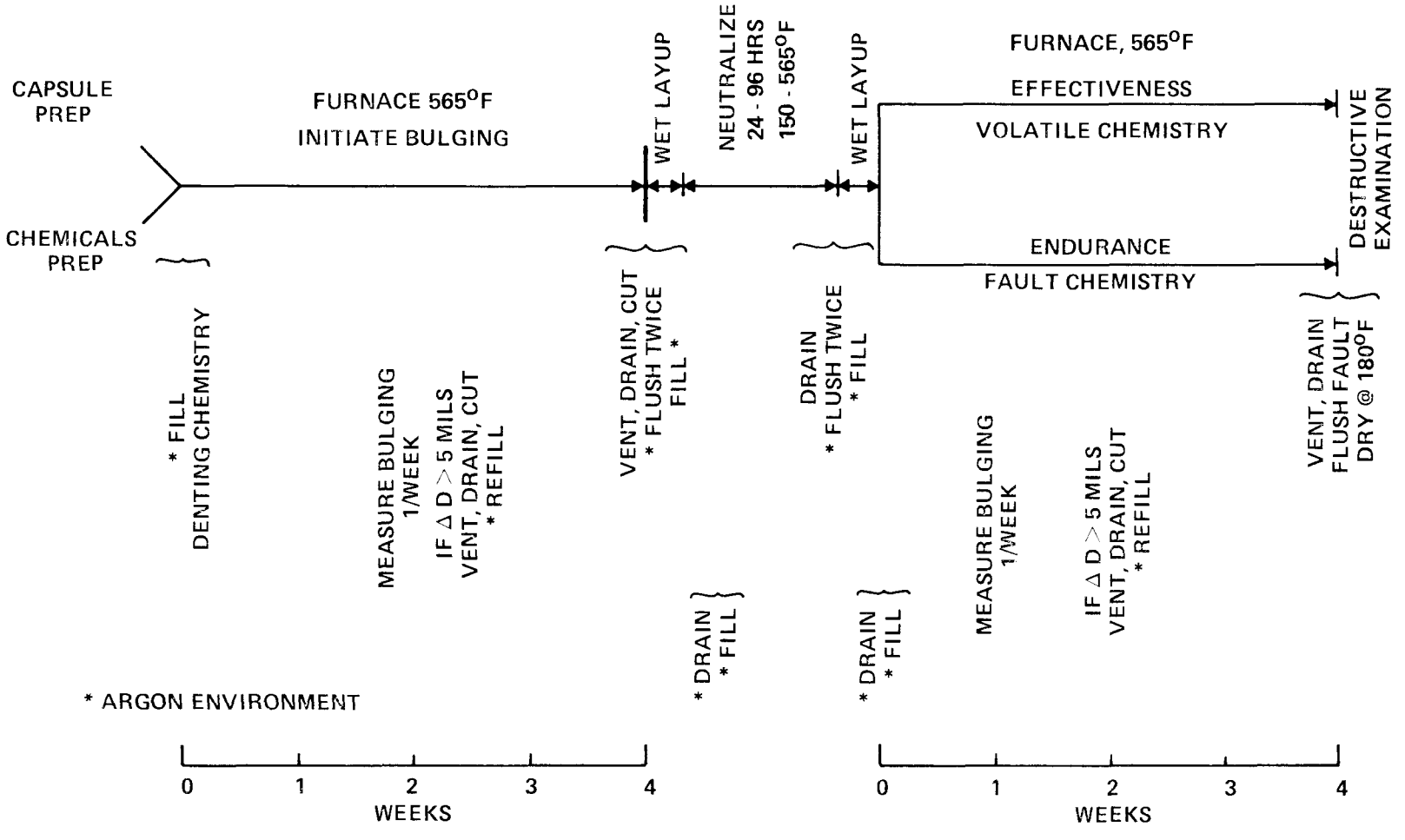

- C-E Reference Denting Environment

  0.1 M $FeCl_2$

  This environment had been selected as the simplest yielding corrosion similar to that in the field. Potter and Mann[1] had studied the "fast linear growth of magnetite" on carbon steel in this environment.

- W/EPRI Reference Denting Evnironment

  0.1 M $CuCl_2$ plus
  0.1 M $NiCl_2$ dissolved in full strength seawater

  This environment had been developed through testing conducted under Task 310 of EPRI Research Project RP-699-1, "PWR Steam Side Chemistry Follow Program". Dents produced from this environment were intended to simulate field dents in chemical composition.

Neutralizer/Soak Application. Following dent initiation, the capsules were subjected to a series of operations which generally included the following:

- pre-flushing to remove residual impurities adsorbed onto exposed interior surfaces;

- isothermal soaking in either an electrically heated furnace ($565^{o}F \pm 10$) or a constant temperature bath ($150^{o}F \pm 5$);

- post-flushing to remove residual neutralizer and/or impurities eluted during the soak.

TABLE 2-1

CAPSULE TESTING MATRIX

| Area | # Of Tests | Denting Chemistry | Soak Conditions (4) Time Hrs. | Temp. °F. | Chemistry |
|---|---|---|---|---|---|
| Water Soaking | 12 | W/EPRI (1) | 24, 96, 168 | 150 | 200 ppm $N_2H_4$, pH = 10 |
| | | | | 565 | ∿20 ppm $N_2H_4$ |
| Phosphate Neutralization | 31 | C-E (2) | 24, 96 | 150 | 300, 1000, 3000 ppm $PO_4$ $Na/PO_4$ = 2.4, 2.8 |
| | | | | 565 | 50, 300 ppm $PO_4$ $Na/PO_4$ = 2.5 |
| | 20 | W/EPRI | 24, 96 | 150 | 1000, 3000, 5000, 10,000 ppm $PO_4$ $Na/PO_4$ = 2.8 |
| | | | | 565 | 50, 300, 1000, 3000 ppm $PO_4$ $Na/PO_4$ = 2.5 |
| Additional Denting Chemistry (3) | 12 | 0.25 M $FeCl_2$ | 96 | 150 | 300, 1000, 3000, 10,000 ppm $PO_4$ $Na/PO_4$ = 2.8 |
| | | | | 565 | 300 ppm $PO_4$ $Na/PO_4$ = 2.5 |
| | 12 | 0.05 M $FeCl_2$ in Full Strength Seawater | | | No soaks performed |

Notes
1. 0.1 M $CuCl_2$ + 0.1 M $NiCl_2$ in Full Strength Seawater
2. 0.1 M $FeCl_2$
3. In addition to above environments
4. Both Effectiveness and Endurance tested on each soak except capsules bulged with 0.25 M $FeCl_2$ were subjected to effectiveness testing only.

For all tests except the water soaks, pre- and post-soak flushes consisted of two one-minute rinses in demineralized water followed by 24 hours of wet layup (200 ppm $N_2H_4$). The wet layup periods were omited for the water soak tests. During the phosphate soak tests, selected capsules were retained as "controls". These were soaked in demineralized water rather than phosphate in order to separate neutralization from soaking.

Post-Soak Testing. The effectiveness and endurance of the soaks were evaluated by observing capsule growth under furnace exposure over the next month. For effectiveness tests, capsules were refilled with demineralized water containing approximately 20 ppm $N_2H_4$. The hydrazine was added to consume oxygen in the demineralized water. Residual hydrazine would decompose to ammonia at temperature, providing an environment simulating volatile chemistry control. Endurance capsules were refilled with demineralized water containing 0.1 M $FeCl_2$ to simulate a fault chemistry environment.

Testing Procedures

In general, all capsule filling was done in an Argon-filled glove box to exclude oxygen. For tests where chemical mass balances were desired, the volumes of all rinses and drains were measured. The solutions were saved for analyses of chloride and, when appropriate, sodium and phosphate.

Capsule diameters were measured after each week of furnace exposure following the first two weeks. Measurements were made with a micrometer at five different locations around the circumference, and the average was recorded. The accuracy of this measurement was $\pm$ 1 mil on the diameter.

The formation of nonprotective magnetite within crevices is accompanied by the formation of hydrogen gas. In the sealed environment of a capsule, hydrogen accumulation could result in

pressure sufficient to rupture the capsule if precautions were not taken. For this reason every capsule was vented to relieve this pressure, after each diametral increase of 5 mils. After each venting, the capsule was drained, and the upper swagelock fitting was cut off to facilitate installation of a new swagelock fitting. Fresh solution was then added to the capsule.

Evaluation of Bulging Data

The raw data consisted of capsule diametral measurements made during assembly and at roughly weekly intervals during the course of testing. Cumulative diametral increases were determined by difference with the initial diameter; these were tabulated and plotted against time.

For screening tests, any growth in excess of 1 mil following a soak was taken as a negative result (no effectiveness or endurance). For quantitative evaluation, bulging rates before and after soaking were calculated from the plots and compared.

Preliminary observations indicated that growth only occurred during periods of furnace exposure. This is consistent with information developed by Westinghouse Electric Corporation under EPRI Contract RP-699-1 (Reference 2) showing that temperature has a strong influence on capsule bulging rates. Therefore, the time used in plotting was furnace exposure time ("days at temperature") including time with neutralizers present. Where dent initiation times varied, time was normalized to the beginning of the neutralization phase. In these plots the number of days before and after neutralization have been indicated by (-) and (+) respectively. By this technique, neutralization occurs at the same time for all capsules in a given plot. Comparison of bulging rates before and after neutralization are thereby simplified.

In most instances, capsule bulging appeared to be a linear function of furnace exposure time. Data were fitted to straight lines via the method of linear regression in order to determine the slope (m) in mils/day, the y-intercept (b) in mils, and the coefficient of correlation (R). Where possible the standard deviation of the slopes were determined by standard statistical methods. These were used to evaluate the statistical significance of the differences observed between pre- and post-soak bulging rates. Reductions at the 95% confidence level were considered significant. In a few cases, a small increase was observed in bulging rate following soaking. Since there appeared to be no physical reason for such an increase these data were assumed to be indicating a bulging rate unaffected by soaking.

Evaluation of Chemistry Data

For a number of capsules, fill, drain, and flush solutions were analyzed in an attempt to perform mass balances for chloride, sodium and phosphate. Concentrations in ppm were converted to absolute milligrams by multiplying each concentration by the volume. These data were then used to account for all chloride added to or removed from the capsules. Sodium and phosphate data were handled in a similar fashion. Capsules, however, ar not very amenable to quantitative techniques such as pouring and flushing because of flow restrictions resulting from the near closing of the slug ID by non-protective magnetite.

Capsule Destructive Examinations

Selected capsules were destructively examined to see if test results would correlate with the structure and chemistry of non-protective magnetite, and thus provide insight into the mechanisms of denting, impurity removal, and neutralization. Specific objectives were as follows:

- to determine the location and concentration of residual chloride and phosphate in the magnetite matrix;

- to determine how differences in the denting environment influence the morphology of non-protective magnetite;

- to determine the location and concentration of sea salts, copper, and nickel (present in the W/EPRI reference environment) in the magnetite matrix.

Eight capsules representing a cross-section of denting environments, soak procedures, and post-soak chemistries were chosen for destructive examination. Table B-1 summarizes the test histories. Capsule DD-12 was examined primarily to determine why the capsule had grown less than anticipated based upon other water soak tests. It was later concluded that DD-12 had inadvertently been exposed to phosphate during testing.

All capsules were examined along a cross section through the center of the bulged region. The non-protective magnetite at this location was farthest from the soak solution. Two capsules (AA-7, DD-7) were examined along a longitudinal section to see how the oxide morphology and chemistry varied from the center to the end of the bulged region.

The transverse sections were examined in an optical metallograph and by SEM (scanning electron microscopy). Concentration gradients across the oxide layer were determined by EMPA (electron microprobe analysis). For each specimen, a number of elements were anlyzed, including those present in the tubing and slug (Cr, Fe, Ni), in the denting environment (Cl and Mg, Ca, Cu when present), and in the soak solution (Na, P). Two specimens (AA-8, DD-8) were also examined by IMMA (ion microprobe mass analysis). IMMA results were examined statistically to determine correlations for the presence or

absence of elements over the areas examined. Such correlations would suggest chemical or physical association among groups of elements.

Destructive examinations were performed by Knolls Atomic Power Laboratory (KAPL), Schenectady, New York, under the general direction of G. E. Galonian of the Steam Generator/Coolant Technology section. Most of the SEM and EMPA work was subcontracted by KAPL to Mechanical Technology, Inc. (MTI), Latham, New York. Table B-2 summarizes the analyses performed on each capsule.

## POT BOILER TESTING

### Overview

Pot boilers are refluxing autoclaves designed to study tubing and support material corrosion at operating temperatures under controlled chemistry conditions. The units contain four tubes which are heated internally by circulating high pressure water simulating reactor coolant. In terms of thermal-hydraulics, pot boilers occupy a middle ground between isothermal capsules and model steam generators. Bare-tube heat fluxes are an order of magnitute lower than field units. The tubes are widely-spaced rather than on a close-packed triangular or square pitch. There is no tube bundle shroud to direct the flow of recirculating water. Steam quality and fluid velocities in the bundle region are low.

The objective of this testing was to comparatively evaluate the three soak procedures shown in Table 2-2 under target plant conditions. Tube bundles were outfitted, as shown in Figure 2-3, with various devices to simulate tube-support plate crevices. Selected concentrating rings were instrumented with high temperature strain gauges which were used to follow the

course of tube denting. Denting was also measured via eddy current examination at different points during testing. Crevices were pre-packed with copper-alloy feedtrain corrosion products to assure that concentration would occur even at the low pot boiler heat fluxes.

There were three phases to pot boiler testing as shown in Table 2-2. In Phase I, denting was induced by operating with seawater and corrosion product ingress. Fault chemistry chloride concentrations were maintained as described in Table 2-2. Following dent initiation, volatile chemistry control was re-established via blowdown and by draining and refilling. Ultimately chloride was reduced to less than 1.0 ppm prior to Phase II. At this point, the pots simulated seawater sited plants with active denting due to prior exposure to condenser leakage.

During Phase II, the soaking procedures shown in Table 2-2 were applied. These procedures were similar to those that would be used in field units, with the exception that temperature was maintained at $150^{O}F$ to assure the comparability of the results. The units were pre-flushed to remove neutralizer prior to restart.

In Phase III, the units were operated for about thirty days on volatile chemistry control, simulating plant operation with a tight condenser. Table 2-3 contains the volatile chemistry specifications applicable during this and other phases described as under volatile control.

The effectiveness of the soaks was judged primarily on the amount of further denting which was observed during post-soak operations. Corrosivity was determined from non-destructive tubing examination, from the destructive examination and from corrosion coupons mounted in the boiler during various phases

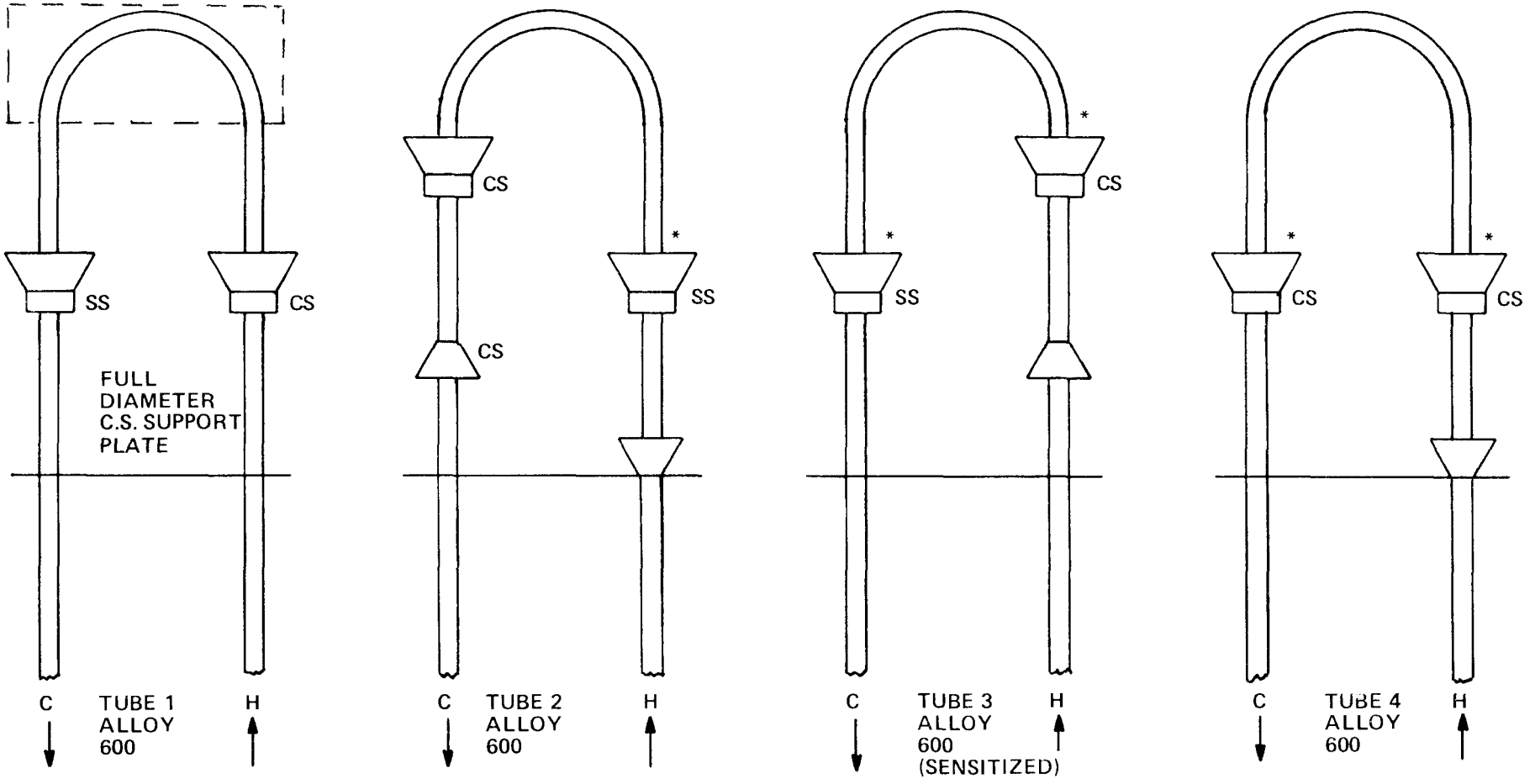


Figure 2-3

SCHEMATIC OF TUBE
BUNDLE FABRICATION
FOR POT BOILER TESTS 9, 11, 7E

TABLE 2-2

TEST OPERATION SUMMARY

| | Water Soak Pot 9 | Phosphate Soaks Pot 11 - 1000 ppm | Pot 7E - 3000 ppm |
|---|---|---|---|
| Phase I - Dent Initiation * | | | |
| Average heat flux 7000 BTU/hr/ft$^2$ | | | |
| Days volatile pre-conditioning | 13 | 13 | 7 |
| Days chloride fault 100-150 ppm $Cl^-$ | 17 | 17 | -- |
| 150 ppm $Cl^-$ | 12 | 12 | 15 |
| 150-175 ppm $Cl^-$ | 30 | 25 | 35 |
| Days Blowdown/Volatile | 5 | 8 | 22 |
| Total | 77 | 75 | 79 |
| Phase II - Watersoak/Neutralization | Water Soak | $PO_4$ Soak | $PO_4$ Soak |
| Soak Specifications | $N_2H_4$ 200 ± 50 ppm<br>pH ~ 10.0<br>96 hrs/150°F | $PO_4$ ~ 1000 ppm<br>Na/P MR 2.8<br>$N_2H_4$ ~ 20 ppm<br>96 hr/150°F | $PO_4$ ~ 3000 ppm<br>Na/P MR 2.8<br>$N_2H_4$ ~ 20 ppm<br>96 hr/150°F |
| Phase III - Volatile Operation | | | |
| Average heat flux 7000 Btu/hr/ft$^2$ | | | |
| Days volatile operation | 37 | 36 | 34 |
| Bulk chloride concentration, ppm | <0.6 | <0.3 | <0.5 |
| | Non-destructive examination | Destructive examinations | |

* Crud consting of 4.8 g $Fe_3O_4$ and 3.2 g CuO was injected times weekly during fault operation.

TABLE 2-3

Volatile Chemistry Specifications
Pot Boiler Testing

| | |
|---|---|
| Chloride | < 0.1 ppm |
| pH | 8.2 - 9.2 |
| Conductivity | < 7 μmhos/cm |

of testing. Other data were generated which provided insight into the mechanisms of denting, impurity elution, and neutralization.

Pot Boiler Examination

Pot boilers were examined following fabrication to establish the baseline condition, at the completion of Phase I - Dent Initiation, and at the end of Phase III - Volatile Operation. The methods used are discussed below.

Visual. Visual examinations, documented by photographs, were conducted to determine the general conditions of the pot boiler internals, to identify areas of localized corrosion, and to identify regions for sampling loose corrosion products. Denting rings were checked to see if they gripped the tubing (usually an indication of crevice corrosion), and support plate annuli were checked for blockage.

Observations are discussed in the "Operating History" section of Appendix C.

Eddy Current Testing. Tube bundles were eddy current tested in order to detect and measure the magnitute of tube dents and to search for gross corrosion of the tubing OD. Tubes were scanned with an EM 3300 ZETEC eddy current tester equipped with a strip-chart recorder and a TEAC 2300 SX magnetic tape recorder. A dual coil differential bobbin-style probe was used. The probe was manually pulled. The following test parameters were established:

| Objective | Frequency | Instrument Sensitivity |
|---|---|---|
| Large ( >20%) Wall Defects | 400 khz. | 50 |
| Small Wall Defects | 100 khz. | 30 |
| Dents | 400 khz. | 10 |

Corrosion Product Sampling. Deposits were collected from areas of interest for characterization by X-ray fluorescence (XRF) and X-ray diffraction (XRD). These results were used to determine whether changes had occurred in the chemical form of corrosion products added, to document corrosion product segregation (variations in composition with respect to location), and to evaluate the relation between deposits found in the vicinity of active dents and the denting process.

Corrosion Coupons/Specimens. Corrosion coupon and double U-bend specimens (present in the two phosphate tests) were examined. Corrosion coupon specimens were cleaned, descaled, and weighed to measure weight loss. The U-bend specimens were examined visually at magnifications up to 60X for crack-like indications. Specimens were then sectioned, polished, etched and examined under high magnification for indications of intergranular cracking.

Destructive Examination. Pots 11 (1000 ppm $PO_4$) and 7E (3000 ppm $PO_4$) were examined. Dents on tube 4 at both carbon steel concentrating rings and at the hot leg support plate were sectioned for optical and scanning electron microscopy (SEM).

For all specimens, the morphology of the oxide in the crevice region was examined in detail by optical microscopy. Comparisons were made of the oxide formations at different locations within the same specimen and between different specimens.

The concentrating ring dents were further examined by scanning electron microscopy (SEM) supplemented by energy dispersive spectrometry (EDS or EDAX) analysis to identify elements present. Areas for SEM/EDS examination were identified from the light microscopy studies. At each area, a low magnification (39-50X) SEM was obtained which was then used to select four to six areas for examination at higher magnification (2100X)

A qualitative search of the magnetite in each area was conducted via EDS to identify chemical species present.

The support plate sections were also examined by SEM. Additionally, the magnetite was examined with the electron microprobe (EMP) supplemented with wave length dispersive spectrometry (WDS), which provided a sensitive X-ray mapping of the elemental distribution. The result was a map of a given area of magnetite on which the distribution of characteristic X-ray emissions is represented by white dots. The number of dots per unit area represents the localized intensity of the characteristic X-radiation and consequently the relative concentration of the given element. A map of this kind is produced to exactly the same scale as an SEM picture and comparison of the map with the SEM picture allows areas in which specific elements (eg. chloride, phosphorus) have concentrated, to be associated with specific structures of the magnetite morphology.

Data Evaluation

Strain Gauge Data. Strain, plotted as a function of time, was used to define the time of dent initiation and to observe changes in the rate of denting resulting from soaking. Strain would begin to increase when enough support material corrosion had occurred to exert compressive forces sufficient to deform the tubing. The rate of strain increase was presumed to be proportional to the denting rate (and hence the support material corrosion rate), although the proportionality constant would be dependent on local geometric conditions.

Eddy Current Test (ET) Results. Eddy current testing served two functions: to establish the magnitude of denting at a given point in testing; and to search for gross corrosion of the tube OD surface. Average denting rates were calculated from sequential ET examinations.

Average denting rates for Phase I, Dent Initiation, utilized strain gauge response as an indication of when denting initiated.

Bulk Water Chemistry Data. With one exception, bulk water chemistry was monitored for the sole purpose of assuring compliance with test specifications. Chloride concentrations were closely monitored during both the soaking phase and post-soak operations, and chloride recoveries (presumably from dented regions) were calculated.

# Section 3

# RESULTS

As described in Section 2, the two types of experimental devices utilized in this study were isothermal capsules and four-tube pot boilers. Similar conclusions regarding dent mititation and neutralization have been drawn from both. The experimental techniques, however, are sufficiently different that the results from each type of device are presented separately.

## CAPSULE TESTING

Measurements of diametral expansion (bulging) were used to derive capsule bulging rates throughout all phases of testing. Post-soak bulging rates were found to be significantly more dependent upon the pre-soak fault chemistry than on soak chemistry or conditions. The most significant difference between the various pre-soak fault chemistries was the chloride concentration which ranged from 7000 to 32000 ppm. For the test procedures followed, soaking was ineffective (bulging was not halted) in all capsules except those bulged with the lowest chloride concentration (7000 ppm). For capsules in which bulging continued subsequent to soaking, chloride residuals were found localized in a band of magnetite adjacent to the carbon steel. Results from bulging measurements, solution chemical analyses, and destructive examinations are presented in the following.

### Bulging Rates

Overview. Capsule bulging data during the dent initiation phase were statistically evaluated for each of the four denting

environments used. The W/EPRI reference environment produced a bulging rate significantly higher than that of the C-E reference environment and 0.25 M $FeCl_2$ which were equal. Significant scatter (± 100%) was observed in all rates. The 0.05 M $FeCl_2$ in full strength seawater environment produced no bulging after 62 days although slugs were wedged indicating that the annular gap had been filled.

The effectiveness and endurance of soaks in hydrazine treated water and alkaline phosphate solutions were evaluated in terms of the reduction in bulging rate observed. Capsules bulged with C-E denting chemistry stopped bulging whenever the fault environment was removed. In other words, corrosion was successfully stifled by all tested water soak and phosphate formulations. Capsules bulged with W/EPRI and 0.25 M $FeCl_2$ fault chemistries continued to grow after soaking irrespective of the soak and post-soak environment.

Fault-Chemistry Bulging Rates. Bulging rates were evaluated for four denting environments, as follows:

- 0.1 M $CuCl_2$ + 0.1 M $NiCl_2$ in full strength seawater (W/EPRI Reference)
- 0.1 M $FeCl_2$ (C-E Reference)
- 0.25 M $FeCl_2$
- 0.05 M $FeCl_2$ in full-strength seawater.

No bulging was observed with the latter environment after sixty-two days at temperature. At the completion of testing, the carbon steel slugs were wedged in the capsules, indicating that the initial radial gap had been filled by corrosion product.

With the other three environments, bulging commenced after about eight days at temperature. This initiation time corresponded to the filling of the annular gap between slug OD and tube ID (about 15 mils) with magnetite. Two rates were determined from the raw data: the apparent gap fill rate (initial gap divided by initiation time) and the radial growth rate, by methods described in Section 2. The experimental data and calculated rates for the 79 capsule tests used in this evaluation are presented in the Appendix, Tables A-2, A-3, and A-4. Summary results, expressed as radial growth rates, are presented in Table 3-1.

In all cases, the gap-fill rate was at least an order of magnitude higher than the radial bulging rate. No statistically-significant difference at the 95% confidence level was found in the gap fill rates for the three different environments. When all the data are considered together, the median value for 70 observations becomes 1.9 mils/day with a standard deviation of 0.8 mils/day.

The radial growth or bulging rate with the W/EPRI reference environment was about 30% greater than with either the C-E reference solution or 0.25 M $FeCl_2$. The latter two environments produced essentially the same bulging rates. Both these observations were statistically significant at the 95% confidence level. As can be seen from the standard deviations in Table 3-1, a significant scatter in capsule bulging rates was observed, ranging from 0.28 mils/day to 0.71 mils/day for the W/EPRI environment and 0.10 mils/day to 0.5 mils/day for the other two environments.

TABLE 3-1

Summary of Capsule Bulging Rates (Radial)
During Dent Initiation

| Fault Chemistry | C-E | 0.25 M $FeCl_2$ | W/EPRI |
|---|---|---|---|
| Gap Fill Rate | $1.9 \pm 0.5$[1] | $2.2 \pm 0.9$[2] | $2 \pm 1$[3] |
| Number of Operations[4] | 25 | 11 | 34 |
| Bulging Rate | $0.16 \pm 0.06$[3] | $0.14 \pm 0.04$[1] | $0.20 \pm 0.08$[3] |
| No. of Observations[4] | 26 | 11 | 34 |

Statistical considerations at the 95% confidence level yield the following:

Common gap-fill rate = $1.9 \pm 0.8$[2] mils/day

W/EPRI bulging rate = = $0.20 \pm 0.08$[3] mils/day

C-E and 0.25 M $FeCl_2$ bulging rate = $0.16 \pm 0.06$[3] mils/day

Notes:

1. The arithmetic mean was used because the distribution was normal.
2. The median was used because the distribution was skewed with about 10% of the values at the high end of the range.
3. The geometric mean was used because the distribution was bimodal.
4. Some observations were excluded because either the initation time could not be determined or the observed rate exceeded the mean by three standard deviations.

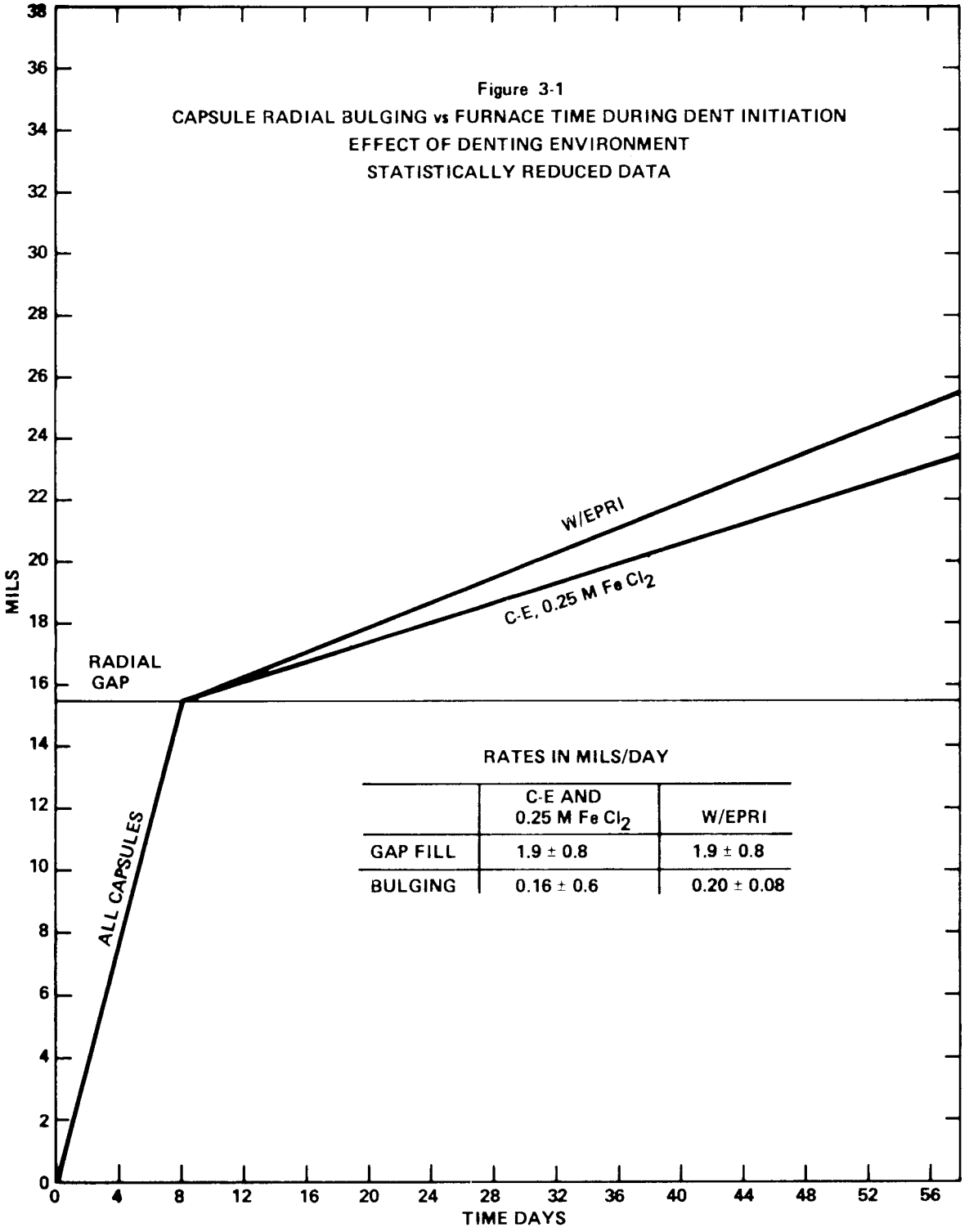
Figure 3-1
CAPSULE RADIAL BULGING vs FURNACE TIME DURING DENT INITIATION
EFFECT OF DENTING ENVIRONMENT
STATISTICALLY REDUCED DATA
MILS
TIME DAYS
RADIAL GAP
W/EPRI
C-E, 0.25 M Fe Cl2
ALL CAPSULES
RATES IN MILS/DAY
C-E AND 0.25 M Fe Cl2
W/EPRI
GAP FILL
1.9 ± 0.8
1.9 ± 0.8
BULGING
0.16 ± 0.6
0.20 ± 0.08

Effects of Water Soaks. A total of twelve capsules, reverse dented with W/EPRI reference solution, were utilized in the water soak test. Quantitative data pertaining to diametral increase, in mils, are listed in Appendix Table A-5 and presented graphically in Figures 3-2 through 3-5. Where reasonable straight lines can be fit to the data, slopes, and the y- intercepts, are presented in the figures along with the coefficients of correlation.

In general all capsules continued to bulge after soaking, as shown on Figures 3-2 through 3-5. Bulging was linear with time up to a total diametral increase of 16-20 mils, after which a reduction in bulging rate was observed. This fall-off at large diametral increases is a characteristic of capsule testing which has been observed previously in these laboratories and by others (2). It is not related to the soak conditions.

The variation in capsule bulging rates which is apparent from these figures is identical to the variance in pre-neutralization bulging for all capsules bulged with W/EPRI reference solution. This variation complicated interpretation of results because a given post-soak bulging rate was dependent on two factors: (1) the affect of soaking and (2) the particular pre-soak bulging rate. In view of this, ratios formed by dividing a post-soak bulging rate by the pre-soak rate were used in evaluating the data. Results in terms of percentage reductions in pre-soak bulging rates are shown on Table 3-2.

The endurance test results cannot be related to the soak conditions. In the effectiveness tests, soak temperature had no significant influence on the results. An incrase in effectiveness was observed when soak time was increased from one to four days, but little further increase was observed from a seven day soak. The results taken in total suggest that water soaking reduced capsule bulging rates by about a third.

TABLE 3-2

EFFECT OF WATER SOAKS ON
CAPSULE BULGING RATES

% REDUCTION IN PRE-SOAK RATE AS
A FUNCTION OF TEST CONDITIONS

| | EFFECTIVENESS TESTS | | ENDURANCE TESTS | |
|---|---|---|---|---|
| Soak Temperature<br>Soak Time | 150°F | 565°F | 150°F | 565°F |
| 1 day | 7 | 0 | 28 | 35 |
| 4 day | 18 | 28 | 49 | 26 |
| 7 day | 21 | 25 | 42 | 37 |

Figure 3-2

EFFECTIVENESS OF WATER SOAKS

TEMPERATURE: 150°F

TIME: 1, 4, 7 DAYS

CHEMISTRY: C-E WET LAYUP (200 ± 50 PPM $N_2H_4$ pH = 10.0)

DENT ENVIRONMENT: W/EPRI REFERENCE SOLUTION

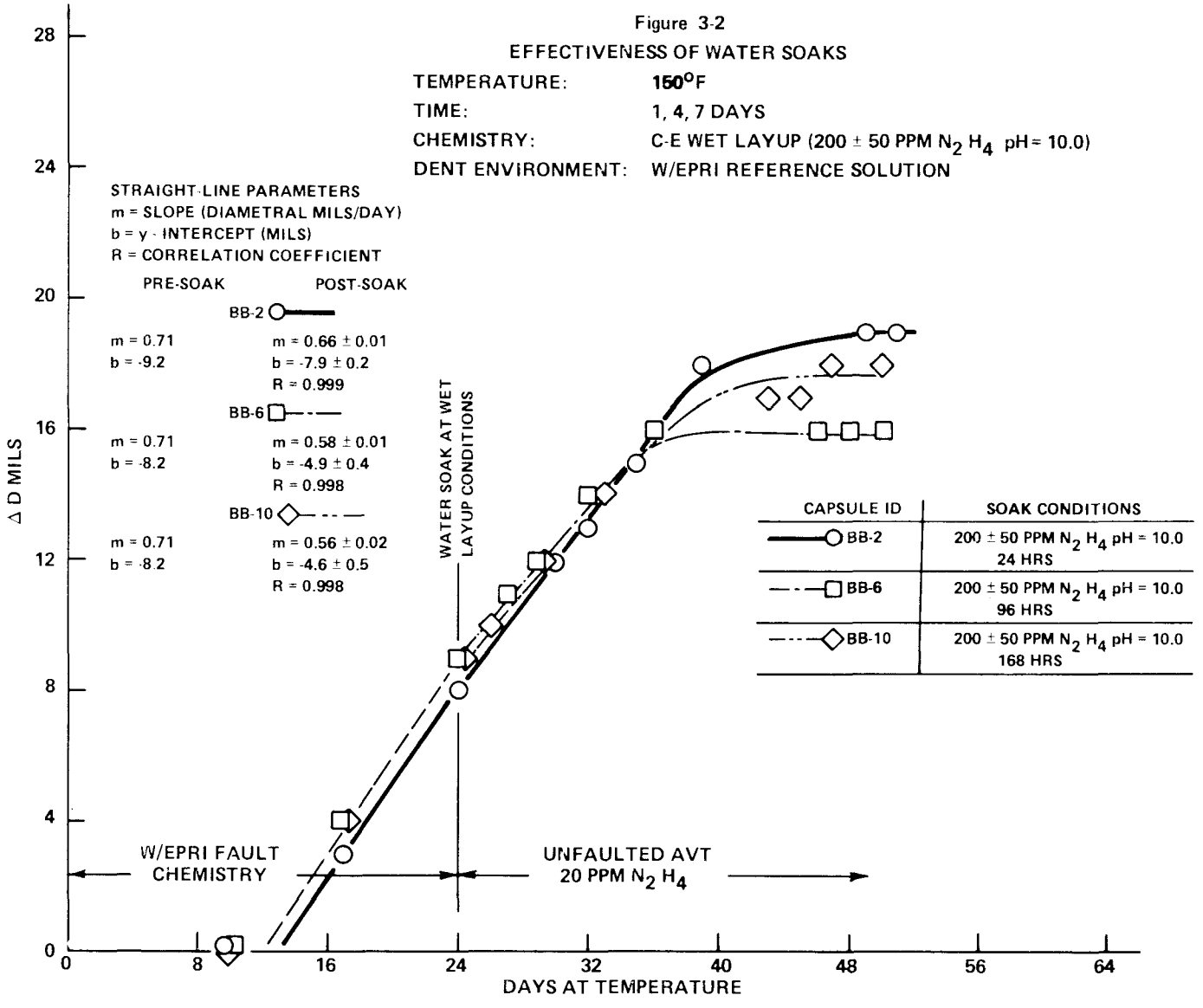

Figure 3-3
ENDURANCE OF WATER SOAKS
TEMPERATURE: 150°F
TIME: 1, 4, 7 DAYS
CHEMISTRY: C-E WET LAYUP (200 ± 50 PPM $N_2H_4$) pH = 10
DENT ENVIRONMENT: W/EPRI REFERENCE SOLUTION

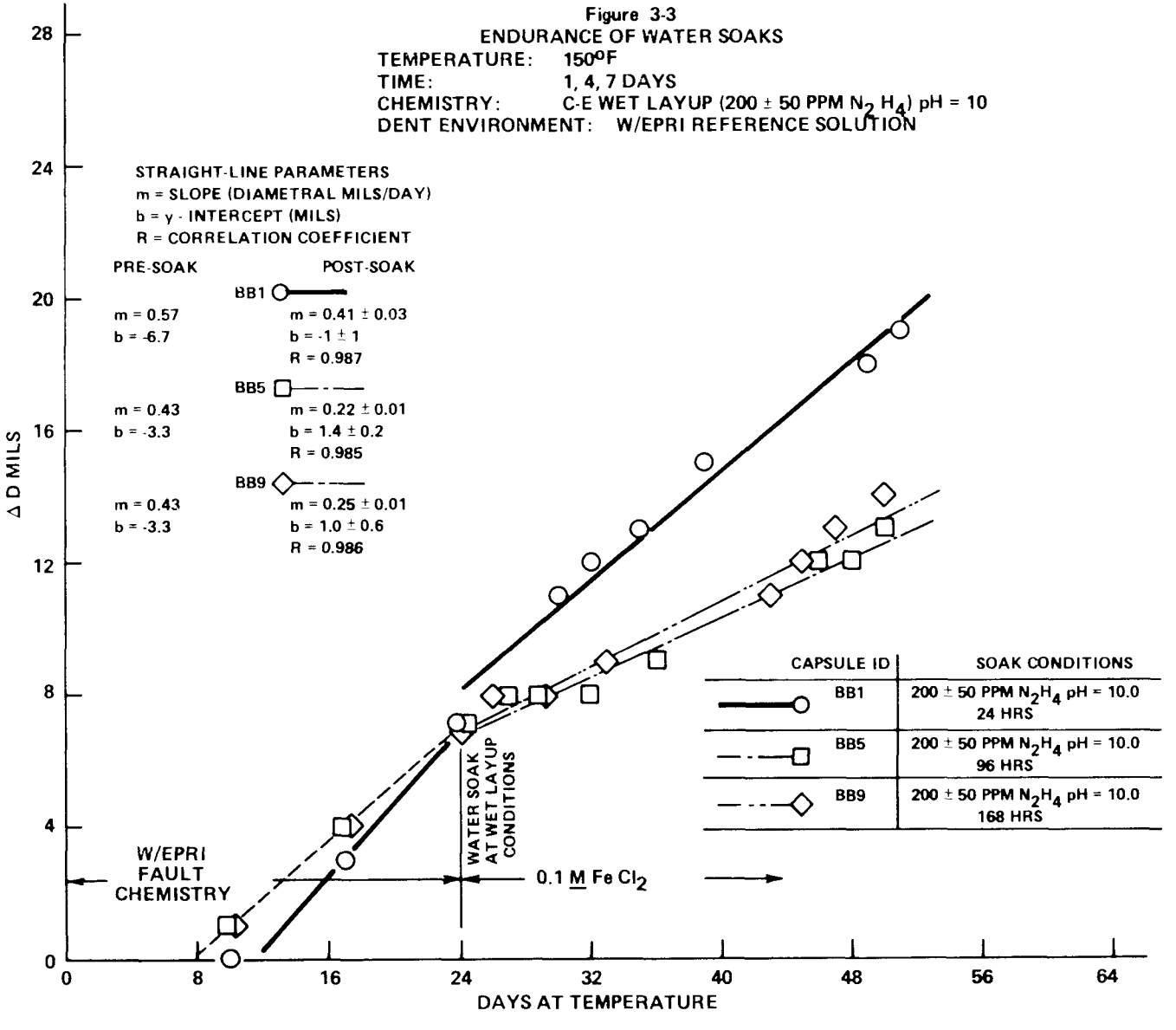

Figure 3-4
EFFECTIVENESS OF WATER SOAKS

TEMPERATURE: 565°F
TIME: 1, 4, 7 DAYS
CHEMISTRY: AVT (20 ppm $N_2H_4$)
DENT ENVIRONMENT: W/EPRI REFERENCE SOLUTION

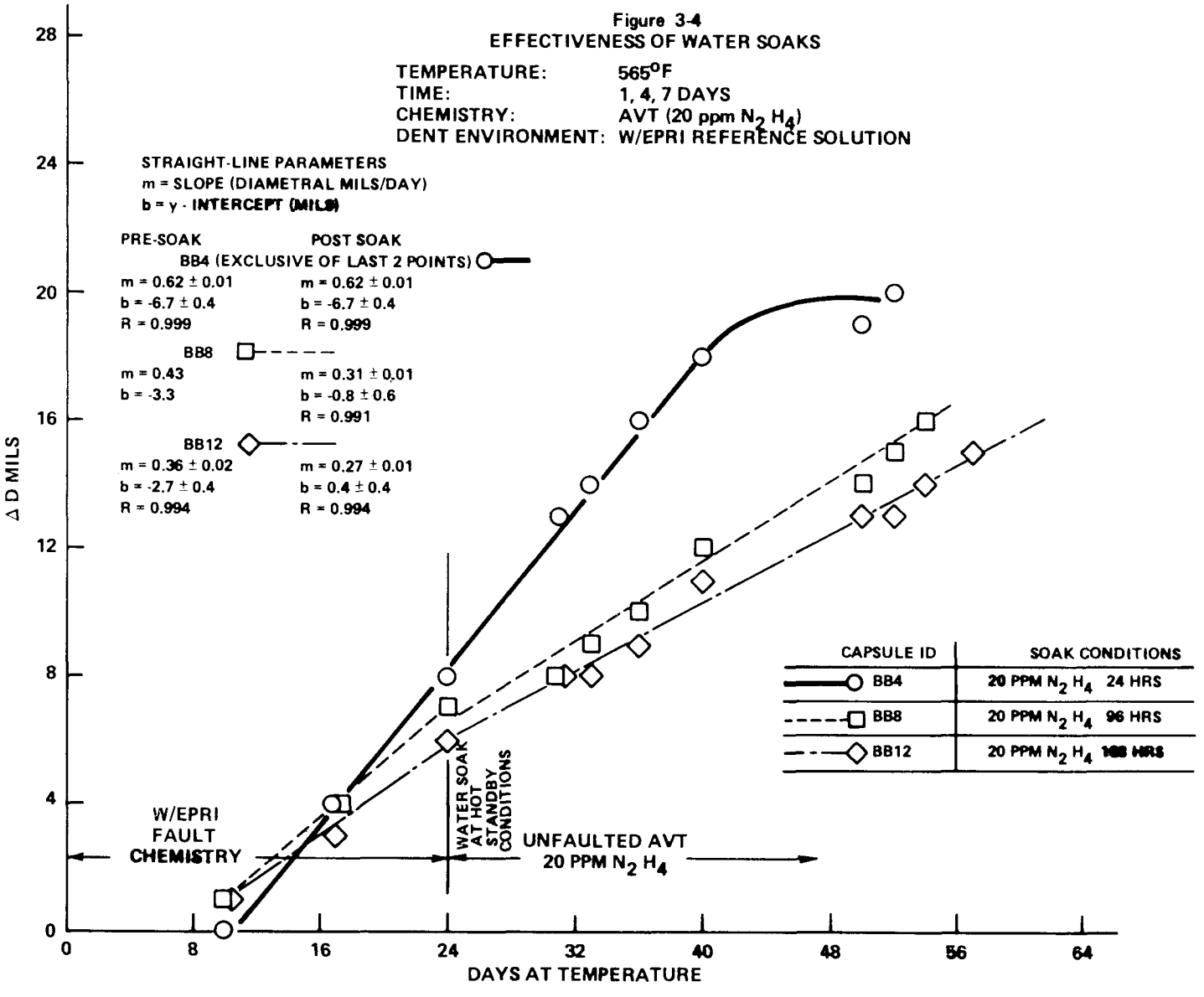

Figure 3-5
ENDURANCE OF WATER SOAKS

TEMPERATURE: 565°F
TIME: 1, 4, 7 DAYS
CHEMISTRY: AVT (200 PPM $N_2 H_4$)
DENT ENVIRONMENT: W/EPRI REFERENCE SOLUTION

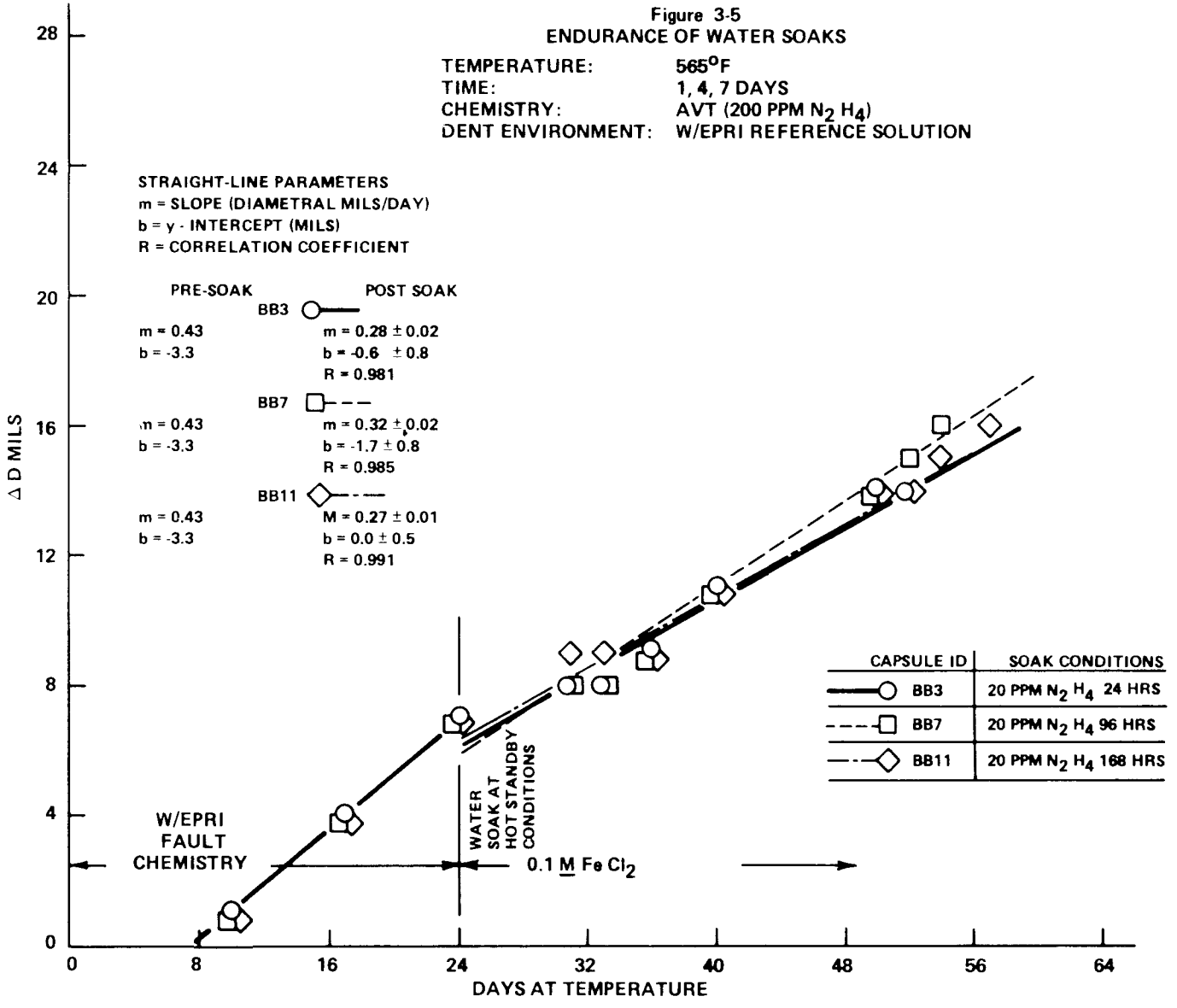

Effect of Phosphate Neutralization. Capsule evaluation of alkaline phospate neutralization was conducted with capsules in which three different fault chemistries had been used to initiate bulging. Capsule bulging rates after phosphate neutralizations were found to be more dependent on the initial denting environment than on soaking parameters. For this reason, the results of phosphate testing in capsules are presented separately for each denting chemistry.

C-E Reference Environment. Bulging data from C-E capsules neutralized with alkaline phosphates are tabulated in Appendix Tables A-6 through A-8. Representative data are plotted in Figures 3-6 through 3-10. As can be seen, diametral growth was limited to less than 2 mils (the experimental error of capsule diametral measurements) in all the "Effectiveness" tests, but continued with little or no change in rate in all the "Endurance" tests. Soak time, temperature, or solution chemistry appeared to have no influence on the results. This is most readily observed in Figure 3-10, which is a plot of data from control capsules. Capsules which were refilled with volatile chemistry stopped bulging whereas those which had been refilled with 0.1 M $FeCl_2$ continued to bulge. Apparently, removal of the denting environment is sufficient to halt corrosion in capsules dented with the C-E reference environment.

Considerable scatter is apparent in Appendix Tables A-6 through A-8 and in Figures 3-6 through 3-10. This scatter is exactly the same as previously discussed for C-E pre-soak bulging rates because the same capsules were involved.

In all of the "Endurance" tests except Z-9 (300 ppm $PO_4$, Na/P=2.8, 150°F, 96 hrs), the post-soak bulging rate was not statistically different from the pre-soak rate. The bulging rate of Z-9 was reduced by 8% following the soak.

Figure 3-6

PHOSPHATE SOAK AT 150°F

EFFECTIVENESS

CAPSULES DENTED WITH C-E REFERENCE SOLUTION

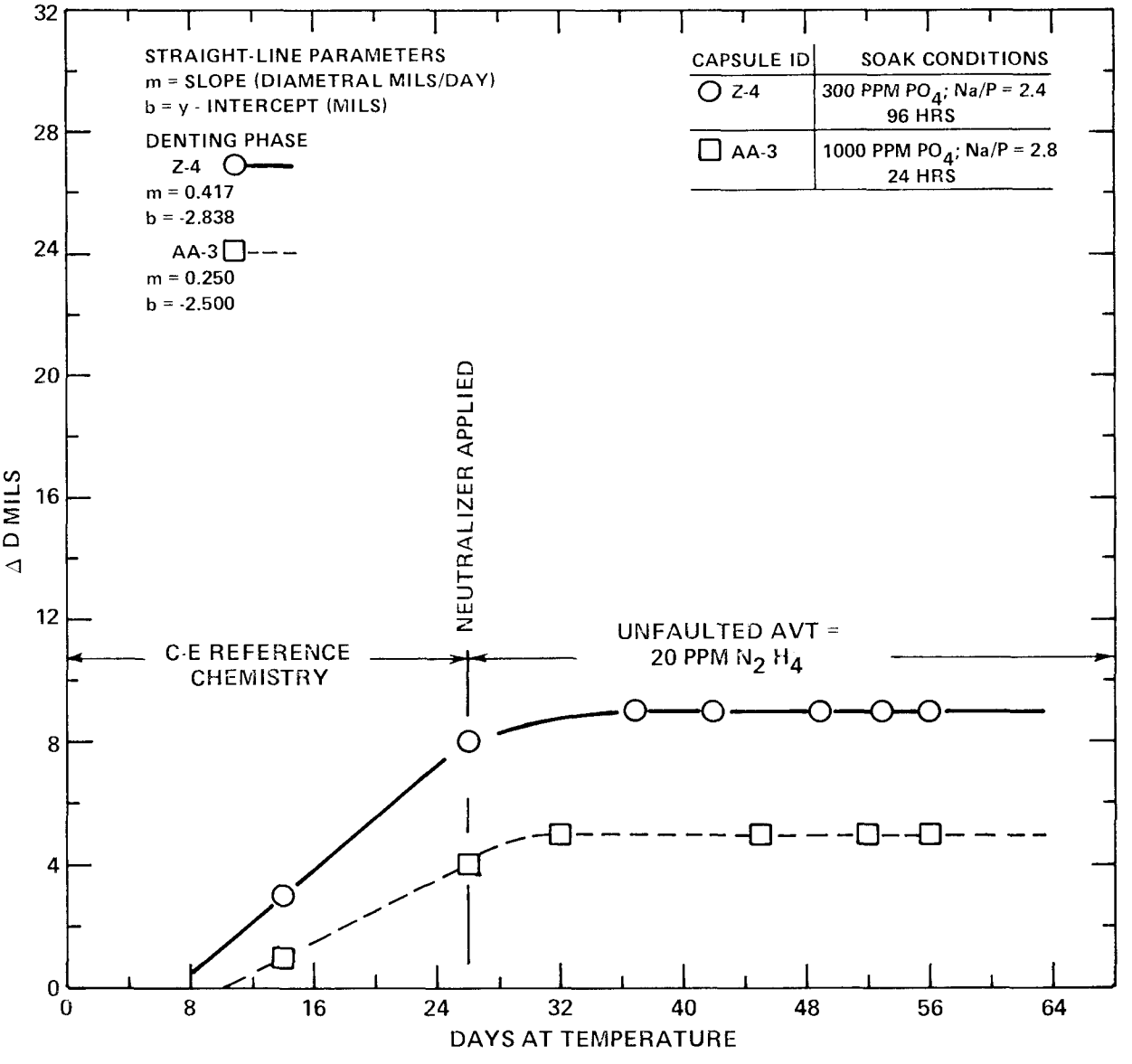

Figure 3-7

PHOSPHATE SOAK AT 150°F

ENDURANCE

CAPSULES DENTED WITH C-E REFERENCE SOLUTION

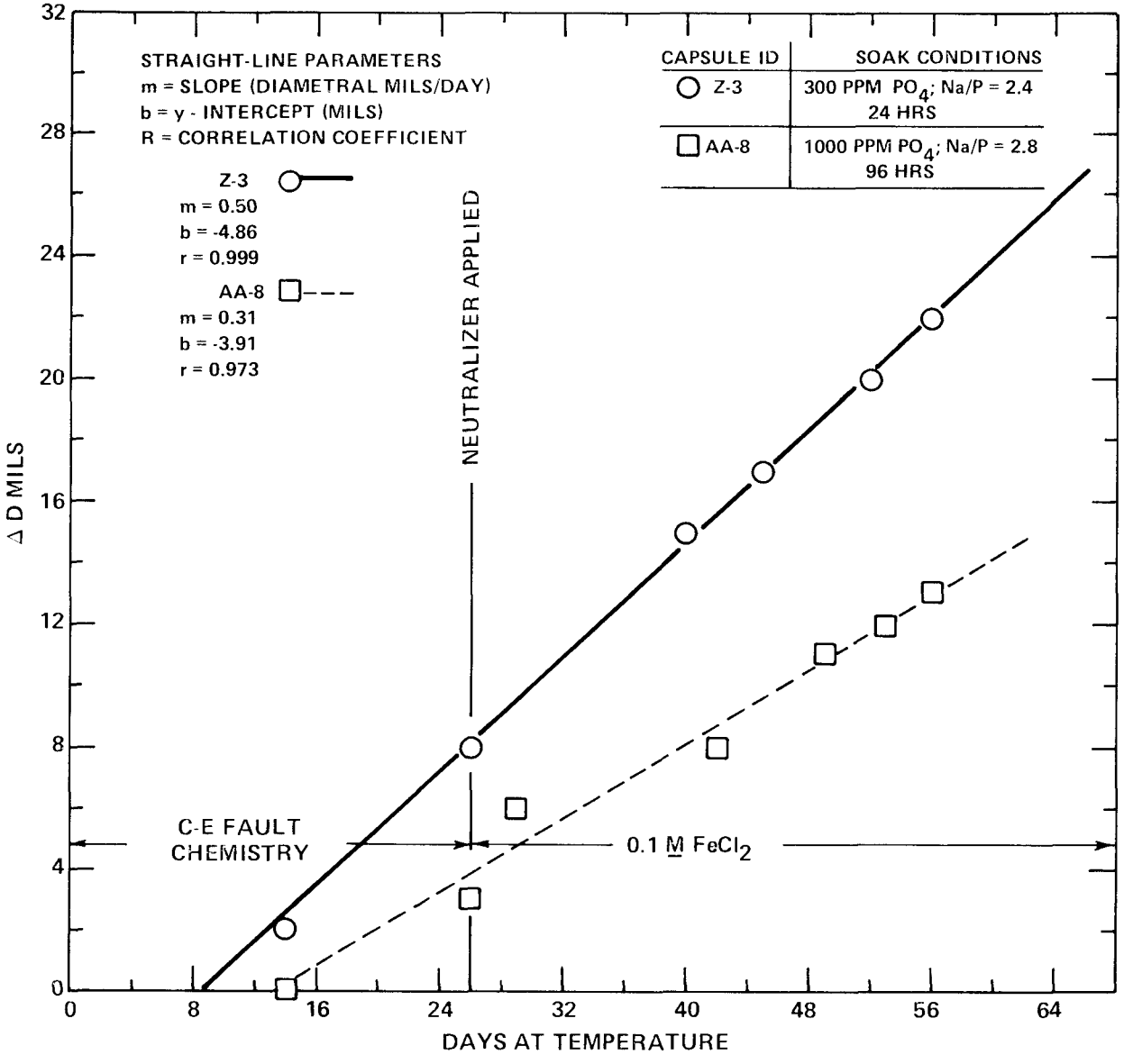

Figure 3-8
PHOSPHATE SOAK AT 565°F
EFFECTIVENESS TEST
CAPSULES DENTED WITH C-E REFERENCE SOLUTION

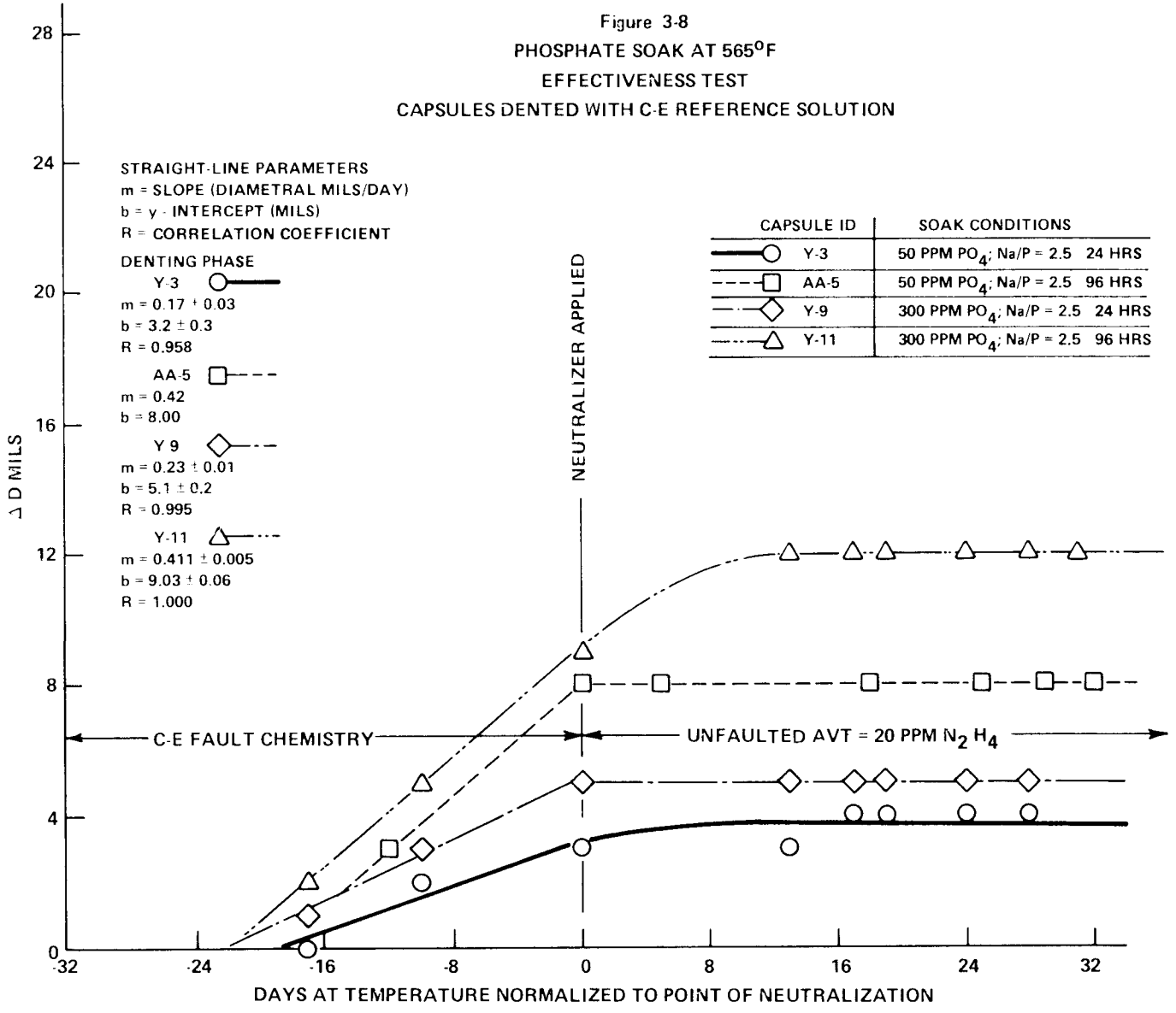

Figure 3-9
PHOSPHATE SOAK AT 565°F
ENDURANCE TEST
CAPSULES DENTED WITH C-E REFERENCE SOLUTION

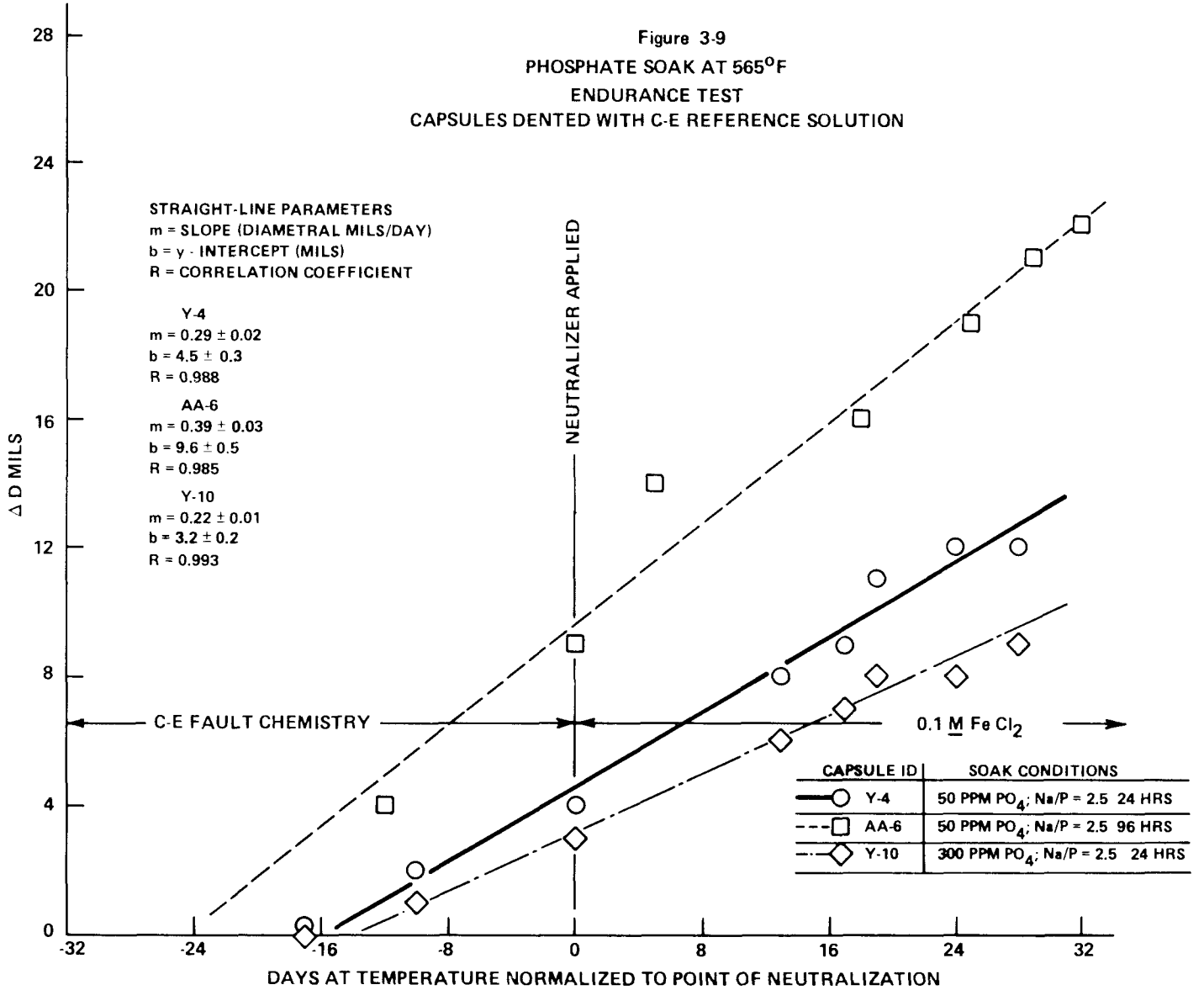

Figure 3-10

CONTROLS FOR PHOSPHATE SOAK TEST AT 150°F

CAPSULES DENTED WITH C-E REFERENCE SOLUTION

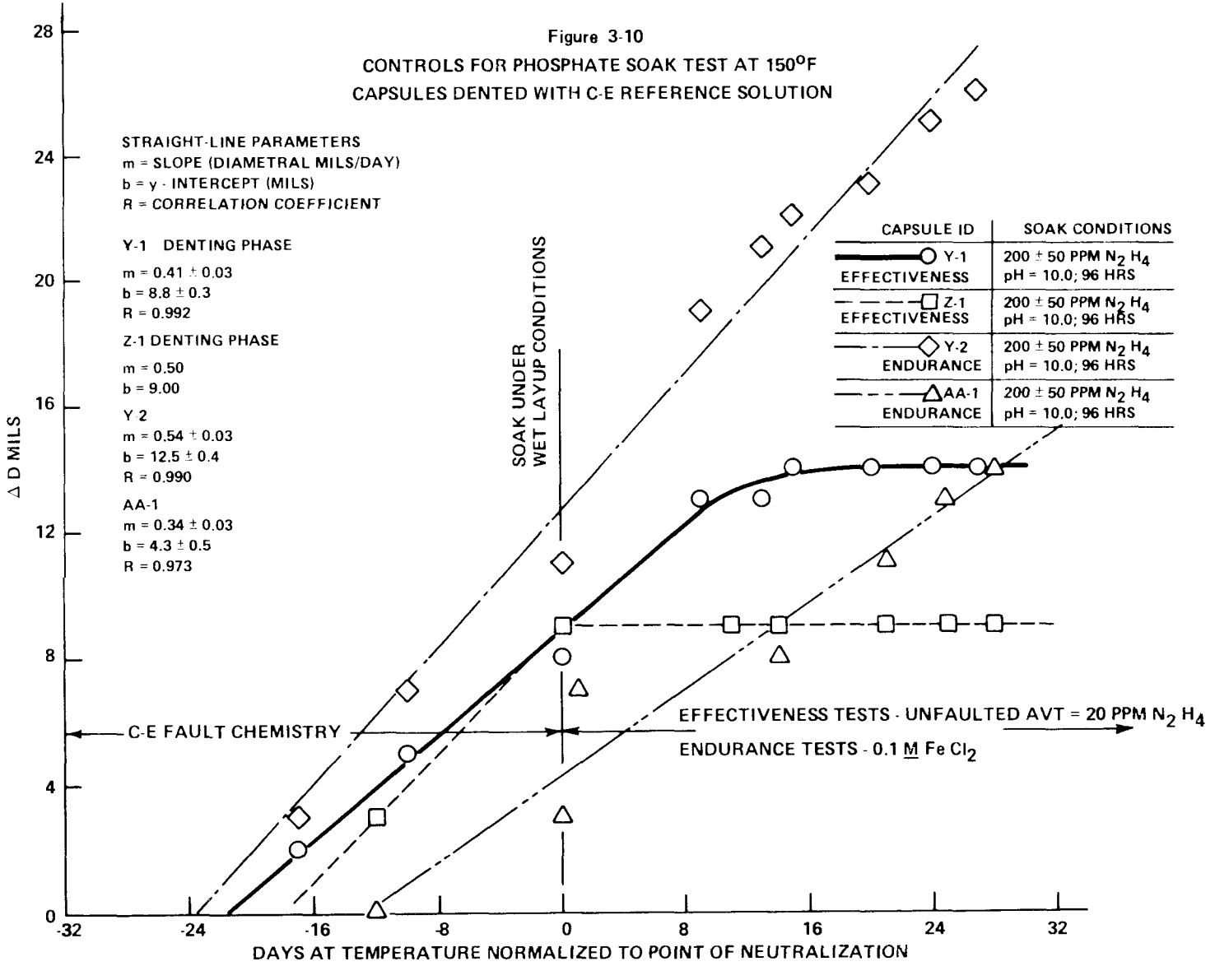

W/EPRI Reference Environment. Bulging data from W/EPRI capsules neutralized with alkaline phosphates are tabulated in Appendix Tables A-9 through A-11. Representative data are presented graphically in Figures 3-11 through 3-15. As can be seen, bulging continued during post-soak testing in all cases. Pre- and post-soak bulging rates were assessed to identify tests in which a reduction in bulging rate was observed. Results are presented in Table 3-3. In eight cases, a reduction in bulging rate was observed following soaking, while none was observed in the other eleven. There was no reasonable correlation between soak conditions and test results except for the "Effectiveness" tests at 150°F. In these tests post-soak bulging rates declined with increasing phosphate concentration in the soak solution. This observation may have been fortuitous, however, given the scatter found in both pre- and post-soak bulging rates. Less correlation was found between the percent reduction in bulging rate and phosphate concentration. The largest reduction, 49%, was found at the intermediate concentration of 5000 ppm $PO_4$. The relationship between phosphate concentration and capsule bulging rates is considered in more detail in Section 4.

Control capsule data are presented in Appendix Tables A-11 and plotted in Figure 3-15. In neither case was there a significant change in the bulging rate associated with the neutralization step.

Figure 3-11

PHOSPHATE SOAK AT 150°F
EFFECTIVENESS
CAPSULES DENTED WITH W/EPRI REFERENCE SOLUTION

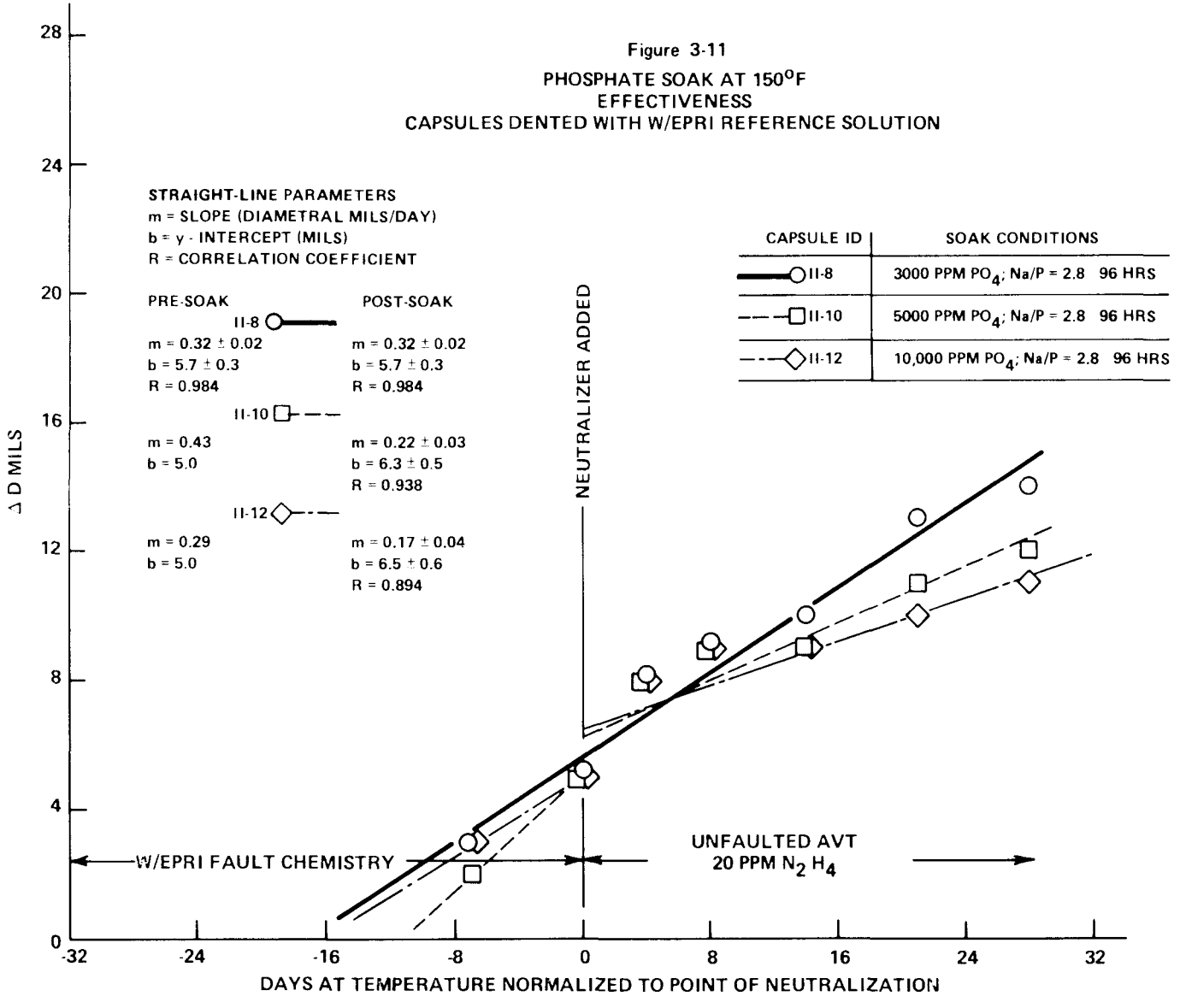

Figure 3-12
PHOSPHATE SOAK AT 150°F
ENDURANCE
CAPSULES DENTED WITH W/EPRI REFERENCE SOLUTION

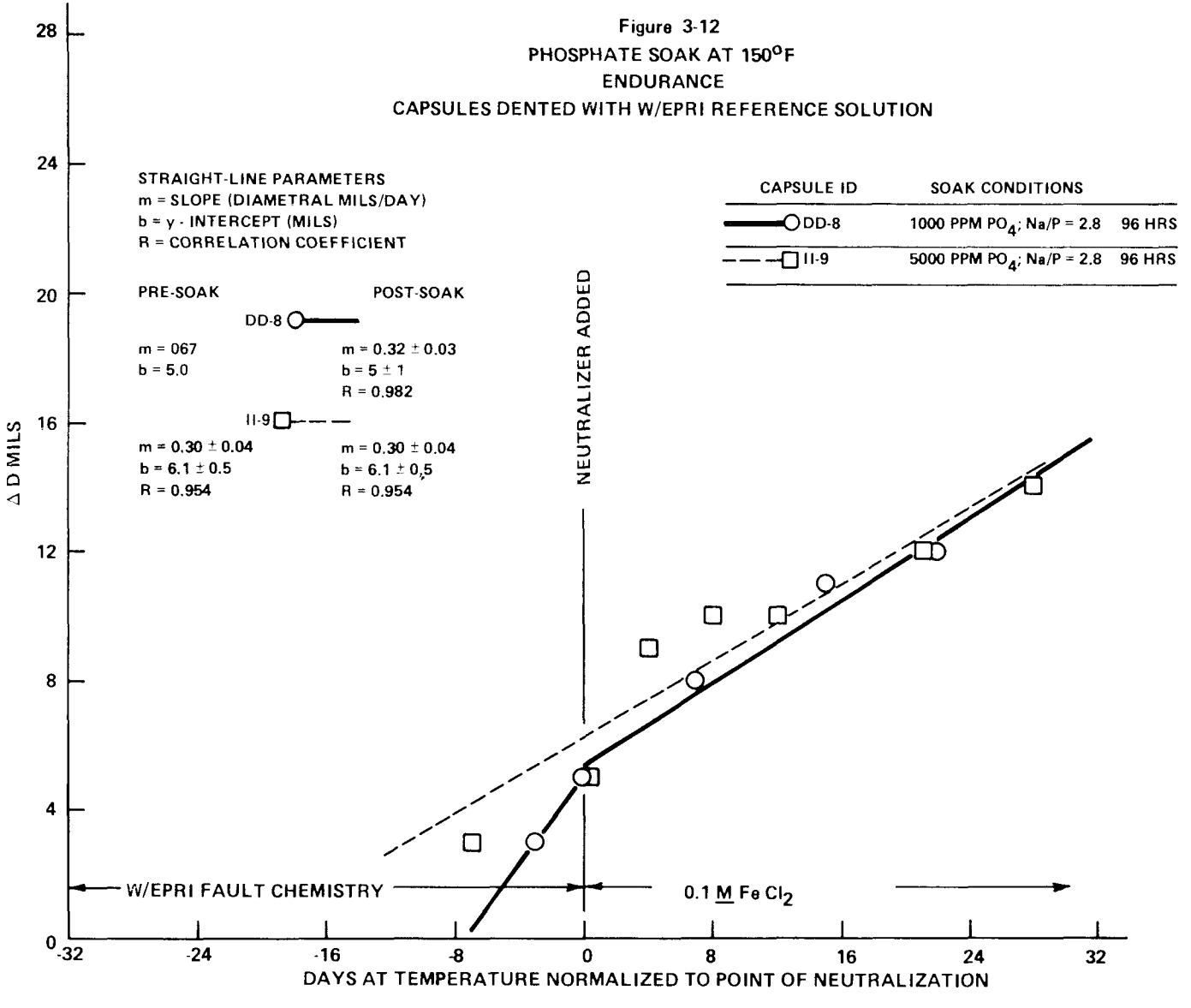

Figure 3-13
PHOSPHATE SOAK AT 565°F
EFFECTIVENESS
CAPSULES DENTED WITH W/EPRI REFERENCE SOLUTION

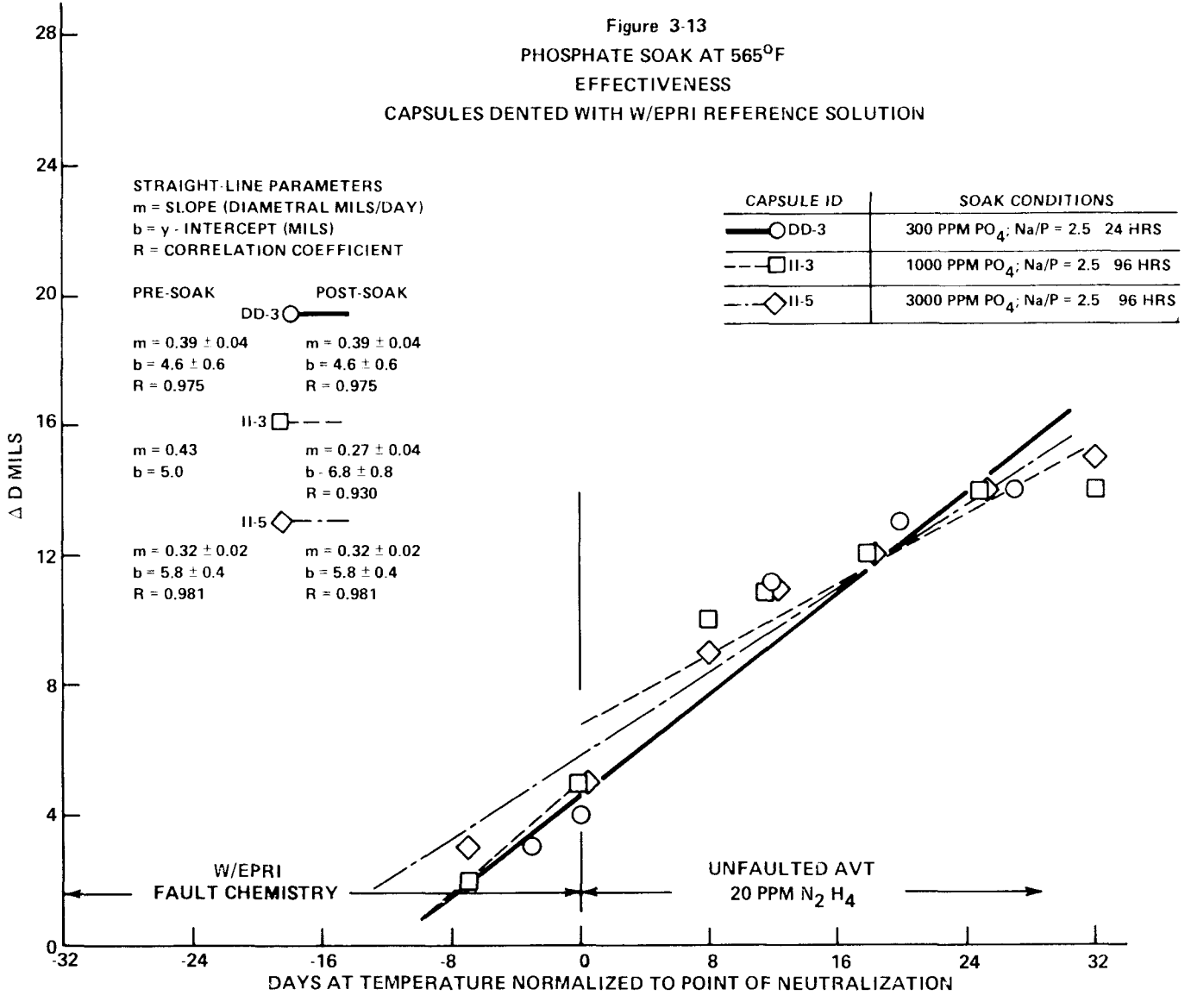

Figure 3-14
PHOSPHATE SOAK AT 565°F
ENDURANCE
CAPSULES DENTED WITH W/EPRI REFERENCE SOLUTION

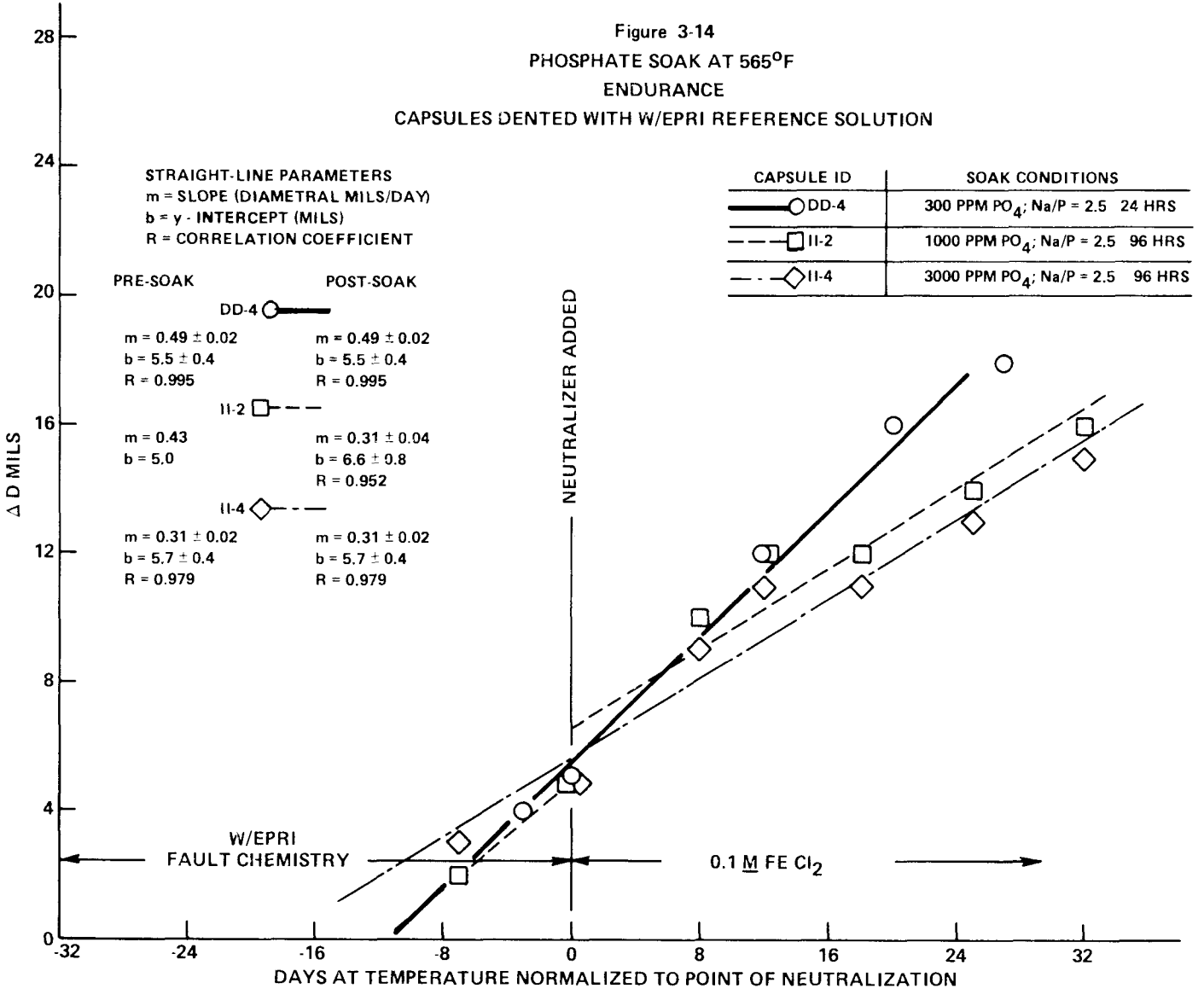

Figure 3-15
CONTROLS FOR PHOSPHATE SOAK
EFFECTIVENESS
CAPSULES DENTED WITH W/EPRI REFERENCE SOLUTION

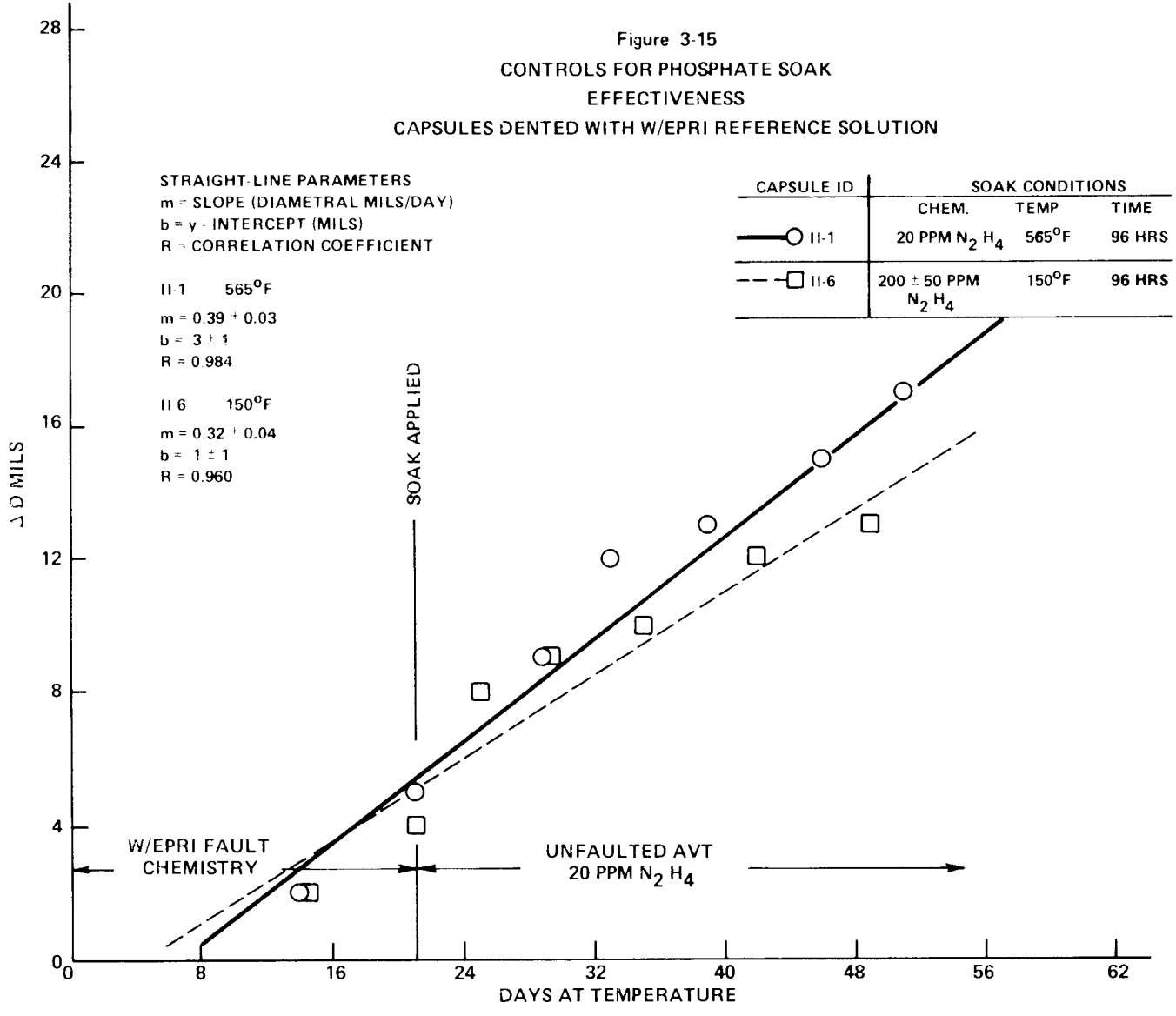

TABLE 3-3

W/EPRI CAPSULE BULGING RATE DATA

| Capsule ID | Soak Conditions |
|---|---|
| | **Capsules in Which Bulging Rate Was Reduced After Soaking** |
| | **150°F Soak For 96 Hrs., Effective Test** |
| II-10 | 5000 ppm $PO_4$, Na/P = 2.8 |
| II-12 | 10000 ppm $PO_4$, Na/P = 2.8 |
| | **150°F Soak For 96 Hrs., Endurance Test** |
| DD-8 | 1000 ppm $PO_4$, Na/P = 2.8 |
| II-7 | 3000 ppm $PO_4$, Na/P = 2.8 |
| | **565°F Soak For 96 Hrs., Effectiveness Test** |
| II-3 | 1000 ppm $PO_4$, Na/P = 2.5 |
| | **565°F Soak, Endurance Test** |
| DD-6 | 50 ppm $PO_4$, Na/P = 2.4, 24 Hrs. |
| DD-2 | 300 ppm $PO_4$, Na/P = 2.5, 96 Hrs. |
| II-2 | 1000 ppm $PO_4$, Na/P = 2.5, 96 Hrs. |
| | **Capsules in Which There Was No Reduction in Bulging Rate After Soaking** |
| | **150°F Soak For 96 Hrs., Effectiveness Test** |
| II-8 | 3000 ppm $PO_4$, Na/P = 2.8 |
| | **150°F Soak For 96 Hrs., Endurance Test** |
| II-9 | 5000 ppm $PO_4$, Na/P = 2.8 |
| II-11 | 10000 ppm $PO_4$, Na/P = 2.8 |

TABLE 3-3

W/EPRI CAPSULE BULGING RATE DATA (continued)

| Capsule ID | Soak Conditions |
|---|---|
| | 565°F Soak, Effectiveness Test |
| DD-5 | 50 ppm $PO_4$, Na/P = 2.5, 24 Hrs. |
| DD-3 | 300 ppm $PO_4$, Na/P = 2.5, 24 Hrs. |
| DD-1 | 300 ppm $PO_4$, Na/P = 2.5, 96 Hrs. |
| II-5 | 3000 ppm $PO_4$, Na/P = 2.5, 96 Hrs. |
| | 565°F Soak, Endurance Test |
| DD-4 | 300 ppm $PO_4$, Na/P = 2.5, 24 Hrs. |
| II-4 | 3000 ppm $PO_4$, Na/P = 2.5, 96 Hrs. |
| | 150°F Control Soak For 96 Hrs., Effectiveness Test |
| II-6 | Hydrazine Treated Water 200 $\pm$ 50 ppm |
| | 565°F Control Soak For 96 Hrs., Effectiveness Test |
| II-1 | Hydrazine Treated Water 200 ppm |

Phosphate Neutralization of 0.25 M $FeCl_2$ Fault Chemistry. The diametral increases as a function of time are presented in Appendix Tables A-12 and A-13. Representative data are plotted in Figures 3-16 and 3-17. Except for the controls, all phosphate neutralizations were performed in duplicate. All tests with this denting environment were "Effectiveness" tests, and all capsules continued to bulge. Of the twelve capsules tested, five showed a reduction in bulging rate associated with soaking and seven did not. These tests are identified in Table 3-4. There was no reasonable correlation found between the change in bulging rate and the concentration of phosphate used in the soak.

Figure 3-16
PHOSPHATE SOAK AT 150°F
EFFECTIVENESS
CAPSULES BULGED WITH 0.25 M Fe $Cl_2$

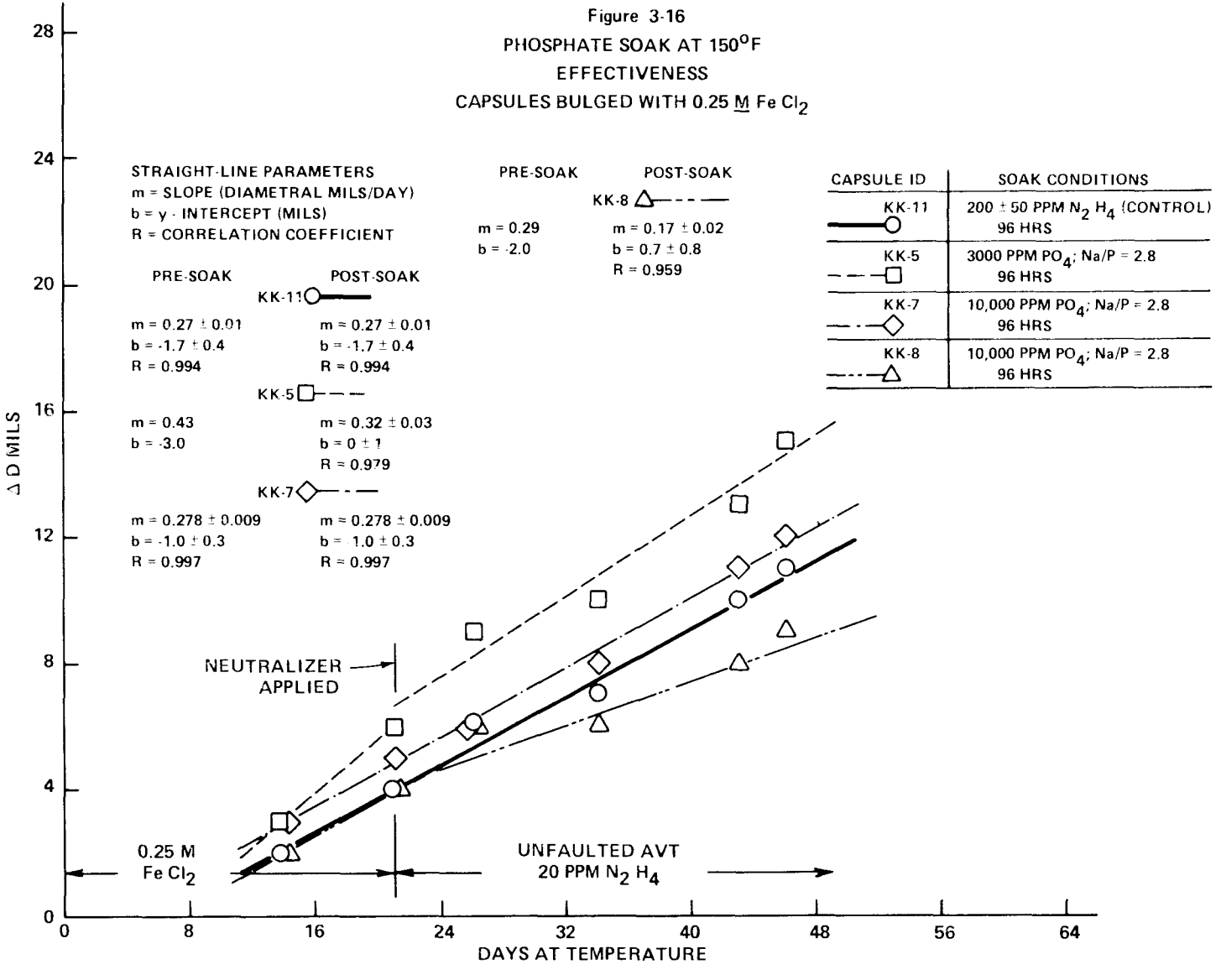

Figure 3-17
PHOSPHATE SOAK AT 565°F
EFFECTIVENESS
CAPSULES BULGED WITH 0.25 M $FeCl_2$

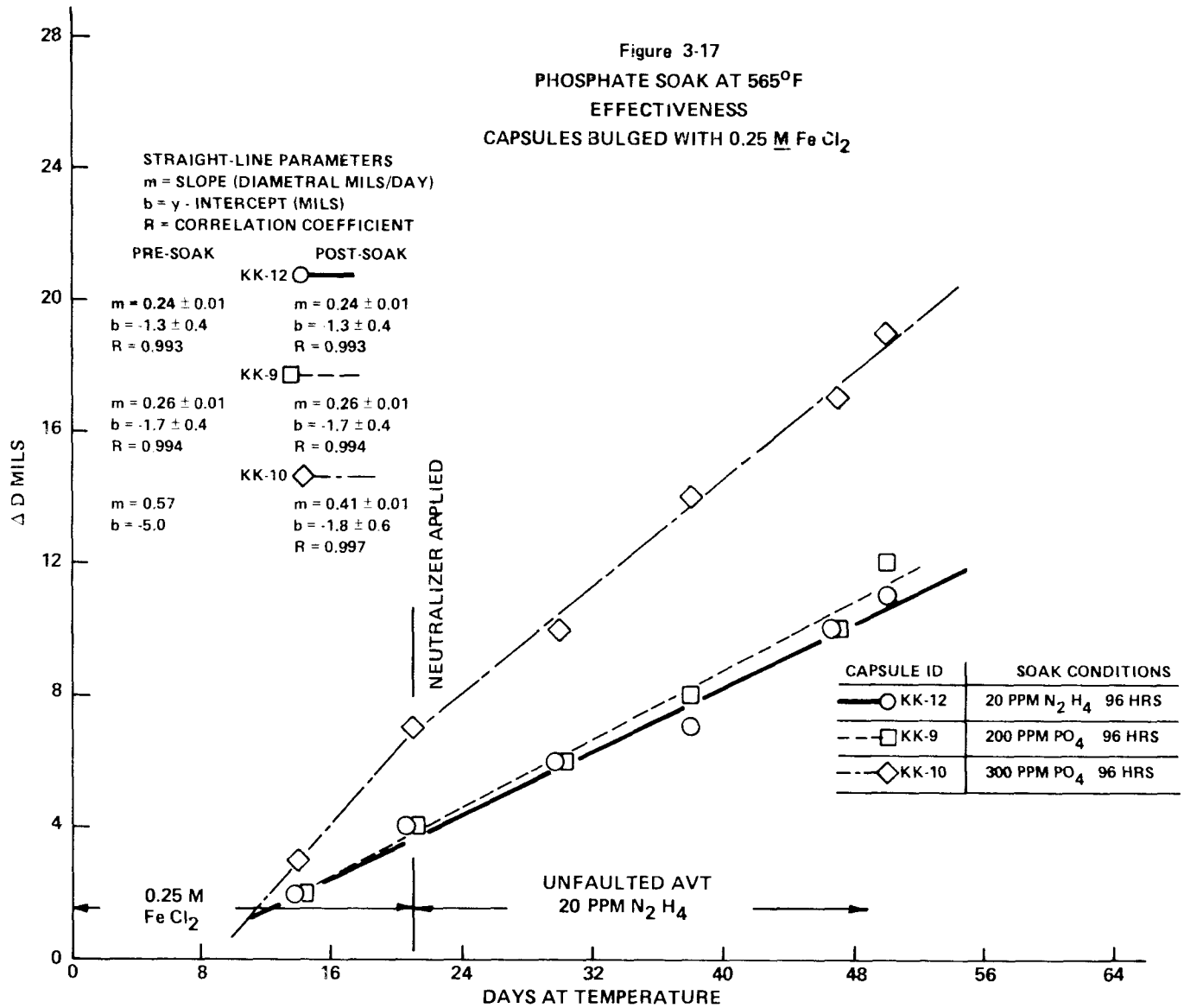

TABLE 3-4

0.25 M $FeCl_2$ CAPSULE BULGING RATE DATA

| Capsule ID | Soak Conditions |
|---|---|
| | **Capsules in Which Bulging Rate Was Reduced After Soaking** |
| | **150°F Soak For 96 Hrs., Effectiveness Test** |
| KK-1 | 300 ppm $PO_4$, Na/P = 2.8 |
| KK-5 | 3000 ppm $PO_4$, Na/P = 2.8 |
| KK-6 | 3000 ppm $PO_4$, Na/P = 2.8 |
| KK-8 | 10000 ppm $PO_4$, Na/P = 2.8 |
| | **565°F Soak For 96 Hrs., Effectiveness Test** |
| KK-10 | 300 ppm $PO_4$, Na/P = 2.5 |
| | **Capsules In Which There Was No Reduction In Bulging Rate After Soaking** |
| | **150°F Soak For 96 HRS., Effectiveness Tests** |
| KK-2 | 300 ppm $PO_4$, Na/P = 2.8 |
| KK-3 | 1000 ppm $PO_4$, Na/P = 2.8 |
| KK-4 | 1000 ppm $PO_4$, Na/P = 2.8 |
| KK-7 | 10000 ppm $PO_4$, Na/P = 2.8 |
| | **565°F Soak For 96 Hrs., Effectiveness Test** |
| KK-9 | 300 ppm $PO_4$, Na/P = 2.5 |
| | **150°F Control Soak For 96 Hrs., Effectiveness Test** |
| KK-11 | Hydrazine treated water 200 ± 50 ppm |
| | **565°F Control Soak For 96 Hrs., Effectiveness Test** |
| KK-12 | Hydrazine treated water 20 ppm |

Chemistry Data

All solutions added to and emptied from W/EPRI capsules were analyzed for chloride and, where appropriate, for phosphate. The objective was to better understand the relationship between the chemical environment and capsule bulging. This subsection contains the results of these analyses. The following observations were made: (1) pre-soak rinses and wet layups generally removed as much or more chloride than the soak procedure, and (2) a larger quantity of chloride is released from capsules soaked at 565°F than at 150°F.

Water Soaks. All chloride-containing solutions which were added to W/EPRI capsules, were analyzed for chloride as were all solutions removed from the capsules. These data were utilized in an attempt to perform a chloride mass balance calculation. Results (presented in Appendix Tables A-15) were poor. In many cases, a large negative value for residual chloride was calculated. These negative values are indicative of the magnitude of error associated with this procedure, since there is no physical meaning for a negative chloride residual. The techniques and analytical procedures utilized were inadequate for mass balance calculations. The data, however, reliably indicate that pre-soak rinses remove as much or more chloride as the soak, and that soaks at 565°F (capsules BB-3, BB-4, BB-7, and BB-8) are more effective in leaching chloride than soaks at 150°F.

Phosphate Soaks. During the various phases of denting, neutralization, and post-neutralization steps with W/EPRI capsules, samples were taken from the capsule solution and analyzed for chlorides, and phosphates (where appropriate). The results of the analyses were tabulated in an attempt to follow the release of chloride and the adsorption of phosphate. Unforturnately the analytical data are incomplete in some instances. For this reason, no attempt was made to

perform a mass balance calculation. Absolute amounts of chloride and phosphate, in milligrams are tabulated in Appendix Tables A-16 through A-19.

In general a substantial amount of chloride was released in the pre-neutralization wet layup. For series DD considerably more chloride was released in the wet layup step than in the neutralization phase. The data also indicate a significant temperature effect.

The average amount of chloride leached from capsules soaked at 565$^{o}$F was 110 mg while the average at 150$^{o}$F was 70 mg. There are individual capsules which are exceptions, but the averages indicate that approximately 60% more chloride is leached from capsules at 565$^{o}$F than from capsules at 150$^{o}$F.

## Capsule Destructive Examinations

Selected capsules were destructively examined to observe crevice-magnetite morphology as well as the distribution of various chemical species. Chloride, when found, was limited to the layer adjacent to the carbon steel. Observations via optical microscopy, SEM, and EMPA are presented below.

Optical Microscopy. Photomicrographs taken at 4X of transverse cross sections of capsules bulged with C-E and W/EPRI reference denting solutions are presented as Figures 3-18 and 3-19. The complete collection of photomicrographs is in Appendix B. Nonprotective magnetite was found on both the ID (inside diameter) of the carbon steel slug and in the annulus between the slug and the Inconel tubing. As can be seen most noticeably in Figure 3-19, the slug was not always centered in the tubing. Whereas corrosion in the 0.1 M $FeCl_2$ appeared to be very uniform, corrosion in the W/EPRI reference environment was irregular, especially on the ID surface.

The structure of the oxide in both the annulus and the ID of the slug was examined in detail at 75X. Photomicrographs are presented in Figures 3-20 through 3-23. Oxides formed from the two denting environments were similar, although the oxides from the W/EPRI environment were generally coarser and showed less fine detail than oxides grown in 0.1 M $FeCl_2$.

The following features were present in varying degrees in all specimens. The background was a medium to dark grey oxide which had a rippled, layered appearance. Layers were closely-spaced (1-2 mil) and ran circumferentially (parallel to the steel interface). Superimposed on this layered structure were boundaries between areas of differing morphology. These boundaries also ran circumferentially, and their number as well

as their prominence correlated well with the previous history of the given capsule. Specifically the radial distance as measured from the photomicrographs between these boundaries and the carbon steel/oxide interface frequently equaled two times the increase in capsule radius at various stages of testing. The factor of two is the approximate ratio of the density of metallic iron to the density of magnetite. As a consequence, the corrosion of 1 mil of carbon steel should cause the carbon steel/oxide interface to retreat by 1 mil but produce an oxide layer 2 mils thick and a resultant increase in the radius of the capsule of 1 mil. Hence, the two-to-one relationship between these layers of magnetite and the radial increase in capsules is a reasonable correlation. The boundaries apparently form when corrosion is halted then restarted, as when a capsule is taken from the furnace for venting or soaking. This is most clearly illustrated in the lower portion of Figure 3-21 for capsule AA-8. The first ridge-like line to the right of the carbon steel surface is thought to have originated with the post-soak venting of hydrogen. The next ridge in like manner can be correlated with the four-day soak at 150$^{o}$F in 1000 ppm $PO_4$.

Scattered throughout this background were discrete areas of lighter oxide which were much more prominent in the annulus oxide of capsules DD-7 and DD-8. In some samples these light areas formed a pattern of radial rays. As shown more clearly in the SEM results which follow, these appeared to be regions of coarse-grained magnetite which had precipitated into former void areas of the original non-protective magnetite. The oxide/steel interface was irregular, with the dimensions of the irregularities (0.5 to 2 mil) reflected in the rippling of the lamellar structure. There was seldom a break at the oxide/steel interface. Cracks were sometimes observed in the annular oxide, but these may have been generated during sectioning and mounting.

The ID oxide, which grew inward without restraint, generally had a more uniform appearance than the annulus oxide. Porosity, as indicated by the size and number of black areas in the photomicrographs, was present throughout the ID oxide in most samples and appeared to increase with distance from the steel interface.

The annulus oxide was characterized by several distinct circumferential bands. The outermost band from the Inconel interface to the point where the discrete light regions disappear was very similar in appearance to the ID oxide. Some very large pores were observed at the Inconel interface; otherwise little porosity was apparent.

The central band consisted of the rippled, layered oxide described above, but without the discrete regions of lighter oxide. Circumferential breaks in the layered pattern were observed as in the ID oxide.

The innermost oxide, a band ranging from 75 to 250 μm (3 to 10 mil) next to the carbon steel interface, was typically a lighter grey than the central band. Its appearance ranged from featureless to mottled. Some oxide cracking was observed, although the interface with the carbon steel was usually continuous. This band was not found in capsule AA-7 which had not grown following the soak (see Figure 3-20).

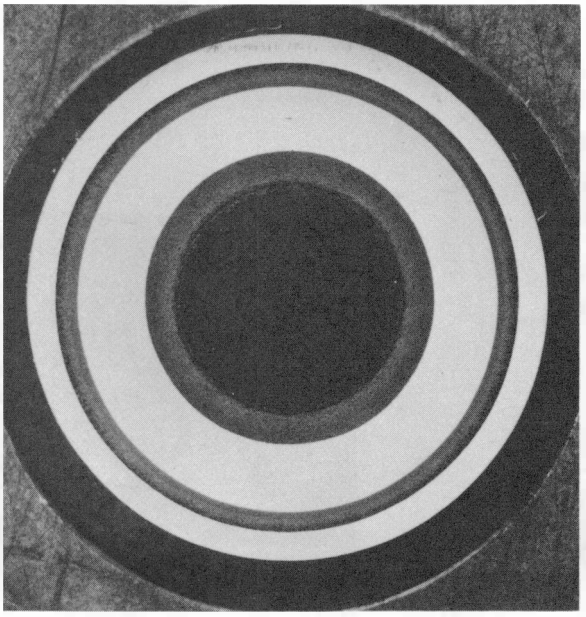

Figure 3-18. Capsule AA-7
Transverse Section (4X)*
C-E Reference Solution (0.1 M $Fe Cl_2$)
150°F/96 hr./1000 ppm $PO_4$/2.8
Volatile

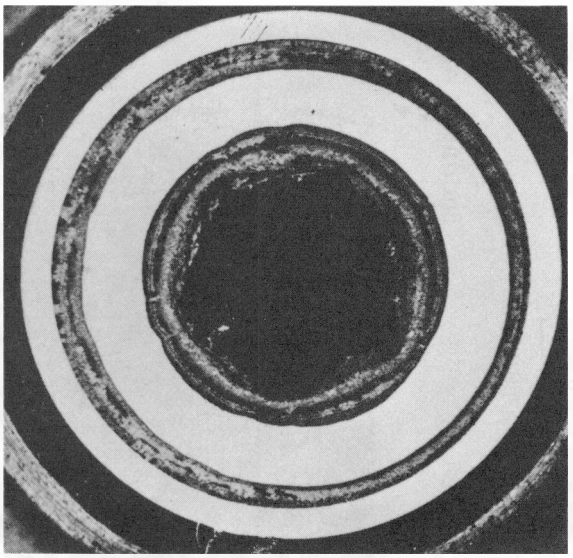

Figure 3-19. Capsule DD-8
Transverse Section (4X)*
W/EPRI Reference Solution (Seawater + 0.1 M $CuCl_2$ + 0.1 M $NiCl_2$)
150°F/96 hr./1000 ppm $PO_4$/2.8
Fault

*Please note that the illustrations on this page have been reduced 10% in printing.

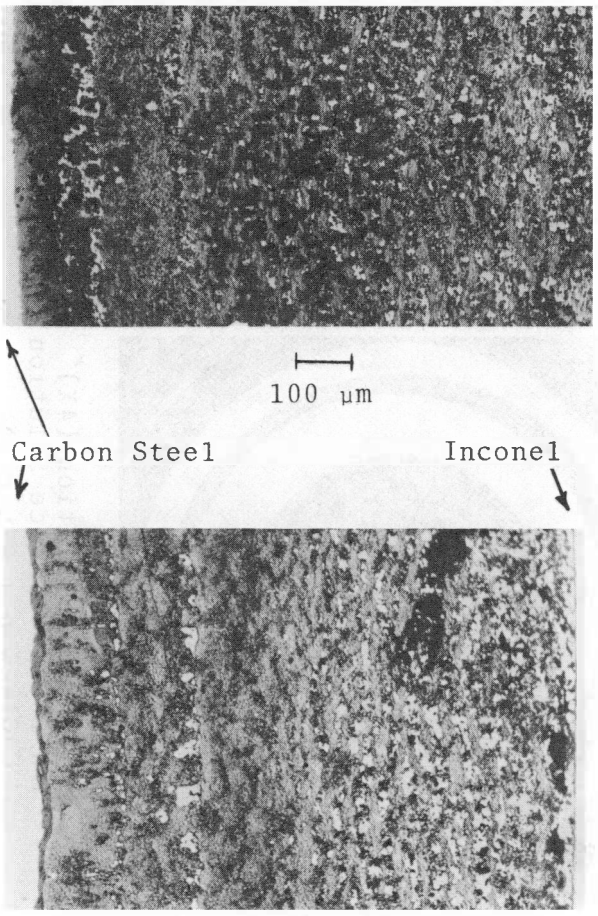


Figure 3-21. Capsule AA-8
Transverse Section at
Middle of Bulge (75X)*

Top: Oxide on ID of Slug
Bottom: Oxide in Annulus

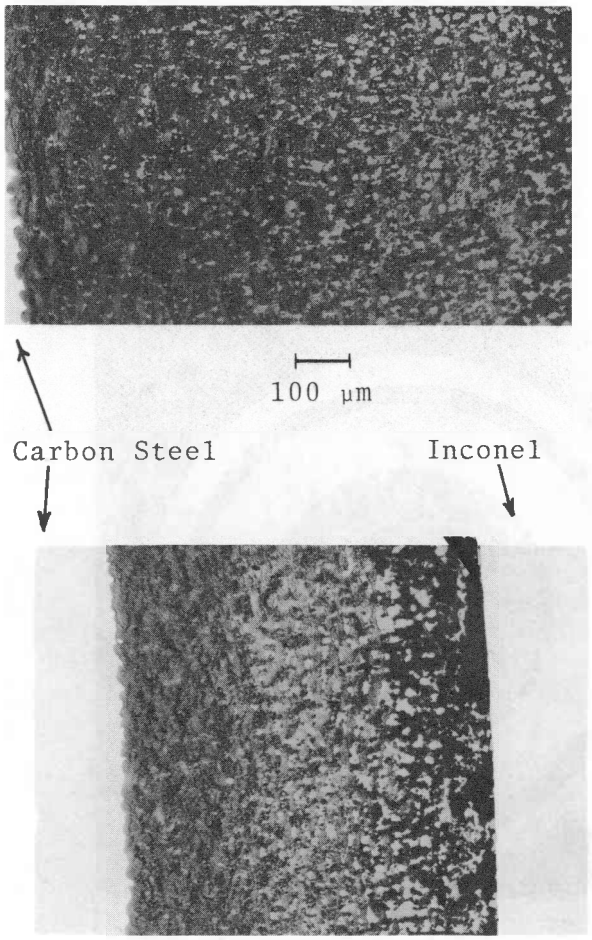


Figure 3-20. Capsule AA-7
Transverse Section at
Middle of Bulge (75X)*

Top: Oxide on ID of Slug
Bottom: Oxide in Annulus

*Please note that the illustrations on this page have been reduced 10% in printing.

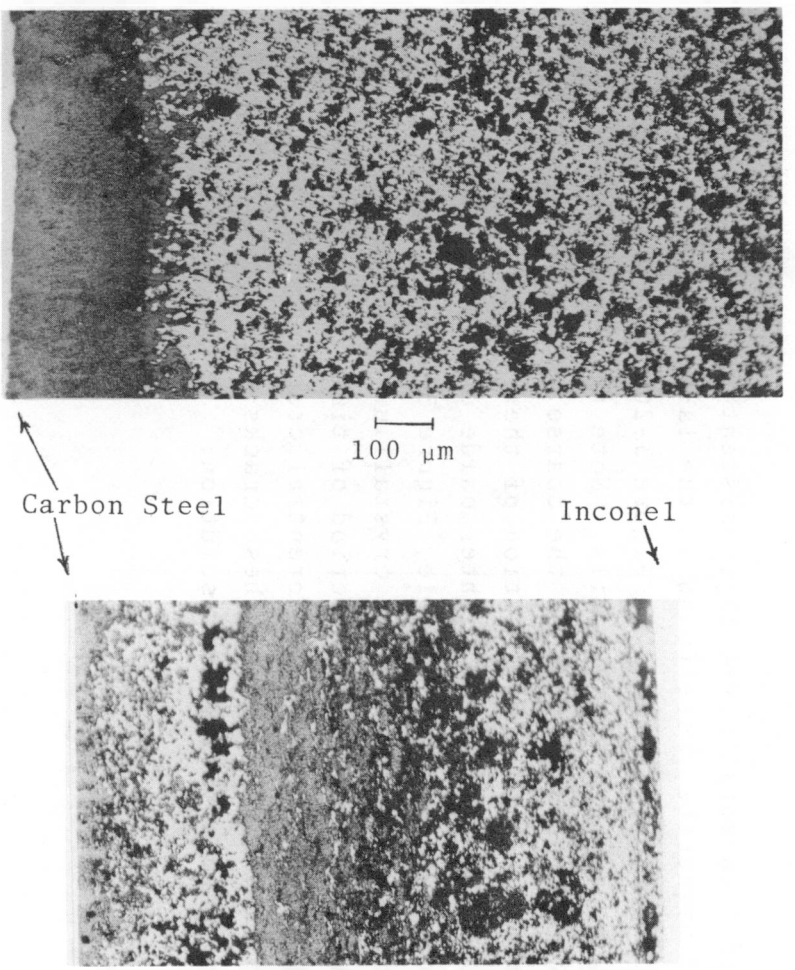


Figure 3-22. Capsule DD-7
Transverse Section Through
Middle of Bulge (75X)*

Top: Oxide on ID of Slug
Bottom: Oxide in Annulus

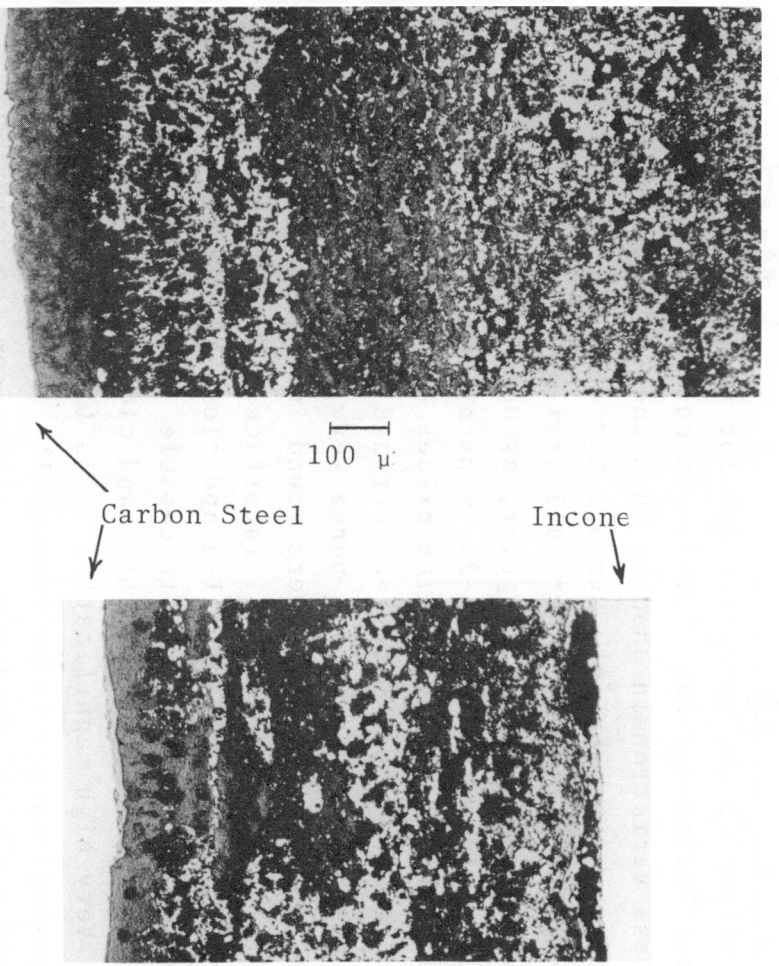


Figure 3-23. Capsule DD-8
Transverse Section Through
Middle of Bulge (75X)*

Top: Oxide on ID of Slug
Bottom: Oxide in Annulus

*Please note that the illustrations on this page have been reduced 10% ir

Scanning Electron Microscopy (SEM). Figures 3-24 and 3-25 provide overviews of the annulus oxide for the samples examined by Mechanical Technology Inc. (MTI). In general, the SEM's exhibited less variation in shading than the light micrographs, but provided more insight into surface textures and porosity. Oxides grown from 0.1 M $FeCl_2$ were all similar. Although the interface was almost always irregular, as best illustrated in higher magnification in Figure 3-24, separation between steel and oxide was seldom observed. The oxides had a smooth appearance from the steel interface outward to about 2/3 of the thickness, beyond which pits and pores were found. Most of the porosity and the largest pores were found in a band of about 250 $\mu$m (10 mil) along the Inconel interface. Cracks were sometimes observed running paralled and close to the steel interface as well as radially. In capsule AA-8, ridge-like lines were observed running parallel and close to the steel interface. Very high magnification SEM's (3000X) revealed a very fine-grained structure of essentially no porosity at the steel interface. With increasing distance from the interface, increasing porosity and regions of coarse, blocky structure were observed.

Well-defined octahedral crystals consistent with the crystal symmetry of magnetite, were found in the large interstices near the Inconel surface, as shown in Figure 3-26. Edges of the octahedra were as large as 0.5 mils. Note that sections through these octahedra produced the coarse, blocky structures described above. Also, the location of these octahedra correspond to the regions of lighter oxide observed in the light micrographs (see for example, Figure 3-20). The octahedra have the appearance of crystalline material which has formed slowly over an extended period of time. It appears that significant porosity and circumferential cracking existed at one time in the oxide and that these cracks were later filled by magnetite precipitating from solution.

The oxide grown in the W/EPRI reference environment (Figure 3-25) was more irregular and coarse than those above. The oxide appeared to consist of three zones of different widths. The innermost zone was about 150 μm (6 mil) thick and was bounded by a ridge-like line similar to that observed in capsule AA-8 parallel to the steel interface. This oxide was smoother in appearance than the other layers, and exhibited a very fine-grained texture with no apparent porosity under higher magnification. The central zone was about 280 μm (11 mil) thick and was bounded by another ridge-like line. This zone contained numerous pits or pores. The outermost zone, about 230 μm (9 mil) exhibited a rough texture with most of the pores concentrated in a band at the Inconel interface.

Coarse, blocky structures characteristic of large $Fe_3O_4$ octrahedra were observed throughout the central and outer zones. Judging from the light micrographs, these also formed the ridge-like lines noted above.

Capsules AA-7 and DD-7 were examined at intervals along longitudinal sections from the center to one end of the slug. No differences were observed in the structure of the oxide in these regions relative to that observed in the transverse section.

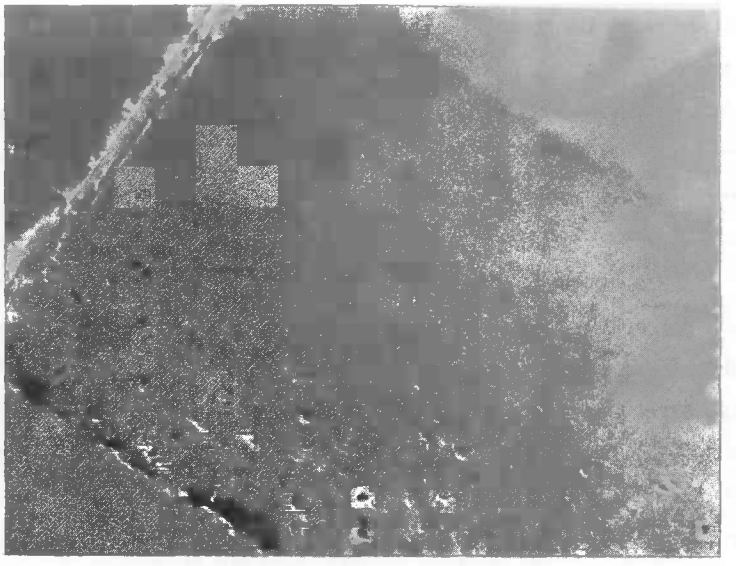


A. 100X*

SEM of the Oxide Layer in the Annulus of Capsule AA-7, C-E Dent Environment, Neutralized with 1000 ppm $PO_4$ for 96 Hrs. at 150°F Followed with Exposure to AVT (Inconel/Oxide/Steel)

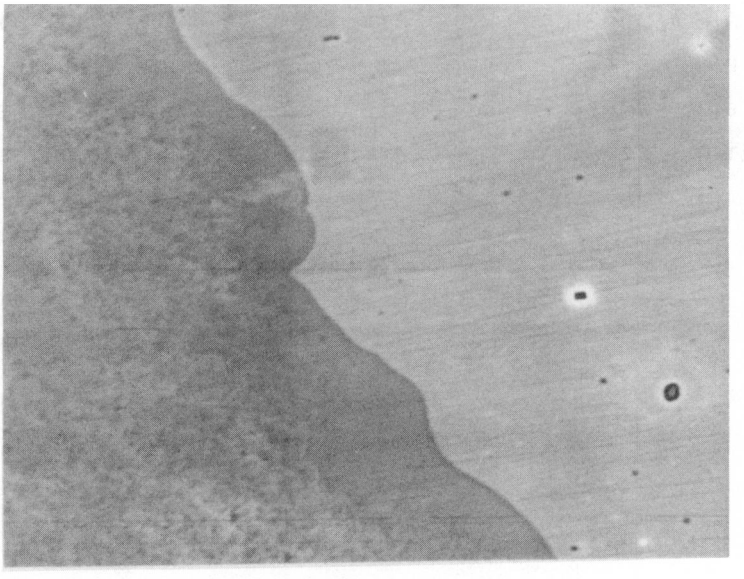


B. 1000X*

Figure 3-24. SEM of the Steel/Oxide Interface - Capsule AA-7, C-E Dent Environment, Neutralized with 1000 ppm $PO_4$ for 96 Hrs. at 150°F Followed with Exposure to AVT

*Please note that the illustrations on this page have been reduced 10% in printing.

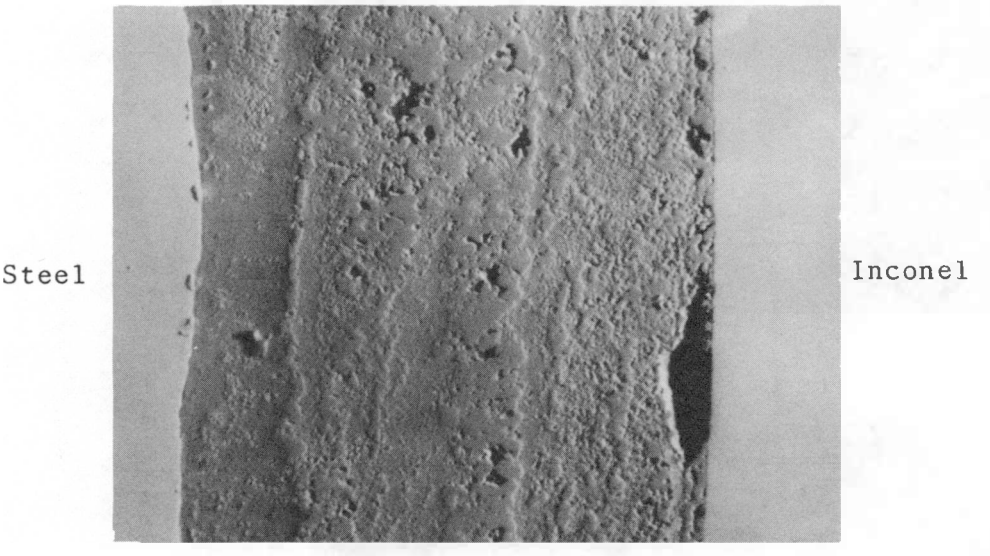


Figure 3-25. SEM of the Oxide Layer in the Annulus of Capsule DD-8, W/EPRI Dent Environment, Neutralized with 1000 ppm $PO_4$ for 96 Hrs. at 150°F Followed with Exposure to 0.1 M $FeCl_2$ (Steel/Oxide/Inconel)

*Please note that the illustrations on this page have been reduced 10% in printing.

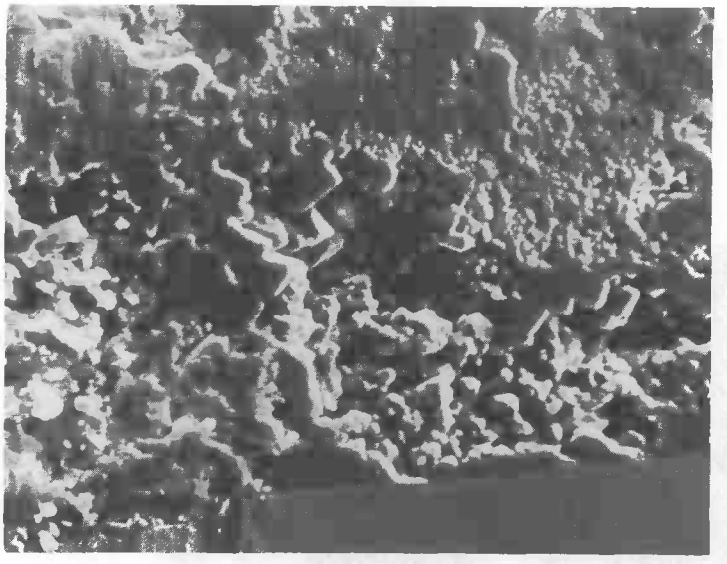


A.

600X*

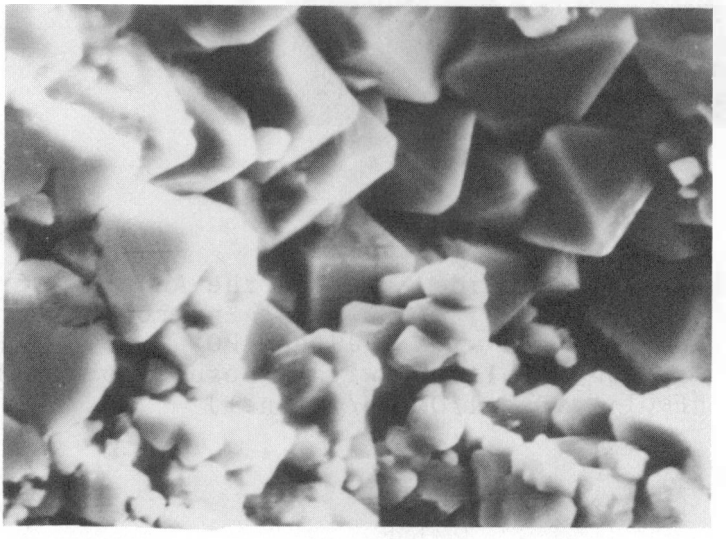

B.

2000X*

Figure 3-26. SEM's of the Octahedral Crystals - Capsule Y-1, C-E Dent Environment, Soaked with Wet Layup Water for 96 Hrs. at 150°F as a Control, Followed with Exposure to AVT

*Please note that the illustrations on this page have been reduced 10% in printing.

Electron Microprobe Analysis (EMPA). EMPA analyses showed that the major constituents of the oxide were iron and oxygen, with the oxide generally slightly richer in iron toward the steel interface. Nickel, chromium, and copper (when analyzed) were just barely detected above background and uniformly distributed. Phosphorus was not found in any of the specimens (Y-1 was not analyzed for P). The lower limit of detection for phosphorus was about 1 (w/o) percent. Significant chlorine was found in 5 samples, confined to a narrow region next to the steel interface. Some chlorine was also detected sporadically in the oxide near the Inconel interface. Table B-9 summarizes the EMPA results for the oxide close to the carbon steel interface.

Figure 3-27 is a higher magnification SEM of the chlorine-rich region in specimen DD-8 on which is superimposed an X-ray line trace for chlorine along the path marked by the white horizontal line. The ridge-like line which marks the boundary of the chlorine-rich region is about 150 μm (6 mil) from the steel interface. The large peak corresponds to a point concentration of approximately 38 (w/o) percent chlorine. Figures 3-28 and 3-29 are similar illustrations for specimens Y-10 and AA-8, with peak concentations of approximately 21 (w/o) percent and approximately 0.4 (w/o) percent respectively.

Capsule DD-7 was further examined at five areas about 1/8" apart along a longitudinal section from the center to the end of the slug. Chlorine was again found only within the 150 μm (6 mil) band of oxide at the steel interface. Figure 3-30 shows the SEM's and chlorine line traces for these five areas. Concentrations varied locally from 1 to 15 (w/o) percent within the band and appeared to be dependent upon the physical appearance of the oxide along the beam path. Areas of high chlorine appeared to be slightly raised and were smooth with scattered pocks while neighboring areas of low chlorine had appearance previously described for this region.

Total chlorine in each area, as estimated by the area under the line traces, was quite variable. However, the last two micrographs show decreasing chlorine content as the end of the slug is approached.

Capsule AA-7 was also examined at selected locations along a longitudinal section. The oxide chemical composition was identical to that found in the transverse section and essentially constant in the longitudinal direction. No significant chlorine was found in any area.

A most interesting feature of the chlorine-rich zone of capsule DD-8 were "starfish-like" growths on the oxide surface which slowly evaporated or decomposed under the electron beam. These are shown in Figure 3-31. Figure 3-32 presents an SEM and a chlorine map of an area containing these growths which shows them to be rich in chlorine. At present the significance of these observations is not known.

They could possibly be a hydrated ferrous chloride such as $FeCl_2$ 4 $H_2O$. This would explain why these structures appeared to decompose under the electron beam inasmuch as all hydrates tend to lose water when heated. In addition, this hydrate has a crystalline symmetry which is consistent with the observed structures. In the absence of additional information, however, this is only conjecture, not identification.

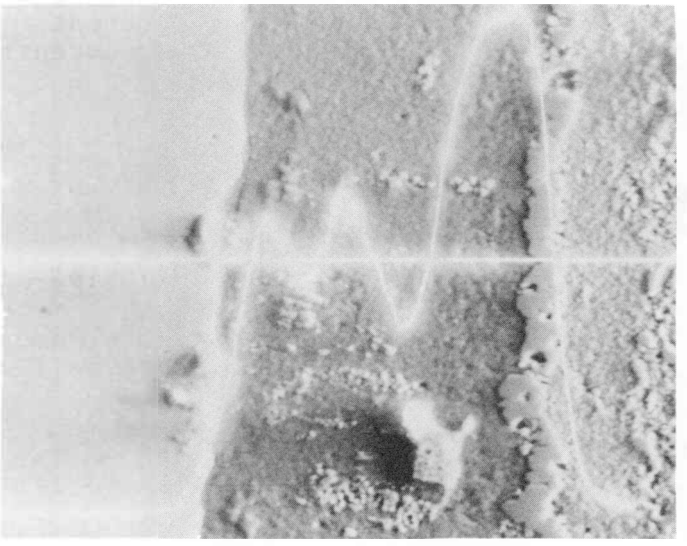


Figure 3-27. SEM of the Steel/Oxide Interface, with a Superimposed X-Ray Line Trace for Chlorine - Capsule DD-8, W/EPRI Dent Environment, Neutralized with 1000 ppm $PO_4$ for 96 Hrs. at 150°F Followed with Exposure to 0.1 M $FeCl_2$

*Please note that the illustrations on this page have been reduced 10% in printing.

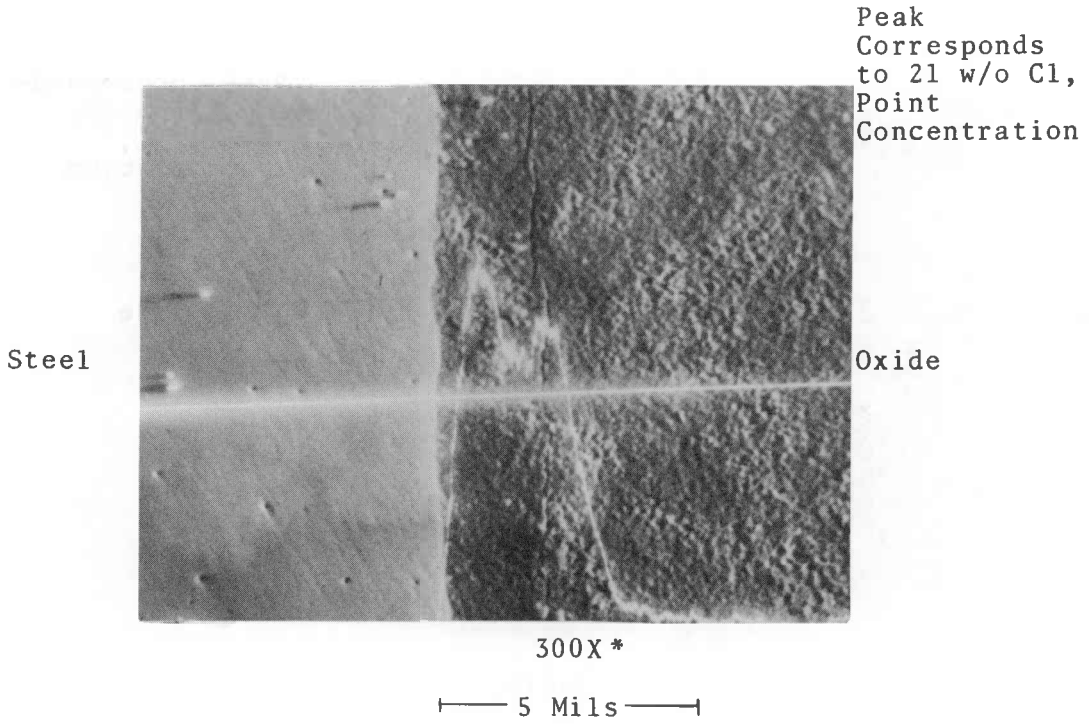


Figure 3-28. SEM of the Steel/Oxide Interface, with a Superimposed X-Ray Line Trace for Chlorine - Capsule Y-10, C-E Dent Environment, Neutralized with 300 ppm $PO_4$ for 24 Hrs. at 565°F Followed with Exposure to 0.1 M $FeCl_2$

*Please note that the illustrations on this page have been reduced 10% in printing.

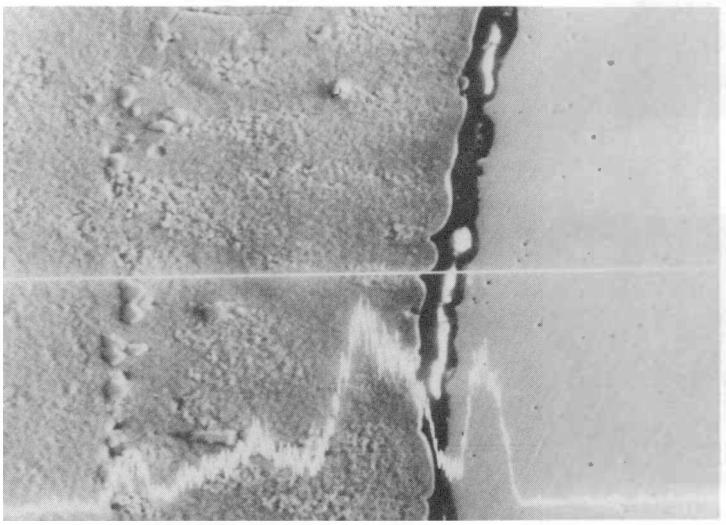


Figure 3-29. SEM of the Steel/Oxide Interface, with a Superimposed X-Ray Line Trace for Chlorine - Capsule AA-8, C-E Dent Environment, Neutralized with 1000 ppm $PO_4$ for 96 Hrs. at 150°F Followed with Exposure to 0.1 M $FeCl_2$

*Please note that the illustrations on this page have been reduced 10% in printing.

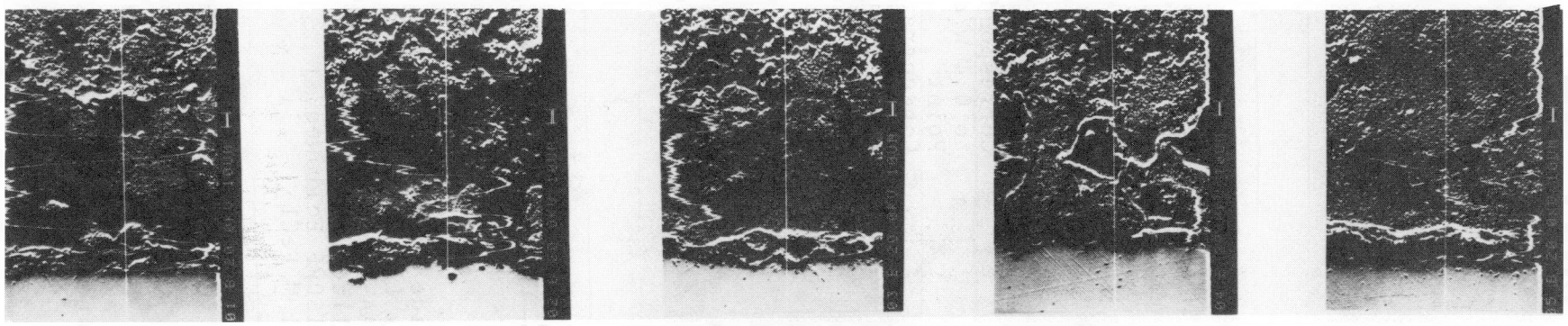

A: Center B: 1/8" From Center C: 1/4" From Center D: 3/8" From Center E: Outer End

Figure 3-30

SEM'S (500X)*of the Longitudinal Section of Capsule DD-7

W/EPRI Dent Environment, Neutralized with 1000 ppm $PO_4$ for 96 Hours at 150° F Followed with Exposure to AVT.



*Please note that the illustrations on this page have been reduced 10% in printing.

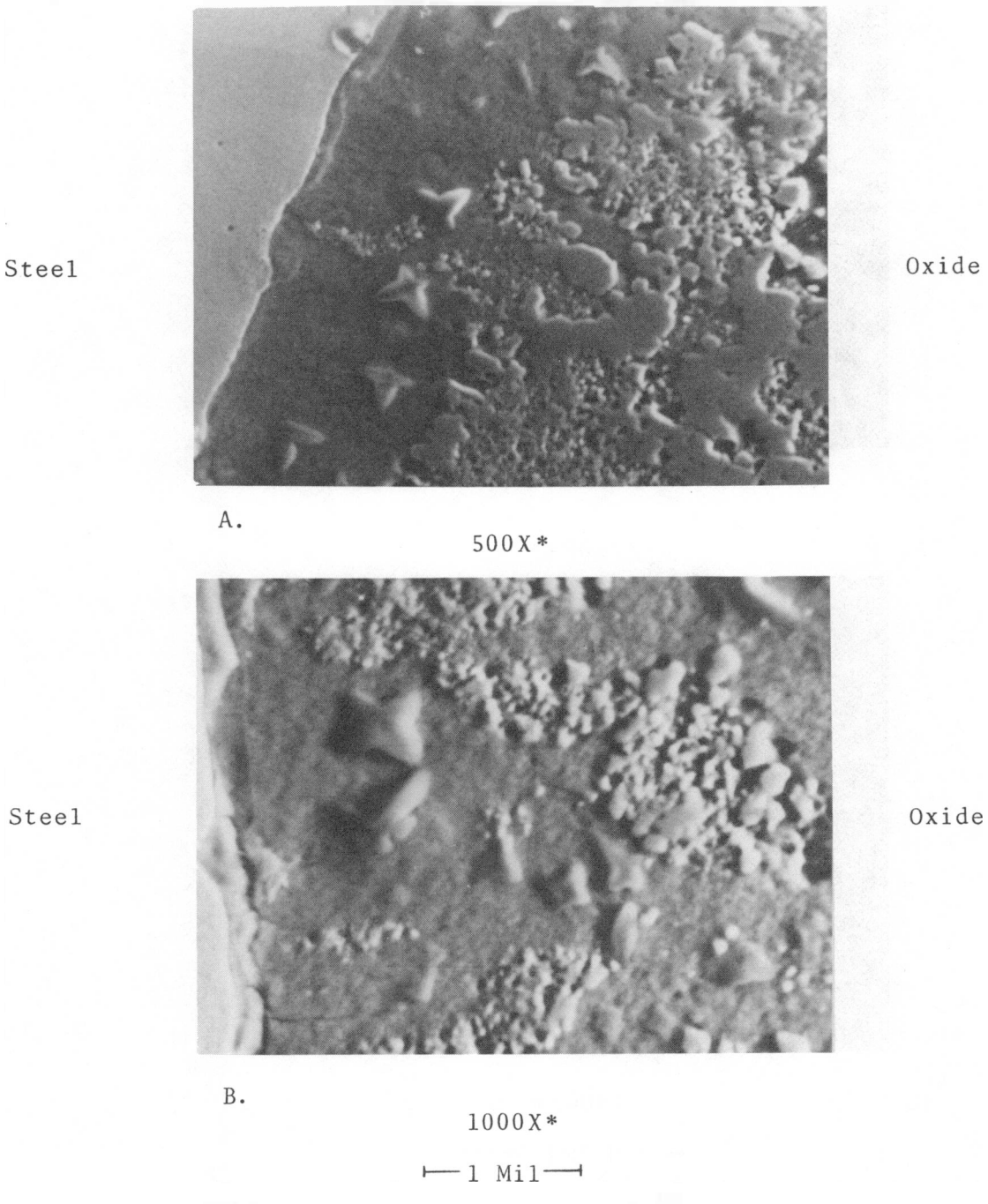


Figure 3-31. SEM's of the "Starfish-Like" Growths in the Oxide Layer at the Steel/Oxide Interface Capsue DD-8, W/EPRI Dent Environment, Neutralized with 1000 ppm $PO_4$ for 96 Hrs. at 150°F, Followed with Exposure to 0.1 M $FeCl_2$

*Please note that the illustrations on this page have been reduced 10% in printing.

A. 1500X*

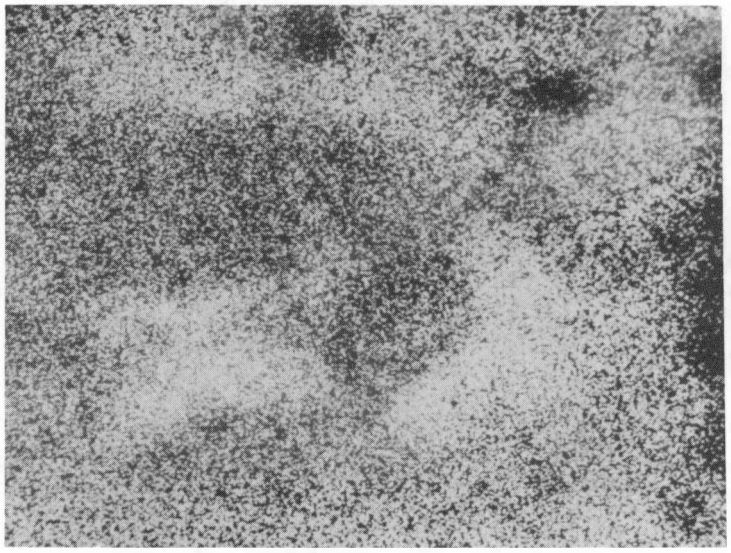

B. 1500X*

1 Mil

Figure 3-32. SEM's of "Starfish-Like" Crystals in the Oxide-Layer at the Steel/Oxide Interface (A), and Corresponding X-Ray Map for Chlorine (B), Capsule DD-8, W/EPRI Dent Environment, Neutralized with 1000 ppm $PO_4$ for 96 Hrs. at 150°F, Followed with Exposure to 0.1 M $FeCl_2$

*Please note that the illustrations on this page have been reduced 10% in printing.

Ion Microprobe Mass Analysis (IMMA). IMMA is a destructive examination in which elements are sputtered off a surface under ion bombardment. The technique is less sensitive than EMPA but has better accuracy due to very low backgrounds. IMMA was not used for quantitative analysis, but rather to determine statistically which groups of elements tended to be found together and which did not.

Ion microprobe analysis of capsule AA-8 showed some chloride, a very small amount of sodium, and approximately 0.5 (w/o) percent silicon. An apparent positive correlation existed for Cl, Mn, and Ca for that small portion of chlorine found near the I600 surface. Also, Ca, P, Mg, and Si exhibited some correlation.

Ion microprobe analysis of capsule DD-8 showed the presence of some sodium (aproximately 1.5 percent) in addition to Fe, Cr, Cu, Cl, and Si. A positive correlation among elements typically found in sea salts (Na, K, Mg, Ca) was found. Ni, Cr and Cu, Ti, Co indicated some correlation. No correlation of chloride with other elements was indicated. A negative correlation existed between iron and the other heavy metals detected.

## POT BOILER TESTING

### Overview

Four-day isothermal soaks at wet-layup conditions (150°F) were evaluated in three pot boilers. The soak chemistries were as follows:

| | |
|---|---|
| Pot 9 | Wet-Layup |
| Pot 11 | 1000 ppm $PO_4$ |
| Pot 7E | 3000 ppm $PO_4$ |

Detailed test conditions are tabulated in Appendix Tables C-3 and C-4. None of these soaks halted denting but post-soak denting rates were reduced in proportion to phosphate concentration. Denting rates were reduced by up to 70% by soaking. No abnormal corrosion was observed. Measurable quantities of chloride were found in crevice magnetite localized to a band near the surface of carbon steel. Phosphate was observed in crevice magnetite only in areas near the I600 surface. Such areas were characterized by porosity, cracks and other discontinuities. No phosphorus was found in other areas of magnetite.

Strain gauge observations of denting rates, absolute dent measurements via eddy current techniques, chemistry data, and corrosion-coupon observations are described in the following. In addition, observations from the destructive examination of the phosphate soak test bundles are presented.

### Strain Gauge Response

As described in Section 2 and Appendix C, five strain gauges were installed in each pot, three at carbon steel concentrating rings and two at 405 stainless steel concentrating rings. Indications of tube denting, as observed

through strain gauges, were monitored during Phase I to establish the initiation of tube denting, and during Phase III to determine the effectiveness of water/phosphate soaks in stifling active denting.

For each of the three pots used in this study, significant strain gauge response was observed at only two of the three carbon steel concentrating rings. Without exception, the strain gauge on the hot leg of tube 4 indicated strain. For pots 7E and 11, strain was also indicated on the cold leg of tube 4. For pot number 9, no strain gauge response was indicated for the cold leg of tube 4; however, the ring on the hot leg of tube 3 showed measurable strain gauge response. This variation between tubes within a given pot boiler and between pots is presumably due to unequal heat flux. It is estimated that the heat flux in tube 4 is between 10000 and 20000 $BTU/ft^2/hr.$, and in tube 3 between 4000 and 8000 $BTU/ft^2/hr.$ Heat fluxes for tube 1 and 2 are less than 500 $BTU/ft^2/hr.$

Strain gauge response during the initial fault chemistry periods are presented in Figures 3-33, 3-34, and 3-35. Strain, indicative of tube denting, occurred at carbon steel concentrating rings after approximately 40-45 days of seawater faulted chemistry operation in Pots 9 and 11, and after approximately 35 days in Pot 7E. Upon initiation of blowdown/volatile operations, the strain rate decreased by up to 70% at all but one location. Strain continued at one hot leg location in Pot 9 at a slightly higher rate than during actual seawater injection operation. Figures 3-36, 3-37 and 3-38 present strain gauge response during the post-soak volatile phase of operation, with comparative data from Phase I. Table 3-5 is a summary of these observations. An increasing strain gauge response throughout post-soak operation occurred at all instrumented locations which had previously dented indicating that denting had not been halted by low

temperature phosphate soaking. Strain rates were reduced by as much as 70% by soaking. Nevertheless, the rate of strain increase during post-soak volatile operation continued at approximately 10-30 μin/in/day.

Figure 3-33

POT 9 - PHASE I FAULT OPERATION
STRAIN GAGE RESPONSE

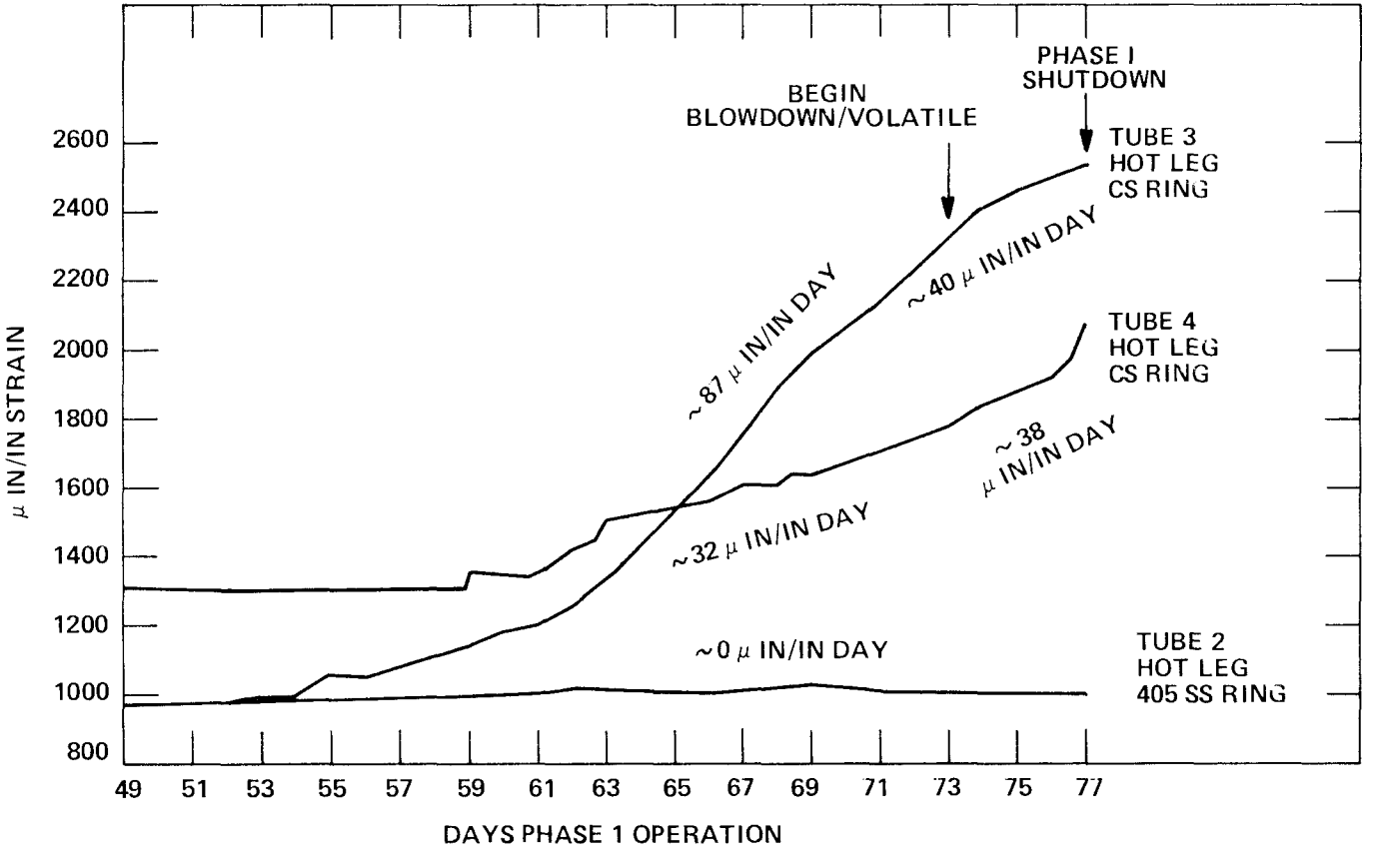


NOTE: PHASE 1 INCLUDED 13 DAYS OF PRECONDITIONING. THE NUMBER OF DAYS OF ACTUAL FAULT OPERATION IS EQUAL TO THE DAYS OF PHASE 1 OPERATION MINUS 13

Figure 3-34

POT 11 - PHASE I FAULT OPERATION
STRAIN GAGE RESPONSE

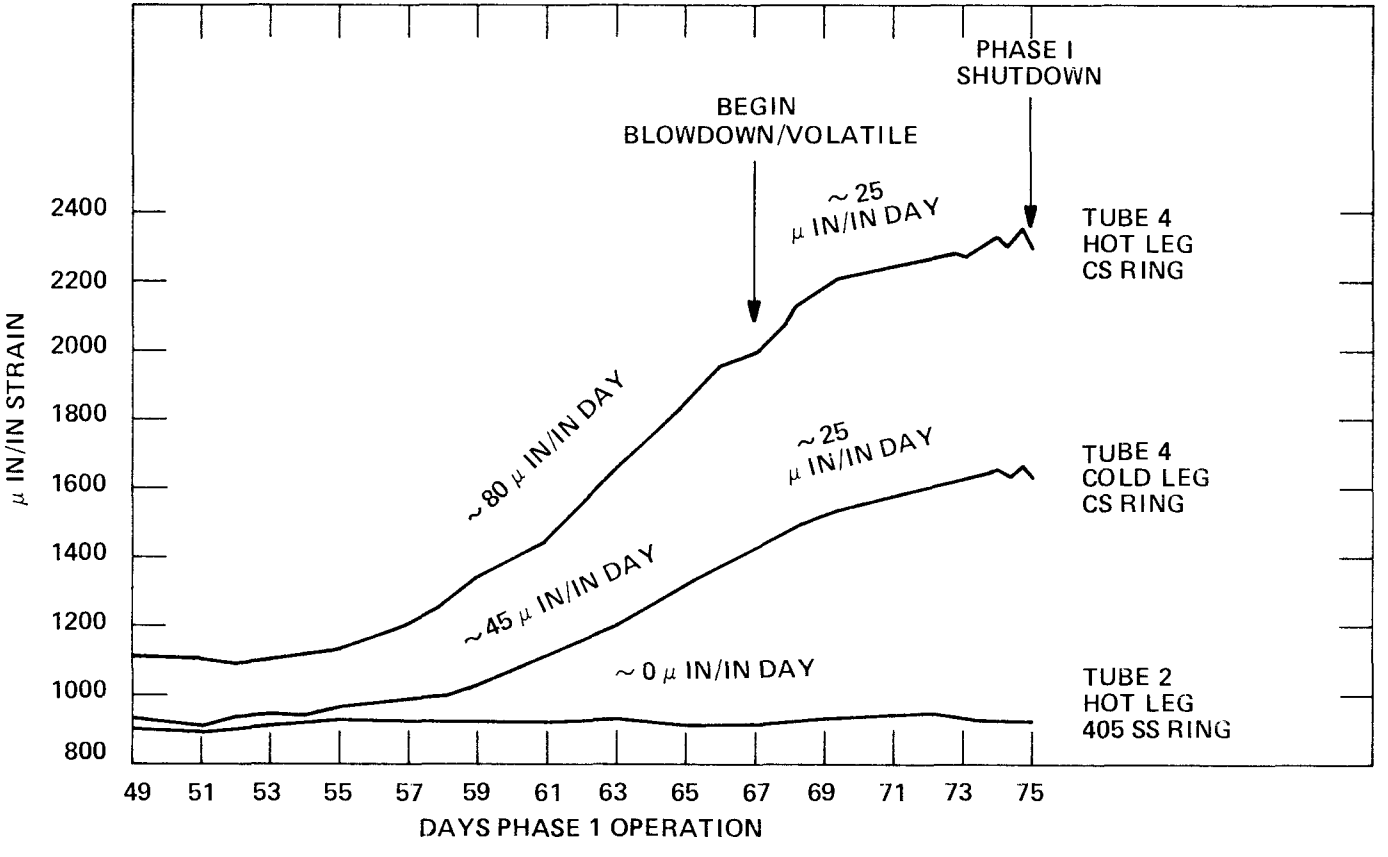


NOTE: PHASE 1 INCLUDED 13 DAYS OF PRECONDITIONING. THE NUMBER OF DAYS OF ACTUAL FAULT OPERATION IS EQUAL TO THE DAYS OF PHASE 1 OPERATION MINUS 13

Figure 3-35
POT 7E - PHASE I FAULT OPERATION
STRAIN GAGE RESPONSE

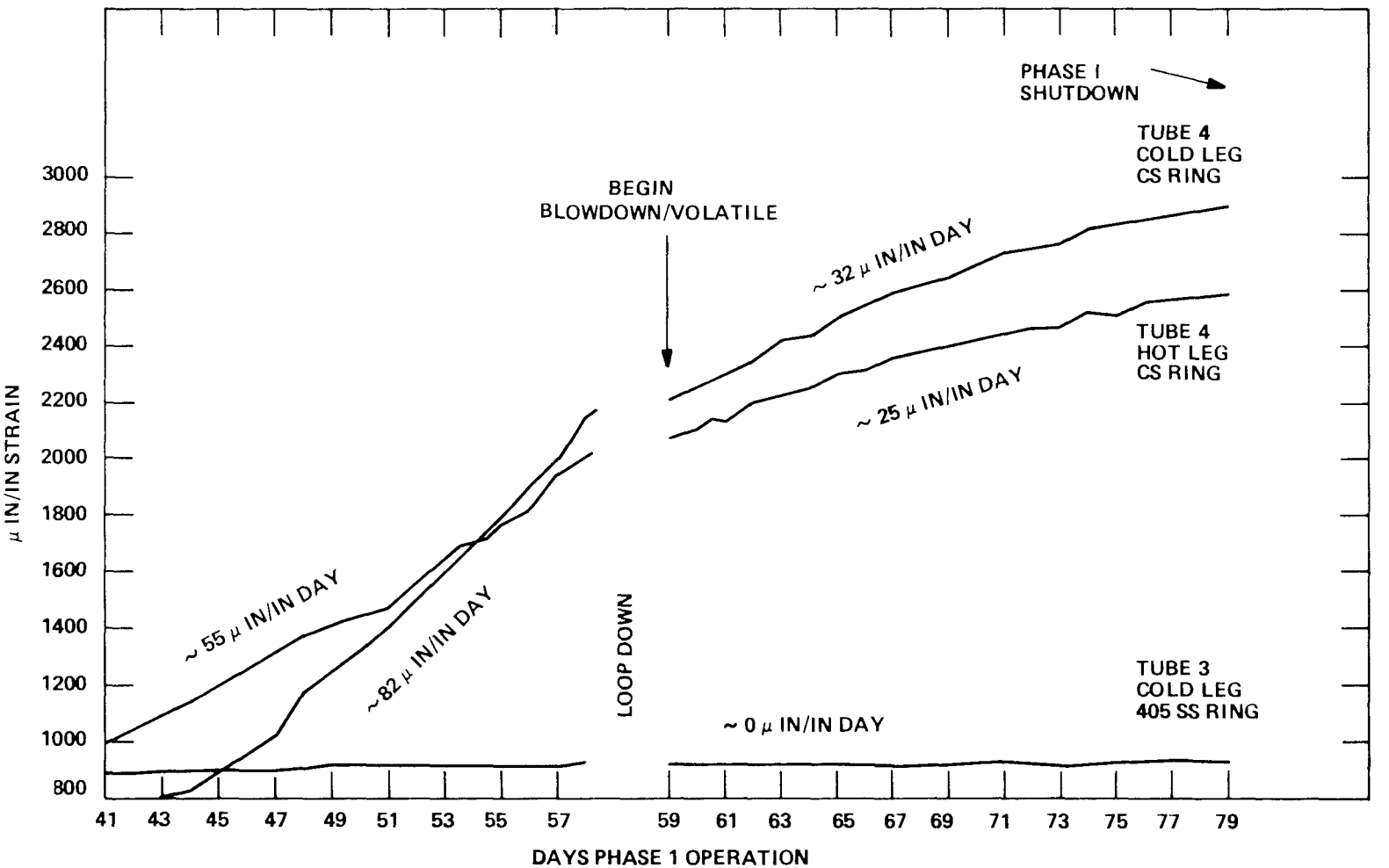


NOTE: PHASE 1 INCLUDED 7 DAYS OF PRECONDITIONING. THE NUMBER OF DAYS OF ACTUAL FAULT OPERATION IS EQUAL TO THE DAYS OF PHASE 1 OPERATION MINUS 7

Figure 3-36

POT 9 - PHASE 3 VOLATILE OPERATION
STRAIN GAGE RESPONSE

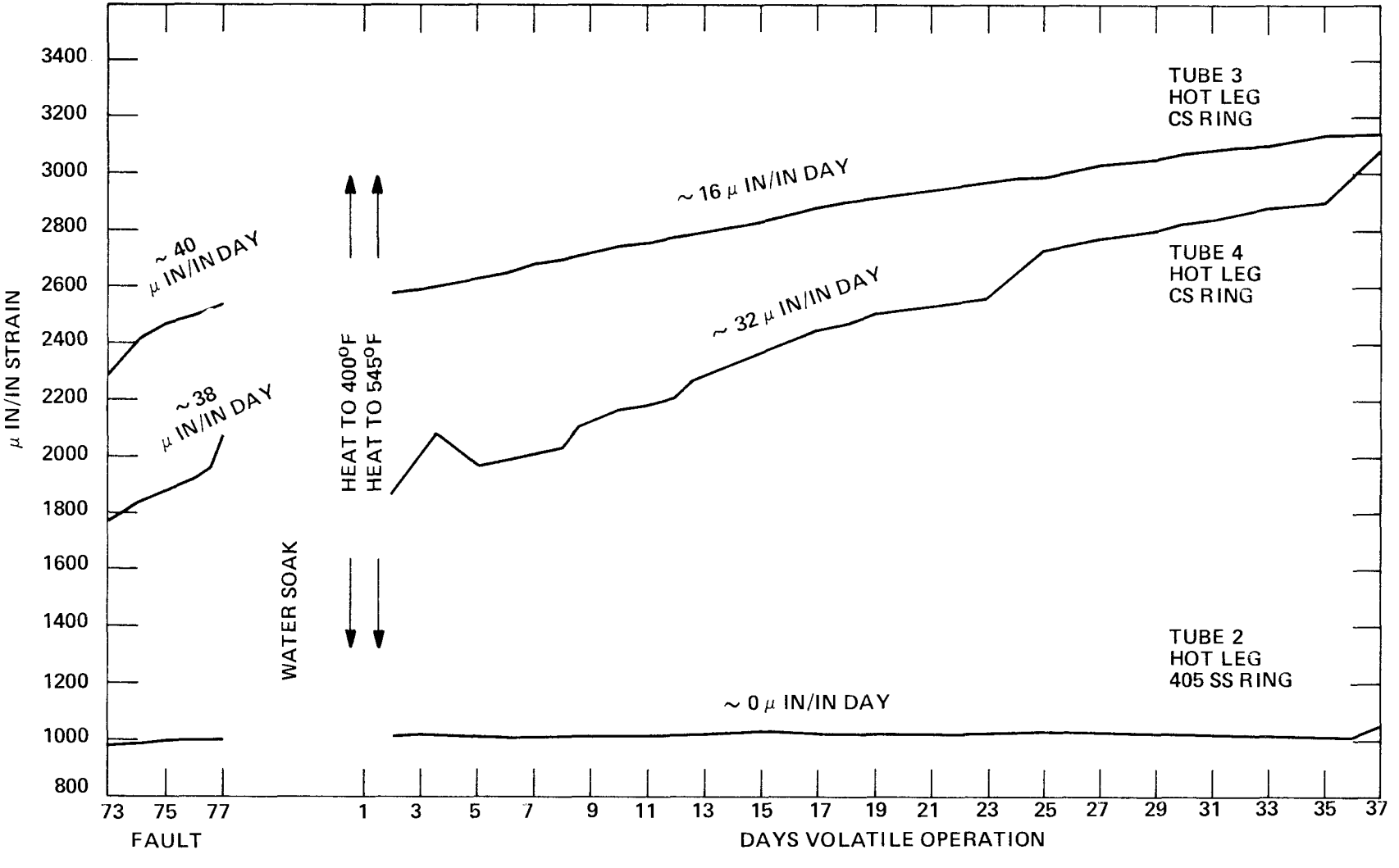

Figure 3-37

POT 11 - PHASE 3 VOLATILE OPERATION
STRAIN GAGE RESPONSE

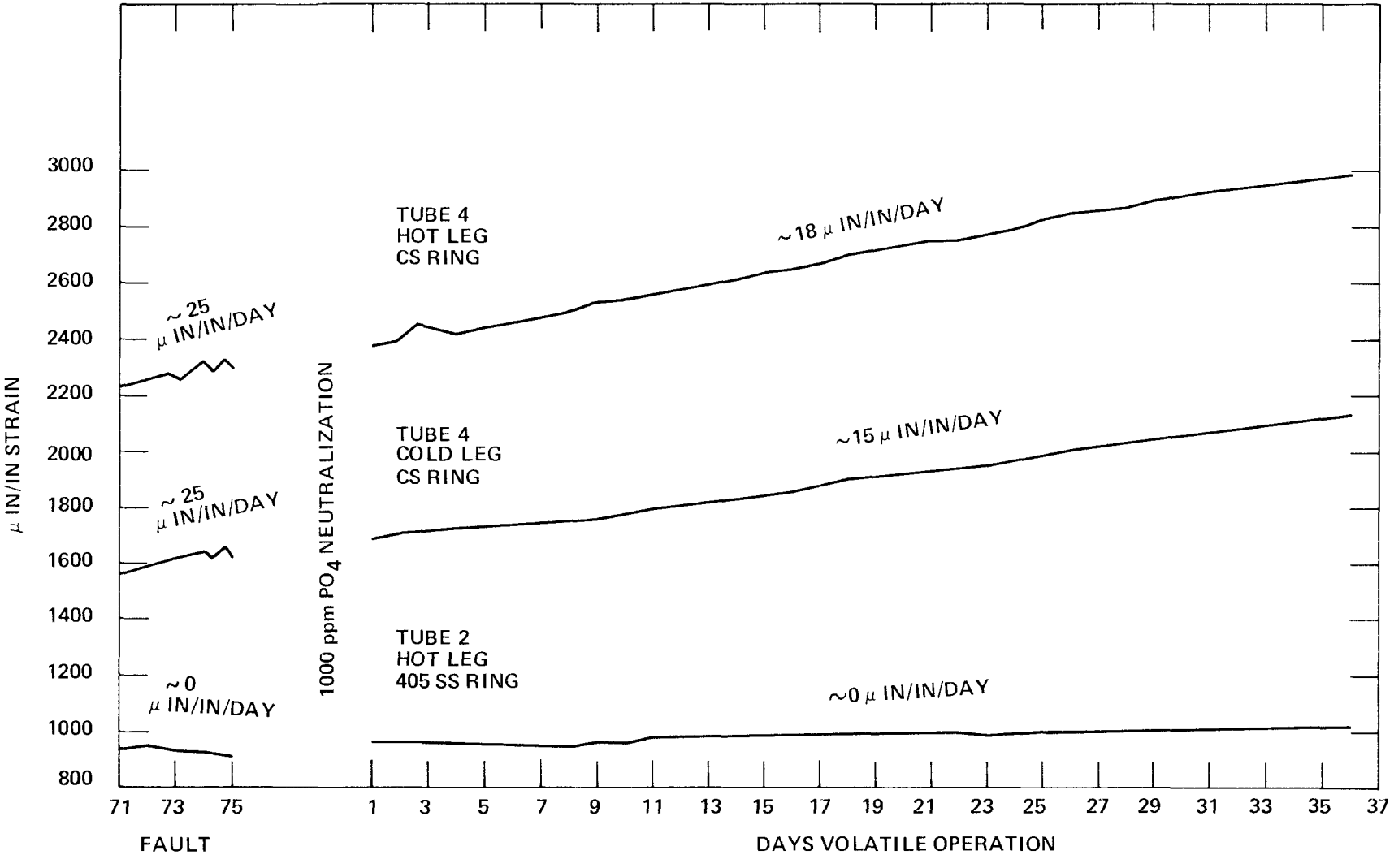

Figure 3-38

POT 7E - PHASE 3 VOLATILE OPERATION

STRAIN GAGE RESPONSE

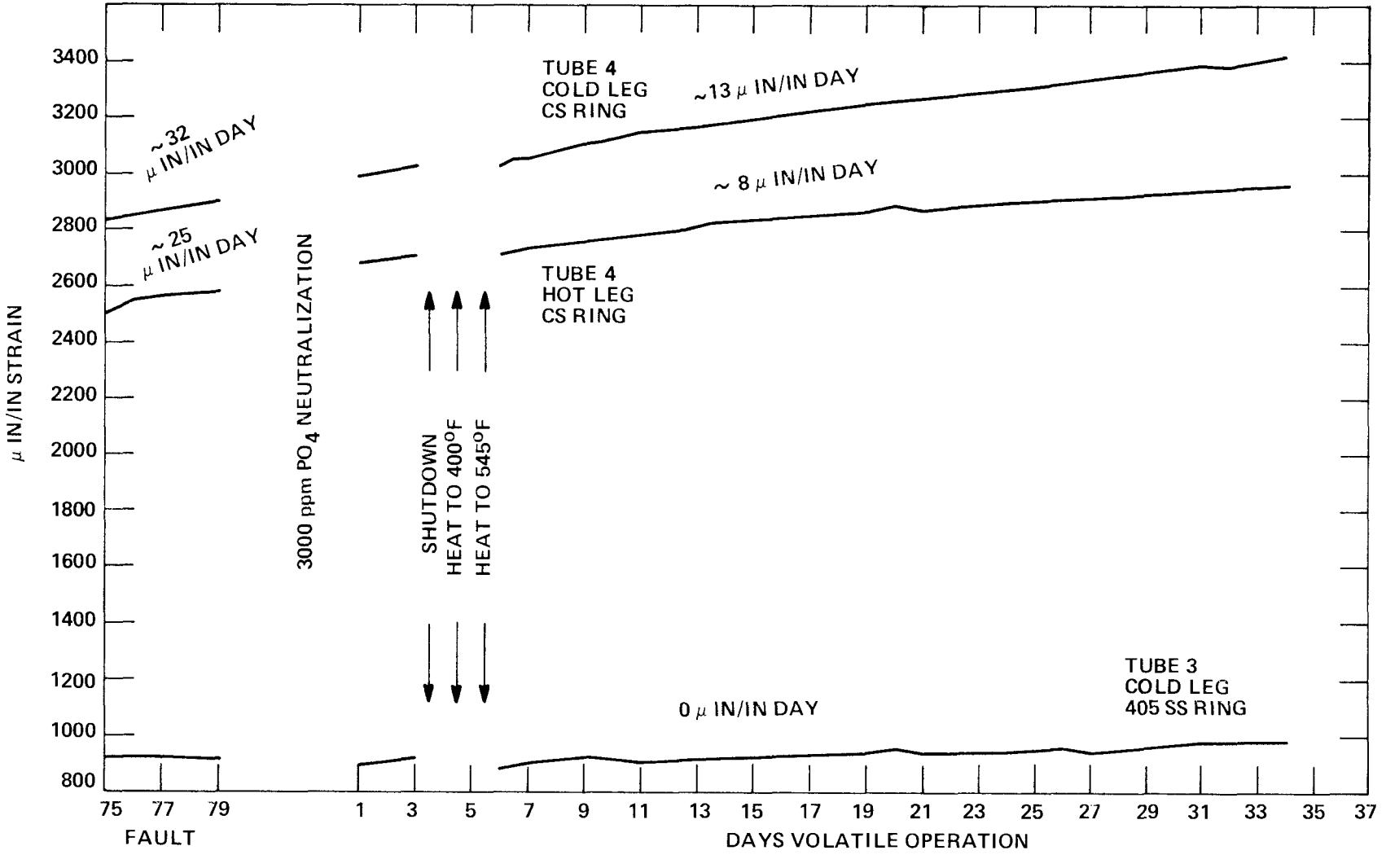

TABLE 3-5

POT BOILER STRAIN RATES

| Pot Number | Soak Conditions | Pre-Soak Strain Rate μin/in/day | Post-Soak Strain Rate μin/in/day | Percent Reduction |
|---|---|---|---|---|
| 9 | Wet Layup | | | |
| | Tube 3 Hot Leg CS Ring | 40 | 16 | 52% |
| | Tube 4 Hot Leg CS Ring | 38 | 32 | 16% |
| | Average | 39 | 24 | 38% |
| 11 | 1000 ppm $PO_4$ | | | |
| | Tube 4 Hot Leg CS Ring | 25 | 18 | 28% |
| | Tube 4 Cold Leg CS Ring | 25 | 15 | 40% |
| | Average | 25 | 16 | 36% |
| 7E | 3000 ppm $PO_4$ | 25 | 8 | 68% |
| | Tube 4 Hot Leg CS Ring | 32 | 13 | 59% |
| | Tube 4 Cold Leg CS Ring | 28 | 10 | 64% |

Eddy Current Examination

Eddy current examinations of the tube bundles were performed after Phase I fault operation and Phase III volatile operation. Results are summarized in Tables 3-6, 3-7 and 3-8. In general, all dents had increased in size during post-soak operation following the water and phosphate soak procedures. Average denting rates calculated from the eddy current data showed a significant reduction following soaks, consistent with reductions predicted by the strain data.

After the initial fault chemistry phase, tube denting indications of approximately 2-5 mils radially were observed at tube 4 concentrating ring and support plate locations of pots 9 and 11. Pot 7E exhibited more severe denting of approximately 5-6 mils radially at Tube 4 rings and approximately 10-11 mils at tube 4 support plate areas. The rates of tube denting during this phase were estimated at 0.1 to 0.3 mils/day for the three units.

After Phase III volatile operation, tube denting indications had increased at ring and plate areas of pot 9 and 11 to approximately 5-11 mils radially, which represented continued denting rates of 0.05 - 0.15 mils/day Additionally, new denting of approximately 2-3 mils had occurred at a support plate and tubesheet location in pot 9. One tubesheet dent in pot 11 remained essentially unchanged after volatile operation. Tube denting in Pot 7E had continued during post-soak volatile operation at rates estimated at 0.02-0.07 mils/day. Denting had increased to approximately 6-7 mils radially at the rings and approximately 12-13 mils at the support plates.

TABLE 3-6

POT 9-WATER SOAK, TUBE DENTING RESULTS

| Dent Location | Eddy Current Results Mils of Radial Denting Phase I | Phase III | Change | Estimated Denting Rate* Mils Per Day Phase I | Phase III | Percent Reduction |
|---|---|---|---|---|---|---|
| Tube 3-Hot Leg Concentrating Ring | 3.8 | 5.5 | +1.7 | 3.8/23 = .17 | 1.7/37 = .05 | 71% |
| Tube 4-Hot Leg Concentrating Ring | 1.7 | 5.0 | +3.3 | 1.7/18 = .09 | 3.3/37 = .09 | 0% |
| Tube 4-Hot Leg Support Plate | 5.0 | 10.5 | +5.5 | 5.0/41 = .12* | 5.5/37 + .15 | -- |
| Tube 3-Hot Leg Support Plate | ---- | 1.8 | +1.8 | ---- | 1.8/37 = .05+ | |
| Tube 4-Hot Leg Tubesheet | ---- | 2.5 | +2.5 | ---- | 2.5/37 = .07+ | |

* Calculation of estimated denting rates was based upon the number of operation days subsequent to the initiation of a positive strain gage response at instrumented locations. Denting rates at non-strain gaged locations were based upon estimated crevice fill times and are therefore subject to a greater degree of uncertainty.

\+ Phase III denting rates for tube 3-hot leg support plate and tube 4-hot leg tubesheet are somewhat uncertain inasmuch as there had been no indication of denting at the conclusion of Phase I. There is no way to establish just when these crevices began to dent. Average rates have been computed assuming dent growth throughout the 37 day period.

TABLE 3-7

POT 11-PHOSPHATE SOAK-1000 PPM, TUBE DENTING RESULTS

| Dent Location | Eddy Current Results Mils of Radial Denting Phase I | Phase III | Change | Estimated Denting Rate* Mils Per Day Phase I | Phase III | Percent Reduction |
|---|---|---|---|---|---|---|
| Tube 4-Cold Leg Concentrating Ring | 4.0 | 7.0 | +3.0 | 4.0/20 = .2 | 3.0/36 = .08 | 60% |
| Tube 4-Hot Leg Concentrating Ring | 3.2 | 4.5 | +1.3 | 3.2/20 = .16 | 1.3/36 = .04 | 75% |
| Tube 4-Hot Leg Support Plate | 5.3 | 10.0 | +4.7 | 5.3/38 = .14* | 4.7/36 = .13 | 7% |
| Tube 4-Hot Leg Tubesheet | 1.7 | 1.8 | + .1 | 1.7/6 = .28* | .1/36 = .00 | 99% |

* See Note on Table 3-6

TABLE 3-8

POT 7E-PHOSPHATE SOAK-3000 PPM, TUBE DENTING RESULTS

| Dent Location | Eddy Current Results Mils of Radial Denting Phase I | Phase III | Change | Estimated Denting Rate* Mils Per Day Phase I | Phase III | Percent Reduction |
|---|---|---|---|---|---|---|
| Tube 4-Cold Leg Concentrating Ring | 5.5 | 6.5 | +1.0 | 5.5/36 = .15 | 1.0/34 = .03 | 80% |
| Tube 4-Hot Leg Concentrating Ring | 5.0 | 5.5 | + .5 | 5.0/38 = .13 | .5/34 = .02 | 85% |
| Tube 4-Cold Leg Support Plate | 11.0 | 12.5 | +1.5 | 11.0/52 = .21* | 1.5/34 = .04 | 81% |
| Tube 4-Hot Leg Support Plate | 9.5 | 12.0 | +2.5 | 9.5/52 = .18* | 2.5/34 = .07 | 61% |

* See Note on Table 3-6

Chemistry Data

For each pot boiler, the release of impurities was monitored during the soak operation as well as the subsequent period of steaming. Total chlorides recovered during Phases II and III of testing, as derived from these data, are presented in Table 3-9. Approximately the same total chloride recovery was observed in all three pots. In the water soak test, most of the chloride was released during post-soak operation. In the 1000 ppm phosphate test, the largest amount of chloride was released during the 96 hour soak, while in the 3000 ppm phosphate test, the major portion of the chloride was relased during post-soak operation. Chloride concentration during operation showed no apparent trends and seemed to be independent of blowdown and sampling losses. For this reason calculated chloride releases consisted of removal through sampling and blowdown, of varying volumes which contained essentially constant chloride concentrations. Hence, chloride releases during operation were primarily dependent on the number of liquid samples drawn and blowdowns performed for chemistry control. Apparently chloride was leached from various pot-boiler internal surfaces until an equilibrium concentration ranging from a few tenths of a ppm to one ppm was established. Varying quantities of this bulk solution were removed through blowdowns and samples for analysis. As bulk solution was replenished with chloride-free makeup water, additional chloride was leached from internal surfaces re-establishing the equilibrium concentration. Blowdowns and analyses were determined by such factors, as the phosphate and sodium concentrations and the conductivity. Hence there is little significance to the plots of chloride concentration versus time in Phase III.

Although a mass balance calculation had not been planned, a chloride mass balance was attempted for pot 7E. During dent initiation, 1.82 liters of seawater (18250 ppm Cl) had been injected resulting in 33.2 g of chloride added. Blowdown and

sampling during this phase accounted for the removal of 24.8 g of chloride. Hence at the conclusion of dent initiation, this calculation indicated roughly 8 g of chloride remaining in the pot. Chloride recovery during soaking and subsequent operation is given in Table 3-9. As is apparent, there is considerable uncertainty as to the amount of chloride removed during these phases. This results from the fact that many chloride analyses taken during this period were reported as less than 0.1 ppm Cl (the lower limit of detection). In any event, the maximum amount of chloride which could be accounted for via this procedure was 0.18 g. This would still leave approximately 8 g of chloride in the pot.

TABLE 3-9

ESTIMATED CHLORIDE REMOVAL DURING
PHASE II - WATER SOAK/NEUTRALIZATION
AND PHASE III - POST NEUTRALIZATION VOLATILE OPERATION
MILLIGRAMS OF CHLORIDE REMOVED

| | Pot 9 Water Soak | Pot 11 1000 ppm $PO_4$ | Pot 7E 3000 ppm $PO_4$ |
|---|---|---|---|
| | Max/Min* | Max/Min | Max/Min |
| Pre-flush | 21/10 | 26/10 | 22/0 |
| 96 Hr. Soak | 22 | 54 | 12 |
| Final Drain | 14 | 11 | 45 |
| Post-flush | 11/0 | 22/0 | 17/12 |
| Phase 3-Volatile Operation | 104/78 | 48/35 | 85/51 |
| Total All Sources | 172/124 | 161/110 | 181/120 |

* Maximum - $Cl^-$ Reported $<0.2 = 0.1$
Minimum - $Cl^-$ Reported $<0.1 = 0$

## Deposit Examinations

Sample deposits were collected from the tube bundles during unit examinations and submitted for chemical analysis which included X-ray diffraction (XRD) and X-ray fluorescence (XRF) techniques. Tables 3-10 through 3-14 present semi-quantitative chemical data including XRF results for the various samples. XRD results are summarized in Table 3-15.

Because all three units had been similarly prepacked, and operated under the same initial seawater faulted chemistry, deposit samples were very similar in chemical composition. Iron in the form of $Fe_3O_4$ and metallic copper were identified as the major components of all samples. Most samples also contained nickel, manganese and magnesium, as well as minor amounts of other seawater salts.

Copper was identified as the primary component of the red deposit coatings noted on many of the tube bundle surfaces. The highest concentrations of copper were present in the spiral patterns at support plate surfaces around tube 4. These samples additionally contained minor amounts of nickel, manganese, and phosphorus, which were present in all final deposit samples from pots 11 and 7E.

Tubesheet deposits from pot 7E were dissimilar. In addition to iron, copper and nickel, the post-dent initiation tubesheet sample contained a relatively high quantity of zinc, in addition to aluminum and silicon. The deposit at the same location, when examined at the conclusion of testing however, was primarily composed of copper with neither zinc, aluminum nor silicon identified as present.

TABLE 3-10

POT BOILER 9, POST-PHASE III DEPOSIT ANALYSIS[1]
SEMI-QUANTITATIVE VALUES REPORTED AS WEIGHT PERCENT

| | | Steam Blanket Umbrellas Deposit | |
|---|---|---|---|
| Element | Assumed Oxide Form | Relative % Element | Relative % As Oxide |
| Sulfur | $SO_3$ | 0.063 | 0.16 |
| Calcium | CaO | 0.032 | 0.045 |
| Chromium | $Cr_2O_3$ | 0.19 | 0.27 |
| Manganese | MnO | 0.77 | 1.0 |
| Iron | $Fe_3O_4$ | 53.1 | 73.4 |
| Nickel | NiO | 1.3 | 1.6 |
| Copper | (Metal) | 14.0 | 14.0 |
| Zinc | ZnO | 0.035 | 0.044 |
| Hydrogen[2] | $H_2O$ | 0.05 | 0.45 |
| Carbon[2] | $CO_2$ | 0.38 | 1.4 |
| Nitrogen[2] | $NO_2$ | 0.03 | 0.099 |
| Sodium[3] | $Na_2O$ | < 0.1 | < 0.1 |
| Magnesium[4] | MgO | 0.51 | 0.85 |

Notes:

1. Analysis was by X-ray fluorescence except as noted.
2. Analysis was by Perkin Elmer #240 carbon, hydrogen, and nitrogen analyzer.
3. Analysis was by flame photometry.
4. Analysis was by atomic absorption.

TABLE 3-11

POT BOILER 9, POST-PHASE I DEPOSIT ANALYSIS[1]
SEMI-QUANTITATIVE VALUES REPORTED AS WEIGHT PERCENT

| | | Steam Blanket Umbrellas Deposit | |
|---|---|---|---|
| Element | Assumed Oxide Form | Relative % Element | Relative % As Oxide |
| Sulfur | $SO_3$ | 0.066 | 0.17 |
| Chlorine | Cl | 0.049 | 0.049 |
| Calcium | CaO | 0.034 | 0.048 |
| Chromium | $Cr_2O_3$ | 0.083 | 0.12 |
| Manganese | MnO | 1.0 | 1.3 |
| Iron | $Fe_3O_4$ | 58.3 | 80.6 |
| Nickel | NiO | 2.8 | 3.5 |
| Copper | (Metal) | 9.5 | 9.5 |
| Zinc | ZnO | 0.028 | 0.035 |
| Hydrogen[2] | $H_2O$ | 0.040 | 0.36 |
| Carbon[2] | $CO_2$ | 0.24 | 0.88 |
| Nitrogen[2] | $NO_2$ | < 0.1 | < 0.1 |
| Sodium[3] | $Na_2O$ | < 0.1 | < 0.1 |
| Magnesium[4] | MgO | 0.36 | 0.60 |

Notes:

See Table 3-10

TABLE 3-12

POT BOILER 11, FINAL EXAMINATION DEPOSIT ANALYSIS[1]
SEMI-QUANTITATIVE VALUES REPORTED AS WEIGHT PERCENT

| | | Tubesheet Deposit | | Steam Blanket Umbrella Deposit | |
|---|---|---|---|---|---|
| Element | Assumed Oxide Form | Relative % Element | Relative % As Oxide | Relative % Element | Relative % As Oxide |
| Silicon | $SiO_2$ | ---- | ---- | 0.28 | 0.61 |
| Phosphorus | $P_2O_5$ | 0.098 | 0.23 | 0.12 | 0.27 |
| Sulfur | $SO_3$ | 0.072 | 0.18 | 0.089 | 0.22 |
| Chlorine | Cl | 0.071 | 0.071 | 0.047 | 0.047 |
| Calcium | CaO | 0.030 | 0.042 | 0.20 | 0.27 |
| Chromium | $Cr_2O_3$ | 0.089 | 0.13 | 0.055 | 0.080 |
| Manganese | MnO | 0.91 | 1.2 | 0.41 | 0.53 |
| Iron | $Fe_3O_4$ | 55.6 | 76.8 | 46.3 | 64.0 |
| Nickel | NiO | 1.7 | 2.1 | 0.43 | 0.55 |
| Copper | (Metal) | 15.4 | 15.4 | 16.9 | 16.9 |
| Hydrogen[2] | $H_2O$ | 0.040 | 0.36 | 0.040 | 0.357 |
| Carbon[2] | $CO_2$ | 0.28 | 1.0 | 0.19 | 0.70 |
| Nitrogen[2] | $NO_2$ | 0.010 | 0.033 | ---- | ---- |
| Sodium[3] | $Na_2O$ | < 0.1 | < 0.1 | < 0.1 | < 0.1 |
| Magnesium[4] | MgO | 0.30 | 0.50 | 0.51 | 0.84 |

Notes:

See Table 3-10

TABLE 3-12
(continued)
POT BOILER 11, FINAL EXAMINATION DEPOSIT ANALYSIS[1]
SEMI-QUANTITATIVE VALUES REPORTED AS WEIGHT PERCENT

| | | Support Plate Spiral Deposit | |
|---|---|---|---|
| Element | Assumed Oxide Form | Relative % Element | Relative % As Oxide |
| Phosphorus | $P_2O_5$ | 0.34 | 0.78 |
| Chlorine | Cl | 0.20 | 0.20 |
| Calcium | CaO | 0.032 | 0.045 |
| Chromium | $Cr_2O_3$ | 0.14 | 0.21 |
| Manganese | MnO | 0.20 | 0.26 |
| Iron | $Fe_3O_4$ | 12.6 | 17.4 |
| Nickel | NiO | 0.38 | 0.48 |
| Copper | (Metal) | 80.2 | 80.2 |
| Hydrogen[2] | $H_2O$ | * | |
| Carbon[2] | $CO_2$ | * | |
| Nitrogen[2] | $NO_2$ | * | |
| Sodium[3] | $Na_2O$ | < 0.1 | < 0.1 |
| Magnesium[4] | MgO | 0.078 | 0.13 |

* Insufficient Sample for Analysis

Notes:

See Table 3-10

TABLE 3-13

POT BOILER 7E, POST PHASE I DEPOSIT ANALYSIS[1]
SEMI-QUANTITATIVE VALUES REPORTED AS WEIGHT PERCENT

| | | Tubesheet Deposit | | Deposit on Tube 4 Concentrating Rings | |
|---|---|---|---|---|---|
| Element | Assumed Oxide Form | Relative % Element | Relative % As Oxide | Relative % Element | Relative % As Oxide |
| Aluminum | $Al_2O_3$ | 0.85 | 1.6 | ---- | ---- |
| Silicon | $SiO_2$ | 0.85 | 1.8 | ---- | ---- |
| Sulfur | $SO_3$ | ---- | ---- | 0.12 | 0.29 |
| Chlorine | Cl | 0.059 | 0.059 | 0.047 | 0.047 |
| Potassium | $K_2O$ | 0.019 | 0.023 | ---- | ---- |
| Calcium | CaO | 0.16 | 0.22 | 0.035 | 0.049 |
| Titanium | $TiO_2$ | 0.084 | 0.14 | ---- | ---- |
| Chromium | $Cr_2O_3$ | 0.16 | 0.23 | 0.062 | 0.091 |
| Manganese | MnO | 0.67 | 0.89 | 0.48 | 0.62 |
| Iron | $Fe_3O_4$ | 34.0 | 47.0 | 41.1 | 56.8 |
| Nickel | NiO | 1.8 | 2.3 | 1.6 | 2.1 |
| Copper | (Metal) | 25.0 | 25.0 | 29.7 | 29.7 |
| Zinc | ZnO | 5.5 | 6.9 | ---- | ---- |
| Hydrogen[2] | $H_2O$ | 0.12 | 1.1 | 0.040 | 0.36 |
| Carbon[2] | $CO_2$ | 0.83 | 3.0 | 0.12 | 0.44 |
| Nitrogen[2] | $NO_2$ | 0.02 | 0.066 | 0.010 | 0.033 |
| Sodium[3] | $Na_2O$ | < 0.1 | < 0.1 | <0.1 | <0.1 |
| Magnesium[4] | MgO | 0.12 | 0.20 | 0.21 | 0.35 |

Notes:

See Table 3-10

TABLE 3-14

POT BOILER 7E, FINAL EXAMINATION DEPOSIT ANALYSIS[1]
SEMI-QUANTITATIVE VALUES REPORTED AS WEIGHT PERCENT

| | | Support Plate Spiral Deposit | | Gray/Green Deposit on Tube 4 Concentrating Rings | |
|---|---|---|---|---|---|
| Element | Assumed Oxide Form | Relative % Element | Relative % As Oxide | Relative % Element | Relative % As Oxide |
| Phosphorus | $P_2O_5$ | 0.15 | 0.35 | 0.098 | 0.23 |
| Sulfur | $SO_3$ | ---- | ---- | 0.13 | 0.34 |
| Calcium | CaO | ---- | ---- | 0.0074 | 0.010 |
| Chromium | $Cr_2O_3$ | 0.044 | 0.064 | 0.048 | 0.070 |
| Manganese | MnO | 0.22 | 0.28 | 0.27 | 0.35 |
| Iron | $Fe_3O_4$ | 20.8 | 28.7 | 45.6 | 63.0 |
| Nickel | NiO | 0.38 | 0.49 | 0.84 | 1.1 |
| Copper | (Metal) | 57.8 | 57.8 | 28.6 | 28.6 |
| Zinc | ZnO | 0.054 | 0.067 | ---- | ---- |
| Hydrogen[2] | $H_2O$ | * | | 0.010 | 0.089 |
| Carbon[2] | $CO_2$ | * | | 0.090 | 0.33 |
| Nitrogen[2] | $NO_2$ | * | | ---- | ---- |
| Sodium[3] | $Na_2O$ | * | | < 0.1 | < 0.1 |
| Magnesium[4] | MgO | | | 0.14 | 0.23 |

* Insufficient Sample for Analysis

Notes:

See Table 3-10

TABLE 3-14
(continued)
POT BOILER 7E, FINAL EXAMINATION DEPOSIT ANALYSIS[1]
SEMI-QUANTITATIVE VALUES REPORTED AS WEIGHT PERCENT

| | | Tubesheet Deposit | |
|---|---|---|---|
| Element | Assumed Oxide Form | Relative % Element | Relative % As Oxide |
| Phosphorus | $P_2O_5$ | 0.28 | 0.63 |
| Chlorine | Cl | 0.059 | 0.059 |
| Chromium | $Cr_2O_3$ | 0.034 | 0.050 |
| Manganese | MnO | 0.16 | 0.20 |
| Iron | $Fe_3O_4$ | 6.2 | 8.6 |
| Nickel | NiO | 0.40 | 0.51 |
| Copper | (Metal) | 84.1 | 84.1 |
| Hydrogen[2] | $H_2O$ | 0.010 | 0.089 |
| Carbon[2] | $CO_2$ | 0.37 | 1.4 |
| Nitrogen[2] | $NO_2$ | 0.07 | 0.23 |
| Sodium[3] | $Na_2O$ | < 0.1 | < 0.1 |
| Magnesium[4] | MgO | 0.36 | 0.60 |

Notes:

See Table 3-10

TABLE 3-15

X-RAY DIFFRACTION ANALYSES RESULTS
POT BOILER 9, 11, 7E DEPOSIT SAMPLES

| Pot Boiler | Sampling Time | Sample Identification | Major Components In Approximate Concentration |
|---|---|---|---|
| 9 | Post-Phase 3 | Steam Blanket Umbrella Deposit | 83% $Fe_3O_4$<br>17% Cu |
| 11 | Post-Phase 1 | Tubesheet Deposit | 89% $Fe_3O_4$<br>11% Cu |
| 11 | Final Exam | Tubesheet Deposit | 75% $Fe_3O_4$<br>25% Cu |
| 11 | Final Exam | Steam Blanket Umbrella Deposit | 73% $Fe_3O_4$<br>27% Cu |
| 11 | Final Exam | Support Plate Spiral Deposit | 85% Cu<br>15% $Fe_3O_4$ |
| 7E | Post-Phase 1 | Tubesheet Deposit | 53% Cu<br>47% $Fe_3O_4$ |
| 7E | Post-Phase 1 | Deposit on Tube 4 Concentrating Rings | 51% Cu<br>49% $Fe_3O_4$ |
| 7E | Final Exam | Support Plate Spiral Deposit | 98% Cu<br>2% $Fe_3O_4$ |
| 7E | Final Exam | Gray/Green Deposit on Tube 4 Concentrating Rings | 52% Cu<br>48% $Fe_3O_4$ |
| 7E | Final Exam | Tubesheet Deposit | 81% Cu<br>19% $Cu_2O$ |

Corrosion Coupon Analyses

Average corrosion coupon data are presented in Table 3-16. (See Appendix D for more detailed data pertaining to corrosion coupons) Observed corrosion rates for the various materials ranked as expected. Carbon steel and the low alloy grades A508 and A533 exhibited the highest corrosion rate. The corrosion rate for 409 SS was significantly lower, and the rate for Alloy 600 was negligible. No significant adverse effects on corrosion rates were noted for any of the materials tested, which could be related to exposure to phosphates.

TABLE 3-16

AVERAGE CORROSION RATES

FROM POT BOILER TESTS

| Material | Pot | PPM of $PO_4$ | Average Corrosion Rate, MPY (1) | $\bar{S}$ (3) | Average Corrosion Rate MDD (2) | $\bar{S}$ (3) |
|---|---|---|---|---|---|---|
| C-Steel | 11 | 1000 | 0.58 | 0.05 | 3.2 | 0.3 |
| | 7E | 3000 | 0.52 | 0.04 | 2.9 | 0.2 |
| A-508 | 11 | 1000 | 0.39 | 0.02 | 2.1 | 0.1 |
| | 7E | 3000 | 0.43 | 0.02 | 2.4 | 0.1 |
| A-533-A | 11 | 1000 | 0.56 | 0.02 | 3.1 | 0.1 |
| | 7E | 3000 | 0.46 | 0.04 | 2.5 | 0.2 |
| 409 SS | 11 | 1000 | 0.16 | 0.01 | 0.88 | 0.08 |
| | 7E | 3000 | 0.13 | 0.01 | 0.72 | 0.08 |
| Alloy 600 | 11 | 1000 | 0.021 | 0.004 | 0.12 | 0.03 |
| | 7E | 3000 | 0.027 | 0.002 | 0.16 | 0.01 |

Notes: (1) Mils per year
(2) Milligrams per square decimeter per day
(3) Standard deviation

Metallographic Examination

The ring and support plate crevices on tube #4 from both pot 11 (1000 ppm $PO_4$) and pot 7E (3000 ppm $PO_4$) were destructively examined. Measureable phosphorus was detected in only one crevice from pot 7E, exclusively in surface cracks and voids in the immediate vicinity of the I600 surface. Chlorine was localized in a band near the surface of the carbon steel. Observations via optical microscopy, scanning electron microscopy, and electron microprobe analysis follow.

Optical Microscopy. The oxide at all locations was voluminous and completely filled the crevice. The oxide thickness shown in the micrographs varied from about 0.020 inch to about 0.066 inch. This thickness included the original crevice (size approximately 0.010 inch), the additional crevice area caused by the denting, plus the depth of attack in the carbon steel.

The corrosion was relatively uniform at different locations in the same specimen and did not vary greatly between different specimens. The oxide generally consisted of successive regions of relatively fine magnetite and relatively coarse magnetite. The laminations were not as evident in some of the photomicrographs as they were during visual examination. The magnetite also exhibited a significant amount of cracking and some porosity, but the amounts varied among different locations. Some plated copper was also observed in a few localized areas near the magnetite/Alloy 600 interfaces.

The above observations are typical of oxides grown on carbon steel in acid chloride environments.

Scanning Electron Microscopy (SEM) of Concentrating Rings. One of the more significant observations is that in none of the energy dispersive spectrometry (EDS) analyses of concentrating

rings was phosphorus present in the oxide. The sensitivity of the typical EDS is approximately one percent. Therefore, phosphorus did not exceed a maximum of one percent of the oxide in the areas analyzed.

In all areas of both specimens from pot 11 (1000 ppm $PO_4$), Cl was clearly present. However, Cl was found in only one area of the two pot 7E specimens. When present in quantities above the threshold of detection, Cl was found in a band 20 mils thick beginning anywhere from 2 to 5 mils from the carbon steel/oxide interface. It tended to diminish as distance from the carbon steel increased. Only at the center of Specimen C-7E-4-D was Cl detected near the Alloy 600/oxide interface. In this instance a small amount of Cl was observed 8 mils from the Alloy 600/oxide interface.

The high magnification SEM's showed that the morphology of the magnetite varied significantly, from very smooth textured surfaces that were essentially featureless to very coarse textured surfaces with many large and small pits, pores, cracks, granules and indentations. Data presented in greater detail in Appendix E suggests that the coarse textured magnetite harbored a greater variety of elements, probably because the many surface features provided locations at which these elements could concentrate. In general, the various structures observed were similar to structures usually observed in magnetite on carbon steel exposed to acid chloride environments.

Electron Microprobe Analysis (EMPA) of Support Plate Crevices. Support plate crevices from both pots were examined by EMPA analysis and suplemented with SEM, EDS, and X-ray mapping.

Phosphorus was detected via X-ray mapping at two locations - near the top and bottom of specimen H-7E-4-K from the 3000 ppm $PO_4$ test. In both cases, the phosphorus was in the vicinity

of the I600/magnetite interface. (See Figure 3-39) Although the oxide was scanned in detail, EDS analysis showed P present only at the bottom of the specimen. This descrepancy was probably the result of the different sensitivities of the two methods. X-ray mapping, which is performed by wave length dispersive spectrometry (WDS), is more sensitive to low concentrations.

Phosphorus was not uniformly dispersed through the magnetite, but was concentrated in localized regions. Comparison of tne X-ray maps with the SEM results indicated that P was confined primarily to the areas of the oxide near the Inconel-600 characterized by porosity, cracks, and other discontinuities, where apparently sufficient surface area was available to adsorb a detectable quantity of phosphate from solution. From the EDS results, the concentration of phosphorus was estimated to be 2% by weight. As with all semi-quantitative EDS work, the error band ranges from a factor of 1/2 to 2. Hence the range for P is 1-4%.

Cl was identified and mapped at the center location of each of the support plate specimens. There were indications by X-ray mapping that some Cl was present near the Alloy 600/magnetite interface, but by far the greatest quantity was near the carbon steel interface (See Figure 3-40). Chloride content was estimated at 8% and 5% at two locations in specimen H-11-4-K (1000 ppm $PO_4$ test), and 6% at one location in specimen H-7E-4-K (3000 ppm $PO_4$ test). Again the error band is 1/2 to 2.

Other elements identified by EDS are tabulated in Appendix E and can be attributed to sea salts (Mg, Ca, Mn, S), tne prepacking material (Cu, Ni), the polishing operation, or the base metals.

The morphology of the oxide itself as observed by SEM, was essentially identical to that found in the concentrating ring specimens.

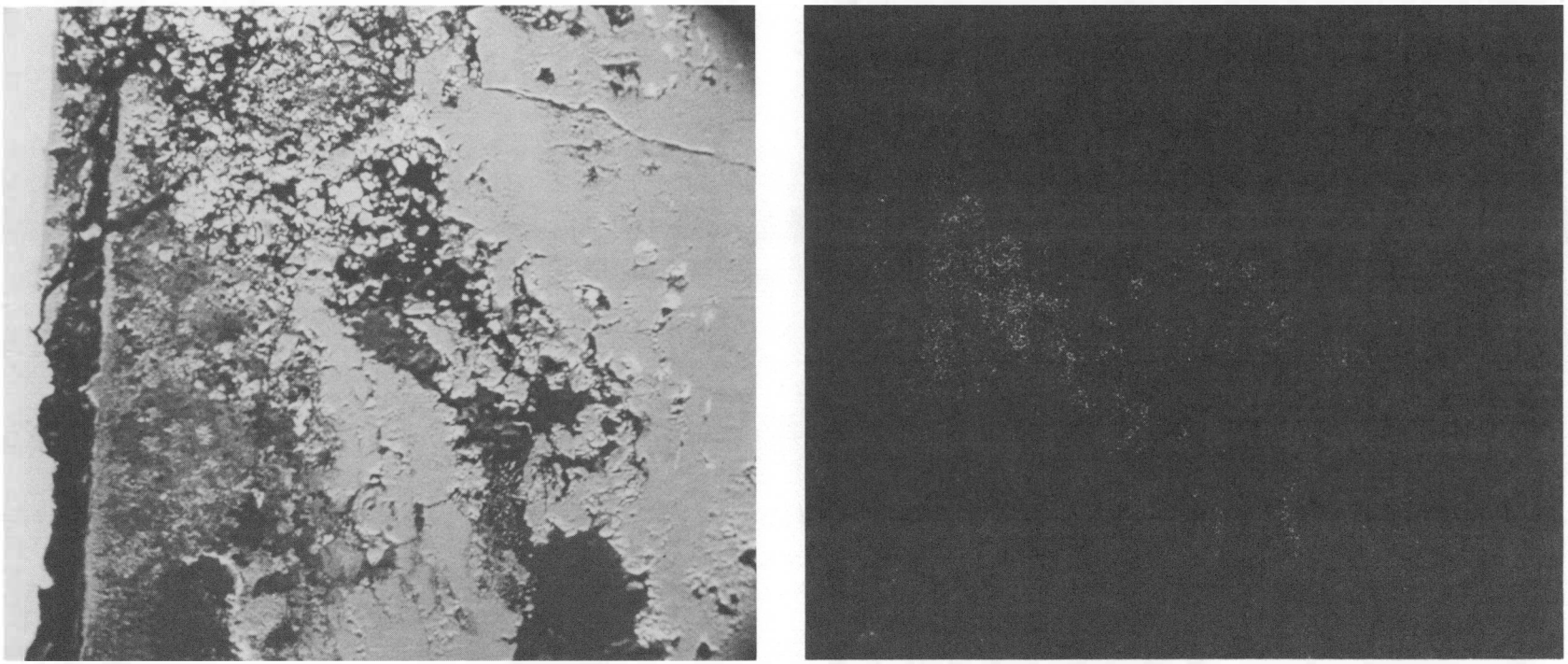

Figure 3-39. SEM and P X-Ray Map of the Area Near the Alloy 600/ Oxide Interface Near the Bottom of Support Plate Specimen H-7E-4-K (150X)*

*Please note that the illustrations on this page have been reduced 10% in printing.

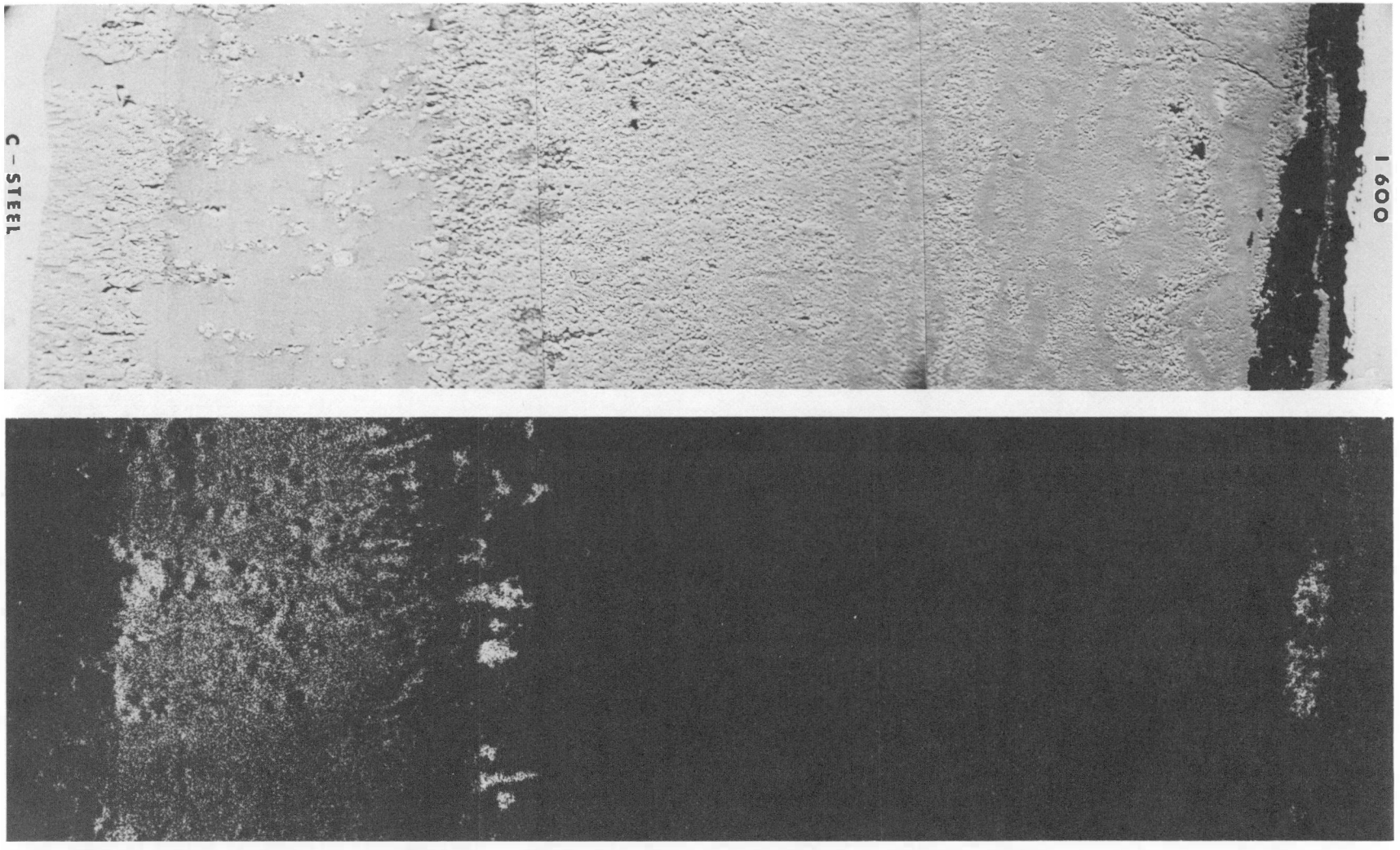


Figure 3-40. SEM and $Cl^-$ X-Ray Map from the Top of Support Plate Specimen H-7E-4-K (150X)*

*Please note that the illustrations on this page have been reduced 10% in printing.

# SECTION 4

# DISCUSSION

## CAPSULE TESTING

The three different fault chemistries which produce capsule bulging are discussed separately in what follows. The C-E reference solution (0.1 M $FeCl_2$) is identical to the solution originally used by Potter and Mann[1] in their work with non-protective magnetite. It contains acidic chloride but no reducible metal species which are found in W/EPRI reference solution (0.1 M $CuCl_2$ + 0.1 M $NiCl_2$ in full strength seawater). The third solution, 0.25 M $FeCl_2$, has the same concentration of acidic chlorides as in the W/EPRI solution, but no reducible metal ions. This solution was tested to evaluate the cause of differences observed in the response of the first two solutions to soaking.

### Capsules Bulged with C-E Reference Solution

All soaks, irrespective of soak conditions, were effective in halting corrosion. None of the soaks possessed endurance; all continued to bulge after being refilled with the denting environment. Similar behavior was observed in all other testing conducted within C-E using this denting environment.[4] Apparently the C-E reference denting environment is sufficiently mild that the denting solution must be maintained in contact with the crevice magnetite in order for capsule bulging to continue. In this respect, these capsules appear to be unlike pot or model boilers, in which dents have continued to grow after chloride-free AVT has been reestablished. Dents in operating steam generators are presumed to be similar to pot and model dents. Any apparent effectiveness of the various tested soak procedures on C-E capsule dents is secondary to the effect of removing the denting environment from the capsule.

Capsules Bulged with W/EPRI Reference Solution

Although denting rates were slowed, all W/EPRI capsules continued to bulge after soaking. A definite relationship was observed between phosphate concentration and degree of reduction in bulging rate in the "Effectiveness" tests at 150°F. This relationship is indicated in Table 4-1 and Figure 4-1. The data were treated in two ways. The post-soak bulging rate was plotted vs. phosphate concentration. This plot, however, does not allow for variation in pre-soak bulging rates which are expected to influence post-soak bulging rates. To account for this, the quotient formed by dividing post-soak bulging rate by the pre-soak bulging rate (rate ratio) was plotted as a function of phosphate concentration. For both plots the X-intercept represents an extrapolation to the phosphate concentration which would be expected to stop bulging. Extrapolation of the post-soak rate data alone yielded a phosphate concentration of 16700 ppm necessary to stop bulging. The rate ratio data indicated a phosphate concentration of 20900 ppm. These extrapolations may not be valid for steam generators and pot boilers inasmuch as the relationship of isothermal capsules bulged with W/EPRI reference solution to actual heat-exchanger devices such as pot boilers and steam generators, has not been established.

Soaks at 565°F were ineffective in reducing bulging rates, even though water soak tests indicated greater chloride release at higher temperatures. The highest phosphate concentration tested was 3000 ppm; the same concentration at 150°F also failed to reduce bulging rate. This observation suggests that a threshold of phosphate concentrations (or total contained phosphate or alkalinity in the capsule) was required in these tests in order to influence bulging rates.

TABLE 4-1

DIAMETRAL W/EPRI BULGING RATES AT 150°F AS
A FUNCTION OF PHOSPHATE CONCENTRATION

ALL CAPSULES BULGED WITH W/EPRI REFERENCE SOLUTION

| Capsule | ppm $PO_4$ | Pre-Soak Denting Rate Mils/day | Post-Soak Denting Rate Mils/day | Rate Ratio Post-Soak/ Pre-Soak |
|---|---|---|---|---|
| II-6 | 0 | 0.39 ± 0.03 | 0.39 ± 0.03 | 1.0 |
| II-8 | 3,000 | 0.32 ± 0.02 | 0.32 ± 0.02 | 1.0 |
| II-10 | 5,000 | 0.43 | 0.22 ± 0.03 | 0.51 |
| II-12 | 10,000 | 0.29 | 0.17 ± 0.04 | 0.59 |

All soak times were 96 hours, and the Na/P mode ratio was 2.8

Linear Regression Parameters for Lines Through These Points

| | Post-Soak Rates | Rate Ratio |
|---|---|---|
| Slope | $-2.25 \times 10^{-5}$ | $-4.72 \times 10^{-5}$ |
| X Intercept | 16,700 | 20,900 |
| Correlation Coefficient | 0.955 | 0.757 |

Figure 4-1

BULGING RATE REDUCTION vs PHOSPHATE CONCENTRATION DATA FROM W/EPRI CAPSULES EFFECTIVENESS TEST AT 150°F

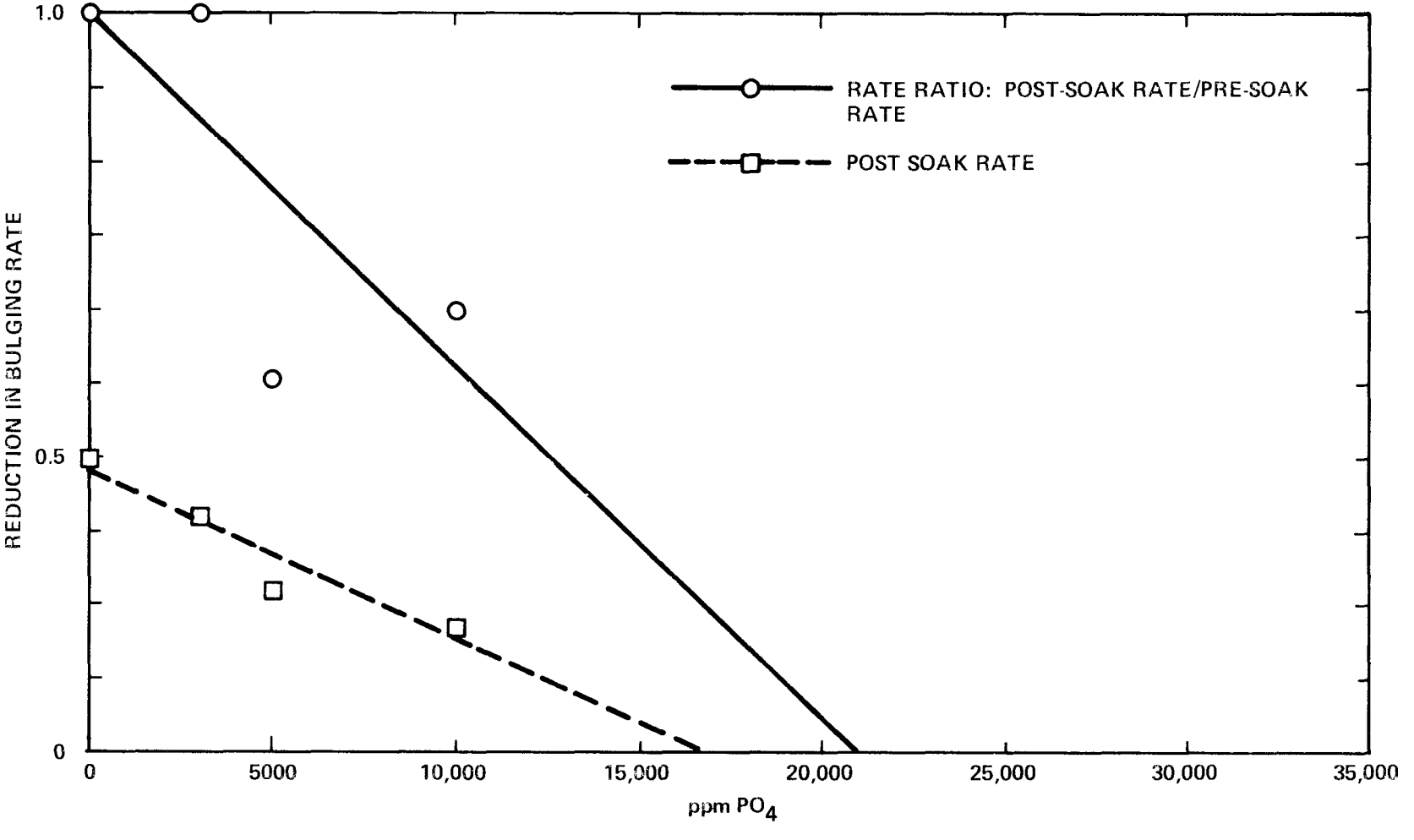

Since none of these soaks was completely effective in halting corrosion, there was no "endurance" in the sense originally conceived. All the "Endurance" tests showed continued growth at rates which could not be correlated with soak conditions. This suggests that post-soak bulging rates were primarily controlled by the post-soak fault environment in the capsules. It also suggests that any reduction in denting rate achieved through phosphate soaking would lack "endurance"; denting rates would be expected to increase again with fresh impurity ingress.

Capsules Bulged with 0.25 M $FeCl_2$.

Capsules bulged with 0.25 M $FeCl_2$ appear to occupy a middle ground between C-E capsules and W/EPRI capsules. The rate at which these capsules bulged was equal to that for C-E capsules, but slower than for W/EPRI capsules. However, while all soaks were effective in C-E capsules, these capsules were similar to W/EPRI capsules in that soaking with either water or solutions of alkaline phosphates produced only sporadic reductions in bulging rate. There was no correlation between rate reduction and neutralizer concentration. Bulging was not halted for any of these capsules. From these observations, it is concluded that the difference in response to soaking observed between the W/EPRI and C-E environment appears to be related to the higher concentration of acidic chloride in the former environment.

## POT BOILER TESTING

In spite of the different physical phenomena utilized in measurements by strain gauges and eddy current, there is a strong correlation between the two techniques. Denting in pot boilers was assessed by both methods. There was no attempt to directly measure tubing diameters. Denting rates as indicated via strain rates are compared in Table 4-2 with eddy current data. A graphic correlation is presented in Figure 4-2. The correlation coefficient, R, is 0.664.

The only pot boiler dent which did not increase during post-soak volatile operation was a tubesheet dent in pot 11. There was no strain gauge in this dent. For this reason it is not shown in Table 4-2.

Reductions in denting rates are readily apparent when post-soak denting rates are divided by pre-soak rates as in Table 4-2 and Figure 4-3. It is seen that reductions of as much as 70% in strain rates were observed. Even greater reductions in denting rate were indicated by eddy current data. These latter observations, however, were based on radial changes of one mil or less which are approximately the same as the experimental uncertainty in eddy current measurements. The strain gauge data are, therefore considered to be more reliable for these crevices.

A definite relationship was observed between phosphate concentration and the degree of reduction in pot boiler denting rates. This is shown in Figure 4-3. Eddy current ratios at any phosphate concentration tended to be smaller than strain gauge ratios. Should a linear relationship between rate ratio and phosphate concentration be assumed, these data can be extrapolated to the X-intercept where the post-neutralization denting rate goes to zero. These extrapolations are indicated in the figure. Working from eddy current data, a phosphate concentration of 4000 ppm should halt denting. Strain gauge data extrapolate to 7100 ppm $PO_4$. All data taken together extrapolated to 5200 ppm $PO_4$.

These extrapolations and those described above for capsule data must be viewed as speculation inasmuch as the assumed linear relationships have not been demonstrated for more concentrated phosphate solutions. There may be reason to doubt such a relationship because residual chlorides appear to be unaffected by the soak procedure as shown below. These residual chlorides, would be expected to reinitiate denting after soaking.

TABLE 4-2

COMPARISON OF STRAIN GAUGE AND EDDY CURRENT DATA FROM POTS

| Crevice Location | Pot 9-Water Soak | | Pot 11-1000 ppm $PO_4$ | | Pot 7E-3000 ppm $PO_4$ | |
|---|---|---|---|---|---|---|
| | Tube 3 Hot Ring | Tube 4 Hot Ring | Tube 4 Hot Ring | Tube 4 Cold Ring | Tube 4 Hot Ring | Tube 4 Cold Ring |
| Strain Rates (μin/in/day) | | | | | | |
| Phase I | 40 | 38 | 25 | 25 | 25 | 32 |
| Phase III | 16 | 32 | 18 | 15 | 8 | 13 |
| Phase III/Phase I Rate Ratio | 0.40 | 0.84 | 0.72 | 0.60 | 0.32 | 0.41 |
| Eddy Current Rates (mil/day) | | | | | | |
| Phase I | 0.17 | 0.09 | 0.16 | 0.20 | 0.15 | 0.15 |
| Phase III | 0.05 | 0.09 | 0.04 | 0.08 | 0.02 | 0.03 |
| Phase III/Phase I Rate Ratio | 0.29 | 1.00 | 0.25 | 0.40 | 0.15 | 0.20 |

Linear Regression Parameters for Line Through all Ratios

Slope = $-1.20 \times 10^{-4}$ $ppm^{-1}$

Y-Intercept = 0.62

R = 0.581

Figure 4-2

POT BOILER CORRELATION OF STRAIN GAUGE DATA AND EDDY CURRENT DATA

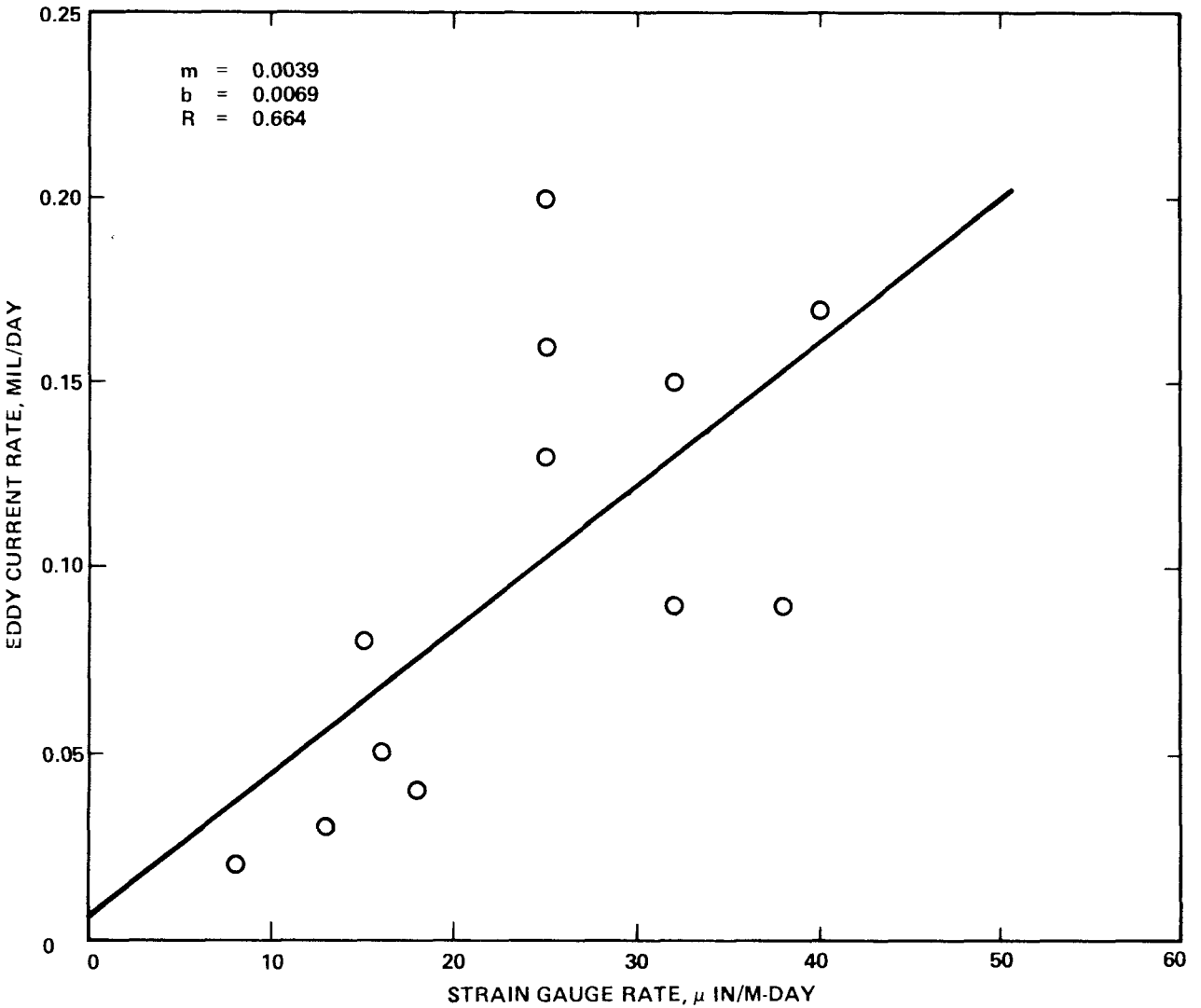

Figure 4-3

DENTING RATE REDUCTION AS A FUNCTION OF PHOSPHATE CONCENTRATION STRAIN GAUGE AND EDDY CURRENT DATA FROM POTS 9, 11, AND 7E

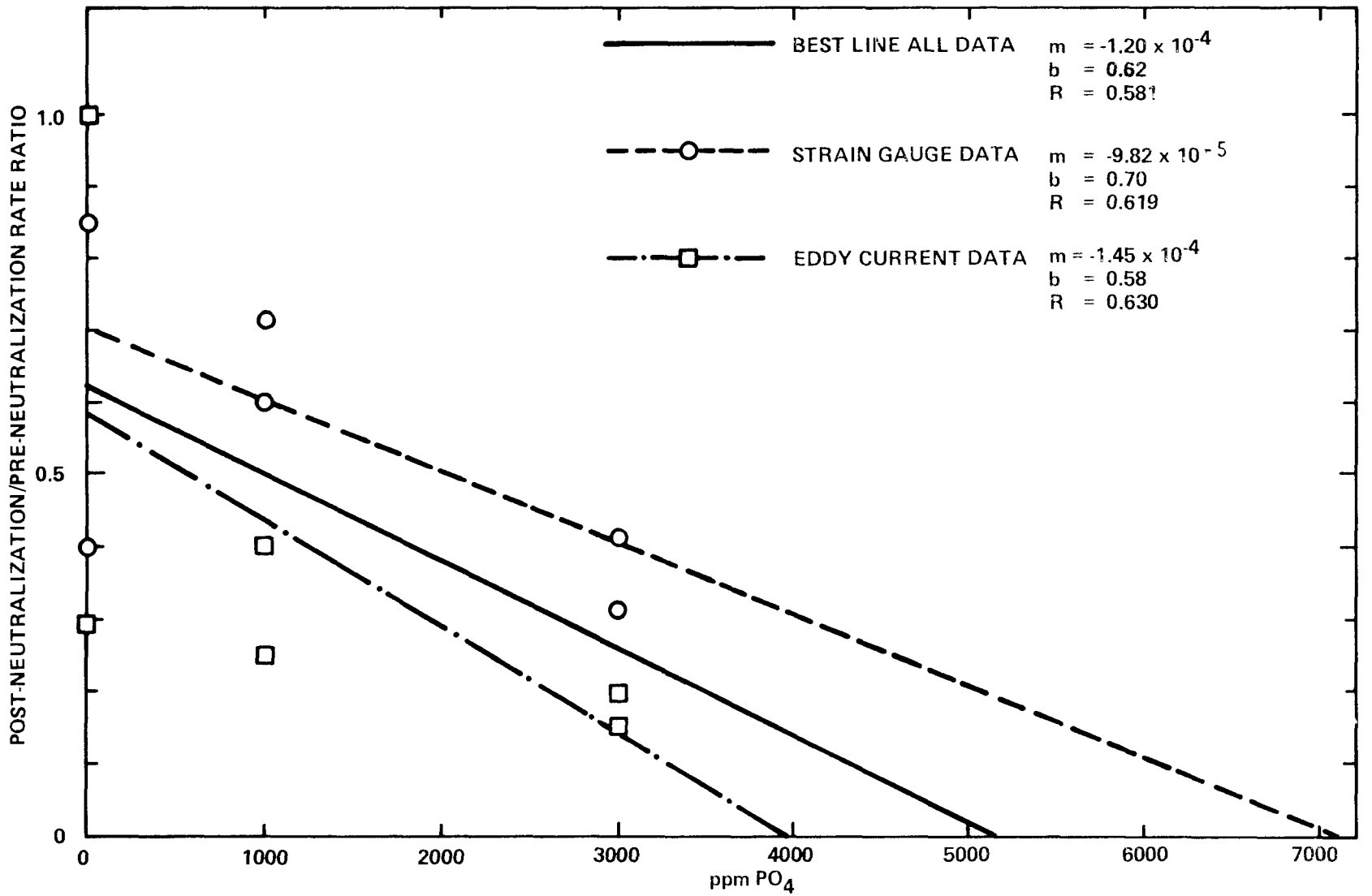

DESTRUCTIVE EXAMINATION

Crevice Chloride and Denting

A striking correlation was observed between continued capsule bulging and chloride residuals within crevice magnetite. C-E capsules (AA-7, Y-1, and Y-11) in which the denting solution had been removed and replaced with hydrazine-treated water, all stopped bulging (see Tables A-6 through A-8 and Figures 3-8 and 3-10). As previously indicated, this behavior is not considered representative of field denting. None of these capsules contained measurable chloride when destructively examined. C-E capsules which had been filled with 0.1 M $FeCl_2$ subsequent to soaking, continued to bulge (see Tables A-6 and A-7 and Figures 3-7 and 3-9). They contained measurable chloride when destructively examined. The chloride residual within these capsules was not uniformly distributed. Instead, chloride was found almost exclusively within a band beginning less than 1 mil from the carbon steel interface and ending about 3 mils from the same interface. In general, this band corresponded to one of the distinct bands observed in the magnetite morphology. Within this band, capsule AA-8 contained 0.4 w/o chloride; capsule Y-10, 2.8 w/o. chloride. In both W/EPRI capsules (DD-7 and DD-8) which were destructively examined, bulging had continued subsequent to soaking (see Table A-9 and Figures 3-11 and 3-12). One of these capsules (DD-7) had been filled with hydrazine-treated water subsequent to soaking and the other (DD-8) had been filled with 0.1 M $FeCl_2$. Both capsules, however, contained residual chloride in a localized band beginning less than 1 mil and ranging out to 6 mils from the carbon steel interface. Within the localized band, capsule DD-7 contained between 1.0 and 10.0 w/o; capsule DD-8, 16.0 w/o.

## Chloride in Pot Boiler Crevices

As indicated in Section 3, all pot boilers continued to dent after the various isothermal soaks. Support-plate dents from two pot boilers were destructively examined, and chloride was found in both crevices. Like the capsules, chloride was localized to a band of magnetite beginning between 2 and 5 mils and ranging out to 20 mils from the carbon steel. Within this band, the chloride in pot 11, which had been soaked with 1000 ppm $PO_4$, was 8.0 w/o; in pot 7E, which had been soaked with 3000 ppm $PO_4$, 5.0 w/o.

## Phosphate in Pot Boiler Crevices

A thorough search for phosphorus was made in all capsule and pot boiler crevices. The detection limit was approximately 1%. No phosphorus was found in any of the capsules, but 1-4 w/o P was observed in one pot boiler crevice. The phosphorus which was found was confined to surface areas, cracks and voids in the vicinity of the I600 interface. There was no indication that phosphate penetrated the magnetite.

# CONCLUSIONS

Reductions of as much as 70% in denting rates were observed, but in no instance was denting stopped by isothermal soaking. This observation is supported by the preceding considerations which may be summarized as follows:

1. Capsule bulging rates were reduced by as much asd 50% as a consequence of isothermal soaking although some capsules continued bulging with no reduction in rate.

2. A correlation between reductions in capsule bulging rates and phosphate concentration was observed.

3. Pot boiler dents continued to increase after soaking at rates reduced by up to 70%.

4. There was a correlation between pot boiler denting rates after soaking, and phosphate concentration.

5. Soaking did not remove residual chlorides from pot boiler crevices, and capsule testing demonstrated that chloride residuals are associated with continued denting.

6. The phosphate neutralizer did not penetrate crevice magnetite beyond surface areas, cracks and voids.

In general, it is concluded that isothermal soaks will not be an effective solution to the denting problem. Consequently no recommendation to utilities has been drawn from this work. Rather it is suggested that techniques to enhance neutralizer penetration of crevice magnetite be evaluated. Such techniques would be pressurization cycling, boiling or application under heat transfer conditions.

REFERENCES


1. E. C. Potter, and G. M. W. Mann, "The Fast Linear Growth of Magnetite on Mild Steel in High-Temperature Aqueous Conditions", British Corrosion Journal 1, pp. 26-35, 1965.

2. G. M. Jouris, M. J. Wootten, and J. T. Patton, PWR Steam Side Chemistry Follow Program - Analysis of Data From Isothermal Capsules EPRI Contract RP699-1 Progress Report, June 1979.

3. M. Wiatrowski. Report on Capsule Testing Conducted by Combustion Engineering Over the Period June 1977 - April 1978 Combustion Engineering Report No. TR-MCD-019.

4. T. A. Beineke, K. E. Marugg, and M. Wiatrowski, Neutralization of Crevice Acids EPRI Contract RP-623-2 Third Progress Report.

5. B. W. Lindgren and G. W. McElrath, "Introduction to Probability and Statistics," Macmillan 1959, p. 231.

6. J. B. Brooks and R. A. Gwinn, Determination and Verification of Required Water Chemistry Limits Combination Third and Fourth Progress Report, July 1979.

Appendix A

# CAPSULE TESTING
# EXPERIMENTAL DETAILS

## EQUIPMENT

### Capsules

Capsules were constructed of Inconel 600 tubing similar to that which is used in C-E nuclear steam generators. The overall design of a capsule is presented in Figure 2-1. The tubing had an outside diameter (OD) of 0.75 in., an inside diameter (ID) of 0.665 in., and generally was cut to lengths of 16 in. A swagelock fitting sealed the bottom. A smaller diameter Inconel 600 tube 2 in. in length was used to support a carbon steel slug. The sleeve was cut lengthwise to improve fluid flow within the capsule. The slug was made from 1018 carbon steel which is similar in composition to support plate material. It was 1.0 in. in length with an OD of 0.635 in., and an ID of 0.375 in. These dimensions provided a radial gap of 15 mils between the slug OD and the capsule ID. After filling, the capsules were sealed at the top with another stainless steel swagelock fitting.

These capsules were designed to contain 30 ml. of test solution. This volume of liquid allowed for fluid expansion at high temperature and, in addition, provided space for the accumulation of hydrogen gas which was evolved during corrosion of the carbon steel slug.

### Furnace

Capsules were heated to test temperatures in a Grieve furnace with an automatic temperature controller. To assure that the temperature controller correctly maintained the furnace

temperature, a temperature profile was measured on February 8, 1979. It consisted of placing 27 calibrated thermocouples at various points inside the furnace. The temperature was set at 550°F and was read and recorded over a period of two hours. The average temperature was 564°F, while the difference between the highest and lowest reading was only 8.5°F, indicating uniform temperature distribution in the furnace.

## PROCEDURES

The testing sequence for evaluating isothermal soaks consisted of three phases: dent (or bulge) initiation, neutralizer/soak application, and post-soak application. These are discussed following the general procedures below.

### General

Capsule diameters at the elevation of the slug were measured after each week of furnace time following the initial two weeks. The recorded measurement was an average of five different measurements made at different angles around the circumference of the capsule. The accuracy of the average measurement was estimated at $\pm$ 1 mil.

Whenever any capsule showed an increase of five mils on its OD, it was opened and the accumulated hydrogen gas was vented to the atmosphere. Venting was necessary in order to prevent a buildup of pressure to levels where capsule failure could occur. Venting upon each five mil dent increase was designed to keep the pressure inside the capsules below 2,500 psia. After venting, the upper swagelock fitting was cut off reducing capsule length by one inch, and a new fitting installed. Capsules were then refilled with fresh solution.

All capsule fillings and most drains (except for vents, above) were done in an Argon filled glove box to exclude air. For those tests where chemical mass balances were desired, the volumes of all rinses and drains were measured and the solutions saved for analyses of chloride and when appropriate, sodium and phosphate.

## Phase I - Dent Initiation

Prior to testing, each capsule's ID (inside diameter) and OD (outside diameter) were measured with a micrometer to the nearest 0.001 inch. Each carbon steel slug was cleaned in acetone, then measured in length and on its OD and ID. In addition, each slug was weighed to the nearest 0.00001 gram. The capsule was then assembled and permanently marked with an alpha-numeric code indicating the test series and capsule number.

Each capsule was filled with 30 mls of the denting solution (discussed below) and sealed with a swagelock cap. The capsules were then inserted into the furnace which was maintained at 565°F. Following the initial two weeks, each capsule was removed from the furnace and the diameter at the elevation of the slug measured. Generally about three weeks of furnace time were required to produce from 1 to 5 mils of diametral bulging.

One of the following solutions was used to initiate capsule bulging.

- C-E Reference Denting Environment

  0.1 M $FeCl_2$

  This environment had been selected as the simplest, yielding corrosion similar to that in the field.

Potter and Mann[1] had studied the "fast linear growth of magnetite" on carbon steel in this environment.

- W/EPRI Reference Denting Environment

  0.1 M $CuCl_2$ and 0.1 M $NiCl_2$ dissolved in full strength seawater (Table A-1)

  This environment had been developed through testing conducted under Task 310 of EPRI Research Project RP 699-1, "PWR Steam Side Chemistry Follow Program." Dents produced from this environment were intended to simulate field dents in chemical composition.

- 0.25 M $FeCl_2$

  This environment contained the same concentration of reducible or hydrolyzable chloride salts as the W/EPRI environment. Bulging rates and soak/neutralization effects on these dents could be compared to those from other environments, in order to gain information on the role of reducible chlorides, total chloride, and other impurities on denting and dent neutralization.

- 0.05 M $FeCl_2$ in Full Strength Seawater

  This environment contained the same concentration of reducible or hydrolyzable chloride salts as the C-E environment, and again was intended to gain additional information on parameters affecting denting and neutralizations.

TABLE A-1

CHEMICAL ANALYSIS OF THE SEAWATER USED FOR DENT INITIATION

| | |
|---|---|
| pH | 7.9 |
| Conductivity @ 72°F ( μmhos) | 45,000 |
| P Alkalinity (as $CaCO_3$) | 0 |
| Alkalinity (as $CaCO_3$) | 172 ppm |

| | ppm |
|---|---|
| Sulfate $SO_4$ | 2,600 |
| Bicarbonate $HCO_3$ | 210 |
| Chloride Cl | 18,250 |
| Phosphate $PO_4$ | < 1.0 |
| TOTAL ANIONS | 21,060 |
| Calcium Ca | 768 |
| Magnesium Mg | 1,051 |
| Sodium Na | 9,750 |
| Potassium K | 515 |
| TOTAL CATIONS | 12,084 |
| Silica $SiO_2$ | < 1.0 |
| TOTAL Dissolved Solids @ 105°C | 34,900 |
| Suspended Solids | < 1.0 |

Phase II - Isothermal/Soaking

Following dent initiation, the capsules were subject to a series of operations which generally included the following:

- pre-flushing to remove residual impurities adsorbed onto exposed interior surfaces;
- isothermal soaking in either the Grieve furnace ($565^{o}F$) or a constant temperature water bath ($150^{o}F$);
- post-flushing to remove residual neutralizer and/or impurities eluted during the soak.

Pre-flushing. Capsules were drained and rinsed twice (one minute per rinse) with demineralized water containing 200 ppm $N_2H_4$. All capsules except those of Series "BB" (the Water Soak tests) were then placed into wet layup for 24 hours to provide further assurance that only crevice impurities remained prior to phosphate neutralization testing. Wet layup conditions were as follows:

$200 \pm 50$ ppm $N_2H_4$
pH $\sim$ 10
$150^{o}F$
24 hrs.

Isothermal Soaking. Capsules were filled with 30 ml of the appropriate soak solution and placed in either a constant temperature bath (for $150^{o}F$ soaks) or back into the furnace (for high temperature soaks) for the required period of time.

Post-Flushing. Capsules were drained and the Pre-flushing procedure was repeated.

Phase III - Post Soak Testing

Capsules were drained and refilled with one of the solutions below in an inert environment, then sealed and placed into the Grieve furnace for an additional three to four weeks. Diametral measurements were taken weekly, and the capsules vented as appropriate, following the procedures for Phase I.

Effectiveness Tests. Capsules were refilled with demineralized water containing 20 ppm $N_2H_4$. The hydrazine was added to consume oxygen in the demineralized water. Residual hydrazine would decompose to ammonia at temperature, providing an environment simulating volatile chemistry control.

Endurance Tests. Capsules were refilled with demineralized water containing 0.1 M $FeCl_2$ to simulate a fault chemistry environment.

TEST CONDITIONS

Capsule tests can be grouped into three general areas: evaluation of water soaks; evaluation of soaks in alkaline phosphate solutions; and evaluation of capsule denting environments.

Water Soaks

A total of 12 capsules were used in evaluating water soaks.

Bulging was initiated with W/EPRI reference denting solution. The parameters evaluated were soaking time and soaking temperature.

| Temperature | $150^{o}F$ | $565^{o}F$ |
|---|---|---|
| Time in hours | 24, 96, 168 | 24, 96, 168 |
| Soak Chemistry | 200 $\pm$ 50 ppm $N_2H_4$ pH = 10.0 | $\sim$ 20 ppm $N_2H_4$ |

Both effectiveness and endurance testing were carried out.

Alkaline Phosphate Soaks

Capsules Bulged with 0.1 M $FeCl_2$. A total of 31 capsules were reverse dented with the C-E reference denting solution. Four of these were retained as "controls," and the remainder were subsequently subjected to various alkaline phosphate neutralizers. The controls were soaked for 96 hours at $150^{o}F$ in wet layup solution; otherwise they were handled in the same manner as the test capsules. Controls were used to separate the effect of the alkaline phosphate neutralization from that of water soaking alone.

Of the 31 phosphate test capsules, four were controls. Hence, 27 different variations of useful data on phosphate neutralization were obtained. The several parameters which were varied are summarized below:

| Temperature | $150^{o}F$ | $565^{o}F$ |
|---|---|---|
| Time in hours | 24, 96 | 24, 96 |
| Sodium/Phosphate molar ratio | 2.4, 2.8 | 2.5 |
| ppm $PO_4$ | 300, 1000, 3000 | 50, 300 |

In addition to effectiveness, these neutralizers were tested for endurance with the reintroduction of impurities.

Capsules Reverse Dented with W/EPRI Reference Dent Solution A total of twenty capsules were reverse dented with W/EPRI reference denting solution. They were subsequently subjected to various alkaline phosphate neutralizers. Of the twenty capsules, two were controls. One capsule was empty at the end of the denting phase. Hence seventeen different variations of useful data were obtained. The several parameters which were varied are summarized below:

| | | |
|---|---|---|
| Temperature | 150°F | 565°F |
| Time in hours | 24, 96 | 24, 96 |
| Sodium/Phosphate molar ratio | 2.8 | 2.5 |
| ppm $PO_4$ | 1000, 3000 5000, 10,000 | 50, 300, 1000,3000 |

In addition to effectiveness, these neutralizers were tested for endurance with the reintroduction of impurities.

Alternate Denting Environments

In addition to the standard C-E and W/EPRI reference denting environments, twenty-four capsules were used to evaluate denting solutions which were presumed to be more corrosive than C-E reference solution but less corrosive than W/EPRI reference solution. Twelve capsules were filled with 0.05 M $FeCl_2$ in full strength seawater, and twelve capsules were filled with 0.25 M $FeCl_2$ in demineralized water. The former solution did not produce capsule bulging throughout the sixty-two day test period. All carbon steel slugs, however, were frozen in the I600 tubing. No soaking tests were conducted on these capsules. Capsules containing 0.25 M $FeCl_2$ bulged in a manner similar to the standard C-E and W/EPRI reference solutions. These capsules were subjected to various alkaline phosphate neutralizers. Of the twelve capsules, two were controls. Ten different variations of

useful neutralization data were obtained. The several parameters which were varied are summarized below:

| | | |
|---|---|---|
| Temperature | 150°F | 565°F |
| Time in hours | 96 | 96 |
| Sodium/Phosphate molar ratio | 2.8 | 2.5 |
| ppm $PO_4$ | 300, 1000, 3000, 10,000 | 300 |

In addition to effectiveness, these neutralizers were tested for endurance with the reintroduction of impurities.

## DATA

### Capsule Bulging Measurements

Pre-soak capsule bulging data are presented for all capsules in Tables A-2 through A-4. Post-soak data for the water soak tests are presented in Table A-5. Data for C-E capsules soaked with alkaline sodium phosphate solutions are listed in Tables A-6 through A-8. Similar data for W/EPRI capsules soaked with alkaline sodium phosphate are tabulated in Tables A-9 through A-11. Phosphate soak data for capsules bulged with 0.25 M $FeCl_2$ are presented in Tables A-12 and A-13. Bulging rates before and after soaking are compared for all capsules in Table A-14. For each capsule, the soak conditions are presented followed by pre-soak and post-soak bulging rates if there was a significant reduction. If there was no significant reduction in bulging rate, the overall bulging rate for all data from the given capsule is presented, under the heading, "All Data."

### Chemical Mass Balance Data

Chemical mass balance calculations require a complete

accounting of all materials added to and removed from each capsule. Accurate measurements of volume and concentration are required for each solution added to or removed from every capsule. The volume in mls. times the concentration in ppm yields the absolute number of milligrams of a given chemical species.

Volumes and concentrations were measured by standard techniques. The volume of every solution added to or removed from a capsule was measured in a graduated cylinder to $\pm$ 1 ml. Chloride concentration was determined with a chloride specific ion electrode. Phosphate was measured via flameless atomic absorption spectroscopy.

Masses in milligrams of chloride and phosphate are tabulated in Tables A-15 through A-17. During phase I - dent initiation and during the pre-soak rinses and pre-soak wet lay-up steps, chloride and phosphate analyses were performed on combined solutions for capsule series BB and DD. That is capsules 1 and 2 were combined as were 3 and 4, etc. since the chemistries were identical up to this point. Some of the analytical data are not available as a consequence of sampling errors. These instances have been entered as dashes in the tables. All zeros in the tables mean either that the mass of chloride was less than 1 milligram (the lower limit of detection) or that no chloride was added. For example, the zeros in rows 5 and 6 of column 7 in Table A-15 indicate that chloride was below the limit of detection. The zeros in column 9 indicate that chloride-free volatile chemistry was added.

TABLE A-2
CAPSULE PRE-SOAK BULGING RATES FOR C-E REFERENCE SOLUTION *
DIAMETRAL INCREASE IN MILS AS A FUNCTION OF TIME
ALL CAPSULES REVERSE DENTED WITH 0.1 M $FeCl_2$

| CAPSULE | DIAMETRAL GAP MILS † | DAYS AT 565°F 14 | 21 | 26 | 31 | BULGING RATE MILS/DAY | X-INTERCEPT | GAP FILL RATE MILS/DAY |
|---|---|---|---|---|---|---|---|---|
| Y-1 | 32 | 2** | 5 | | 8 | 0.35 | 8.7 | 3.7 |
| Y-2 | 31 | 3 | 7 | | 11 | 0.47 | 7.0 | 4.4 |
| Y-3 | 33 | 0 | 2 | | 3 | 0.10 | 1.0 | 33.0 †† |
| Y-4 | 31 | 0 | 2 | | 4 | 0.20 | 11.0 | 2.8 |
| Y-9 | 31 | 1 | 3 | | 5 | 0.23 | 9.1 | 3.4 |
| Y-10 | 34 | 0 | 1 | | 3 | 0.20 | 16.0 | 2.1 |
| Y-11 | 28 | 2 | 5 | | 9 | 0.41 | 9.0 | 3.1 |
| Y-12 | 33 | 0 | 1 | | 3 | 0.20 | 16.0 | 2.1 |
| Z-1 | 30 | 3 | | 9 | | 0.50 | 8.0 | 3.8 |
| Z-2 | 30 | 0 | | 3 | | – | – | – |
| Z-3 | 29 | 2 | | 8 | | 0.50 | 10.0 | 2.9 |
| Z-4 | 31 | 3 | | 8 | | 0.42 | 6.8 | 4.6 |
| Z-5 | 31 | 0 | | 3 | | – | – | – |
| Z-6 | 31 | 3 | | 8 | | 0.42 | 6.8 | 4.6 |
| Z-7 | 30 | 1 | | 3 | | 0.17 | 8.0 | 3.8 |
| Z-8 | 29 | 3 | | 8 | | 0.42 | 6.8 | 4.3 |
| Z-9 | 31 | 3 | | 9 | | 0.50 | 8.0 | 3.9 |
| Z-10 | 31 | 3 | | 8 | | 0.42 | 6.8 | 4.6 |
| Z-11 | 31 | 2 | | 7 | | 0.42 | 9.2 | 3.4 |
| Z-12 | 31 | 2 | | 8 | | 0.50 | 10.0 | 3.1 |
| AA-1 | 30 | 0 | | 3 | | – | – | – |
| AA-2 | 32 | 2 | | 8 | | 0.50 | 10.0 | 3.2 |
| AA-3 | 31 | 1 | | 4 | | 0.25 | 10.0 | 3.1 |
| AA-4 | 32 | 0 | | 3 | | – | – | – |
| AA-5 | 30 | 3 | | 8 | | 0.42 | 6.8 | 4.4 |
| AA-6 | 30 | 4 | | 9 | | 0.42 | 4.4 | 6.8 |
| AA-7 | 30 | 2 | | 5 | | 0.25 | 6.0 | 5.0 |
| AA-8 | 31 | 0 | | 3 | | – | – | – |
| AA-9 | 32 | 0 | | 2 | | – | – | – |
| AA-10 | 31 | 3 | | 8 | | 0.42 | 6.8 | 4.6 |
| A-11 | 31 | 1 | | 4 | | 0.25 | 10.0 | 3.1 |
| AA-12 | 30 | 3 | | 8 | | 0.42 | 6.8 | 4.4 |
| MEAN | 30.9 | | | | | 0.36 | 8.4 | 3.8 |
| $\sigma$ | 1.2 | | | | | 0.12 | 3.0 | 1.0 |
| N | 32 | | | | | 26 | 26 | 25 |

* C-E REFERENCE SOLUTION IS 0.1 M $FeCl_2$

** THE TABULATED VALUES ARE THE TOTAL DIAMETRAL INCREASE IN MILS. EACH VALUE IS THE AVERAGE OF A MINIMUM OF FIVE INDEPENDENT MICROMETER MEASUREMENTS

† THERE WAS NO ATTEMPT TO CENTER THE PLUG WITHIN THE CAPSULE

†† THE DENT RATE BETWEEN DAYS 21 AND 31 WAS SO SLOW THAT THE X-INTERCEPT (DAY 1) OBTAINED BY EXTRAPOLATION, WHEN DIVIDED INTO THE DIAMETRAL GAP RESULTED IN AN UNREASONABLY HIGH GAP FILL RATE. THIS RATE IS MORE THAN 3 $\sigma$ GREATER THAN THE MEAN GAP FILL RATE, AND WAS THEREFORE REJECTED

MEAN RADIAL GAP FILL RATE = 1.9 ± 0.5 MILS/DAY

RADIAL BULGING RATE GEOMETRIC MEAN = 0.16 ± 0.06 MILS/DAY

TABLE A-3

CAPSULE BULGING RATE FOR W/EPRI REFERENCE SOLUTION *

DIAMETRAL INCREASE IN MILS AS A FUNCTION OF TIME

ALL CAPSULES REVERSE DENTED WITH W/EPRI REFERENCE SOLUTION

| CAPSULE | DIAMETRAL GAP MILS † | DAYS AT 565°F 10 | 14 | 17 | 19 | 21 | 26 | BULGING RATE MILS/DAY | X-INTERCEPT | GAP FILL RATE MILS/DAY |
|---|---|---|---|---|---|---|---|---|---|---|
| BB-1 | 29 | 0** | | | 3 | | 7 | 0.57 | 13.7 | 2.1 |
| BB-2 | 29 | 0 | | | 3 | | 8 | 0.71 | 14.8 | 2.0 |
| BB-3 | 30 | 1 | | | 4 | | 7 | 0.37 | 8.6 | 3.5 |
| BB-4 | 31 | 0 | | | 4 | | 8 | 0.57 | 12.0 | 2.6 |
| BB-5 | 31 | 1 | | | 4 | | 7 | 0.37 | 8.6 | 3.6 |
| BB-6 | 32 | 0 | | | 4 | | 9 | 0.71 | 13.4 | 2.4 |
| BB-7 | 31 | 1 | | | 4 | | 7 | 0.37 | 8.6 | 3.6 |
| BB-8 | 29 | 1 | | | 4 | | 7 | 0.37 | 8.6 | 3.4 |
| BB-9 | 31 | 1 | | | 4 | | 7 | 0.37 | 8.6 | 3.6 |
| BB-10 | 29 | 0 | | | 4 | | 9 | 0.71 | 13.4 | 2.2 |
| BB-11 | 31 | 1 | | | 4 | | 7 | 0.37 | 8.6 | 3.6 |
| BB-12 | 30 | 1 | | | 3 | | 6 | 0.31 | 8.5 | 3.5 |
| DD-1 | 27 | | 3 | 4 | | | | 0.33 | 5.0 | 5.4 |
| DD-2 | 28 | | 3 | 5 | | | | 0.67 | 9.5 | 2.9 |
| DD-3 | 29 | | 3 | 4 | | | | 0.33 | 5.0 | 5.8 |
| DD-4 | 26 | | 4 | 5 | | | | 0.33 | 2.0 | 13.0 †† |
| DD-5 | 29 | | 3 | 4 | | | | 0.33 | 5.0 | 5.8 |
| DD-6 | 30 | | 4 | 6 | | | | 0.67 | 8.0 | 3.8 |
| DD-8 | 27 | | 3 | 5 | | | | 0.67 | 9.5 | 2.8 |
| DD-9 | 29 | | 4 | 7 | | | | 1.00 †† | 10.0 | 2.9 |
| DD-10 | 28 | | 4 | 6 | | | | 0.67 | 8.0 | 3.5 |
| DD-11 | 29 | | 3 | 4 | | | | 0.33 | 5.0 | 5.8 |
| DD-12 | 29 | | 2 | 3 | | | | 0.33 | 7.9 | 3.7 |
| II-1 | 32 | | 2 | | | 5 | | 0.43 | 9.3 | 3.4 |
| II-2 | 32 | | 2 | | | 5 | | 0.43 | 9.3 | 3.4 |
| II-3 | 30 | | 2 | | | 5 | | 0.43 | 9.3 | 3.2 |
| II-4 | 30 | | 3 | | | 5 | | 0.29 | 3.5 | 8.6 |
| II-5 | 30 | | 3 | | | 5 | | 0.28 | 3.5 | 8.6 |
| II-6 | 30 | | 2 | | | 4 | | 0.29 | 7.0 | 4.3 |
| II-7 | 28 | | 3 | | | 6 | | 0.43 | 7.0 | 4.0 |
| II-8 | 28 | | 3 | | | 5 | | 0.29 | 3.5 | 8.0 |
| II-9 | 28 | | 3 | | | 5 | | 0.29 | 3.5 | 8.0 |
| II-10 | 32 | | 2 | | | 5 | | 0.43 | 9.3 | 3.4 |
| II-11 | 30 | | 2 | | | 4 | | 0.29 | 7.0 | 4.3 |
| II-12 | 30 | | 3 | | | 5 | | 0.29 | 3.5 | 8.6 |
| MEAN | 29.6 | | | | | | | 0.43 | 8.0 | 4.3 |
| $\sigma$ | 1.4 | | | | | | | 0.15 | 3.2 | 2.0 |
| N | 35 | | | | | | | 34 | 35 | 34 |

* W/EPRI REFERENCE SOLUTION IS 0.1 M $CuCl_2$ + 0.1 M $NiCl_2$ IN FULL STRENGTH TURKEY POINT SEAWATER

** THE TABULATED VALUES ARE THE TOTAL DIAMETRAL INCREASE IN MILS. EACH VALUE IS THE AVERAGE OF A MINIMUM OF FIVE INDEPENDENT MICROMETER MEASUREMENTS

† THERE WAS NO ATTEMPT TO CENTER THE PLUG WITHIN THE CAPSULE

†† THESE VALUES WERE REJECTED BECAUSE THEY WERE MORE THAN 3 $\sigma$ GREATER OR SMALLER THAN THE MEAN

RADIAL GAP FILL RATE ARITHMETIC MEAN = 22% MILS/DAY

RADIAL BULGING RATE GEOMETRIC MEAN = 0.20 ± 0.08 MILS/DAY

TABLE A-4

CAPSULE BULGING RATES FOR 0.25 M $FeCl_2$

DIAMETRAL INCREASE IN MILS AS A FUNCTION OF TIME

ALL CAPSULES REVERSE DENTED WITH 0.25 M $FeCl_2$

| CAPSULE | DIAMETRAL GAP MILS † | DAYS AT 565°F 14 | 21 | BULGING RATE MILS/DAY | X-INTERCEPT | GAP FILL RATE MILS/DAY |
|---|---|---|---|---|---|---|
| KK-1 | 32 | 1* | 4 | 0.43 | 11.7 | 2.7 |
| KK-2 | 33 | 1 | 2 | 0.14 | 7.0 | 4.7 |
| KK-3 | 35 | 2 | 3 | 0.14 | 0.0 | – |
| KK-4 | 31 | 2 | 4 | 0.29 | 7.0 | 4.4 |
| KK-5 | 31 | 3 | 6 | 0.43 | 7.0 | 4.4 |
| KK-6 | 29 | 3 | 5 | 0.29 | 3.5 | 8.3 |
| KK-7 | 29 | 3 | 5 | 0.29 | 3.5 | 8.3 |
| KK-8 | 31 | 2 | 4 | 0.29 | 7.0 | 4.4 |
| KK-9 | 32 | 2 | 4 | 0.29 | 7.0 | 4.6 |
| KK-10 | 31 | 3 | 7 | 0.57†† | 8.7 | 3.6 |
| KK-11 | 29 | 2 | 4 | 0.29 | 7.0 | 4.1 |
| KK-12 | 33 | 2 | 4 | 0.29 | 7.0 | 4.7 |
| MEAN | 31.3 | | | 0.29 | 6.4 | 4.9 |
| $\sigma$ | 1.8 | | | 0.09 | 2.9 | 1.8 |
| N | 12 | | | 11 | 12 | 11 |

* THE TABULATED VALUES ARE THE TOTAL DIAMETRAL INCREASE IN MILS. EACH VALUE IS THE AVERAGE OF A MINIMUM OF FIVE INDEPENDENT MICROMETER MEASUREMENTS

† THERE WAS NO ATTEMPT TO CENTER THE PLUG WITHIN THE CAPSULE

†† THIS VALUE WAS REJECTED BECAUSE IT WAS MORE THAN 3 $\sigma$ GREATER THAN THE MEAN

RADIAL GAP FILL RATE MEDIAN = 2.2 ± 0.9 MILS/DAY

MEAN RADIAL BULGING RATE = 0.14 ± 0.04 MILS/DAY

TABLE A-5

WATER SOAK TEST

DIAMETRAL INCREASE (IN MILS) AS A FUNCTION OF TIME FOR W /EPRI DENTS

| CAPSULE | T°F | HRS | POST SOAK | DAYS AT TEMPERATURE | | | | | | | | | | | | | | | | | | | | | |
|---|---|---|---|---|---|---|---|---|---|---|---|---|---|---|---|---|---|---|---|---|---|---|---|---|---|
| | | | | 10 | 17 | 24 | | 26 | 27 | 29 | 30 | 32 | 33 | 35 | 36 | 39 | 43 | 45 | 46 | 47 | 48 | 49 | 50 | 51 |
| BB-2 | 150° | 24 | VOLATILE | 0 | 3 | 8 | WATER SOAK | | | | 12 | 13 | | 15 | | 18 | | | | | | 19 | | 19 |
| BB-6 | | 96 | | 0 | 4 | 9 | | | 11 | 12 | | 14 | | | 16 | | | | 16 | | 16 | | 16 | |
| BB-10 | | 168 | | 0 | 4 | 9 | | 10 | | 12 | | | 14 | | | | 17 | 17 | | 18 | | | 18 | |
| BB-1 | | 24 | FAULT | 0 | 3 | 7 | | | | | 11 | 12 | | 13 | | 15 | | | | | | 18 | | 19 |
| BB-5 | | 96 | | 1 | 4 | 7 | | | 8 | 8 | | 8 | | | 9 | | | | 12 | | 12 | | 13 | |
| BB-9 | | 168 | | 1 | 4 | 7 | | 8 | | 8 | | | 9 | | | | 11 | 12 | | 13 | | | 15 | |

| | | | | DAYS AT TEMPERATURE | | | | | | | | | | | | | | | | | | | | | |
|---|---|---|---|---|---|---|---|---|---|---|---|---|---|---|---|---|---|---|---|---|---|---|---|---|---|
| | | | | 10 | 17 | 24 | | | | 31 | | 33 | | 36 | | 40 | | 50 | 52 | | 54 | | 57 | | |
| BB-4 | 565° | 24 | VOLATILE | 0 | 4 | 8 | WATER SOAK | | | 13 | | 14 | | 16 | | 18 | | 19 | 20 | | | | | | |
| BB-8 | | 96 | | 1 | 4 | 7 | | | | 8 | | 9 | | 10 | | 12 | | 14 | 15 | | 16 | | | | |
| BB-12 | | 168 | | 1 | 3 | 6 | | | | 8 | | 8 | | 9 | | 11 | | 13 | 13 | | 14 | | 15 | | |
| BB-3 | | 24 | FAULT | 1 | 4 | 7 | | | | 8 | | 8 | | 9 | | 11 | | 14 | 14 | | | | | | |
| BB-7 | | 96 | | 1 | 4 | 7 | | | | 8 | | 8 | | 9 | | 11 | | 14 | 15 | | 16 | | | | |
| BB-11 | | 168 | | 1 | 4 | 7 | | | | 9 | | 9 | | 9 | | 11 | | 14 | 14 | | 15 | | 16 | | |

NOTES:

THE WATER SOAK WAS INITIATED ON THE 24TH DAY. HENCE THE FIRST THREE COLUMNS PRESENT DATA FROM THE DENTING PHASE, AND THE REMAINING COLUMNS PRESENT DATA FROM THE POST-SOAK PHASE.

ALL CAPSULES WERE EXPOSED TO W/EPRI REFERENCE DENTING SOLUTION (0.1 M $Ni\,Cl_2$ + 0.1 M $Cu\,Cl_2$ IN FULL STRENGTH SEAWATER) AT 565°F FOR 24 DAYS TO PRODUCE 7 TO 8 MILS OF DIAMETRAL INCREASE PRIOR TO SOAKING

CAPSULES SOAKED AT 150°F CONTAINED WET LAYUP CHEMISTRY (200 ± 50 PPM $N_2H_4$; pH = 10.0); CAPSULES SOAKED AT 565°F CONTAINED VOLATILE CHEMISTRY (20 PPM $N_2H_4$); POST-SOAK FAULT CHEMISTRY WAS 0.1 M $Fe\,Cl_2$.

TABLE A-6

PHOSPHATE SOAK TEST AT 150°F

DIAMETRAL INCREASE (IN MILS) AS A FUNCTION OF TIME

ALL CAPSULES REVERSE DENTED WITH C-E REFERENCE SOLUTION

| CAPSULE | ppm $PO_4$ | Na/P | HRS | POST SOAK | DAYS AT TEMPERATURE 14 | 26 | | 27 | 30 | 35 | 38 | 40 | 43 | 47 | 50 | 51 | 54 |
|---|---|---|---|---|---|---|---|---|---|---|---|---|---|---|---|---|---|
| Z-2 | 300 | 2.4 | 24 | VOLATILE CHEMISTRY | 0 | 3 | | | | | 3 | | 4 | | 4 | | 4 |
| Z-4 | 300 | 2.4 | 96 | | 3 | 8 | | | | 9 | | 9 | | 9 | | 9 | 9 |
| Z-6 | 300 | 2.8 | 24 | | 3 | 8 | | | | | 8 | | 8 | | 8 | | 9 |
| Z-8 | 300 | 2.8 | 96 | | 3 | 8 | | | | 8 | | 8 | | 8 | | 9 | 9 |
| Z-10 | 1000 | 2.4 | 24 | | 3 | 8 | | | | | 9 | | 9 | | 9 | | 9 |
| Z-12 | 1000 | 2.4 | 96 | | 2 | 8 | | | | 8 | | 8 | | 8 | | 8 | 8 |
| AA-3 | 1000 | 2.8 | 24 | | 1 | 4 | | | 5 | | | | 5 | | 5 | | 5 |
| AA-7 | 1000 | 2.8 | 96 | | 2 | 5 | | 5 | | | | 5 | | 5 | | 5 | 5 |
| AA-9 | 3000 | 2.4 | 24 | | 0 | 2 | | | 2 | | | | 2 | | 2 | | 2 |
| AA-11 | 3000 | 2.4 | 96 | | 1 | 4 | | 4 | | | | 4 | | 4 | | 4 | 4 |
| Z-3 | 300 | 2.4 | 24 | FAULT | 2 | 8 | | | | | 15 | | 17 | | 20 | | 22 |
| Z-5 | 300 | 2.4 | 96 | | 0 | 3 | | | | 7 | | 8 | | 12 | | 14 | 15 |
| Z-7 | 300 | 2.8 | 24 | | 1 | 3 | | | | | 9 | | 10 | | 13 | | 14 |
| Z-9 | 300 | 2.8 | 96 | | 3 | 9 | | | | 14 | | 16 | | 19 | | 21 | 22 |
| Z-11 | 1000 | 2.4 | 24 | | 2 | 7 | | | | | 14 | | 16 | | 19 | | 20 |
| AA-2 | 1000 | 2.4 | 96 | | 2 | 8 | | 13 | | | | 15 | | 18 | | 20 | 21 |
| AA-4 | 1000 | 2.8 | 24 | | 0 | 3 | | | 7 | | | | 8 | | 11 | | 12 |
| AA-8 | 1000 | 2.8 | 96 | | 0 | 3 | | 6 | | | | 8 | | 11 | | 12 | 13 |
| AA-10 | 3000 | 2.4 | 24 | | 3 | 8 | | | 14 | | | | 15 | | 18 | | 20 |
| AA-11 | 3000 | 2.4 | 96 | | 3 | 8 | | 12 | | | | 14 | | 18 | | 19 | 20 |

NEUTRALIZER APPLIED

NOTE:

THE NEUTRALIZATION STEP (INCLUDING THE PRE-SOAK IN WET LAYUP) WAS INITIATED ON DAY 26.
ALL CAPSULES WERE EXPOSED TO C-E REFERENCE DENTING SOLUTION (0.1 M $Fe Cl_2$ IN DEIONIZED WATER) AT 565°F FOR 26 DAYS TO PRODUCE 5-9 MILS OF DIAMETRAL INCREASE PRIOR TO NEUTRALIZATION.

WET LAYUP SOLUTION IN DEIONIZED WATER CONTAINING 200 ± 50 PPM $N_2 H_4$ ; pH = 10.0; VOLATILE CHEMISTRY IN DEIONIZED WATER WITH APPROXIMATELY 20 PPM $N_2 H_4$; FAULT CHEMISTRY IS 0.1 M $Fe Cl_2$

TABLE A-7

PHOSPHATE SOAK TEST AT 565°F

DIAMETRAL INCREASE (IN MILS) AS A FUNCTION OF TIME

ALL CAPSULES REVERSE DENTED WITH C-E REFERENCE SOLUTION

| CAPSULE | ppm $PO_4$ | Na/P | HRS | POST SOAK | DAYS AT TEMPERATURE | | | | | | | | | | | |
|---|---|---|---|---|---|---|---|---|---|---|---|---|---|---|---|---|
| | | | | | 14 | 21 | 26 | 31 | 44 | 48 | 50 | 51 | 55 | 58 | 59 | 62 |
| Y-3 | 50 | 2.5 | 24 | VOLATILE | 0 | 2 | | 3 | 3 | 4 | 4 | | 4 | | 4 | |
| AA-5 | 50 | 2.5 | 96 | VOLATILE | 3 | | 8 | 8 | 8 | | | 8 | 8 | 8 | | |
| Y-9 | 300 | 2.5 | 24 | VOLATILE | 1 | 3 | | 5 | 5 | 5 | 5 | | 5 | | 5 | |
| Y-11 | 300 | 2.5 | 96 | VOLATILE | 2 | 5 | | 9 | 12 | 12 | 12 | | 12 | | 12 | 12 |
| Y-4 | 50 | 2.5 | 24 | FAULT | 0 | 2 | | 4 | 8 | 9 | 11 | | 11 | | 12 | |
| AA-6 | 50 | 2.5 | 96 | FAULT | 4 | | 9 | 14 | 16 | | | 19 | 21 | 22 | | |
| Y-10 | 300 | 2.5 | 24 | FAULT | 0 | 1 | | 3 | 6 | 7 | 8 | | 8 | | 9 | |

NOTES:

THE NEUTRALIZATION STEP (INCLUDING THE PRE-SOAK IN WET LAYUP) WAS INITIATED ON DAY 26 FOR SERIES AA AND ON DAY 31 FOR SERIES Y.

ALL CAPSULES WERE EXPOSED TO C-E REFERENCE DENTING SOLUTION (0.1 M $FeCl_2$) at 565°F FOR 26 TO 31 DAYS TO PRODUCE 3-9 MILS OF DIAMETRAL INCREASE PRIOR TO NEUTRALIZATION

FAULT CHEMISTRY IS THE SAME AS C-E REFERENCE DENTING SOLUTION

TABLE A-8

CONTROLS FOR PHOSPHATE SOAK TEST AT 150°F

DIAMETRAL INCREASE (IN MILS) AS A FUNCTION OF TIME

ALL CAPSULES REVERSE DENTED WITH C-E REFERENCE SOLUTION

| | | | DAYS AT TEMPERATURE | | | | | | | | | | | | | |
|---|---|---|---|---|---|---|---|---|---|---|---|---|---|---|---|---|
| CAPSULE | HRS | POST SOAK | 14 | 21 | 26 | 27 | 31 | 35 | 40 | 44 | 46 | 47 | 51 | 54 | 55 | 58 |
| Y-1 | 96 | VOL. | 2 | 5 | | | 8 | | 13 | 13 | 14 | | 14 | | 14 | 14 |
| Z-1 | 96 | VOL. | 3 | | 9 | | | 9 | 9 | | | 9 | 9 | 9 | | |
| Y-2 | 96 | FAULT | 3 | 7 | | | 11 | | 19 | 21 | 22 | | 23 | | 25 | 26 |
| AA-1 | 96 | FAULT | 0 | | 3 | 7 | | | 8 | | | 11 | 13 | 14 | | |

NOTES:

THE NEUTRALIZATION STEP (INCLUDING THE PRE-SOAK IN WET LAYUP) WAS INITIATED ON DAY 26 FOR SERIES AA AND Z AND ON DAY 31 FOR SERIES Y

ALL CAPSULES WERE EXPOSED TO C-E REFERENCE DENTING SOLUTION (0.1 M $Fe Cl_2$) AT 565°F FOR 26 TO 31 DAYS TO PRODUCE 3-11 MILS OF DIAMETRAL INCREASE PRIOR TO NEUTRALIZATION

FAULT CHEMISTRY IS THE SAME AS C-E REFERENCE DENTING SOLUTION

TABLE A-9

PHOSPHATE SOAK TEST AT 150°F

DIAMETRAL INCREASE (IN MILS) AS A FUNCTION OF TIME

ALL CAPSULES REVERSE DENTED WITH W/EPRI REFERENCE SOLUTION

| CAPSULE | ppm $PO_4$ | Na/P | HRS | POST SOAK | DAYS AT TEMPERATURE 14 | 17 | 21 | 24 | 25 | 29 | 32 | 35 | 39 | 42 | 49 |
|---|---|---|---|---|---|---|---|---|---|---|---|---|---|---|---|
| DD-7 (1) | 1000 | 2.8 | 96 | VOLATILE | 4 | 7 | | 7 | | | 10 | | 10 | | |
| II-8 | 3000 | 2.8 | 96 | VOLATILE | 3 | | 5 | | 8 | 9 | | 10 | | 13 | 14 |
| II-10 | 5000 | 2.8 | 96 | VOLATILE | 2 | | 5 | | 8 | 9 | | 9 | | 11 | 12 |
| II-12 | 10,000 | 2.8 | 96 | VOLATILE | 3 | | 5 | | 8 | 9 | | 9 | | 10 | 11 |
| DD-8 | 1000 | 2.8 | 96 | FAULT | 3 | 5 | | 8 | | | 11 | | 12 | | |
| II-7 | 3000 | 2.8 | 96 | FAULT | 3 | | 6 | | 9 | 9 | | 10 | | 12 | 14 |
| II-9 | 5000 | 2.8 | 96 | FAULT | 3 | | 5 | | 9 | 10 | | 10 | | 12 | 14 |
| II-11 | 10,000 | 2.8 | 96 | FAULT | 2 | | 4 | | 8 | 9 | | | | 11 | 13 |

NOTES:

1. CAPSULE DD-7 WAS EMPTY AT THE END OF THE DENTING PHASE
2. THE NEUTRALIZATION STEP (INCLUDING THE PRE-SOAK IN WET LAYUP) WAS INITIATED ON DAY 17 FOR SERIES DD AND ON DAY 21 FOR SERIES II
3. ALL CAPSULES WERE EXPOSED TO W/EPRI REFERENCE DENTING SOLUTION (0.1 M $Ni\,Cl_2$ + 0.1 M $Cu\,Cl_2$ IN FULL STRENGTH SEAWATER) AT 565°F FOR 17 TO 21 DAYS TO PRODUCE 4 - 7 MILS OF DIAMETRAL INCREASE PRIOR TO NEUTRALIZATION
4. WEY LAYUP SOLUTION IN DEIONIZED WATER CONTAINING 200 ± 50 PPM $N_2H_4$; pH = 10.0; VOLATILE CHEMISTRY IN DEIONIZED WATER WITH APPROXIMATELY 20 PPM $N_2H_4$; FAULT CHEMISTRY IS 0.1 M $Fe\,Cl_2$

TABLE A-10

PHOSPHATE SOAK TEST AT 565°F

DIAMETRAL INCREASE (IN MILS) AS A FUNCTION OF TIME

ALL CAPSULES REVERSE DENTED WITH W/EPRI REFERENCE SOLUTION

| CAPSULE | ppm $PO_4$ | Na/P | HRS | POST SOAK | DAYS AT TEMPERATURE | | | | | | | | | | | | |
|---|---|---|---|---|---|---|---|---|---|---|---|---|---|---|---|---|---|
| | | | | | 14 | 17 | 21 | 28 | 29 | 33 | 36 | 37 | 39 | 43 | 44 | 46 | 53 |
| DD-5[1] | 50 | 2.5 | 24 | VOLATILE | 3 | 4 | | | 10 | | | 14 | | | 17 | | |
| DD-3[1] | 300 | 2.5 | 24 | | 3 | 4 | | | 11 | | | 13 | | | 14 | | |
| DD-1 | 300 | 2.5 | 96 | | 3 | 4 | | 9 | | | 12 | | | 15 | | | |
| II-3 | 1000 | 2.5 | 96 | | 2 | | 5 | | 10 | 11 | | | 12 | | | 14 | 14 |
| II-5 | 3000 | 2.5 | 96 | | 3 | | 5 | | 9 | 11 | | | 12 | | | 14 | 15 |
| DD-6[1] | 50 | 2.5 | 24 | FAULT | 4 | 6 | | | 13 | | | 16 | | | 19 | | |
| DD-4[1] | 300 | 2.5 | 24 | | 4 | 5 | | | 12 | | | 16 | | | 18 | | |
| DD-2 | 300 | 2.5 | 96 | | 3 | 5 | | 10 | | | 13 | | | 15 | | | |
| II-2 | 1000 | 2.5 | 96 | | 2 | | 5 | | 10 | 12 | | | 12 | | | 14 | 16 |
| II-4 | 3000 | 2.5 | 96 | | 3 | | 5 | | 9 | 11 | | | 11 | | | 13 | 15 |

NOTES:

1. THE POST-SOAK 24-HOUR WET LAYUP WAS OMITTED FOR CAPSULES DD-3, DD-4 AND DD-6.
2. THE NEUTRALIZATION STEP (INCLUDING THE PRE-SOAK IN WET LAYUP) WAS INITIATED ON DAY 17 FOR SERIES DD AND ON DAY 21 FOR SERIES II
3. ALL CAPSULES WERE EXPOSED TO W/EPRI REFERENCE DENTING SOLUTION (0.1 M $NiCl_2$ + 0.1 M $CuCl_2$ IN FULL STRENGTH SEAWATER) AT 565°F FOR 17 TO 21 DAYS TO PRODUCE 4 - 6 MILS OF DIAMETRAL INCREASE PRIOR TO NEUTRALIZATION
4. WET LAYUP SOLUTION IN DEIONIZED WATER CONTAINING 200 ± 50 PPM $N_2H_4$ ; pH = 10.0; VOLATILE CHEMISTRY IN DEIONIZED WATER WITH APPROXIMATELY 20 PPM $N_2H_4$; FAULT CHEMISTRY IS 0.1 M $FeCl_2$

TABLE A-11

CONTROLS FOR PHOSPHATE SOAK TEST

DIAMETRAL INCREASE (IN MILS) AS A FUNCTION OF TIME

ALL CAPSULES REVERSE DENTED WITH W/EPRI REFERENCE SOLUTION

| CAPSULE | TEMP $^{0}F$ | HRS | POST SOAK | DAYS AT TEMPERATURE 14 | 21 | 25 | 29 | 33 | 35 | 39 | 42 | 46 | 49 | 53 |
|---|---|---|---|---|---|---|---|---|---|---|---|---|---|---|
| II-1 | 565 | 96 | VOL. | 2 | 5 | | 9 | 12 | | 13 | | 15 | | 17 |
| II-6 | 150 | 96 | VOL. | 2 | 4 | 8 | 9 | | 10 | | 12 | | 13 | |

NOTES:

1. THE SOAK SOLUTION FOR CAPSULE II-1 AT 565$^{0}$F WAS VOLATILE CHEMISTRY (APPROXIMATELY 20 PPM $N_2 H_4$); THE SOAK SOLUTION FOR CAPSULE II-6 AT 150$^{0}$F WAS WET LAYUP SOLUTION (200 ± 50 PPM $N_2 H_4$ WITH pH = 10.0)

2. THE NEUTRALIZATION STEP (INCLUDING THE PRE-SOAK IN WET LAYUP) WAS INITIATED ON DAY 21

3. ALL CAPSULES WERE EXPOSED TO W/EPRI REFERENCE DENTING SOLUTION (0.1 M $Ni Cl_2$ + 0.1 M $Cu Cl_2$ IN FULL STRENGTH SEAWATER) AT 565$^{0}$F FOR 21 DAYS TO PRODUCE 4 - 5 MILS OF DIAMETRAL INCREASE PRIOR TO NEUTRALIZATION

TABLE A-12

PHOSPHATE SOAK EFFECTIVENESS TEST WITH 0.25 M $FeCl_2$ AT 150° F

DIAMETRAL INCREASE (IN MILS) AS A FUNCTION OF TIME

| CAPSULE | ppm $PO_4$ | HRS | DAYS AT TEMPERATURE 7 | 14 | 21 | 26 | 34 | 43 | 46 | PRE-NEUT SLOPE | POST-NEUT SLOPE | OVERALL SLOPE |
|---|---|---|---|---|---|---|---|---|---|---|---|---|
| KK-11 | 0 | 96 | 0 | 2 | 4 | 6 | 7 | 10 | 11 | .29 | .27 | .27 |
| KK-1 | 300 | 96 | 0 | 1 | 4 | 6 | 8 | 11 | 13 | .43 | .34 | .35 |
| KK-2 | 300 | 96 | 0 | 1 | 2 | 4 | 5 | 7 | 8 | .14 | .22 | .21 |
| KK-3 | 1000 | 96 | 0 | 2 | 3 | 5 | 5 | 7 | 8 | .14 | .18 | .18 |
| KK-4 | 1000 | 96 | 0 | 2 | 4 | 6 | 7 | 9 | 11 | .29 | .25 | .26 |
| KK-5 | 3000 | 96 | 0 | 3 | 6 | 9 | 10 | 13 | 15 | .43 | .32 | .35 |
| KK-6 | 3000 | 96 | 0 | 3 | 5 | 7 | 8 | 10 | 11 | .29 | .22 | .24 |
| KK-7 | 10,000 | 96 | 0 | 3 | 5 | 6 | 8 | 11 | 12 | .29 | .28 | .28 |
| KK-8 | 10,000 | 96 | 0 | 2 | 4 | 6 | 6 | 8 | 9 | .29 | .18 | .20 |

NEUTRALIZER APPLIED

NOTES:

1. NEUTRALIZER WAS APPLIED ON DAY 21
2. FOR ALL CAPSULES THE Na/P MOLE RATIO WAS 2.8
3. ALL CAPSULES WERE FILLED WITH VOLATILE CHEMISTRY AFTER NEUTRALIZATION

TABLE A-13

PHOSPHATE SOAK EFFECTIVENESS TEST WITH 0.25 M $FeCl_2$ AT 565°F

DIAMETRAL INCREASE (IN MILS) AS A FUNCTION OF TIME

| CAPSULE | ppm $PO_4$ | HRS | DAYS AT TEMPERATURE 7 | 14 | 21 | 30 | 38 | 47 | 50 | PRE-NEUT. SLOPE | POST-NEUT. SLOPE | OVERALL SLOPE |
|---|---|---|---|---|---|---|---|---|---|---|---|---|
| KK-12 | 0 | 96 | 0 | 2 | 4 | 6 | 7 | 10 | 11 | .29 | .24 | .24 |
| KK-9 | 300 | 96 | 0 | 2 | 4 | 6 | 8 | 10 | 12 | .29 | .26 | .26 |
| KK-10 | 300 | 96 | 0 | 3 | 7 | 10 | 14 | 17 | 19 | .57 | .41 | .43 |

NOTES:

1. NEUTRALIZER WAS APPLIED ON DAY 21

2. FOR ALL CAPSULES THE Na/P MOLE RATIO WAS 2.5

3. ALL CAPSULES WERE FILLED WITH VOLATILE CHEMISTRY AFTER NEUTRALIZATION

TABLE A-14

STRAIGHT LINE PARAMETERS FROM CAPSULE BULGING DATA

| CAPSULE ID | SOAK CONDITIONS | PRE-SOAK m | PRE-SOAK b | PRE-SOAK R | POST-SOAK m | POST-SOAK b | POST-SOAK R | ALL DATA m | ALL DATA b | ALL DATA R |
|---|---|---|---|---|---|---|---|---|---|---|
| | W/EPRI CAPSULES, 150°F WATER - SOAK EFFECTIVENESS TEST | | | | | | | | | |
| BB-2 | 24 HRS | 0.71 | -9.2 | | 0.66 ± 0.01 | -7.9 ± 0.2 | 0.999 | | | |
| BB-6 | 96 HRS | 0.71 | -8.2 | | 0.58 ± 0.01 | -4.9 ± 0.4 | 0.998 | | | |
| BB-10 | 168 HRS | 0.71 | -8.2 | | 0.56 ± 0.02 | -4.6 ± 0.5 | 0.998 | | | |
| | W/EPRI CAPSULES, 150°F WATER - SOAK ENDURANCE TEST | | | | | | | | | |
| BB-1 | 24 HRS | 0.57 | -6.7 | | 0.41 ± 0.03 | -1 ± 1 | 0.987 | | | |
| BB-5 | 96 HRS | 0.43 | -3.3 | | 0.22 ± 0.01 | 1.4 ± 0.2 | 0.985 | | | |
| BB-9 | 168 HRS | 0.43 | -3.3 | | 0.25 ± 0.01 | 1.0 ± 0.6 | 0.986 | | | |
| | W/EPRI CAPSULES 565°F WATER - SOAK EFFECTIVENESS TEST | | | | | | | | | |
| BB-4 | 24 HRS | | | | | | | 0.62 ± 0.01 | -6.7 ± 0.4 | 0.999 |
| BB-8 | 96 HRS | 0.43 | -3.3 | | 0.31 ± 0.01 | -0.8 ± 0.6 | 0.991 | | | |
| BB-12 | 168 HRS | 0.36 ± 0.02 | -2.7 ± 0.4 | 0.994 | 0.27 ± 0.01 | -0.4 ± 0.4 | 0.994 | | | |
| | W/EPRI CAPSULES, 565°F WATER - SOAK ENDURANCE TEST | | | | | | | | | |
| BB-3 | 24 HRS | 0.43 | -3.3 | | 0.28 ± 0.02 | -0.6 ± 0.8 | 0.981 | | | |
| BB-7 | 96 HRS | 0.43 | -3.3 | | 0.32 ± 0.02 | -1.7 ± 0.8 | 0.985 | | | |
| BB-11 | 168 HRS | 0.43 | -3.3 | | 0.27 ± 0.01 | 0.0 ± 0.5 | 0.991 | | | |

m = SLOPE (BULGING RATE IN DIAMETRAL MILS/DAY)

b = y - INTERCEPT (MILS)

R = CORRELATION COEFFICIENT

TABLE A-14 (Cont'd)

STRAIGHT LINE PARAMETERS FROM CAPSULE BULGING DATA

| CAPSULE ID | SOAK CONDITIONS (1) | PRE-SOAK m | PRE-SOAK b | PRE-SOAK R | POST-SOAK m | POST-SOAK b | POST-SOAK R | ALL DATA m | ALL DATA b | ALL DATA R |
|---|---|---|---|---|---|---|---|---|---|---|
| | C-E CAPSULES, 150°F PHOSPHATE SOAK, EFFECTIVENESS TEST | | | | | | | | | |
| Z-3 | 300, 2.4, 24 | -- (2) | -- | | 0 (3) | 4.0 | | | | |
| Z-4 | 300, 2.4, 96 | 0.42 | -2.8 | | 0 | 9.0 | | | | |
| Z-6 | 300, 2.8, 24 | 0.42 | -2.8 | | 0 | 8.2 | | | | |
| Z-8 | 300, 2.8, 96 | 0.42 | -2.8 | | 0 | 8.2 | | | | |
| Z-10 | 1000, 2.4, 24 | 0.42 | -2.8 | | 0 | 9.0 | | | | |
| Z-12 | 1000, 2.4, 96 | 0.50 | -5.0 | | 0 | 8.0 | | | | |
| AA-3 | 1000, 2.8, 24 | 0.25 | -2.5 | | 0 | 5.0 | | | | |
| AA-7 | 1000, 2.8, 96 | 0.25 | -2.5 | | 0 | 5.0 | | | | |
| AA-9 | 3000, 2.4, 24 | -- | -- | | 0 | 2.0 | | | | |
| AA-11 | 3000, 2.4, 96 | 0.25 | -2.5 | | 0 | 4.0 | | | | |
| | C-E CAPSULES, 150°F PHOSPHATE SOAK, ENDURANCE TEST | | | | | | | | | |
| Z-3 | 300, 2.4, 24 | | | | | | | 0.50 ± 0.01 | -4.8 ± 0.4 | 0.999 |
| Z-5 | 300, 2.4, 96 | (2) | | | | | | 0.44 ± 0.02 | -8.5 ± 0.9 | 0.995 |
| Z-7 | 300, 2.8, 24 | | | | | | | 0.35 ± 0.02 | -4.6 ± 0.9 | 0.990 |
| Z-9 | 300, 2.8, 96 | 0.50 | -4.0 | | 0.46 ± 0.01 | -2.6 ± 0.5 | 0.998 | | | |
| Z-11 | 1000, 2.4, 24 | | | | | | | 0.47 ± 0.02 | -4.5 ± 0.6 | 0.997 |

m = SLOPE (BULGING RATE IN DIAMETRAL MILS/DAY)

b = y - INTERCEPT (MILS)

R = CORRELATION COEFFICIENT

NOTES: (1) SOAK CONDITIONS ARE ppm $PO_4$ FOLLOWED BY THE Na/P MOLE RATE, FOLLOWED BY TOTAL HOURS OF SOAK

(2) THE PRE-SOAK BULGING RATE COULD NOT BE CALCULATED FOR THESE CAPSULES SINCE ONLY ONE PRE-SOAK DATA POINT WAS AVAILABLE

(3) WHEN BULGING STOPPED AFTER SOAKING, THE SLOPE IS REPORTED AS IDENTICALLY ZERO. THE y-INTERCEPT IS THE FINAL VALUE OF $\Delta D$

TABEL A-14 (Cont'd)

STRAIGHT LINE PARAMETERS FROM CAPSULE BULGING DATA

| CAPSULE ID | SOAK CONDITIONS (1) | PRE-SOAK m | PRE-SOAK b | PRE-SOAK R | POST-SOAK m | POST-SOAK b | POST-SOAK R | ALL DATA m | ALL DATA b | ALL DATA R |
|---|---|---|---|---|---|---|---|---|---|---|
| | C-E CAPSULES, 150°F PHOSPHATE SOAK, ENDURANCE TEST (Continued) | | | | | | | | | |
| AA-2 | 1000, 2.4, 96 | | | | | | | 0.44 ± 0.04 | -3 ± 2 | 0.970 |
| AA-4 | 1000, 2.8, 24 (2) | | | | | | | 0.28 ± 0.04 | -3 ± 2 | 0.948 |
| AA-8 | 1000, 2.8, 96 (2) | | | | | | | 0.31 ± 0.03 | -4 ± 1 | 0.973 |
| AA-10 | 3000, 2.4, 24 | | | | | | | 0.40 ± 0.05 | -1 ± 2 | 0.963 |
| AA-11 | 3000, 2.4, 96 | | | | | | | 0.41 ± 0.03 | -2 ± 1 | 0.979 |
| | C-E CAPSULES, 565°F, PHOSPHATE SOAK, EFFECTIVENESS TEST | | | | | | | | | |
| Y-3 | 50, 2.5, 24 | 0.17 ± 0.03 | 3.2 ± 0.3 (4) | 0.958 | 0 (3) | 4 | | | | |
| AA-5 | 50, 2.5, 96 | 0.42 | 8.0 | | 0 | 8 | | | | |
| Y-9 | 300, 2.5, 24 | 0.23 ± 0.01 | 5.1 ± 0.2 | 0.995 | 0 | 5 | | | | |
| Y-11 | 300, 2.5, 96 | 0.411 ± 0.005 | 9.03 ± 0.06 | 1.000 | 0 | 12 | | | | |
| | C-E CAPSULES, 565°F PHOSPHATE SOAK, ENDURANCE TEST | | | | | | | | | |
| Y-4 | 50, 2.5, 24 | | | | | | | 0.29 ± 0.02 | 4.5 ± 0.3 | 0.988 |
| AA-6 | 50, 2.5, 96 | | | | | | | 0.39 ± 0.03 | 9.6 ± 0.5 | 0.985 |
| Y-10 | 300, 2.5, 24 | | | | | | | 0.22 ± 0.01 | 3.2 ± 0.2 | 0.993 |

m = SLOPE (BULGING RATE IN DIAMETRAL MILS/DAY)

b = y - INTERCEPT (MILS)

R = CORRELATION COEFFICIENT

NOTES: (1) SOAK CONDITIONS ARE ppm $PO_4$, FOLLOWED BY Na/P MOLE RATIO, FOLLOWED BY TOTAL HOURS OF SOAK

(2) THE PRE-SOAK BULGING RATE COULD NOT BE CALCULATED FOR THESE CAPSULES SINCE ONLY ONE PRE-SOAK DATA POINT WAS AVAILABLE

(3) WHEN BULGING STOPPED AFTER SOAKING, THE SLOPE IS REPORTED AS IDENTICALLY ZERO. THE y - INTERCEPT IS THE FINAL VALUE OF $\Delta D$.

(4) FOR BOTH SERIES OF EFFECTIVENESS TESTS AT 565°F THE y - INTERCEPT WAS CALCULATED BASED ON DAYS AT TEMPERATURE NORMALIZED TO POINT OF NEUTRALIZATION

TABLE A-14 (Cont'd)

STRAIGHT LINE PARAMETERS FROM CAPSULE BULGING DATA

| CAPSULE ID | SOAK CONDITIONS[1] | PRE-SOAK m | PRE-SOAK b | PRE-SOAK R | POST-SOAK m | POST-SOAK b | POST-SOAK R | ALL DATA m | ALL DATA b | ALL DATA R |
|---|---|---|---|---|---|---|---|---|---|---|
| | C-E CAPSULES, 150°F CONTROLS FOR PHOSPHATE SOAK EFFECTIVENESS TEST | | | | | | | | | |
| Y-1 | 96 HRS | 0.41 ± 0.03 | 8.8 ± 0.3 [2] | 0.992 | | 0 [3] | 14 | | | |
| Z-1 | 96 HRS | 0.50 | 9.0 | | | 0 | 9 | | | |
| | C-E CAPSULES, 150°F CONTROLS FOR PHOSPHATE SOAK ENDURANCE TEST | | | | | | | | | |
| Y-2 | 96 HRS | | | | | | | 0.54 ± 0.03 | 12.5 ± 0.4 | 0.990 |
| AA-1 | 96 HRS | | | | | | | 0.34 ± 0.07 | 4 ± 1 | 0.973 |
| | W/EPRI CAPSULES, 150°F PHOSPHATE SOAK, EFFECTIVENESS TEST | | | | | | | | | |
| II-8 | 3000, 2.8, 96 | | | | | | | 0.32 ± 0.02 | 5.7 ± 0.3 | 0.984 |
| II-10 | 5000, 2.8, 96 | 0.43 | 5.0 | | 0.22 ± 0.03 | 6.3 ± 0.5 | 0.938 | | | |
| II-12 | 10,000, 2.8, 96 | 0.29 | 5.0 | | 0.17 ± 0.04 | 6.5 ± 0.6 | 0.894 | | | |
| | W/EPRI CAPSULES, 150°F PHOSPHATE SOAK, ENDURANCE TEST | | | | | | | | | |
| DD-8 | 1000, 2.8, 96 | 0.67 | 5.0 | | 0.32 ± 0.03 | 5 ± 1 | 0.982 | | | |
| II-7 | 3000, 2.8, 96 | 0.43 | 6.0 | | 0.25 ± 0.03 | 6.9 ± 0.4 | 0.970 | | | |
| II-9 | 5000, 2.8, 96 | | | | | | | 0.30 ± 0.04 | 6.1 ± 0.5 | 0.954 |
| II-11 | 10,000, 2.8, 96 | | | | | | | 0.30 ± 0.04 | 5.1 ± 0.5 | 0.954 |

m = SLOPE (BULGING RATE IN DIAMETRAL MILS/DAY)

b = y - INTERCEPT (MILS)

R = CORRELATION COEFFICIENT

NOTES: (1) SOAK CONDITIONS ARE ppm $PO_4$, FOLLOWED BY THE Na/P MOLE RATIO, FOLLOWED BY TOTAL HOURS OF SOAK

(2) ALL y - INTERCEPTS ON THIS PAGE WERE CALCULATED BASED ON DAYS AT TEMPERATURE NORMALIZED TO POINT OF NEUTRALIZATION

(3) WHEN BULGING STOPPED AFTER SOAKING, THE SLOPE IS REPORTED AS IDENTICALLY ZERO. THE y - INTERCEPT IS THE FINAL VALUE OF $\Delta D$

TABLE A-14 (Cont'd)

STRAIGHT LINE PARAMETERS FROM CAPSULE BULGING DATA

| CAPSULE ID | SOAK CONDITIONS[1] | PRE-SOAK m | PRE-SOAK b | PRE-SOAK R | POST-SOAK m | POST-SOAK b | POST-SOAK R | ALL DATA m | ALL DATA b | ALL DATA R |
|---|---|---|---|---|---|---|---|---|---|---|
| | W/EPRI CAPSULES, 565°F PHOSPHATE SOAK EFFECTIVENESS TEST | | | | | | | | | |
| DD-5 | 50, 2.5, 24 | | | | | | | 0.477 ± 0.097 | 4.3 ± 0.1[2] | 0.999 |
| DD-3 | 300, 2.5, 24 | | | | | | | 0.39 ± 0.04 | 4.6 ± 0.6 | 0.975 |
| DD-1 | 300, 2.5, 96 | | | | | | | 0.417 ± 0.006 | 4.18 ± 0.09 | 1.000 |
| II-3 | 1000, 2.5, 96 | 0.43 | 5.0 | | 0.27 ± 0.04 | 6.8 ± 0.8 | 0.930 | | | |
| II-5 | 3000, 2.5, 96 | | | | | | | 0.32 ± 0.02 | 5.8 ± 0.4 | 0.981 |
| | W/EPRI CAPSULES, 565°F PHOSPHATE SOAK ENDURANCE TEST | | | | | | | | | |
| DD-6 | 50, 2.5, 24 | 0.67 | 6.0 | | 0.48 ± 0.03 | 6.5 ± 0.4 | 0.995 | | | |
| DD-4 | 300, 2.5, 24 | | | | | | | 0.49 ± 0.02 | 5.5 ± 0.4 | 0.995 |
| DD-2 | 300, 2.5, 96 | 0.67 | 5.0 | | 0.39 ± 0.02 | 5.3 ± 0.3 | 0.995 | | | |
| II-2 | 1000, 2.5, 96 | 0.43 | 5.0 | | 0.31 ± 0.04 | 6.6 ± 0.8 | 0.952 | | | |
| II-4 | 3000, 2.5, 96 | | | | | | | 0.31 ± 0.02 | 5.7 ± 0.4 | 0.979 |
| | W/EPRI CAPSULES CONTROLS FOR PHOSPHATE SOAK EFFECTIVENESS TEST | | | | | | | | | |
| II-6 | 96 HRS, 150°F | | | | | | | 0.39 ± 0.03 | -3 ± 1 | 0.984 |
| II-1 | 96 HRS, 565°F | | | | | | | 0.32 ± 0.04 | -1 ± 1 | 0.960 |

m = SLOPE (BULGING RATE IN DIAMETRAL MILS/DAY)

b = y - INTERCEPT (MILS)

R = CORRELATION COEFFICIENT

NOTES: (1) SOAK CONDITIONS ARE ppm $PO_4$, FOLLOWED BY THE Na/P MOLE RATIO, FOLLOWED BY TOTAL HOURS OF SOAK

(2) ALL y - INTERCEPTS ON THIS PAGE WERE CALCULATED BASED ON DAYS AT TEMPERATURE NORMALIZED TO POINT OF NEUTRALIZATION.

TABLE A-14 (Cont'd)

STRAIGHT LINE PARAMETERS FROM CAPSULE BULGING DATA

| CAPSULE ID | SOAK CONDITIONS (1) | PRE-SOAK m | PRE-SOAK b | PRE-SOAK R | POST-SOAK m | POST-SOAK b | POST-SOAK R | ALL DATA m | ALL DATA b | ALL DATA R |
|---|---|---|---|---|---|---|---|---|---|---|
| | 0.25 M $FeCl_2$ CAPSULES 150°F PHOSPHATE SOAK EFFECTIVENESS TEST | | | | | | | | | |
| KK-11 | 0, –, 96 (2) | | | | | | | 0.27 ± 0.01 | -1.7 ± 0.4 | 0.994 |
| KK-1 | 300, 2.8, 96 | 0.43 | -5.0 | | 0.34 ± 0.02 | -3.1 ± 0.6 | 0.993 | | | |
| KK-2 | 300, 2.8, 96 | | | | | | | 0.22 ± 0.01 | -2.1 ± 0.4 | 0.993 |
| KK-3 | 1000, 2.8, 96 | | | | | | | 0.18 ± 0.02 | -0.4 ± 0.5 | 0.976 |
| KK-4 | 1000, 2.8, 96 | | | | | | | 0.26 ± 0.02 | -1.4 ± 0.6 | 0.987 |
| KK-5 | 3000, 2.8, 96 | 0.43 | -3.0 | | 0.32 ± 0.03 | 0 ± 1 | 0.979 | | | |
| KK-6 | 3000, 2.8, 96 | 0.29 | -1.9 | | 0.22 ± 0.02 | 0.7 ± 0.5 | 0.988 | | | |
| KK-7 | 10,000, 2.8, 96 | | | | | | | 0.279 ± 0.009 | -1.0 ± 0.3 | 0.997 |
| KK-8 | 10,000, 2.8, 96 | 0.29 | -2.0 | | 0.17 ± 0.02 | 0.7 ± 0.8 | 0.959 | | | |
| | 0.25 M $FeCl_2$ CAPSULES 565°F PHOSPHATE SOAK EFFECTIVENESS TEST | | | | | | | | | |
| KK-12 | 0, –, 96 (2) | | | | | | | 0.24 ± 0.01 | -1.3 ± 0.4 | 0.993 |
| KK-9 | 300, 2.5, 96 | | | | | | | 0.26 ± 0.01 | -1.7 ± 0.4 | 0.994 |
| KK-10 | 300, 2.5, 96 | 0.57 | -5.0 | | 0.41 ± 0.01 | -1.8 ± 0.6 | 0.997 | | | |

m = SLOPE (BLUGING RATE IN DIAMETRAL MILS/DAY)

b = y - INTERCEPT (MILS)

R = CORRELATION COEFFICIENT

NOTES: (1) SOAK CONDITIONS ARE ppm $PO_4$, FOLLOWED BY THE Na/P MOLE RATIO, FOLLOWED BY TOTAL HOURS OF SOAK

(2) THE CONTROLS ARE LISTED ALONG WITH THE OTHER DATA. 0 INDICATES NO PHOSPHATE, AND THE – INDICATES NO Na/P RATIO

TABLE A-15

CHLORIDE MASS BALANCE FOR THE WATER SOAK TEST (SERIES BB)

ALL VALUES ARE IN MILLIGRAMS OF CHLORIDE

| SOAK CONDITION | CAPSULE NUMBER | DENT SOLUTION IN | DENT SOLUTION OUT | RINSE 1 OUT | RINSE 2 OUT | WATER SOAK OUT | RINSE 1 OUT | RINSE 2 OUT | REFILL IN | CUT 1 OUT | CUT 1 IN | FINAL SOLUTION OUT | RESIDUAL CHLORIDE |
|---|---|---|---|---|---|---|---|---|---|---|---|---|---|
| 150°F | | | | | | | | | | | | | |
| 24 HR; V[3] | BB-2 | 972 | 672 | 160 | 64 | 136 | 7 | 3 | 0 | 78 | 0 | 19 | -167 |
| 96 HR; V | BB-6 | 972 | 672 | 160 | 64 | 89 | 1 | 1 | 0 | 64 | 0 | 14 | -93 |
| 168 HR; V | BB-10 | 972 | 672 | 160 | 64 | – | – | – | 0 | 55 | 0 | 14 | – |
| 24 HR; F[3] | BB-1 | 972 | 672 | 160 | 64 | 136 | 7 | 3 | 210 | 192 | 175 | 139 | -16 |
| 96 HR; F | BB-5 | 972 | 672 | 160 | 64 | 89 | 1 | 1 | 210 | – | – | 149 | 46 |
| 168 HR; F | BB-9 | 972 | 672 | 160 | 64 | – | – | – | 210 | – | – | 109 | – |
| 565°F | | | | | | | | | | | | | |
| 24 HR; V | BB-4 | 972 | 646 | 78 | 51 | 208 | 6 | 2 | 0 | 42 | 0 | 8 | -69 |
| 96 HR; V | BB-8 | 972 | 646 | 75 | 51 | 212 | 2 | 2 | 0 | 62 | 0 | 7 | -85 |
| 168 HR; V | BB-12 | 972 | 646 | 75 | 51 | – | – | – | 0 | 63 | 0 | 8 | – |
| 24 HR; F | BB-3 | 972 | 646 | 78 | 51 | 208 | 6 | 2 | 175 | – | – | 84 | 72 |
| 96 HR; F | BB-7 | 972 | 646 | 75 | 51 | 212 | 2 | 2 | 175 | – | – | 93 | 96 |
| 168 HR; F | BB-11 | 972 | 646 | 75 | 51 | – | – | – | 210 | – | – | 123 | – |

NOTES:

1. ZEROS INDICATE EITHER THAT THE MASS OF CHLORIDE WAS LESS THAN 1 MILLIGRAM (THE LOWER LIMIT OF DETECTION), OR FOR REFILLS, THAT CHLORIDE-FREE VOLATILE CHEMISTRY WAS ADDED
2. DASHES INDICATE EITHER THAT THE DATA WAS UNAVAILABLE OR THAT THE PARTICLES COLUMN DOES NOT APPLY. FOR EXAMPLE CAPSULES BB-3, BB-5, BB-7, BB-9, AND BB-11 WERE NOT CUT TO RELIEVE HYDROGEN PRESSURE. HENCE NO CHLORIDE WAS REMOVED OR ADDED
3. V INDICATES THAT THE CAPSULE WAS REFILLED WITH VOLATILE CHEMISTRY AFTER SOAKING, AND F INDICATES THAT THE CAPSULE WAS REFILLED WITH 0.1 M $FeCl_2$ AFTER SOAKING

TABLE A-16

CHLORIDE ADDED TO AND RELEASED FROM PHOSPHATE SOAK CAPSULES

ALL CAPSULES WERE BULGED WITH W/EPRI REFERENCE SOLUTION

ALL VALUES ARE IN MILLIGRAMS OF CHLORIDE

| SOAK CONDITION ppm $PO_4$ | HR. | CAPSULE NUMBER | DENT SOLUTION IN | DENT SOLUTION OUT | PRE-SOAK RINSE 1 OUT | PRE-SOAK RINSE 2 OUT | PRE-SOAK WET L-UP OUT | NEUT. OUT | POST-SOAK RINSE 1 OUT | POST-SOAK RINSE 2 OUT | POST-SOAK WET L-UP OUT | REFILL IN | CUT 1 OUT | CUT 1 IN |
|---|---|---|---|---|---|---|---|---|---|---|---|---|---|---|
| 150°F; Na/P RATIO = 2.8 REFILL WITH VOLATILE | | | | | | | | | | | | | | |
| 1000 | 96 | DD-7 | 972 | 0[3] | 40 | 38 | 141 | 101 | 69 | 37 | -- | 0 | -- | -- |
| 3000 | 96 | II-8 | 972 | 941 | 59 | 48 | 24 | 67 | 7 | 3 | 8 | 0 | 31 | 0 |
| 5000 | 96 | II-10 | 972 | 590 | 160 | 95 | 107 | 61 | 3 | 1 | 2 | 0 | 30 | 0 |
| 10,000 | 96 | II-12 | 972 | 639 | 148 | 94 | 30 | 105 | 10 | 5 | 8 | 0 | 4 | 0 |
| 0 = CONTROL | 96 | II-6 | 972 | 983 | 27 | 13 | 38 | 24 | 2 | 1 | 3 | 0 | 24 | 0 |
| 150°F; Na/P RATIO = 2.8 REFILL WITH FAULT | | | | | | | | | | | | | | |
| 1000 | 96 | DD-8 | 972 | 1102 | 40 | 38 | 141 | 10 | 20 | 0 | -- | 210 | -- | -- |
| 3000 | 96 | II-7 | 972 | 707 | 101 | 61 | 40 | 108 | 14 | 10 | 20 | 210 | 175 | 175 |
| 5000 | 96 | II-9 | 972 | 603 | 150 | 84 | 31 | 38 | 29 | 16 | 18 | 210 | 188 | 175 |
| 10,000 | 96 | II-11 | 972 | 657 | 124 | 92 | 175 | 38 | 8 | 4 | 4 | 210 | 174 | 175 |
| 565°F; Na/P RATIO = 2.5 REFILL WITH VOLATILE | | | | | | | | | | | | | | |
| 50 | 24 | DD-5 | 972 | 736 | 11 | 28 | 229 | 72 | 3 | 1 | -- | 0 | 17 | 0 |
| 300 | 24 | DD-3 | 972 | 704 | 114 | 118 | 221 | 33 | 0 | 1 | -- | 0 | 14 | 0 |
| 300 | 96 | DD-1 | 972 | 1208 | 90 | 13 | 165 | 19 | 5 | 1 | 3 | 0 | 6 | 0 |
| 1000 | 96 | II-3 | 972 | 870 | 26 | 11 | 27 | 212 | 8 | 4 | 6 | 0 | 9 | 0 |
| 3000 | 96 | II-5 | 972 | 610 | 25 | 3 | 113 | 259 | 15 | 8 | 15 | 0 | 13 | 0 |
| 0 = CONTROL | 96 | II-1 | 972 | 616 | 78 | 65 | 93 | 33 | 14 | 9 | 10 | 0 | 17 | 0 |

TABLE A-16 (Cont'd)

CHLORIDE ADDED TO AND RELEASED FROM PHOSPHATE SOAK CAPSULES

ALL CAPSULES WERE BULGED WITH W/EPRI REFERENCE SOLUTION

ALL VALUES ARE IN MILLIGRAMS OF CHLORIDE

| SOAK CONDITION ppm $PO_4$ | HR | CAPSULE NUMBER | DENT SOLUTION IN | DENT SOLUTION OUT | PRE-SOAK RINSE 1 OUT | PRE-SOAK RINSE 2 OUT | PRE-SOAK WET L-UP OUT | PRE-SOAK NEUT. OUT | POST-SOAK RINSE 1 OUT | POST-SOAK RINSE 2 OUT | POST-SOAK WET L-UP OUT | REFILL IN | CUT 1 OUT | CUT 1 IN |
|---|---|---|---|---|---|---|---|---|---|---|---|---|---|---|
| $565^0$F; Na/P = 2.5 REFILL WITH FAULT | | | | | | | | | | | | | | |
| 50 | 24 | DD-6 | 972 | 784 | 11 | 28 | 229 | 38 | 1 | 1 | – | 210 | – | 140 |
| 300 | 24 | DD-4 | 972 | 676 | 114 | 118 | 221 | 65 | 7 | 4 | – | 210 | – | 140 |
| 300 | 96 | DD-2 | 972 | 741 | 90 | 13 | 165 | 38 | 5 | 1 | 3 | 175 | – | 140 |
| 1000 | 96 | II-2 | 972 | 871 | 35 | 26 | 16 | 55 | 6 | 3 | 4 | 175 | 148 | 140 |
| 3000 | 96 | II-4 | 972 | 690 | 68 | 48 | 53 | 218 | 16 | 8 | 9 | 175 | 135 | 140 |

NOTES;

1. ZEROS INDICATE EITHER THAT THE MASS OF CHLORIDE WAS LESS THAN 1 MILLIGRAM (THE LOWER LIMIT OF DETECTION, OR FOR REFILLS, THAT CHLORIDE-FREE VOLATILE CHEMISTRY WAS ADDED
2. DASHES INDICATE THAT THE SPECIFIED STEP WAS OMITTED OR THAT THE DATA WERE UNAVAILABLE
3. CAPSULE DD-7 WAS EMPTY AT THE END OF PHASE I.

TABLE A-17

PHOSPHATE ADDED TO AND RELEASED FROM THE PHOSPHATE SOAK CAPSULES

ALL CAPSULES WERE BULGED WITH W/EPRI REFERENCE SOLUTION

ALL VALUES ARE IN MILLIGRAMS OF PHOSPHATE

| SOAK CONDITION | | CAPSULE NUMBER | NEUTRALIZER IN | NEUTRALIZER OUT | RINSE 1 OUT | RINSE 2 OUT | POST-SOAK WET LAYUP OUT | CUT 1 OUT |
|---|---|---|---|---|---|---|---|---|
| ppm $PO_4$ | HR | | | | | | | |
| $150^0$F; Na/P RATIO = 2.8 REFILL WITH VOLATILE | | | | | | | | |
| 1000 | 96 | DD-7 | 30 | – | 10 | 7 | 2 | – |
| 3000 | 96 | II-8 | 90 | 0 | 2 | 11 | 11 | 11 |
| 5000 | 96 | II-10 | 150 | 116 | 11 | 1 | 2 | 0 |
| 10,000 | 96 | II-12 | 300 | 218 | 23 | 20 | 2 | 8 |
| 0 = CONTROL | 96 | II-6 | 0 | 2 | 2 | 0 | 0 | 4 |
| $150^0$F; Na/P RATIO = 2.8 REFILL WITH FAULT | | | | | | | | |
| 1000 | 96 | DD-8 | 30 | 15 | 5 | 5 | 2 | – |
| 3000 | 96 | II-7 | 90 | – | – | 2 | 3 | 8 |
| 5000 | 96 | II-9 | 150 | 176 | 7 | 5 | 2 | – |
| 10,000 | 96 | II-11 | 300 | 195 | 12 | 20 | 9 | 15 |
| $565^0$F; Na/P RATIO = 2.5 REFILL WITH VOLATILE | | | | | | | | |
| 50 | 24 | DD-5 | 1 | – | – | – | – | 1 |
| 300 | 24 | DD-3 | 9 | – | – | – | – | 1 |
| 300 | 96 | DD-1 | 9 | – | 7 | 1 | 2 | 2 |
| 1000 | 96 | II-3 | 30 | 8 | 0 | 3 | 2 | 0 |
| 3000 | 96 | II-5 | 90 | 3 | 4 | 2 | 1 | 4 |
| 0 = CONTROL | 96 | II-1 | 0 | – | 8 | 0 | 0 | 4 |

TABLE A-17 (Cont'd)

PHOSPHATE ADDED TO AND RELEASED FROM PHOSPHATE SOAK CAPSULES

ALL CAPSULES WERE BULGED WITH W/EPRI REFERENCE SOLUTION

ALL VALUES ARE IN MILLIGRAMS OF PHOSPHATE

| SOAK CONDITIONS ppm $PO_4$ | HR | CAPSULE NUMBER | NEUTRALIZER IN | NEUTRALIZER OUT | RINSE 1 OUT | RINSE 2 OUT | POST-SOAK WET LAYUP OUT | CUT 1 OUT |
|---|---|---|---|---|---|---|---|---|
| $565^0F$; Na/P = 2.5 REFILL WITH FAULT | | | | | | | | |
| 50 | 24 | DD-6 | 1 | – | – | – | – | 20 |
| 300 | 24 | DD-4 | 9 | 5 | – | – | – | 6 |
| 300 | 96 | DD-2 | 9 | 4 | 3 | 0 | 2 | 8 |
| 1000 | 96 | II-2 | 30 | 2 | 2 | 1 | 0 | 23 |
| 3000 | 96 | II-4 | 90 | 7 | 0 | 3 | 0 | 40 |

NOTES:

1. ZEROS INDICATE EITHER THAT THE MASS OF CHLORIDE WAS LESS THAN 1 MILLIGRAM (THE LOWER LIMIT OF DETECTION, OR FOR REFILLS, THAT CHLORIDE-FREE VOLATILE CHEMISTRY WAS ADDED

2. DASHES INDICATE THAT THE SPECIFIED STEP WAS OMITTED OR THAT THE DATA WERE UNAVAILABLE

Appendix B

# CAPSULE METALLOGRAPHY

## EXPERIMENTAL

### Summary

Eight capsules, identified in Table B-1 were selected for destructive examination. All were examined on a transverse section through the center of the bulged region. In addition, two capsules (AA-7, DD-7) were examined along a longitudinal section from the center to one end of the bulged region. All transverse sections were examined via light and SEM (scanning election microscopy). Concentration gradients across the oxide layer were determined by EMPA (electron microprobe analysis). Two transverse sections (AA-8, DD-8) were also examined by IMMA (ion microprobe mass analysis) to determine associations among groups of elements. Work was performed by Knolls Atomic Power Laboratory (KAPL), Schenectady, New York under the general direction of G. E. Galonian of the Steam Generator/Coolant Technology section. Most of the SEM and EMPA work was subcontracted by KAPL to Mechanical Technology, Inc. (MTI), Latham, New York. Table B-2 summarizes the analyses performed on each capsule.

### Preparation

Storage procedures prior to destructive examination differed and may have influenced the chemical composition of the oxide. Capsules AA-7, AA-8, Y-1, Y-10, and Y-11 were drained and flushed with de-ionized water upon the completion of testing, dried for twenty-four hours at 150$^{o}$F, and stored in air (caps loosly attached) until examined about six weeks later. The three "DD" capsules were not opened upon completion of testing,

TABLE B-1

CAPSULES SELECTED FOR DESTRUCTIVE EXAMINATION

| Capsule | Denting Chemistry | Soak Conditions | Post Soak Conditions |
|---|---|---|---|
| AA-7 | 0.1 M $FeCl_2$ | 150°F-96 hr-1000 ppm $PO_4$, Na/P=2.8 | Volatile[1] |
| AA-8 | 0.1 M $FeCl_2$ | 150°F-96 hr-1000 ppm $PO_4$, Na/P=2.8 | Fault[2] |
| DD-7 | EPRI REF[3] | 150°F-96 hr-1000 ppm $PO_4$, Na/P=2.8 | Volatile |
| DD-8 | EPRI REF[3] | 150°F-96 hr-1000 ppm $PO_4$, Na/P=2.8 | Fault |
| Y-11 | 0.1 M $FeCl_2$ | 565°F-96 hr-300 ppm $PO_4$, Na/P=2.5 | Volatile |
| Y-10 | 0.1 M $FeCl_2$ | 565°F-24 hr-300 ppm $PO_4$, Na/P=2.5 | Fault |
| Y-1 | 0.1 M $FeCl_2$ | 150°F-96 hr-200 ppm $N_2H_4$ | Volatile |
| DD-12[4] | EPRI REF | 565°F-96 hr-Volatile | Volatile |

Notes:

1. Volatile - the capsule was refilled with a solution of approximately 20 ppm $N_2H_4$ in demineralized water.

2. Fault - the capsule was refilled with a solution of 0.1 M $FeCl_2$ in demineralized water

3. EPRI REF - a solution of 0.1 M $CuCl_2$ and 0.1 M $NiCl_2$ dissolved in full strength Turkey Point seawater.

4. DD-12 - Results from this test were anomalous. Subsequent review revealed that this capsule had been inadvertently exposed to neutralizer during testing.

but were stored at room temperature with slugs immersed until examined about two weeks later.

The capsules were prepared for examination as follows. The capsules were opened, vented, and drained as necessary. The location of the slug (marked on the capsule OD) was verified by X-ray or measurement, after which the bulged section was cut out with a hacksaw. These specimens were then cut in half on a plane perpendicular to the tube axis at the center of the bulged region. One of the two resultant pieces for each capsule was mounted in a standard metallographic mounting epoxy and polished to reveal the transverse section at the center of the bulge. For capsules AA-7 and DD-7, the other half was sectioned again lengthwise along a plane slightly off the diametral plane of the specimen. This was done to reduce the tendency of the Inconel-600 tube "sheath" to relax and break away from the corroded slug. After sectioning, the exposed surface was polished by standard metallographic procedures. All sectioning was done dry (without lubricant) with a circular diamond saw.

Light Metallography

This work was performed by KAPL. All transverse sections were inspected, and photo-micrographs of the overall section were taken at 4X. In addition, 75X photomicrographs were taken of both the oxide in the annulus and that on the ID of the slug.

SEM and EMPA

Specimens were mounted and electrically grounded to the stage of the SEM using methods developed by KAPL and MTI for their respective equipment. The samples were then examined microscopically and the morphology of the oxide layer in each

annulus was recorded in SEM's. A qualitative search in the oxide layer for the presence of the elements enumerated in Table B-2 then was performed by EMPA.

After this cursory inspection, quantitative measurements were made of the intensity of the X-rays emanating from each of the elements found to be present. These readings were then compared with those taken on "standard" samples of the elements, to determine the relative concentrations of these elements in the oxide layer. No attempt was made to correct the readings taken for absorption of the X-rays of one element by any of the others present. Therefore, caution should be exercised in the interpretation of this quantitative data. Furthermore, the validity of the presence or absence of elements in concentrations of 0.10 w/o and below, although calculated and reported, is doubtful, since this concentration range is below the valid detection limit of EMPA.

The quantitative measurements were taken from a number of areas along a representative path across the oxide layer, from the steel interface to the Inconel 600 interface. When a more detailed examination of the concentration distribution of an element was warranted, two other EMPA display techniques were used, namely, an X-ray line trace and an elemental X-ray map.

IMMA (Ion Microprobe Mass Analysis)

All IMMA work was performed by KAPL. Transverse sections of capsules AA-8 and DD-8 were examined for the following elements.

Na, Mg, K, Ca
Al, Si, P, S, Cl
Ti, V, Cr, Mn, Fe, Co, Ni, Cu

TABLE B-2

SUMMARY OF EXAMINATIONS PERFORMED

| Specimen | Sample Prep | LM[1] | SEM/EMPA Tab/elements scanned |
|---|---|---|---|
| AA7-T[2] | KAPL | 4X, 75X | KAPL/ O, Na P Cl Cr, Fe, Ni<br>MTI /O, Na P, S, Cl Cr, Fe, Ni |
| AA7-L | MTI | - - | MTI/ Na P Cl Cr, Fe, Ni |
| AA8-T | KAPL | 4X, 75X | MTI/ O, Na P Cl Cr, Fe, Ni, Cu |
| DD7-T | KAPL | 4X, 75X | KAPL/ O, Na P Cl Cr, Fe, Ni, Cu |
| DD7-L | KAPL | - - | KAPL/ Cl |
| DD8-T | KAPL | 4X, 75X | MTI/ O, Na, Mg, P Cl, Ca, Cr, Fe, Ni, Cu |
| Y11-T | KAPL | 4X, 75X | KAPL/ O, Na P Cl Cr, Fe, Ni |
| Y10-T | KAPL | 4X, 75X | KAPL/ O, Na P Cl Cr, Fe, Ni<br>MTI/ O, Na P Cl Cr, Fe, Ni, Cu |
| Y1-T | KAPL | 4X, 75X | KAPL/ O, Na P Cl Cr, Fe, Ni<br>MTI/ O S, Cl Cr, Fe, Ni |
| DD12-T | KAPL | 4X, 75X | KAPL/ O, Na P Cl Cr, Fe, Ni |

Notes: 1. LM - Light Metallography, magnification of photomicrographs given

SEM - Scanning Electron Microscopy

EMPA - Electron Mircoprobe Analysis

IMMA - Ion Microprobe - Mass Analysis

KAPL - Knolls Atomic Power Laboratory, Schenectady, NY

MTI - Mechanical Technology Inc., Latham, NY

2. T - Transverse section through center of bulged regions

L - Longitudinal section from center of bulge to one end.

Data from the above examinations was statistically analyzed to determine correlation coefficients for groups of elements. A large (>0.8 on a scale of 0 to 1) positive correlation coefficient for two elements would indicate a high probability of finding both of them at any location where one of them was detected. This might imply that the elements were physically or chemically associated. A large negative coefficient would indicate a high probability of not finding both elements at any location where one of them was detected.

## RESULTS

### Light Microscopy

Photomicrographs of transverse cross sections of the eight capsules taken at 4X are presented as Figures B-1 through B-8. Non-protective magnetite was found on both the ID (inside diameter) of the carbon steel slug and in the annulus between the slug and the Inconel tubing. As can be seen most noticeably in Figure B-4, the slug was not always centered in the tubing. Whereas corrosion in the 0.1 M $FeCl_2$ appeared to be very uniform, corrosion in the W/EPRI reference environment was irregular, especially on the ID surface.

The structure of the oxide in both the annulus and on the ID of the slug was examined in detail at 75X. Photo-micrographs are presented in Figures B-9 through B-16. Oxides formed from the two denting environments were similar. The following features were present in varying degrees on all specimens. The background was a medium to dark grey oxide which had a rippled, layered appearance. Layers were closely-spaced (1-2 mil) and ran circumferentially (parallel to the steel interface). Discontinuities in this pattern were sometimes

observed, as in the bottom micrograph of Figure B-10. These apparently form when corrosion is halted then restarted, as when a capsule is taken from the furnace for venting or soaking. Scattered throughout this background were discrete areas of lighter oxide. These light areas were much more prominent in the annulus oxide of capsules DD-7 and DD-8. In some samples this lighter oxide formed a pattern of radial rays. As shown more clearly in the SEM results which follow, these appeared to be regions of coarse-grained magnetite which had precipitated into former void areas of the original non-protective magnetite. The oxide/steel interface was irregular, with the dimensions of the irregularities (0.5 to 2 mil) reflected in the rippling of the lamellar structure. Seldom was there a break at the oxide/steel interface. Cracks were sometimes observed in the annular oxide, but these may have been generated during sectioning and mounting.

The ID oxide, which grew inward without restraint, generally had a more uniform appearance than the annulus oxide. Porosity as indicated by the size and number of black areas in the photomicrographs, was present throughout the ID oxide in most samples and appeared to increase with distance from the steel interface. This latter effect may have been due to the buckling of older, outer layers of oxide as they were moved inward toward a region of smaller circumferential area. For most capsules, the ID oxide was 1.3 - 1.5 mm thick (50 - 60 mil). Presuming an oxide/metal volume ratio of 2, this would result in an inward movement of up to 0.8 mm (30 mil) on the radius. For the average slug ID of 9.58 mm (0.377 in), this represents a decrease of $\sim$15% in circumference at the oxide surface.

The annulus oxide was characterized by several distinct circumferential bands. The outermost band, from the Inconel

interface to the point where the discrete light regions disappear, was very similar in appearance to the ID oxide. Some very large pores were observed at the Inconel interface; otherwise, little porosity was apparent. Radial cracks would tend to develop and widen as the older, outer layers of oxide were moved outward toward a region of larger circumferential area. For most capsules, the annulus oxide was 1.0-1.3 mm thick (40-50 mil). Presuming an oxide/metal volume ratio of 2, this would result in an outward movement of up to 0.6 mm (24 mil) on the radius. For the average slug OD of 16.1 mm (0.635 in) this represents an increase of $\sim$ 8% in circumference at the oxide surface.

The central band consisted of the rippled, layered oxide observed previously, but without the discrete regions of lighter oxide. Circumferential breaks in the layered pattern were observed as in the ID oxide.

The innermost oxide, a band ranging from 75 to 250 $\mu$m (3 to 10 mil) next to the carbon steel interface, was typically a lighter grey than the central band. Its appearance ranged from featureless to mottled. Some oxide cracking was observed, although the interface with the carbon steel was generally continuous. This band was not found in capsule AA-7 which had not grown following the soak (see Figure B-9).

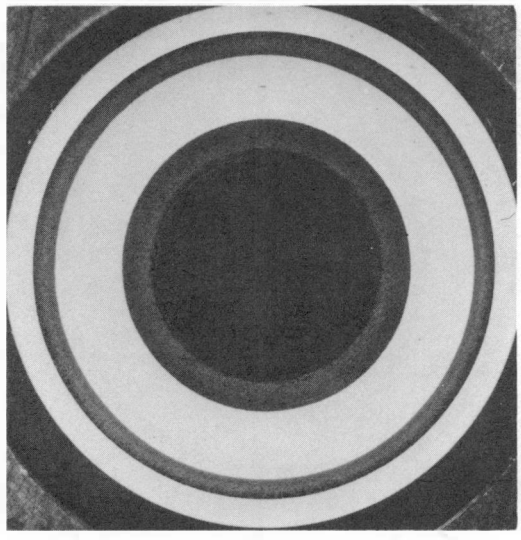

Figure B-1
Capsule AA-7
Transverse Section (4X)*
0.1 M $FeCl_2$
150°F/96hr/1000 ppm $PO_4$/2.8
Volatile

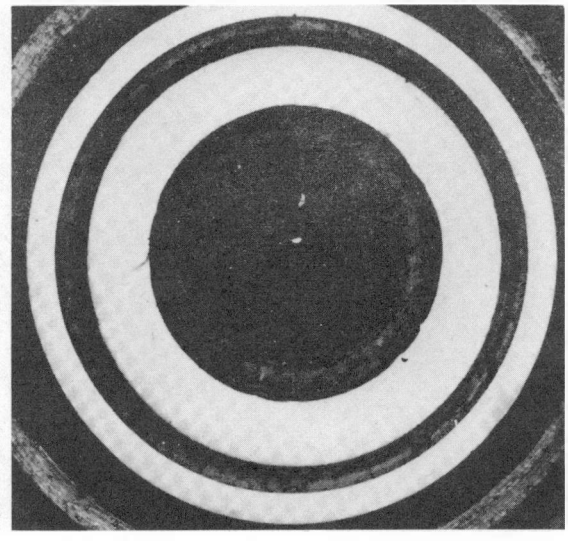

Figure B-2
Capsule AA-8
Transverse Section (4X)*
0.1 M $FeCl_2$
150°F/96hr/1000 ppm
$PO_4$/2.8
Fault

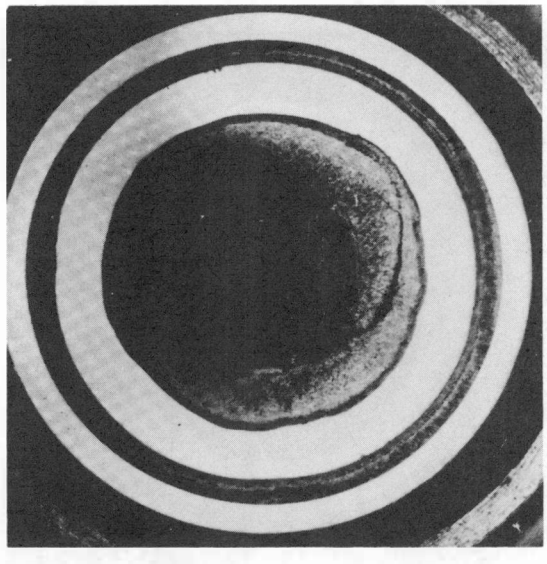

Figure B-3
Capsule DD-7
Transverse Section (4X)*
Seawater + 0.1 M $CuCl_2$ +
0.1 M $NiCl_2$
150°F/96hr/1000 ppm $PO_4$/2.8
Volatile

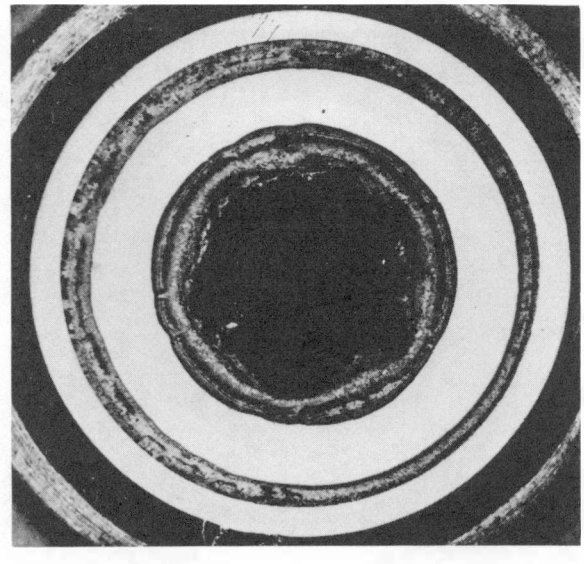

Figure B-4
Capsule DD-8
Transverse Section (4X)*
Seawater + 0.1 M $CuCl_2$
+ 0.1 M $NiCl_2$
150°F/96hr/1000 ppm
$PO_4$/2.8
Fault

*Please note that the illustrations on this page have been reduced 10% in printing.

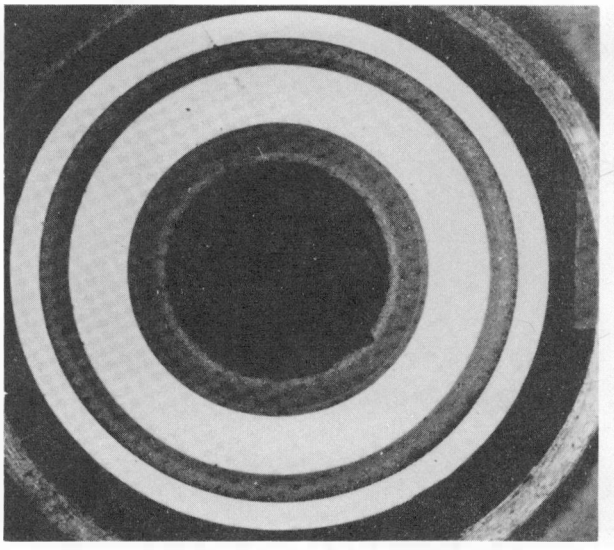

Figure B-5

Capsule Y-11
Transverse Section (4X)*
0.1 M $FeCl_2$
565°F/96hr/300 ppm $PO_4$/2.5
Volatile

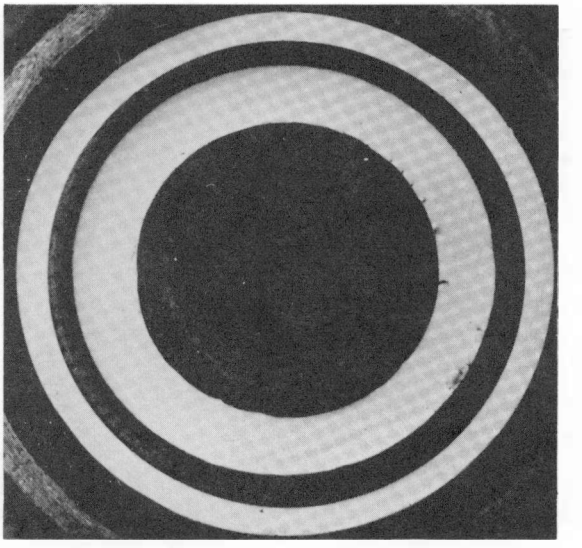

Figure B-6

Capsule Y-10
Transverse Section (4X)*
0.1 M $FeCl_2$
565°F/96 hr/300 ppm
$PO_4$/2.5
Fault

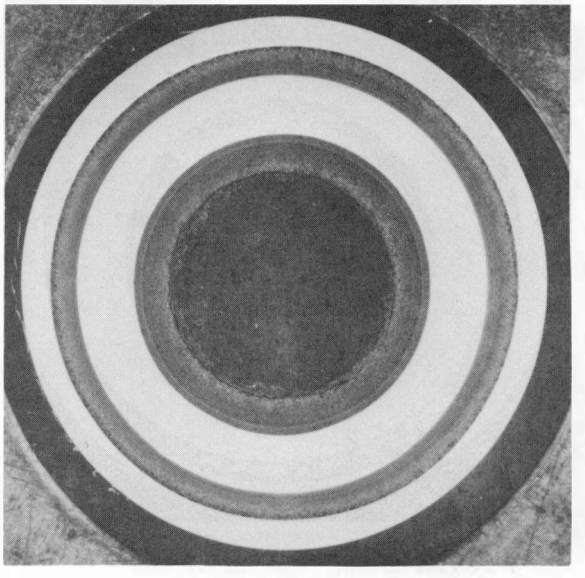

Figure B-7
Capsule Y-1
Transverse Section (4X)*
0.1 M $FeCl_2$
150°F/96hr/200 ppm $N_2H_4$
Volatile

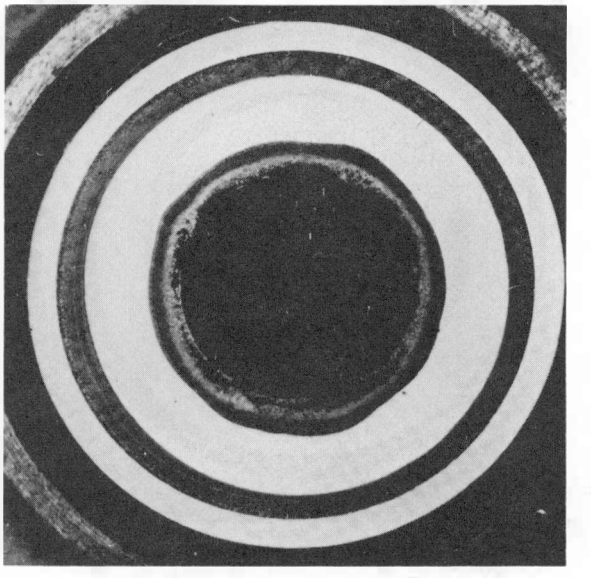

Figure B-8
Capsule DD-12
Transverse Section (4X)*
Seawater + 0.1 M $CuCl_2$ +
0.1 M $NiCl_2$
Soak Conditions unknown
Volatile

*Please note that the illustrations on this page have been reduced 10% in printing.

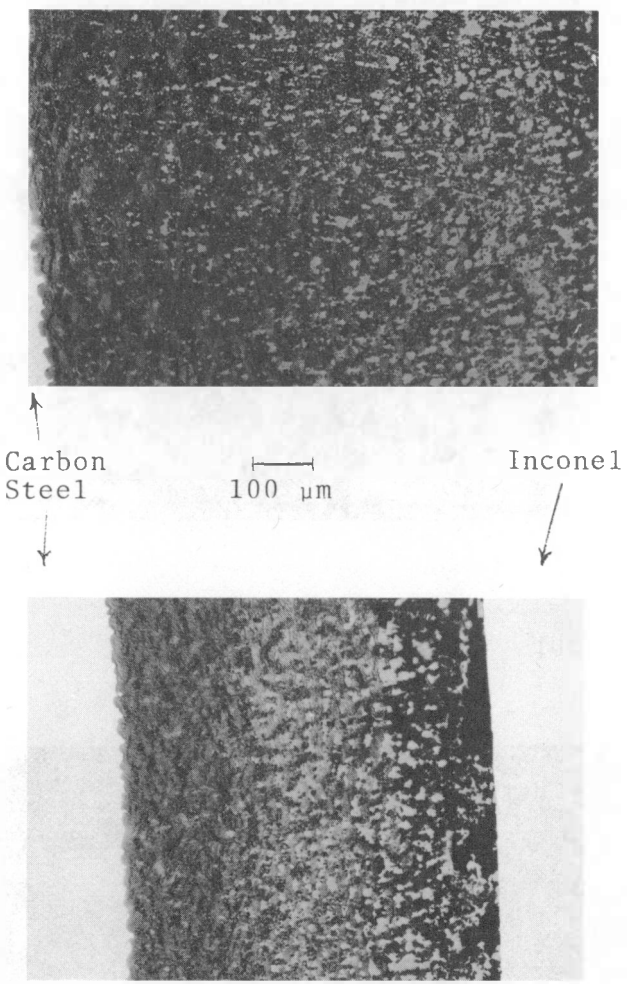


Figure B-9

Capsule AA-7
Transverse Section
at Middle of Bulge
Top: Oxide on ID of Slug
Bottom: Oxide in annulus

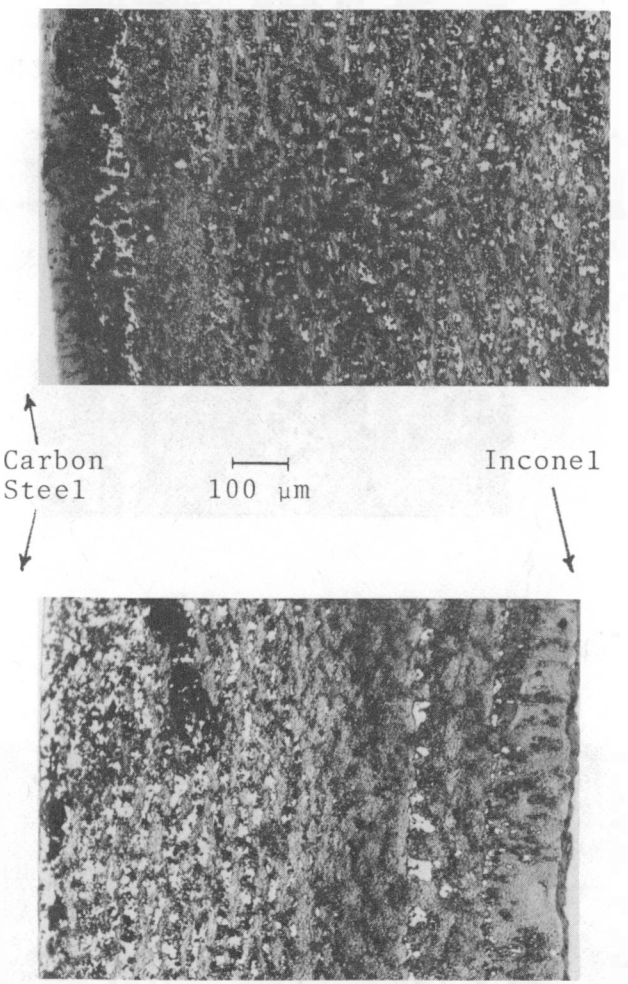


Figure B-10

Capsule AA-8
Transverse Section
at Middle of Bulge
Top: Oxide on ID of Slug
Bottom: Oxide in annulus

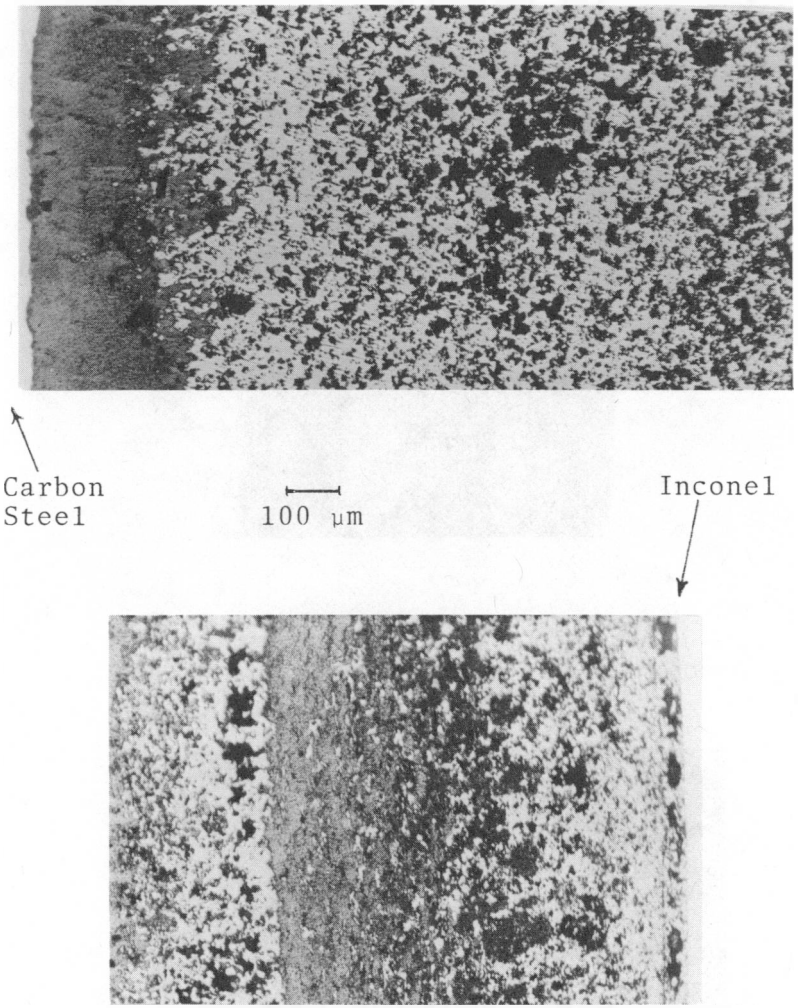


Figure B-11 Capsule DD 7
Transverse Section
Through Middle of
Bulge
Top: Oxide on ID of Slug
Bottom: Oxide in annulus

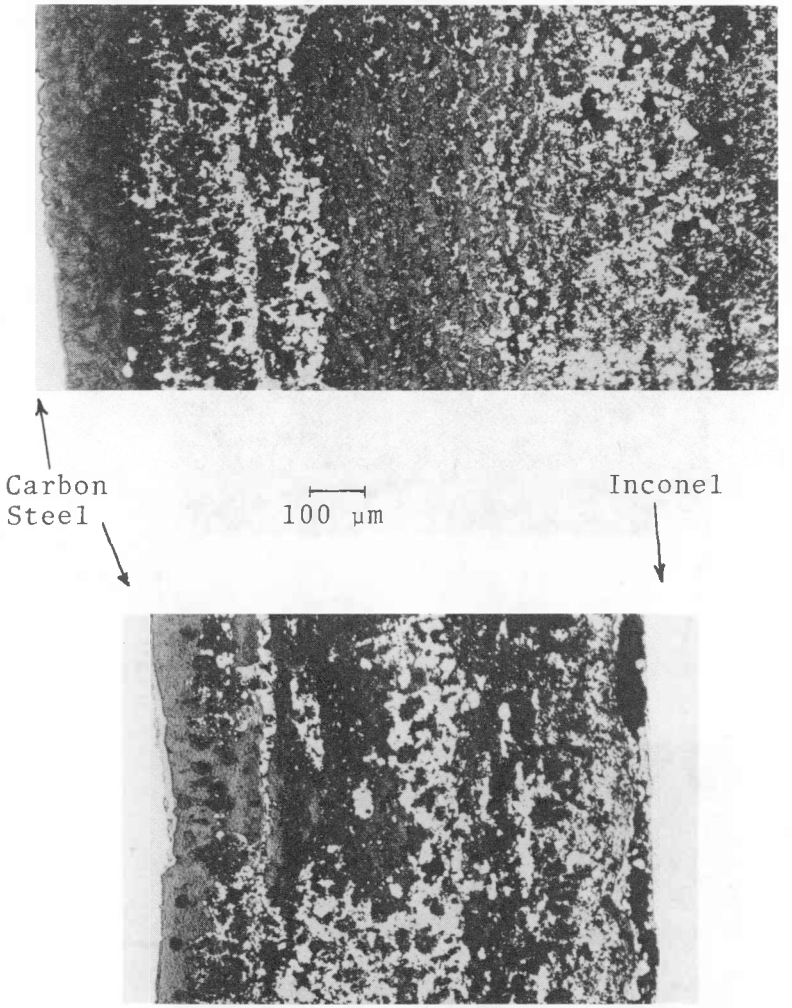


Figure B-12 Capsule DD 8
Transverse Section
Through Middle of
Bulge
Top: Oxide on ID of Slug
Bottom: Oxide in annulus

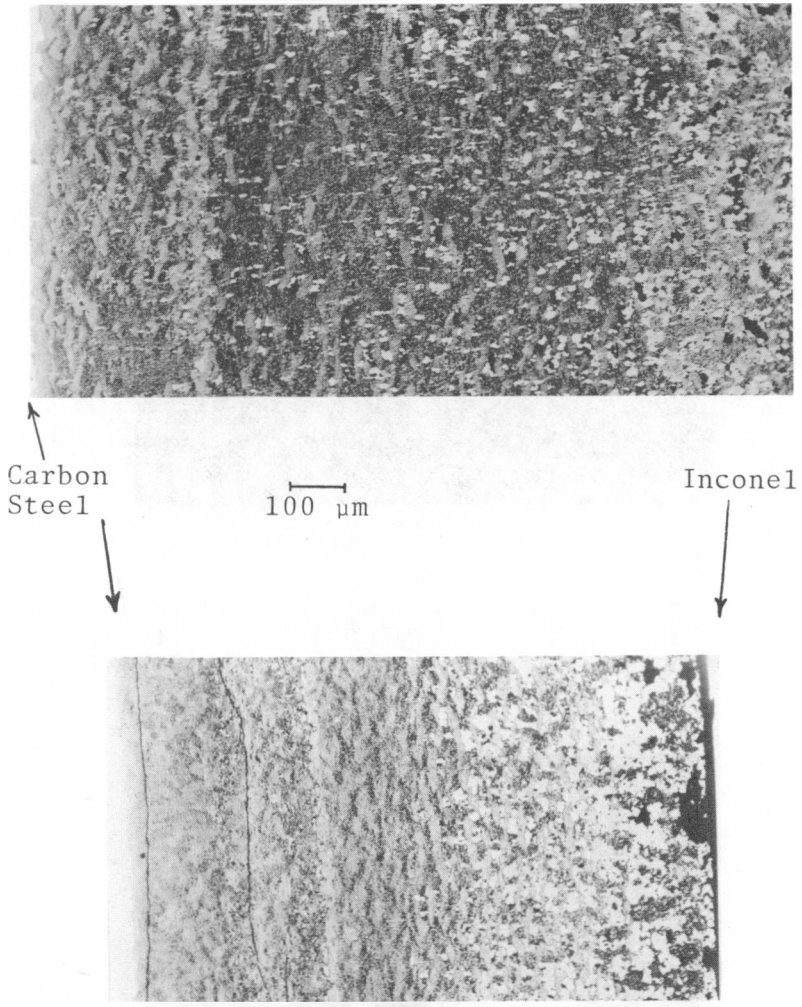


Figure B-13 Capsule Y-11
Transverse Section at
Middle of Bulge
Top: Oxide on ID of Slug
Bottom: Oxide in annulus

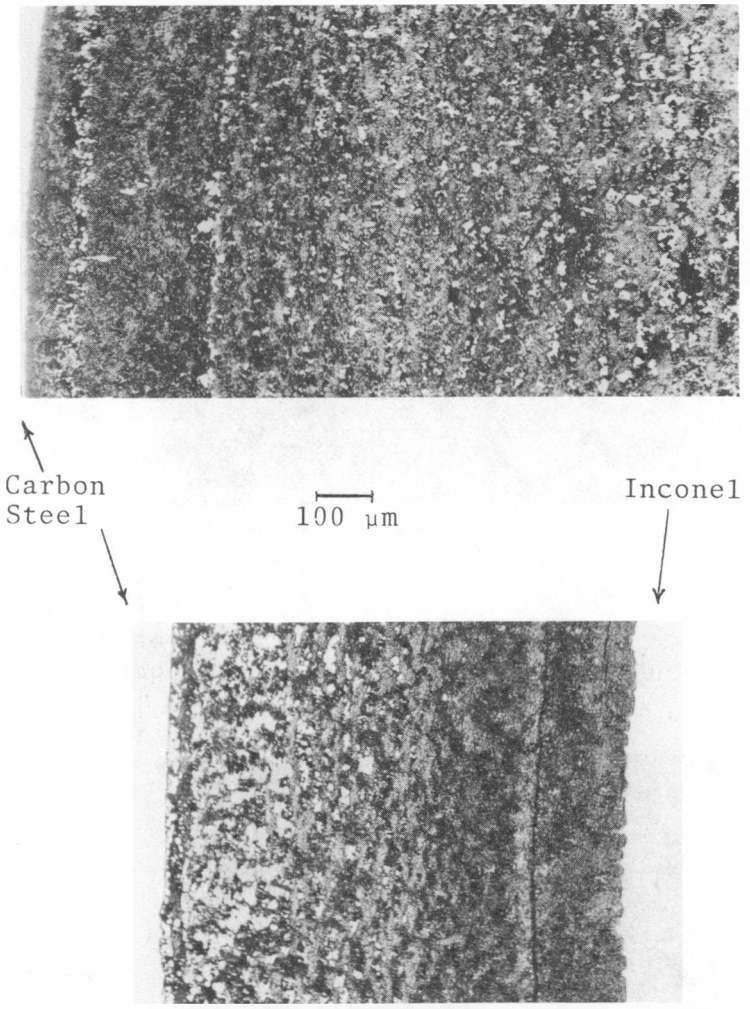


Figure B-14 Capsule Y-10
Transverse Section at
Middle of Bulge
Top: Oxide on ID of Slug
Bottom: Oxide in annulus

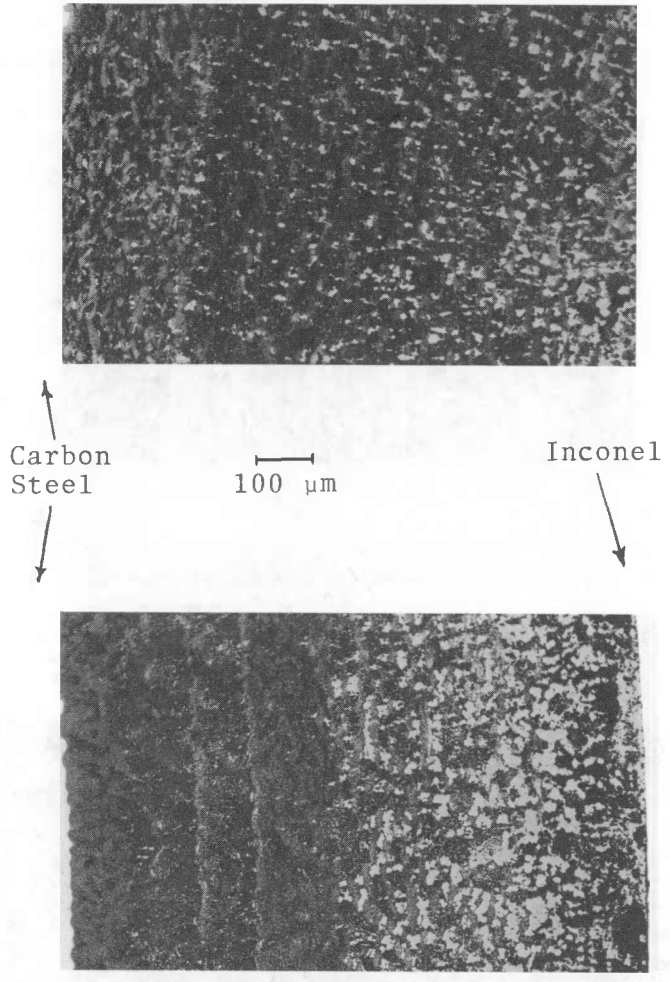


Figure B-15 Capsule Y-1
Transverse Section at
Middle of Bulge
Top: Oxide on ID of Slug
Bottom: Oxide in Annulus

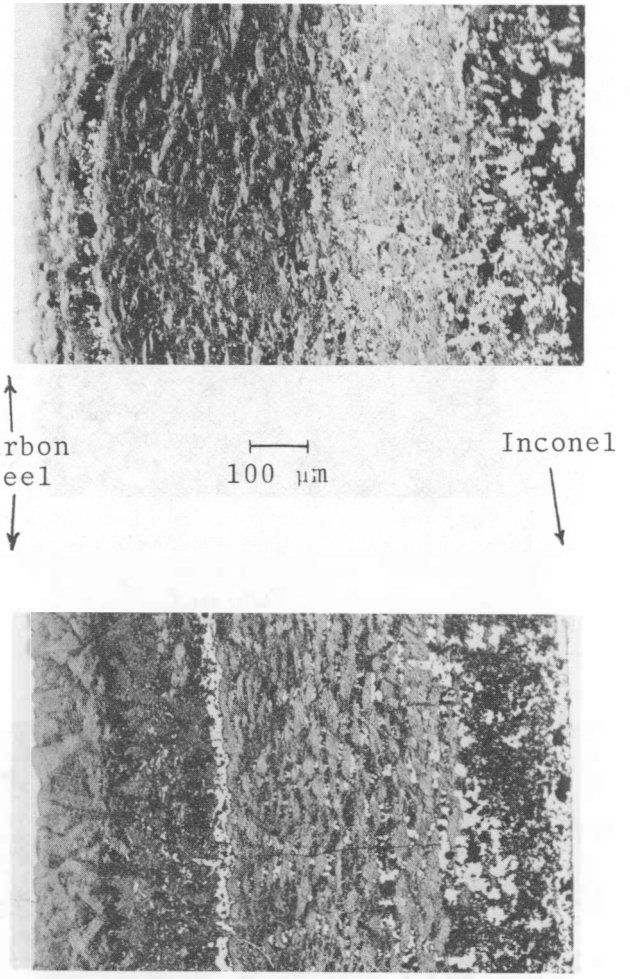


Figure B-16 Capsule DD 12
Transverse Section at
Middle of Bulge
Top: Oxide on ID of Slug
Bottom: Oxide in Annulus

SEM and EMPA

Sample AA-7, Transverse Section. A representative portion of the oxide layer in the annulus of Sample AA-7 is shown in the SEM of Figure B-17; the steel plug is at the upper right, the Inconel tube is at the lower left, the oxide layer is in the center, and a fiducial line is at the upper left. The oxide layer is about 0.028 inch wide. The oxide has a smooth appearance from the steel interface out to about 0.016 inch, where pits or pores are found, which increase in number and size toward the Inconel, with a concentration of large pores at the interface. Although, no separation between metal and oxide exists at the steel interface, the interface is irregular, as shown in Figure B-17, and at a higher magnification in Figure B-18.

The element distribution across the area shown in Figure B-17 is given in Table B-3. The oxide layer was found to consist of iron and oxygen and the relative concentrations of each were found to remain constant from one metal interface to the other. The reason for the abnormally low values for oxygen content is the extremely large mass absorption coefficient of the iron at the wave length of oxygen X-radiation. The presence of chromium and nickel was just barely detected above the background radiation. No X-ray signal above background level was found for chlorine, sulfur, sodium or phosphorus.

An interesting feature of this sample is the presence of well-defined octahedral crystals (Figure B-19 and B-20), which are believed to be magnetite ($Fe_3O_4$) crystals, in the large interstitial areas near the Inconel interface.

TABLE B-3

ELEMENT DISTRIBUTION OF SAMPLE AA-7
TRANSVERSE SECTION

| Area | w/o Fe | w/o Cr | w/o Ni | w/o Cl | w/o S | w/o O | w/o Na | w/o P |
|---|---|---|---|---|---|---|---|---|
| A1 (near steel) | 65.5 | 0.093 | 0.090 | N.D.* | N.D. | 22.4 | N.D. | N.D. |
| A2 | 65.7 | 0.115 | 0.072 | N.D. | N.D. | 22.9 | N.D. | N.D. |
| A3 | 66.7 | 0.052 | 0.056 | N.D. | N.D. | 23.1 | N.D. | N.D. |
| A4 | 65.8 | 0.058 | 0.034 | N.D. | N.D. | 21.0 | N.D. | N.D. |
| A5 | 67.0 | 0.052 | 0.079 | N.D. | N.D. | 21.9 | N.D. | N.D. |
| A6 (near Inconel) | 65.8 | 0.041 | 0.063 | N.D. | N.D. | 22.0 | N.D. | N.D. |

Note * N.D. = Not detected above background radiation

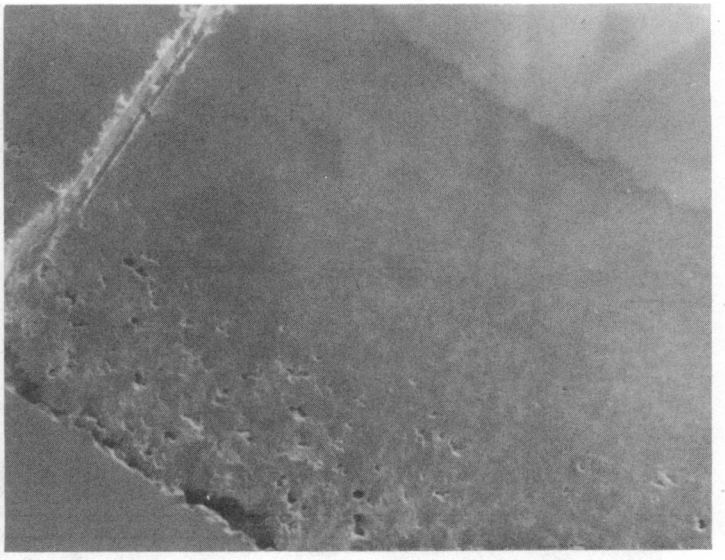


100X*

Figure B-17. SEM of the Oxide Layer in the Annulus of Sample AA-7. (Inconel/Oxide/Steel)

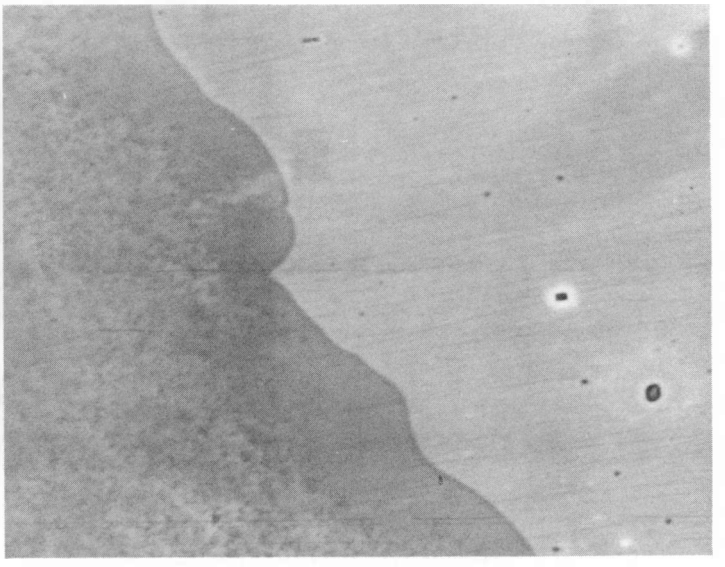


1000X*

Figure B-18. SEM of the Steel/Oxide Interface - Sample AA-7.

*Please note that the illustrations on this page have been reduced 10% in printing.

Inconel

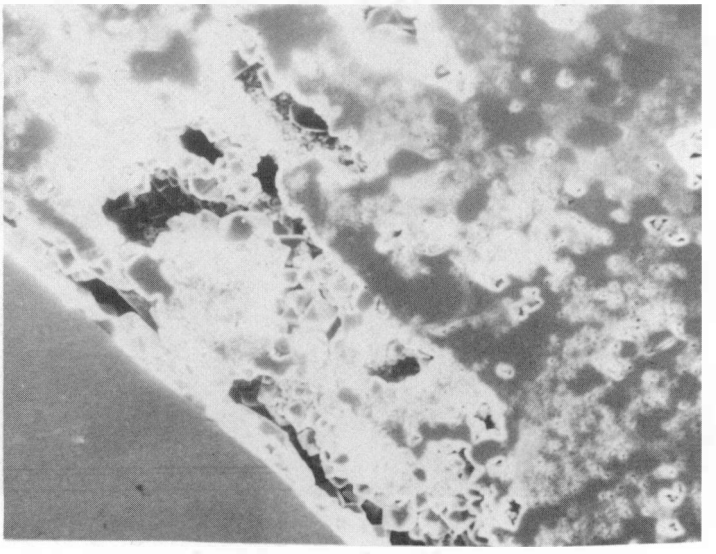

Oxide

300X*

Figure B-19. SEM of Octahedral Crystals
Sample AA-7

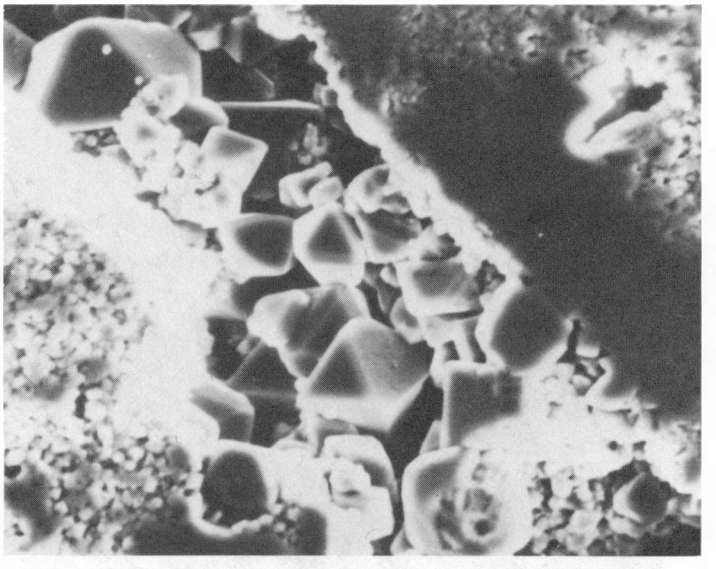

1000X*

Figure B-20 SEM of Octahedral Crystals
Sample AA-7

*Please note that the illustrations on this page have been reduced 10% in printing.

Sample AA-7, Longitudinal Section. Figure B-21 is a light micrograph of the lengthwise section of sample AA-7. Examinations were made of four areas along the length of the axial layer. These areas (designated I, II, III, and IV) were situated at positions approximately 1/5, 2/5, 3/5, and 4/5 of the distance from the midpoint of the capsule previously examined in transverse section, to the outer end of the carbon steel plug. Scanning electron micrographs of these areas are shown in Figures B-22 through B-25 at higher magnification. The Inconel is at the top, the oxide is in the center, and the steel is at the bottom in all four micrographs.

The morphology of the oxide along the length of the section and from the steel to the Inconel interface was the same as that previously described for the transverse section. The oxide appears smooth near the steel even though the interface line is irregular (Figure B-22 through B-25). Pits and pores are found near the middle of the oxide which increase in number and size toward the Inconel with a concentration of large pores at the interface.

The element distribution was determined at five sites in each of the areas examined: 1) in the steel near the oxide, 2) in the oxide near the steel, 3) in the middle of the oxide, 4) in the oxide near the Inconel, and 5) in the Inconel near the oxide. Results are given in Table B-4. No X-ray signal above background level was found for phosphorus. Signals in the oxide for nickel, chromium, chlorine, and sodium were just barely detected above background, and only in very isolated spots for the latter two elements. Some high counts for nickel were found in the oxide near the Inconel in Areas II, III, and IV; however, upon closer microscopic examination, metal appears to have been smeared from the Inconel onto the oxide during polishing, and possibly was trapped in the numerous pores of this region.

Iron and oxygen were found to be the major constituents of the oxide. The iron concentration remains constant along the length of the annulus, with the oxide being slightly richer in iron toward the steel interface.

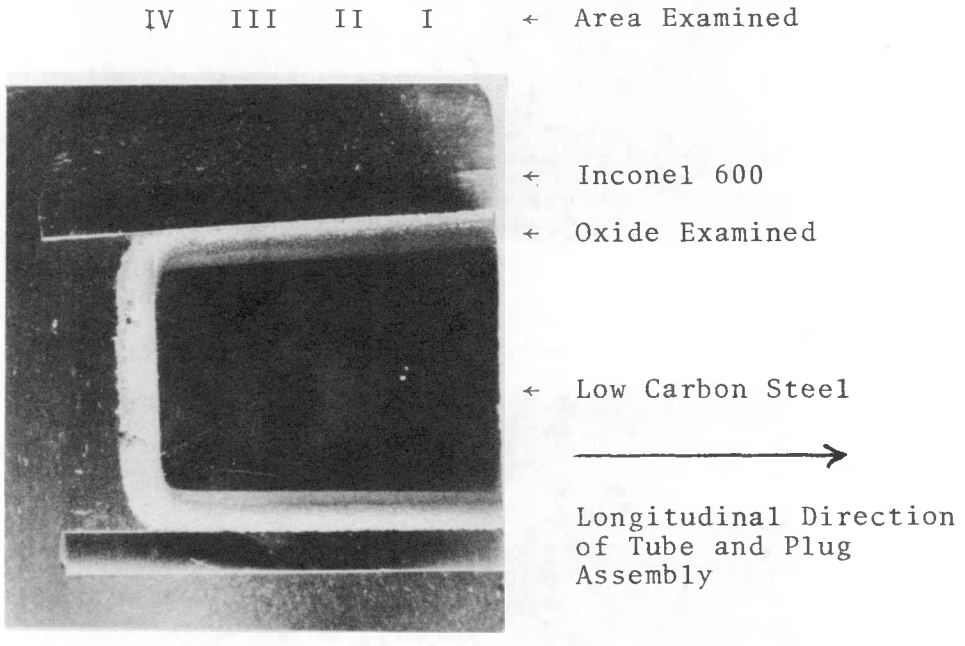


Figure B-21. Lengthwise Section of Sample AA-7

*Please note that the illustrations on this page have been reduced 10% in printing.

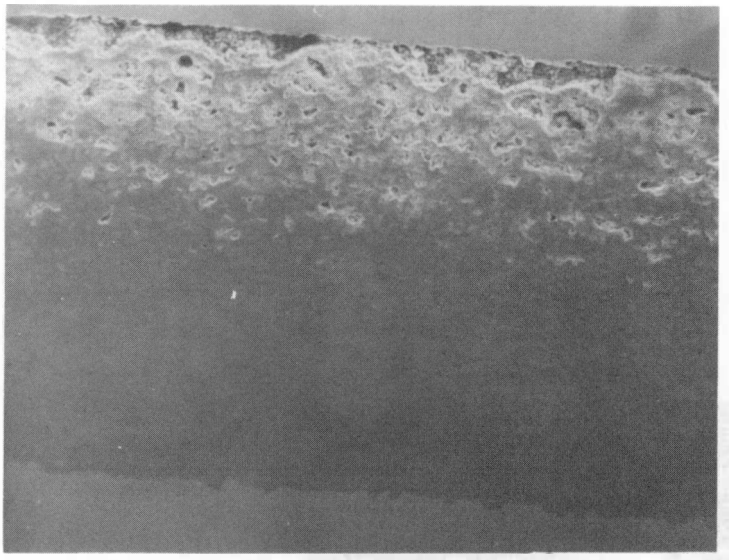


Figure B-22. 50X*

SEM of Area I of the
Oxide Layer Investigated

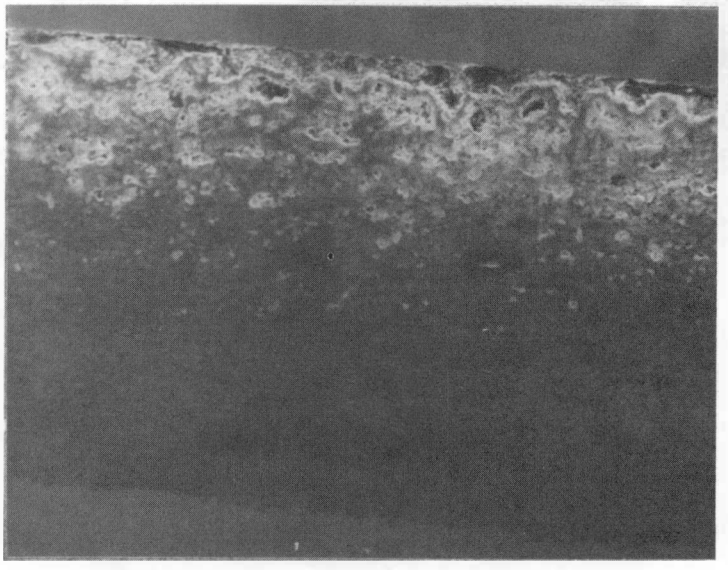


Figure B-23. 50X*

SEM of Area II of the
Oxide Layer Investigated

*Please note that the illustrations on this page have been reduced 10% in printing.

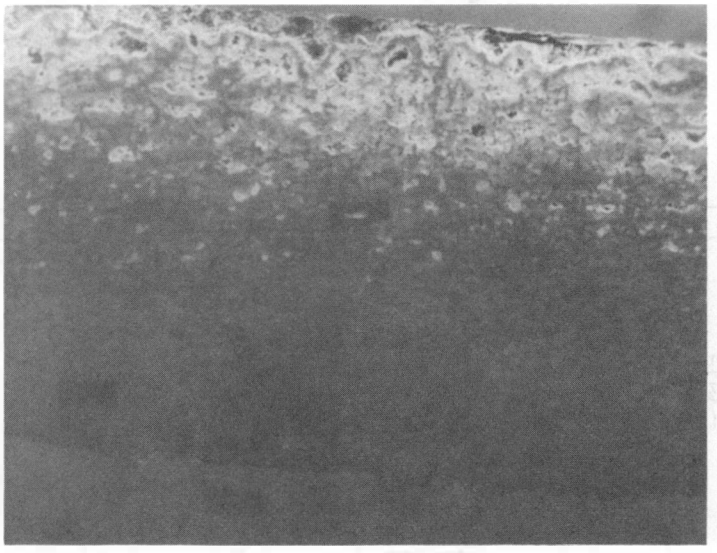


Figure B-24. 50X*

SEM of Area III of
the Oxide Layer


Figure B-25. 50X*

SEM of Area IV of
the Oxide Layer

*Please note that the illustrations on this page have been reduced 10% in printing.

TABLE B-4

ELEMENT DISTRIBUTION OF SAMPLE AA-7
LONGITUDINAL SECTION

| Site | w/o Fe | w/o Ni | w/o Cr | w/o P | w/o Cl | w/o Na |
|---|---|---|---|---|---|---|
| | | | AREA I | | | |
| Inconel (1) | 9.49 | 54.7 | 16.2 | N.D.* | N.D. | 0.084 |
| Oxide near Inconel (2) | 53.1 | 0.114 | 0.058 | N.D. | N.D. | N.D. |
| Middle of Oxide (3) | 59.4 | 0.014 | 0.039 | N.D. | N.D. | 0.056 |
| Oxide near Steel (4) | 59.3 | N.D. | 0.058 | N.D. | 0.049 | 0.077 |
| Steel (5) | 97.3 | N.D. | 0.039 | N.D. | N.D. | 0.035 |
| | | | AREA II | | | |
| (1) | 9.44 | 57.3 | 15.6 | N.D. | N.D. | N.D |
| (2) | 50.3 | 1.55** | 0.276 | N.D. | 0.029 | N.D. |
| (3) | 59.7 | 0.020 | 0.021 | N.D. | 0.019 | N.D. |
| (4) | 60.4 | 0.007 | 0.035 | N.D. | N.D. | 0.063 |
| (5) | 92.7 | 0.005 | 0.047 | N.D. | N.D. | N.D. |
| | | | AREA III | | | |
| (1) | 9.5 | 58.5 | 15.9 | N.D. | 0.019 | N.D. |
| (2) | 53.1 | 1.82** | 0.140 | N.D. | N.D. | 0.056 |
| (3) | 61.3 | 0.047 | 0.054 | N.D. | N.D. | N.D. |
| (4) | 59.0 | N.D. | 0.013 | N.D. | N.D. | N.D. |
| (5) | 96.2 | 0.008 | 0.028 | N.D. | N.D. | N.D. |
| | | | AREA IV | | | |
| (1) | 9.1 | 57.4 | 15.4 | N.D. | N.D. | N.D. |
| (2) | 58.4 | 1.11** | 0.038 | N.D. | N.D. | N.D. |
| (3) | 58.5 | 0.068 | 0.036 | N.D. | 0.019 | 0.028 |
| (4) | 57.4 | 0.033 | 0.051 | N.D. | 0.024 | N.D. |
| (5) | 88.9 | 0.008 | 0.057 | N.D. | N.D. | N.D. |

* Not detectd above background radiation.

** Material looked to be smeared from Inconel during polishing.

Samples AA-8. A representative portion of the oxide layer in the annulus of sample AA-8 is shown in Figure B-26. The steel is at the left of the micrograph and the Inconel is at the right. The total width of the oxide layer is approximately 0.040 inch. This oxide layer appears to have three zones. The first zone extends from the steel interface out to 0.006 inch, where there is a ridge running parallel to the interface. Another zone, similar to the first extends approximately 0.004 inch further out toward the Inconel tube. The material in these regions appears smooth except for the ridges. From the end of the second zone to the Inconel interface, the oxide becomes increasingly more porous, with the pits growing in both number and size. A feature of this oxide layer is the numerous transverse (radial) cracks, like the one shown in Figure B-26. This particular crack seems to have initiated at one of the large holes in the oxide at the Inconel interface. Wide cracks in the oxide parallel to the steel interface also were found, as shown in the SEM of Figure B-27, which are located at approximately 0.006 inch from the steel interface.

The data of Table B-5 shows the distribution of elements across an area like that shown in Figure B-26. The oxide consists predominantly of iron and oxygen; the iron content is higher near the steel interface. No phosphorus was detected in the sample. Only minute amounts of sodium, chromium, nickel, and copper were found in the oxide. Chlorine was found confined to a narrow region next to the steel interface. Figure B-28 is a SEM of a portion of the steel/oxide interface and superimposed on it is an X-ray line trace for chlorine. The chlorine is confined to a band of the oxide approximately 0.006 inch wide. This band width is the same as that of the first zone (described above), and its outer boundry coincides with the location of the wide crack shown in Figure B-27. The peak in this line trace corresponds to a chlorine content of approximately 0.41 w/o.

TABLE B-5

ELEMENT DISTRIBUTION FOR SAMPLE AA-8

| Area | w/o Fe | w/o Cr | w/o Ni | w/o Cu | w/o O | w/o Cl | w/o Na | w/o P |
|---|---|---|---|---|---|---|---|---|
| Low carbon steel | 99.5 | 0.028 | N.D. | 0.023 | 0.041 | N.D. | N.D. | N.D. |
| "Oxide" near steel | 70.3 | 0.032 | 0.033 | 0.021 | 20.7 | 0.413 | N.D. | N.D. |
| Middle of "oxide" | 64.9 | 0.022 | 0.180 | 0.020 | 20.2 | 0.078 | 0.007 | N.D. |
| "Oxide" near Inconel | 55.9 | 0.033 | 0.864 | 0.021 | 19.4 | 0.078 | 0.042 | N.D. |
| Inconel | 10.8 | 15.4 | 64.5 | 0.342 | N.D. | N.D. | N.D. | N.D. |

Steel

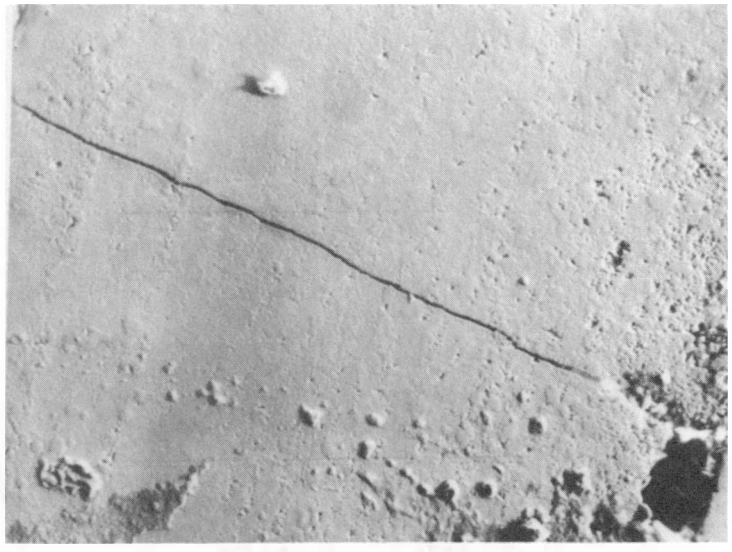

Inconel

100X*

Figure B-26. SEM of the Oxide in the Annulus of Sample AA-8. (Steel/Oxide/Inconel)

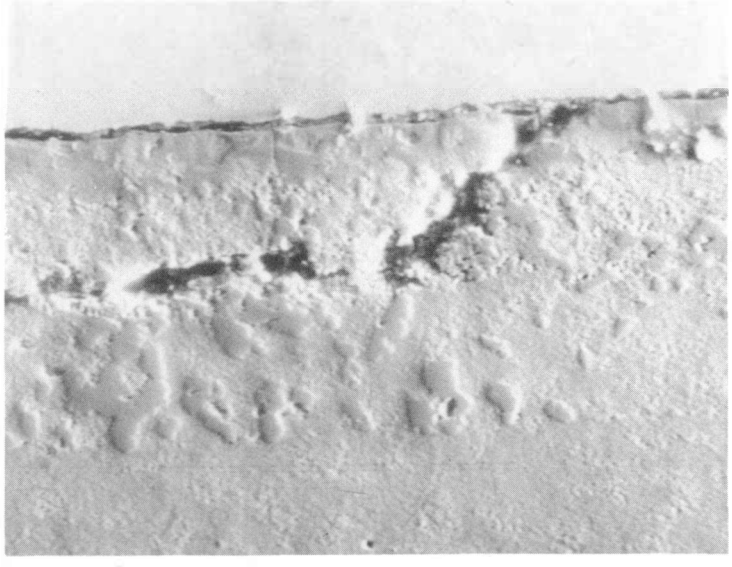

150X*

Figure B-27. SEM of the Steel/Oxide Interface, Showing Crack/ Crevice - Sample AA-8.

*Please note that the illustrations on this page have been reduced 10% in printing.

Oxide

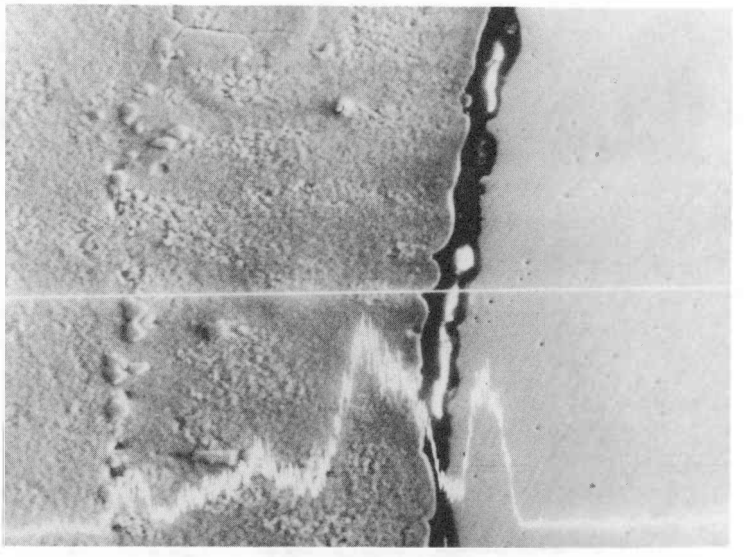

Steel

300X*

Figure B-28. SEM of the Steel/Oxide Interface, With a Superimposed X-ray Line Trace for Chlorine - Sample AA-8.

*Please note that the illustrations on this page have been reduced 10% in printing.

Sample DD-8. A representative portion of the annulus of Sample DD-8 is shown in the SEM of Figure B-29; the steel slug is at the left, the Inconel tube is at the right, and the oxide layer is in the center.

The oxide layer appears to consist of three zones of different widths; the total thickness is about 0.026 inch. The boundary of the first zone is a ridge-like line parallel to the steel interface. This layer is about 0.006 inch thick, and has a smoother appearance than that of the other layers. The second zone is approximately 0.011 inch thick, and terminates at another ridge-like boundary; it contains many pits or pores. The third zone extends the rest of the distance (0.009 inch) to the Inconel; it exhibits a rough texture with most of the pores concentrated in a band at the Inconel 600 interface.

The element distribution across an area like that shown in Figure B-29 is given in Table B-6. The oxide layer consists predominantly of iron and oxygen, with only trace amounts of nickel and chromium. It is iron-rich near the steel interface, and lower in iron towards the Inconel interface, so that practically all of the iron present in the oxide must have originated from the steel; that is, the oxide layer represents, almost entirely, the oxidation product of the steel. Neither phosphorous nor magnesium was detected. Copper, sodium, and calcium were found only in minute amounts in highly localized spots.

The most striking finding is that a high concentration of chlorine exists in the first zone of the oxide layer, near the steel interface. Figure B-30 is a SEM of a portion of the steel slug and the adjacent oxide layer; the steel is at the left, and the ridge-like boundary of the first zone is at the right. Superimposed on the SEM is an X-ray line trace for chlorine; the straight line running through the center is the path actually

scanned for chlorine X-radiation. The trace and the chlorine data in Table B-6 clearly show that the chlorine is highly concentrated in this first zone of the oxide layer. Also present in major amounts in this zone are oxygen and iron, but neither element exhibits a strong concentration gradient like that of chlorine. The concentrations of chlorine indicated by the peaks in the X-ray line trace are greater than the concentration reported in Table B-6 for this area. The data of Table B-6 was generated from an area-count of the X-ray intensities and therefore represents an average value. The line trace is a collection of point counts from each point on the scanned line, and therefore may give individual readings higher than the average. The two small peaks of the line trace of Figure B-30 correspond to 19.6 w/o chlorine and the large peak to 38.0 w/o chlorine. Another feature of this zone of the oxide layer, that is related to the chlorine concentration, is the "starfish-like" growths on the oxide surface (Figure B-31A and B), which slowly evaporate or decompose under the electron beam. Nevertheless, it was possible to determine by EMPA that they are rich in chlorine. Figure B-32A is a SEM of a few of these "starfish" at higher magnification, and Figure B-32B is a chlorine X-ray map of this same area. The brightest regions of Figure B-32B correspond to the shape of the "starfish" of Figure B-32A.

TABLE B-6

ELEMENT DISTRIBUTION FOR SAMPLE DD-8

| Area | w/o Fe | w/o Cr | w/o Ni | w/o Cu | w/o O | w/o Cl | w/o Na | w/o P | w/o Mg | w/o Ca |
|---|---|---|---|---|---|---|---|---|---|---|
| Low Carsteel | 100.2 | 0.017 | 0.018 | 0.007 | 0.219 | N.D. | N.D. | N.D. | N.D. | N.D. |
| "Oxide" near steel | 50.9 | 0.011 | 0.014 | N.D.* | 21.9 | 16.40 | N.D. | N.D. | N.D. | N.D. |
| Middle of "oxide" | 63.1 | 0.030 | 0.041 | 0.013 | 23.7 | 0.121 | N.D. | N.D. | N.D. | N.D. |
| "Oxide" near Inconel | 62.5 | 0.017 | 0.084 | 0.147 | 23.8 | 0.092 | 0.028 | N.D. | N.D. | N.D. |
| Inconel | 9.25 | 15.6 | 60.3 | 0.340 | N.D. | 0.015 | 0.035 | N.D. | N.D. | N.D. |

* N.D. not detected above background radiation

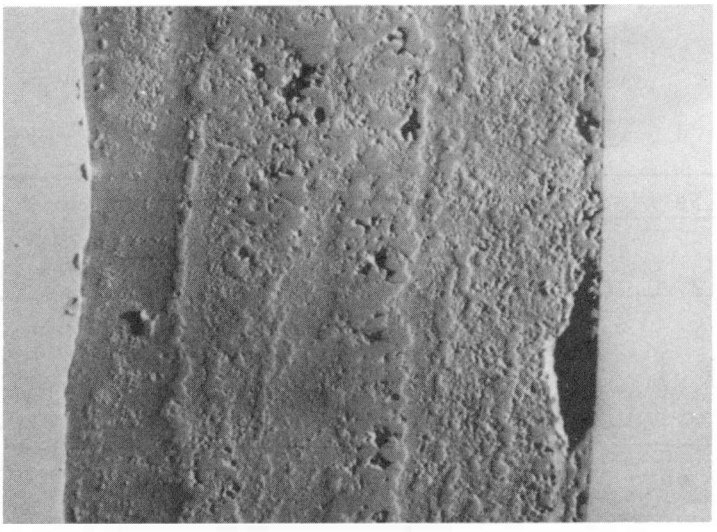


100X*

Figure B-29. SEM of the Oxide Layer in the Annulus of Sample DD-8. (Steel/Oxide/Inconel)

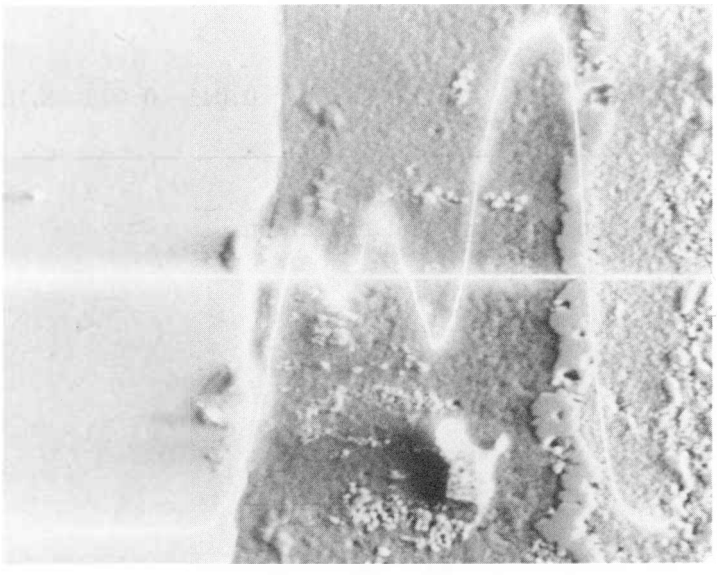


300X*

Figure B-30. SEM of the Steel/Oxide Interface, With a Superimposed X-ray Line Trace for Chlorine - Sample DD-8.

*Please note that the illustrations on this page have been reduced 10% in printing.

Steel

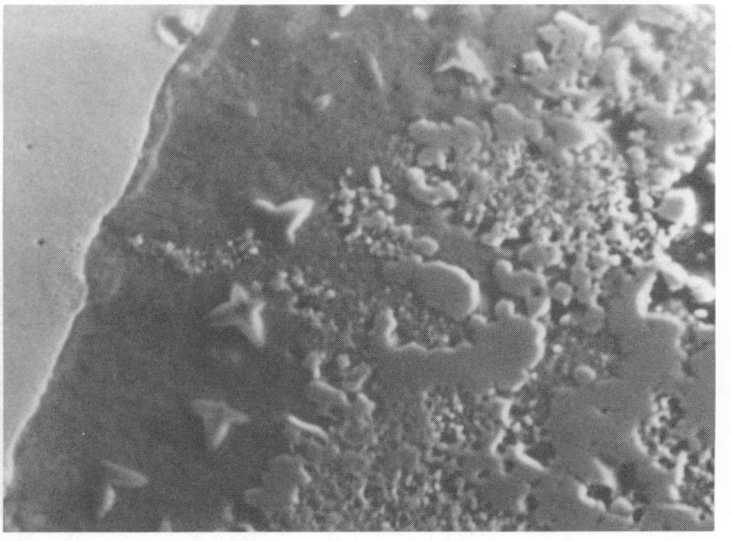

Oxide

A. 500X*

Steel

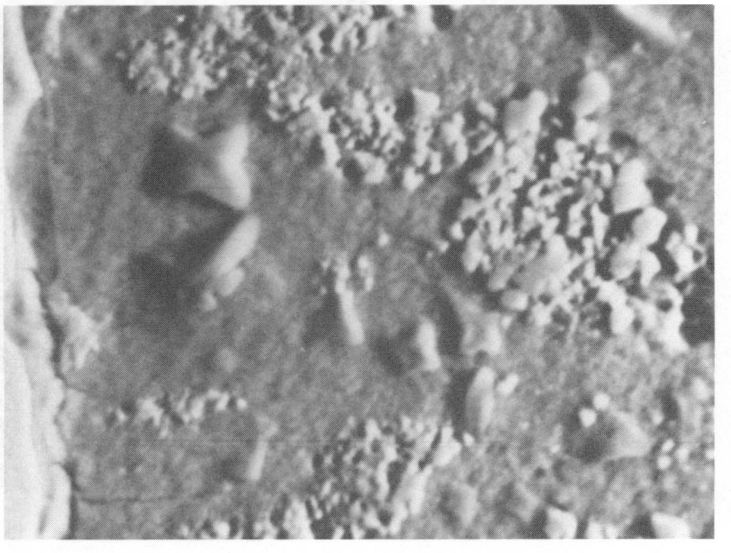

Oxide

B. 1000X*

Figure B-31. SEM's of the "Starfish-like" Growths in the Oxide Layer at the Steel/Oxide Interface - Sample DD-8.

*Please note that the illustrations on this page have been reduced 10% in printing.

A. 1500X*

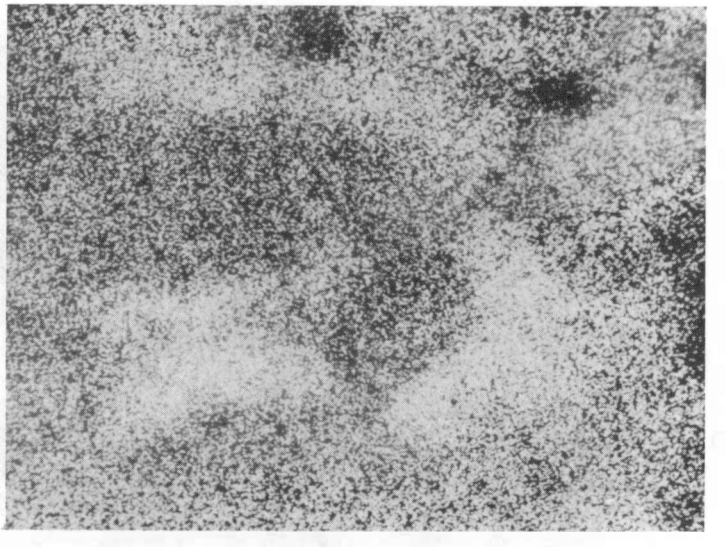

B. 1500X*

Figure B-32. SEM of Starfish-like Crystals in the Oxide Layer at the Steel/Oxide Interface (A), and Corresponding X-ray Map for Chlorine (B).

*Please note that the illustrations on this page have been reduced 10% in printing.

Sample Y-10. Figure B-33 is a SEM of a representative portion of the oxide layer in the annulus of Specimen Y-10. The steel slug is at the left, and the Inconel tube is at the right. The total width of this oxide layer was measured to be approximately 0.035 inch. The most notable feature of this sample is a crack running parallel to the steel interface, at approximately 0.006 inch from the metal. The oxide has a rather smooth surface in a region extending 0.015 inch from the steel interface outward, toward the Inconel. Beyound this region, pits and holes begin to increase in number and size, with the largest holes existing at the Inconel interface. In the region shown in Figure B-33, a separation in the oxide was so great that the mounting epoxy intruded into this gap (bright, flared, streak).

The composition profile across an area like that shown in Figure B-33 is given in Table B-7. The oxide layer was found to be composed of primarily iron and oxygen, with the iron content decreasing with distance from the steel interface. No phosphorus was detected, and only occasional spots contained sodium. Very small amounts of chromium, nickel, and copper were found in the oxide layer. A sharp gradient in the chlorine content was found near the steel interface. The SEM of Figure B-34 shows a portion of the steel and oxide layer at the interface with an X-ray line trace for chlorine superimposed. The trace clearly shows that the chlorine is concentrated in zone of oxide bordered by the crack (mentioned above) and appears to peak in the center of this area, and at the crack itself. The large peak corresponds to a chlorine content of 20.6 w/o and the small peak to 15.4 w/o. Iron and oxygen are major constituents of this zone, but again do not exhibit any marked concentration gradients.

TABLE B-7

ELEMENT DISTRIBUTION FOR SAMPLE Y-10

| Area | w/o Fe | w/o Cr | w/o Ni | w/o Cu | w/o O | w/o Cl | w/o Na | W/o P |
|---|---|---|---|---|---|---|---|---|
| Low carbon steel | 93.9 | 0.017 | N.D. | 0.008 | N.D. | N.D. | N.D. | N.D. |
| "Oxide" near steel | 77.4 | 0.025 | 0.012 | N.D. | 24.5 | 2.80 | N.D. | N.D. |
| Middle of "oxide: | 70.8 | 0.024 | 0.005 | 0.012 | 25.2 | N.D. | 0.028 | N.D. |
| "Oxide" near Inconel | 63.5 | 0.164 | 0.003 | 0.010 | 24.5 | N.D. | N.D. | N.D. |
| Inconel | 9.98 | 17.5 | 57.3 | 0.277 | N.D. | 0.010 | N.D. | N.D. |

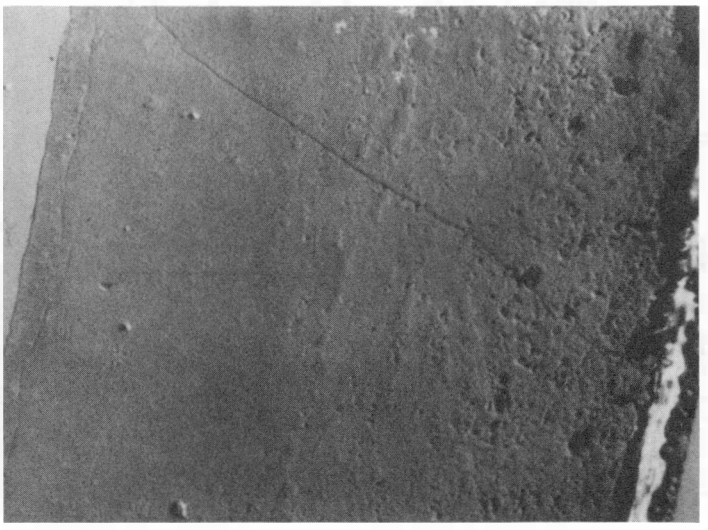


100X*

Figure B-33. SEM of the Oxide in the Annulus of Sample Y-10. (Steel/Oxide/Inconel)

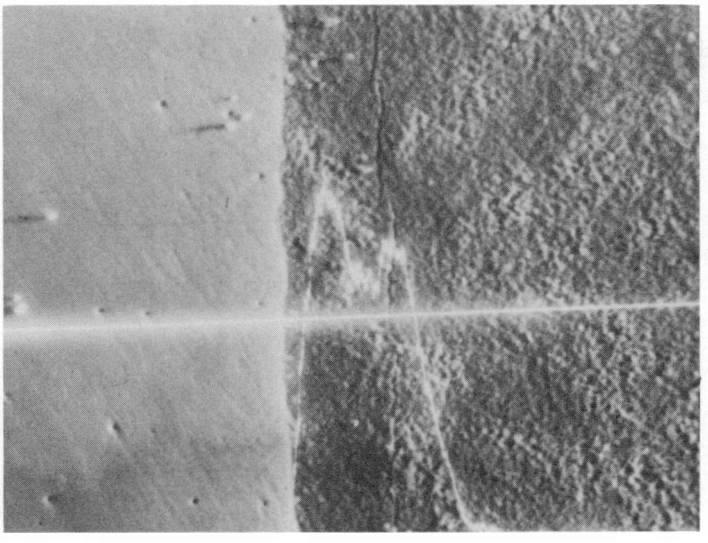


300X*

Figure B-34. SEM of the Steel/Oxide Interface, With a Superimposed X-ray Line Trace for Chlorine - Sample Y-10.

*Please note that the illustrations on this page have been reduced 10% in printing.

Sample Y-1. A representative portion of the oxide layer in the annulus of Sample Y-1 is shown in the SEM of Figure B-35; the steel slug is at the top, the Inconel is at the bottom, the oxide layer is in the center and a fiducial line is at the left, extending from top to bottom. The oxide layer is about 0.038 inch wide. The oxide has a rather smooth appearance from the steel interface out to about 0.020 inch, where small pits or pores are found. Most of the pores, however, are found in a band 0.010 inch wide along the Inconel interface. A notable feature of this sample is the presence of cracks running parallel to the steel interface and approximately 0.008 inch from it (Figure B-35). Figure B-36 is a SEM of a portion of the crack at a higher magnification.

The element distribution across the area shown in Figure B-35 is given in Table B-8. The oxide layer was found to consist of iron and oxygen. No concentration gradient for either element was found across the oxide layer. Chromium and nickel were barely detected, and no evidence of chlorine or sulfur was found above the background radiation.

Well-defined octahedral crystals believed to be magnetite were present in large crevices near the Inconel interface. (Figures B-37, A and B)

TABLE B-8

ELEMENT DISTRIBUTION OF SAMPLE Y-1

| Area | w/o Fe | w/o Cr | w/o Ni | w/o Cl | w/o S | w/o O |
|---|---|---|---|---|---|---|
| C1 (near steel | 67.3 | 0.054 | 0.058 | N.D. | N.D. | 21.2 |
| C2 | 71.1 | 0.062 | 0.082 | N.D. | N.D. | 21.9 |
| C3 | 66.8 | 0.057 | 0.073 | N.D. | N.D. | 20.4 |
| C4 | 69.1 | 0.074 | 0.079 | N.D. | N.D. | 20.0 |
| C5 | 67.3 | 0.063 | 0.073 | N.D. | N.D. | 20.1 |
| C6 (near Inconel) | 68.8 | 0.112 | 0.254 | N.D. | N.D. | 20.1 |

* N.D. = not detected above background radiation.

Steel

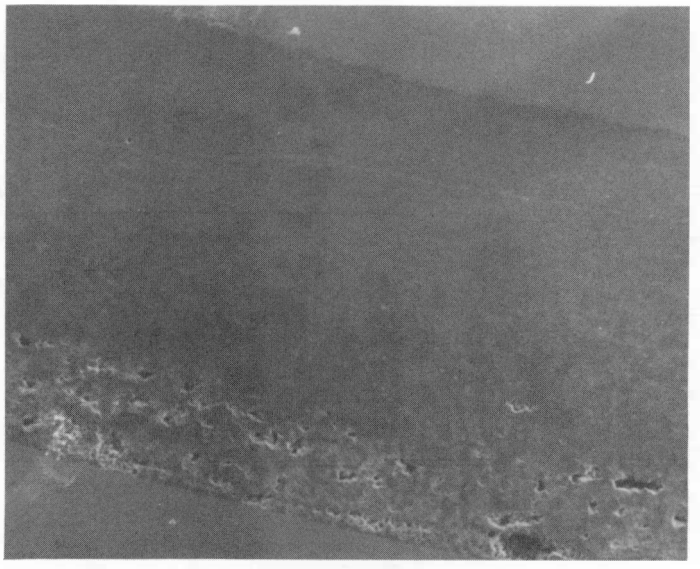

Inconel

60X*

Figure B-35. SEM of the Oxide Layer in the Annulus of Sample Y-1. (Inconel/Oxide/Steel)

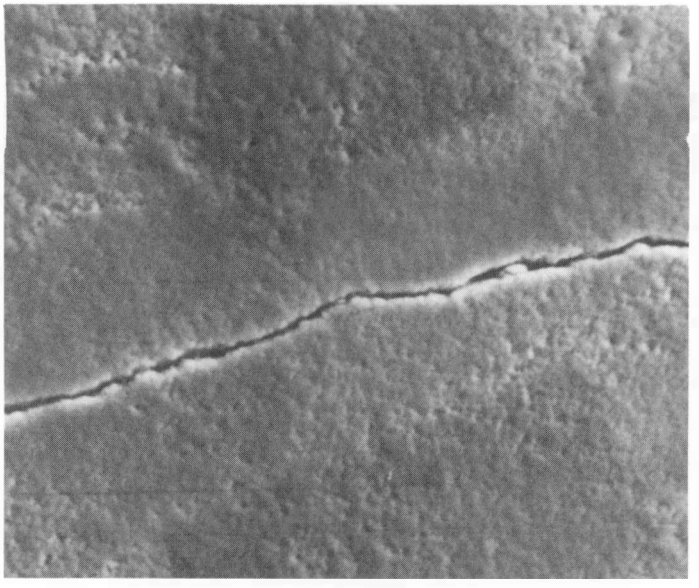

1000X*

Figure B-36. SEM of the Crack Near the Steel Interface - Sample Y-1.

*Please note that the illustrations on this page have been reduced 10% in printing.

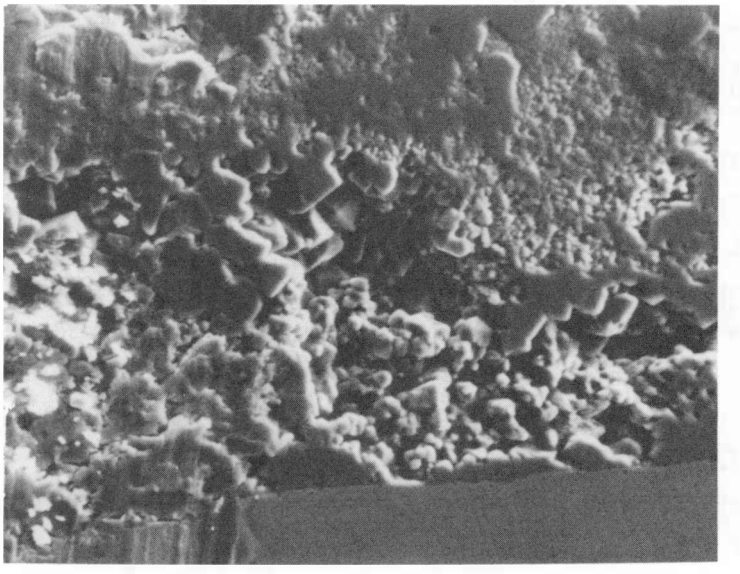


A. 600X*

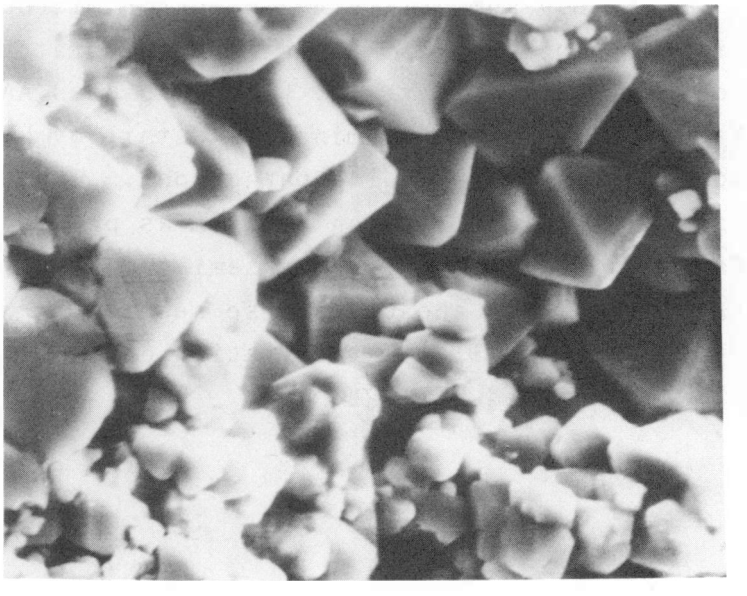

B. 2000X*

Figure B-37. SEM's of the Octahedral Crystals - Sample Y-1.

*Please note that the illustrations on this page have been reduced 10% in printing.

DD-7 Longitudinal Section. The section was examined for chlorine at five areas approximately 1/8" apart from the center of the bulged region to the end of the slug. Chlorine was found only within a 6 mil band of oxide at the steel interface. Figure B-38 shows the SEM electron beam photomicrographs of the chloride concentrations in these regions. Chlorine concentration varied locally from 1 to 15 (w/o) percent within the 6 mil band and appeared to be dependant upon the physical appearance of the oxide along the beam path. As shown in Figure 38A, areas associated with high chloride were smooth with scattered pocks while neighboring areas of low chloride had a textured fine-grained appearance. The total chlorine in the 6 mil area, estimated from the area under the curves, was quite variable but in general decreased as the end of the slug was approached. The sensitivity of the chlorine measurement to the particular features of the local regioned examined made quantification difficult.

EMPA Summary. Table B-9 summarizes the electron microprobe studies performed by both Knolls Atomic Power Laboratory (KAPL) and Mechanical Technology Inc. (MTI) Capsules AA-7, AA-8, DD-8, Y-10, and Y-1 were examined in detail by MTI and have been described in the preceding paragraphs. Capsule DD-7 was examined in longitudinal section by KAPL as previously described. Capsules Y-11 and D-12 were semi-quantitatively examined by KAPL along with the transverse section of capsule DD-7. Table B-9 contains all the imformation on these capsules which was supplied by KAPL.

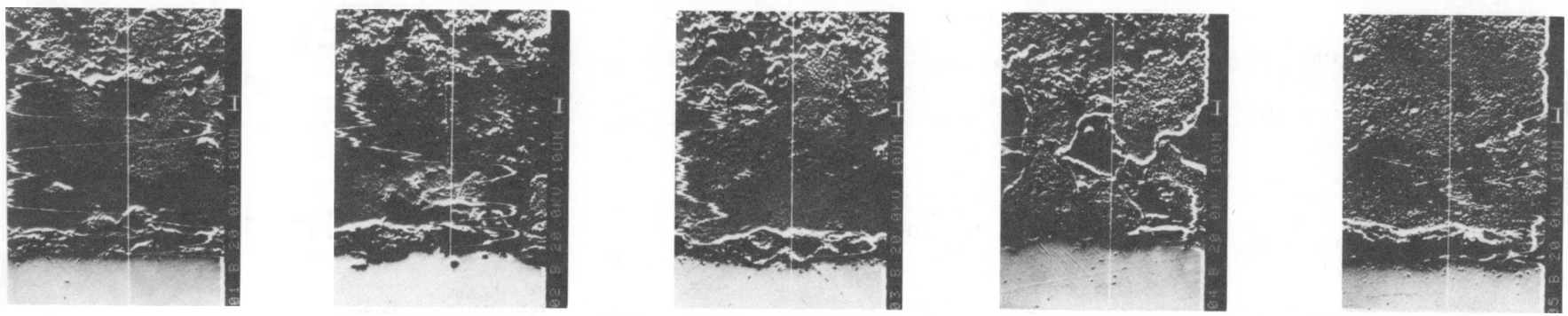

A: Center

B: 1/8" From Center

C: 1/4" From Center

D: 3/8" From Center

E: Outer End

Figure B-38

Longitudinal Sections of Capsule DD-7

The vertical white line in each image is the path of the electron scan. Chloride concentration along the path is indicated by the varying white line. The orientation is such that increasing chlorides are indicated as this line moves to the left.

TABLE B-9

SUMMARY OF EMPA RESULTS
ANNULUS OXIDE NEAR STEEL INTERFACE

| Capsule No. | Dent Solution | Neutralization | Post Neutralization Condition | Oxide Thickness (Mils) A600/Slug Annulus | Microprobe Results - % Element Alloy 600/Steel Slug Annulus | | | | | | | | | |
|---|---|---|---|---|---|---|---|---|---|---|---|---|---|---|
| | | | | | S | Mg | Ca | $Cl^-$ | P | Na | Cu | Ni | Fe | Cr | O | Lab |
| Y-1 | 565°F 0.1M FeCl's | 200 ppm $N_2H_4$ 150°F, 96 hrs. | AVT 20 ppm $N_2H_4$ 565°F, 4 wks. | 39 | N.D | | | <0.1 N.D. | <0.1 -- | <0.1 -- | -- -- | 0.2 0.058 | 70 67.3 | 0.1 0.054 | 30 21.1 | KAPL MTI |
| AA-7 | Same | 1000 ppm $PO_4$ 2.8 $Na/PO_4$ 150°F, 96 hrs. | AVT 20 ppm $N_2H_4$ 565°F, 4 wks. | 22 | N.D N.D | | | <0.03 N.D | <0.1 N.D. | <0.1 N.D. | -- -- | 0.2 0.090 | 70 65.5 | 0.1 0.093 | 30 22.4 | KAPL MTI |
| AA-7 Longitudinal 5 locations from center to end of slug | | | | | | | | N.D. | N.D | N.D[2] | N.D. | N.D. | 59.3 | 0.058 | | MTI |
| AA-8 | Same | Same as AA-7 | 0.1M $FeCl_2$ 565°F, 4 wks. | 41 | | | | 0.413 | N.D. | N.D | 0.021 | 0.033 | 70.3 | 0.032 | 20.7[1] | |
| Y-10 | Same | 300 ppm $PO_4$ 2.5 $Na/PO_4$ 565°F, 24 hrs. | Same as above | 48 | | | | 2.80 | N.D. | N.D. | N.D. | 0.012 | 77.4 | 0.025 | 24.5[1] | MT |
| Y-11 | Same | Same as Y-10 except 96 hr. soak | AVT 20 ppm $N_2H_4$ 565°F, 4 wks. | 45 | | | | < 0.1 | < 0.1 | < 0.1 | -- | 0.1 | 70 | 0.1 | 30 | KAPL |
| DD-7 | 565°F 0.1M $CuCl_2$ + 0.1M $NiCl_2$ in seawater | 1000 ppm $PO_4$ 2.8 $Na/PO_4$ 150°Fm 96 hrs. | AVT 20 ppm $N_2H_4$ 565°F, 4 wks. | 38 | | | | 1.0 (10 in one spot) | <0.1 | <0.1 | 0.1 | 0.1 | 70 | 0.1 | 30 | KAPL |
| DD-8 | Same | Same as DD-7 | 0.1M $FeCl_2$ 565°F, 4 wks. | 31 | | N.D. | N.D. | 16.40 | N.D. | N.D. | N.D. | 0.014 | 50.9 | 0.011 | 21.9[1] | |
| DD-12 | Same | 20 ppm $N_2H_4$ 96 hr. 565°F Possible Contamination | AVT 20 ppm $N_2H_4$ 565°F, 4 wks. | 38 | | | | 0.1 | <0.1 | <0.1 | | 0.1 | 70 | 0.1 | 30 | KAPL |

Note: 1. Low values for oxygen due to extremely large mass absorption coefficient of iron for oxygen X-radiation.

2. Na, Cl were just barely detected above background, and only in very isolated spots.

# APPENDIX C

## POT BOILER TESTING
## EXPERIMENTAL DETAILS

### EQUIPMENT

#### Facility Description

C-E Windsor Pot Boiler Test Facility is a two-loop system of pot boiler units installed in a high pressure, high temperature loop, a schematic of which is shown in Figure C-1. The Primary test loop circulates hot, pressurized water through the pot boiler tubes, transferring heat to the surrounding secondary water. The cooled primary water leaves the pot boiler, is reheated and recycled.

The heated secondary water produces steam which is condensed by the heat exchanger-cooler combination, located above each pot boiler. This provides low-flow gravity water return to complete the secondary cycle.

System operating conditions average as follows:

| | Temperature | Pressure |
|---|---|---|
| Primary Loop | 600°F | 2200 psig |
| Pot Boiler Units | 546°F | 1000 psig |

Each pot boiler test vessel is constructed from 11" OD carbon steel pipe, and is bolted to a 600 pound carbon steel flange, which serves as the tubesheet. Each unit stands approximately 48" high. The tubesheet can contain up to four tubes, which can be fitted with various devices to produce concentration of bulk water impurities in steam blanketed regions on heat transfer surfaces.

Figure C-1
POT BOILER TEST FACILITY SCHEMATIC

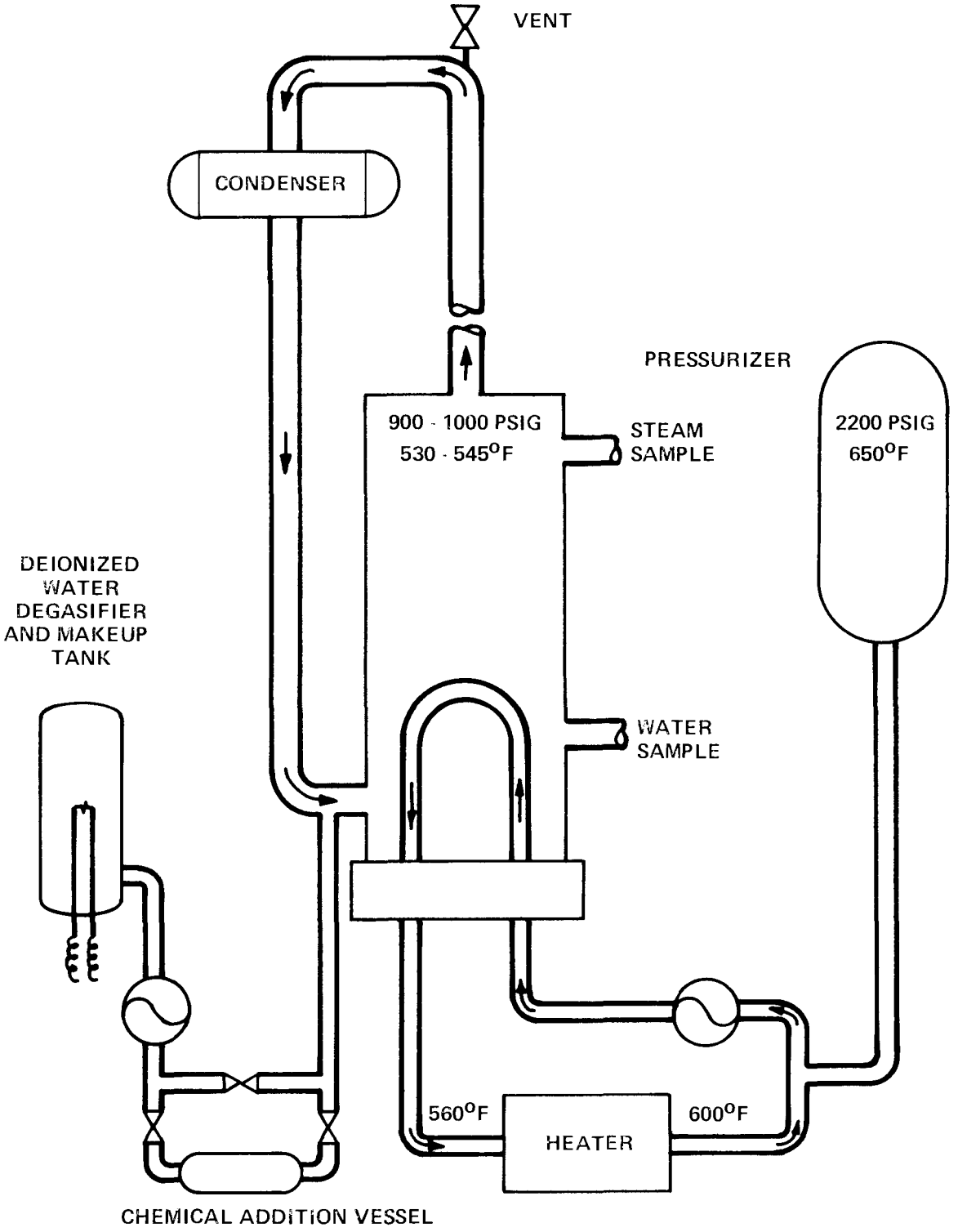

Tube Bundle Buildup

Three identical tube bundles were fabricated for these tests. Figure 2-3 provides a schematic of the tube/hardware arrangement. Each bundle consisted of four tubes which were outfitted with a full diameter carbon steel support plate and with rings of various materials to simulate concentrating tube-support crevices in field units. Selected crevices were outfitted with high temperature strain gauges to allow changes in the rate of denting to be observed during operation. Strain gauge mounting is illustrated in Figure C-2. Crevices were prepacked with a mixture of 71% $Fe_3O_4$, 12% NiO, 12% CuO, and 5% Cu, all feedtrain corrosion products, to accelerate dent initiation. Pre-packing was done by adding the mixture to funnel device above each crevice and wedging the material into the crevice with a spatula. There was no attempt to mechanically shake the material into crevices nor was there any quantitative measure of degree of pre-packing. Other devices, such as umbrellas and U-bend sandwich plates, were installed to provide steam blanketed regions for evaluation of the corrosivity of concentrated bulk water constituents on tubing material, independent of the tube denting phenomena. Various corrosion coupons were also included in order to evaluate potential corrosive effects of the bulk water environment on steam generator materials. Tables C-1 and C-2 present the specific materials used in bundle fabrication. Figure C-3 shows a completed tube bundle prior to operation.

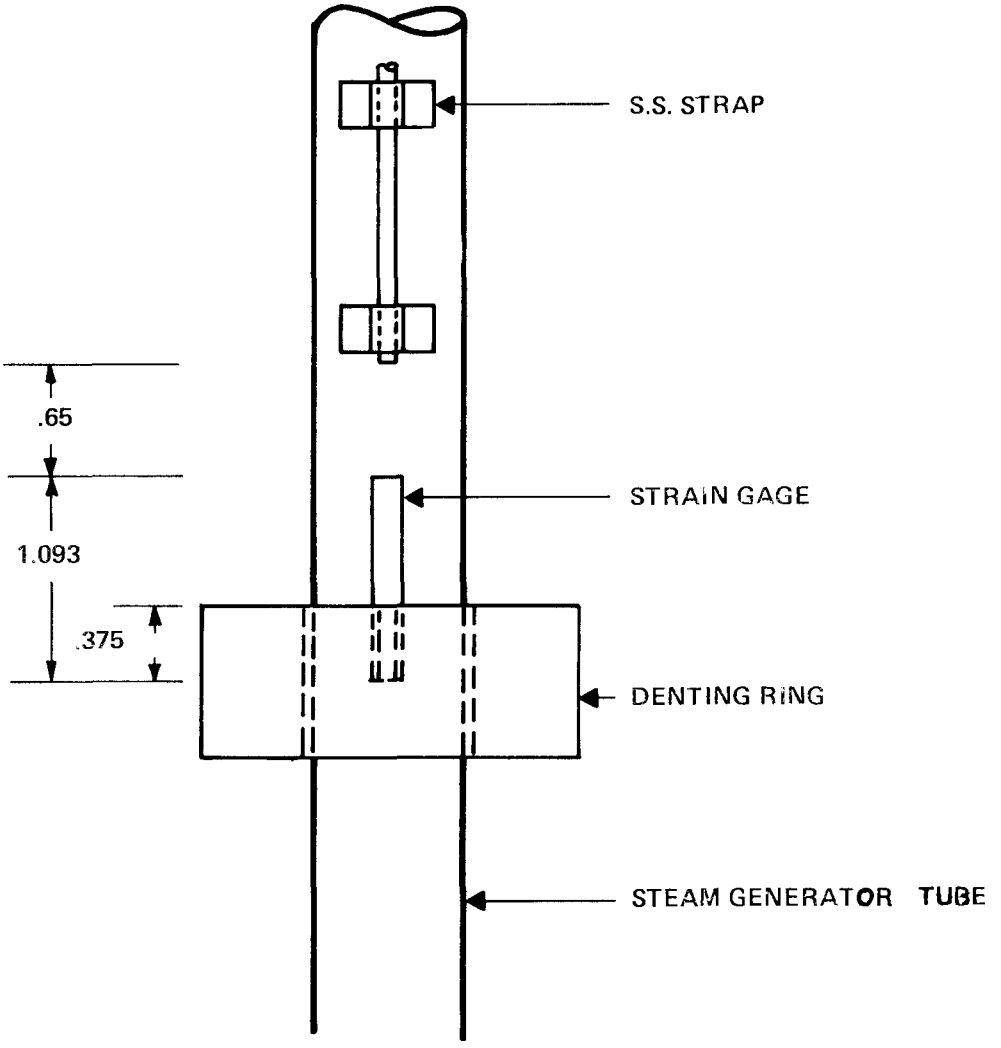


Figure C-2
STRAIN GAGE INSTALLATION IN DENTING RING ANNULUS

TABLE C-1

MATERIALS SUMMARY FOR
TUBE BUNDLE FABRICATION

1. Four Alloy 600 tubes - three mill annealed and one sensitized - 3/4" OD x .042" average wall - 2 1/2" radius U-bend. The chemical composition and mechanical properties of the tubing are provided in Table C-2.

2. Five 1010/1020 carbon steel concentrating rings.

3. Three 405 stainless steel concentrating rings.

4. Four 1010/1020 carbon steel umbrella concentrating devices.

5. One 1010/1020 carbon steel full diameter support plate - 3/4" thickness.

All tube/support annuli were prepacked with a corrosion product mixture of 71% $Fe_3O_4$, 5% Cu, 12% CuO, 12% NiO.

Following Phase I fault operation, Pots 11 and 7E were modified as follows:

1. A 1010/1020 carbon steel sandwich plate set was affixed to the U-bend of one tube.

2. Corrosion coupon specimens, secured to a supporting rack, were added such that all coupons were suspended in the bulk water. Each test unit contained nine coupons of 409SS, 508CS, 1010CS, and Alloy 600 materials, and three double U-bends with Alloy 600 inner and 1010 carbon steel-outer members.

TABLE C-2

CHEMICAL AND MECHANICAL PROPERTIES OF TUBING UTILIZED IN POT BOILER TESTS 9, 11, 7E

Chemical Composition (wt %)

| Heat No. | C | Al | Ti | B | P | S | Si | Cu | Mn | Fe | Cr | Ni | Co | Mg |
|---|---|---|---|---|---|---|---|---|---|---|---|---|---|---|
| NX9539 Alloy 600 Tubes 1, 3, 4 | .03 | .21 | .20 | .003 | .011 | .003 | .17 | .28 | .21 | 8.58 | 16.32 | 74.71 | .04 | <.06 |
| NX9270 Alloy 600 Tube 2 | .03 | .19 | .17 | .003 | .010 | .003 | .13 | .39 | .18 | 9.52 | 14.99 | 74.76 | .04 | .009 |

Mechanical Properties

| Heat No. | Tens. Str. | Yield Str. (@0.2% offset) | Elong. (in.50 mm) |
|---|---|---|---|
| NX9539 Alloy 600 Tubes 1, 3, 4 | 101,000 psi | 53,000 psi | 40% |
| NX9270 Alloy 600 Tube 2 | 100,000 psi | 44,000 psi | 40% |

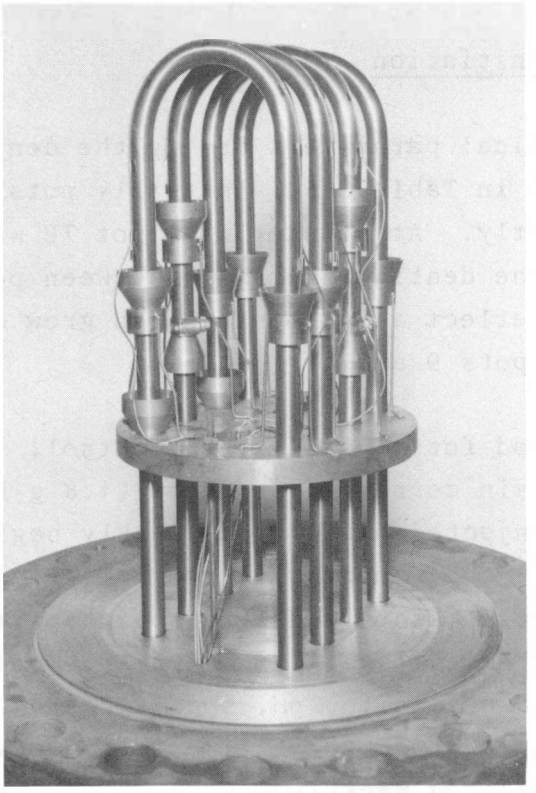

Figure C-3. Fabricated Tube Bundle Arrangement Prior to Testing

OPERATING HISTORY

The operating history of the three pots used in these tests is summarized on Table C-4. Each phase of operation is discussed separately in the following sections.

Phase I - Dent Initiation

Chemistry. Chemical parameters during the dent initiation phase are listed in Table C-3. Initially pots 9 and 11 were dented concurrently. At a later date pot 7E was dented. Differences in the denting chemistry between pot 7E and the other two pots reflect adjustments which grew out of the experience with pots 9 and 11.

Hydrazine was used for pH and oxygen control. A mixture of simulated feedtrain corrosion products (4.8 g $Fe_3O_4$ and 3.2 g CuO) was injected three times weekly beginning on day 18 for pots 9 and 11 and immediately for pot 7E. Chloride concentrations were maintained with seawater injection. Table A-1 provides a chemical analysis of the seawater which was used. Chemical analyses for pH, specific conductivity, Cl, Na, and Cu were performed three times each week. Oxygen and ammonia were monitored weekly.

Operations. Steaming operations began with a pre-conditioning period, during which time normal volatile chemistry control was established via blowdown and venting procedures. Pot boilers 9 and 11, which were newly constructed, required a longer pre-conditioning period with extensive blowdown to remove the protective coatings used in vessel fabrication by the manufacturer.

Fault chemistry conditions were established and maintained with seawater injection. Chloride hideout to concentrating areas was noted, and regular injection was required to

maintain the specified chloride concentration. Approximately two liters of seawater was added to each of the three units during the fault chemistry period. Corrosion product input amounted to approximately 120 grams $Fe_3O_4$ and 70 grams CuO per unit.

Fault conditions were maintained for 50 to 60 days, until a positive strain gauge response was noted indicative of tube denting. Blowdowns were then performed to reduce cnloride levels in the bulk prior to shutdown. Chloride concentrations, initially at approximately 175 ppm, were reduced to less than 0.5 ppm in pot 9 and 0.15 in pot 11. Pot 7E operated for approximately three weeks on volatile chemistry pending finalization procedures. Bulk chloride concentrations of less than 0.1 ppm was achieved during this time.

At the conclusion of the denting phase and blowdown, primary heat was discontinued allowing the unit to cool to less than 150$^{o}$F within six to eight hours. At this point the pot boilers simulated a field unit which had recovered from a period of condenser inleakage prior to going into a cold shutdown.

Visual Examination. Upon completion of Phase I, pot boilers 7E and 11 were drained and opened for examination. Pot 9 was not drained but remained soaking under a nitrogen blanket for approximately five days prior to flushing at the start of Phase II. Pot 9 was not opened between Phases I and II.

The overall appearance of the tube bundles of pot 11 and 7E following dent initiation was similar as shown in Figures C-4 and C-5. A black oxide film covered all tube and hardware surfaces. Substantial amounts of deposits were present at steam blanketed and tubesneet locations. Black and silver crystalline deposit formations were visible at concentrating

umbrella areas of both units. Deposit material had also accumulated on the tubesheets and appeared as in Figure C-6 upon initial draining of the pot boiler. Upon drying, the material hardened and cracked, forming the deposit layers shown in Figure C-7.

A red coating of deposit material, which when analyzed by X-ray fluorescence was found to consist substantially of elemental copper, was evident at several tube bundle locations. Tube 4 concentrating ring devices (Figure C-8), in addition to the support plate areas adjacent to tube 4, displayed substantial copper metal plateout. Copper was particularly evident in pot 7E, in the form of spiral patterns on the underside of the support plate around tube 4.

Concentrating rings were examined for evidence of crevice blockage. All crevices appeared blocked with deposited material and/or the initial prepacked corrosion product mixture. Evidence of non-protective magnetite growth, shown in Figure C-9, was apparent at tube 4 hot leg ring of pot 7E which was particularly distorted. The ring appeared swelled and corroded at the base of the umbrella cup, with hard deposit formations on outside ring surfaces. Pot 11 displayed frozen concentrating rings at tube 4 hot, cold and tube 2 cold legs. Rings on tube 3 were tight, but some circular movement was possible. Tube 1 hot, and tubes 3 and 4 hot and cold leg rings in pot 7E were also frozen in place. All other rings exhibited some movement around the tube.

TABLE C-3

| Pot Number | 7E | 9 | 11 |
|---|---|---|---|
| pH | 7.5-8.5 | 7.5-8.5 | 7.5-8.5 |
| Initial days at 100-125 ppm $Cl^-$ | --- | 17 | 17 |
| Days at ~150 ppm $Cl^-$ | 15 | 12 | 12 |
| Day at 175-200 ppm $Cl^-$ | 35 | 30 | 25 |

TABLE C-4

TEST OPERATION SUMMARY

| | Water Soak Pot 9 | Phosphate Soaks Pot 11-1000 ppm | Pot 7E-3000 ppm |
|---|---|---|---|
| Phase I<br>Dent Initiation*<br>Average heat flux<br>7000 BTU/hr/ft$^2$ | | | |
| Days volatile pre-conditioning | 13 | 13 | 7 |
| Days chloride fault | | | |
| 100-150 ppm $Cl^-$ | 17 | 17 | -- |
| 150 ppm $Cl^-$ | 12 | 12 | 15 |
| 150-175 ppm $Cl^-$ | 30 | 25 | 35 |
| Days Blowdown/Volatile | 5 | 8 | 22 |
| Total | 77 | 75 | 79 |

Phase II
Watersoak/Neutralization

| | Water Soak | $PO_4$ Soak | $PO_4$ Soak |
|---|---|---|---|
| Soak Specifications | $N_2H_4$ 200 ± 50 ppm<br>pH ∿ 10.0<br>96 hrs/150°F | $PO_4$ ∿ 1000 ppm<br>Na/P MR 2.8<br>$N_2H_4$ ∿ 20 ppm<br>96 hr/150°F | $PO_4$ ∿ 3000 ppm<br>Na/P MR 2.8<br>$N_2H_4$ ∿ 20 ppm<br>96 hr/150°F |

Phase III
Volatile Operation
Average heat flux
7000 BTU/hr/ft$^2$

| | | | |
|---|---|---|---|
| Days volatile operation | 37 | 36 | 34 |
| Bulk Chloride concentration, ppm | <0.6<br>Non-Destructive Examination | < 0.3 | <0.5<br>Destructive Examinations |

* Crud consisting of 4.8 g $Fe_3O_4$ and 3.2 g CuO was injected 3 times weekly during fault operation.

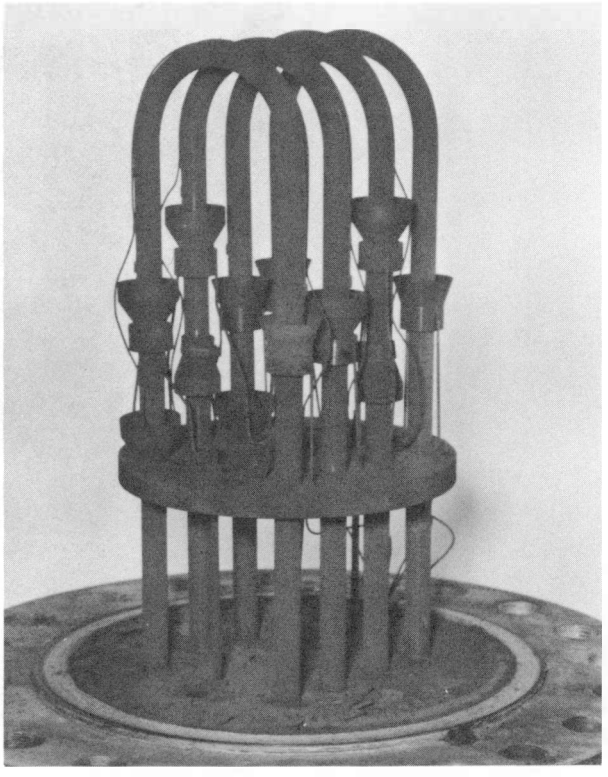

Figure C-4. Pot 11
Tube Bundle
Post-Phase I

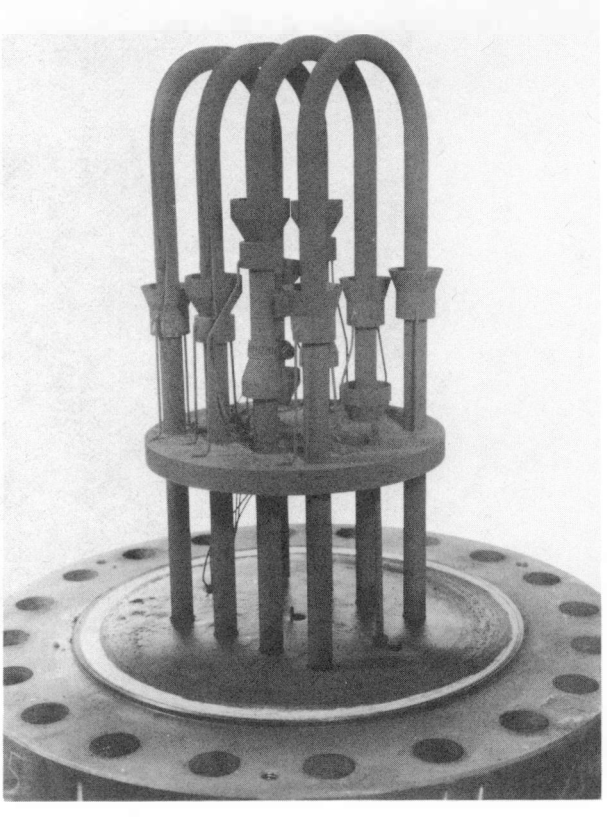

Figure C-5. Pot 7E
Tube Bundle
Post-Phase I

Figure C-6. Tubesheet Deposit Material Upon Draining Pot Boiler
Pot 7E

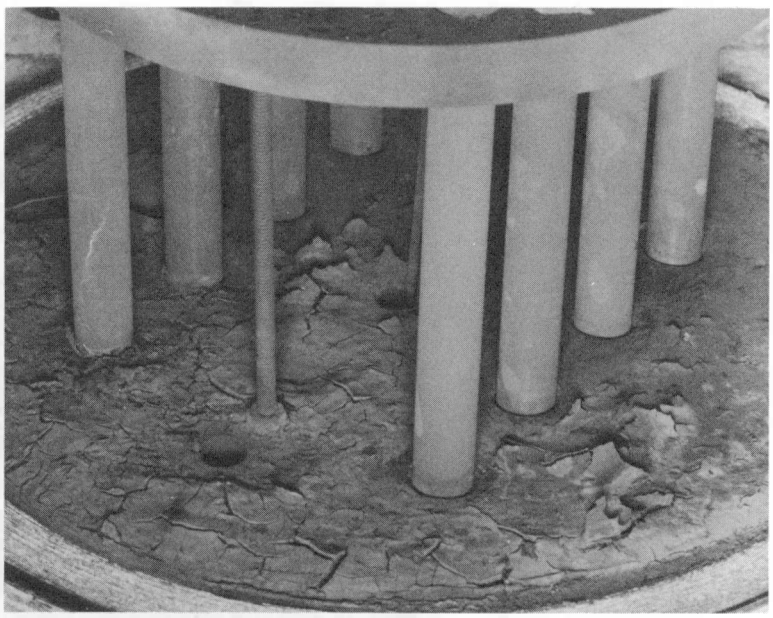

Figure C-7. Dry plus Hardened Tubesheet Material
Pot 11

Figure C-8.

Copper Plateout on
Tube 4 Concentrating
Ring
Pot 7E

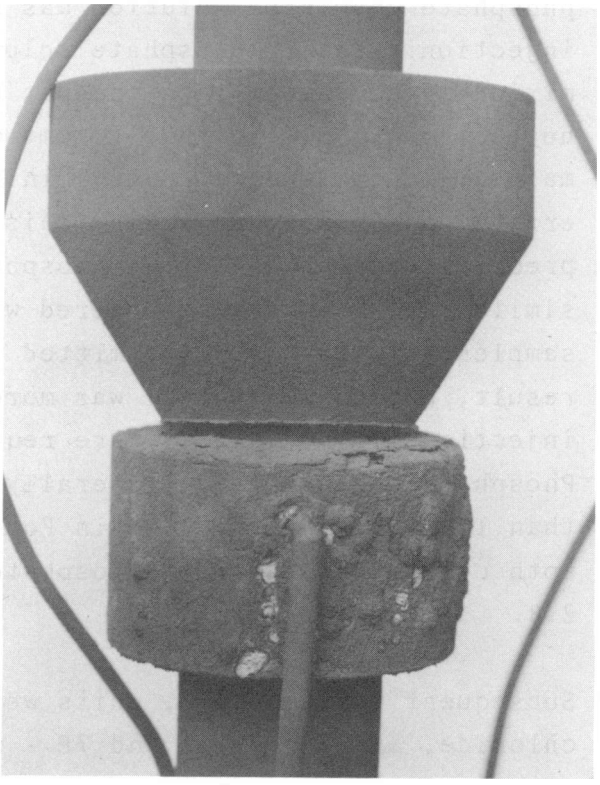

Figure C-9.

Distorted Ring
at Tube 4 Hot Leg
Pot 7E

Phase II - Water Soak/Neutralization

Chemistry. Water and phosphate soak solutions tested are outlined in Table C-5. These were maintained for a 96 hr. period at 150°F. Chemistry sampling was performed every eight hours and adjustments were made as necessary to maintain chemistry.

Operation History. Phase II operation commenced with a series of flushes to reduce residual chloride concentrations prior to soaking.

Wet layup chemistry conditions were established in Pot 9 under low temperature. Chemistry operation during the soak period is shown graphically in Figure C-10. Hydrazine, which began to deplete midway through the soak, was replenished twice.

Phosphate neutralizer soaks in Pots 11 and 7E were similarly maintained at low temperature. Figures C-11 and C-12 graphically present chemistry parameters during the soak and flush procedure. Pot 11 was filled with DI water and heated to 150°F. A phosphate chemistry solution was established via chemical injection. Pot 7E phosphate solution was initially prepared in a mixing tank, pumped into the pot boiler unit, and subsequently heated to 150°F. Initially some difficulty was experienced in maintaining phosphate control in Pot 11, due to inconsistent and erratic phosphate analyses. This resulted in a somewhat less precise description of the phosphate concentration in Pot 11. A similar problem was encountered with Pot 7E; however, duplicate samples were taken and submitted for independent analyses. As a result, phosphate control was more reliable for Pot 7E. Periodic injections of phosphates were required during the soak periods. Phosphate concentration generally remained at equal to or less than 1000 ppm and 3000 ppm in Pots 11 and 7E respectively. In both cases the sodium to phosphate molar ratio was approximately 2.8.

Subsequent to the soaks, units were flushed to reduce levels of chloride, and in Pot 11 and 7E - phosphate and sodium.

TABLE C-5

PHASE II SOAKING CONDITIONS

| | Wet Layup Water Soak | Phosphate Soaks | |
|---|---|---|---|
| | Pot 9 | 1000 ppm-Pot 11 | 3000 ppm-Pot 7E |
| **Initial Pre-Flush** | | | |
| Chemistry Specifications | Fill plus drain under $N_2$ Blanket with solution of $N_2H_4$ (1.5 x $O_2$ concentration, maximum of 20 ppm) in DI water. 1/2 hour soaks at ambient temperature with $N_2$ gas agitation. | | |
| Chemistry Analyses | Drain effluent analyzed for pH, $N_2H_4$, Cl. | | |
| Duration | Until Cl $\leq$ 0.2 ppm | | |
| **Soaks** | | | |
| Chemistry Specifications | pH $\sim$ 10.0<br>$N_2H_4 \sim 200$ ppm $\pm$ 50 ppm<br>150°F | $PO_4$-1000 ppm<br>$Na/PO_4$ M.R 2.8<br>$N_2H_4 \sim 20$ ppm<br>150°F | $PO_4$-3000 ppm<br>$Na/PO_4$ M.R. 2.8<br>$N_2H_4 \sim 20$ ppm<br>150°F |
| | $N_2$ gas agitation every 8 hours, prior to sampling, after chemical addition. | | |
| Chemical Analyses 3 X Daily | pH, Specific Conductivity, $N_2H_4$, Cl | | pH, Specific, Conductivity, $PO_4$, Na, Cl, $N_2H_4$ |
| Duration | 96 Hours | | 96 Hours |
| **Post-Flush** | | | |
| Chemistry Specifications | Same As Pre-Flush | | |
| Chemical Analyses | pH, Specific Conductivity, Cl, $N_2H_4$ | | pH, Specific Conductivity, $PO_4$, Na, Cl, $N_2H_4$ |
| Duration | Until Cl $<$ 0.2 ppm | | Until Cl $<$ 0.2 ppm<br>$PO_4$ $<$ 2 ppm<br>Na $<$ 0.2 ppm |

Figure C-10
POT 9 - WATER SOAK,
PHASE IICHEMISTRY DATA

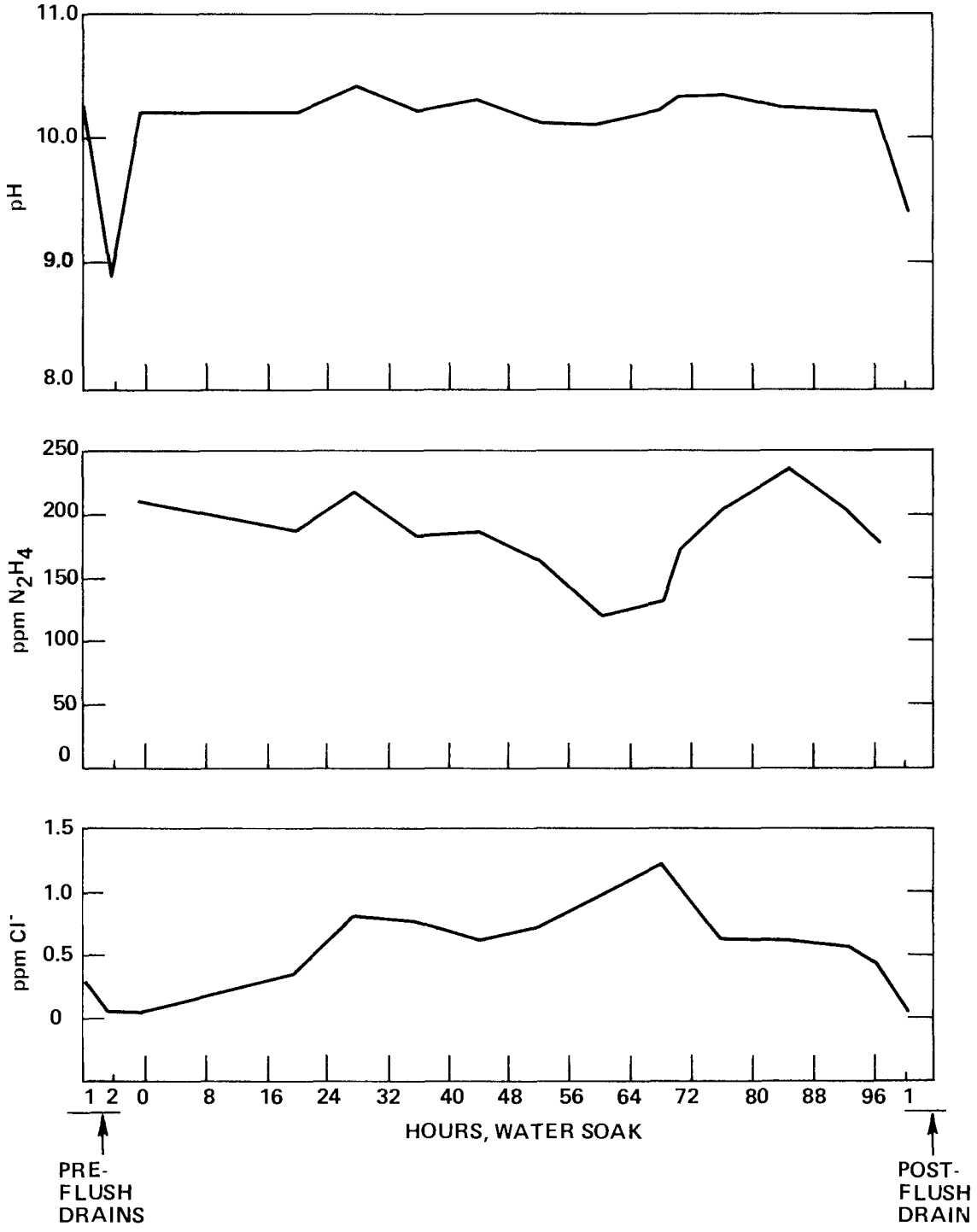

Figure C-11
POT 11 - 1000 ppm PHOSPHATE SOAK,
PHASE IICHEMISTRY DATA

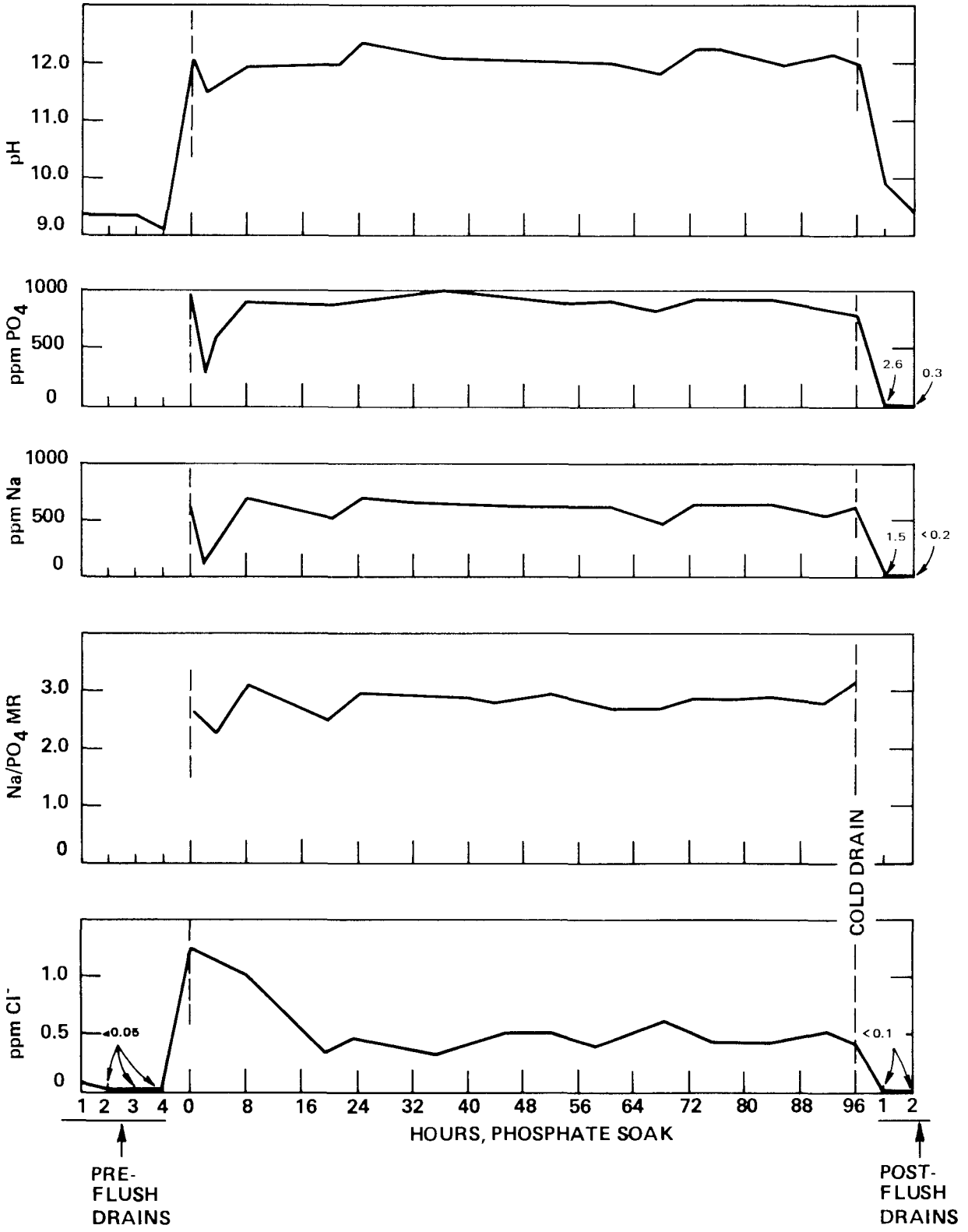

Figure C-12
POT 7E - 3000 ppm PHOSPHATE SOAK,
PHASE II CHEMISTRY DATA

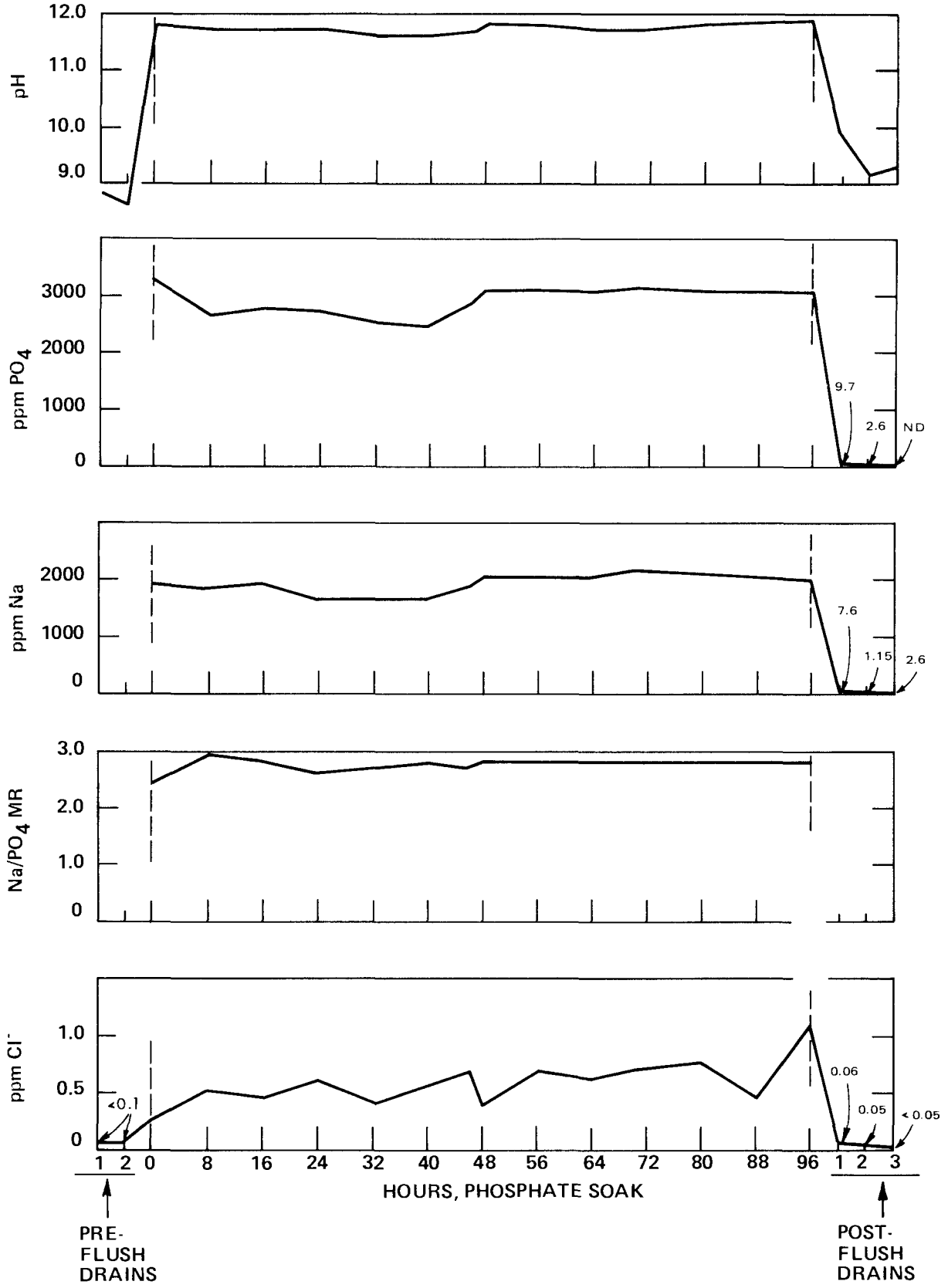

Phase III - Post-Soak Operation

Chemistry. Chemistry specifications maintained during the post-neutralization volatile phases are given in Table C-6.

Operation. All units were refilled in preparation for volatile steaming operation. Chemistry graphs of the volatile test operation are provided in Figures C-13 through C-15.

Pot 9 was stabilized at 400°F, and chloride monitored over three consecutive four-hour periods to ensure concentrations of less than 0.1 ppm chloride prior to steaming at 545°F. With the exception of a four-day holiday period during which time chloride increased to approximately 0.6 ppm, blowdown was performed on a daily basis to reduce concentrations which generally remained at 0.1-0.2 ppm.

Pot 11 began steaming operations at 545°F and experienced initial chloride levels of up to approximately 0.3 ppm. Frequent blowdown reduced chloride levels to less than 0.1 ppm, although sodium remained high, at 0.2-0.3 ppm levels. Phosphate was not detected in the bulk after initial test blowdown.

Pot 7E began initial steaming operations at 545°F, but was shutdown when chloride, phosphate, and sodium levels remained high despite repeated blowdown efforts. The unit was drained and refilled twice, and heated to 400°F. Blowdown operation was continued to reduce out-of-spec chloride and sodium levels. Steaming operations then proceeded at 545°F. Chemistry remained at specified levels throughout the volatile testing.

Visual Examination. The tubes, concentrating rings and umbrellas of pot boilers 9, 11, and 7E were visually examined upon completion of Phase III-Volatile operation. The

test units, shown in Figures C-16, C-17 and C-18 exhibited a protective black oxide film on all unit surfaces. Copper metal plateout, identified by X-ray analyses, was particularly heavy on pots 11 and 7E. Pot 7E (3000 ppm $PO_4$) additionally displayed a heavy gray/green coating on tube 4 concentrating rings (Figure C-19 and C-20), with bright green/gold flecks of deposit material on the support plate and tubesheet. Minimal amounts of gray and white deposit material were present at steam blanketed umbrella areas. Figure C-21 depicts a typical deposit formation.

Copper deposits were present on most unit surfaces and corrosion coupons specimens, and were particularly dense at tube 4 concentrating rings. Additionally, spiral patterns of deposited copper were present on the under side of the support plate for each of the three tube bundles. These are shown in Figures C-22, C-23, and C-24.

Concentrating rings were examined to ascertain the extent of crevice fouling. Most crevice areas appeared blocked allowing either little or no light passage. Upon examination for circular movement around the tube, rings at the following tube locations were found frozen in place:

| | |
|---|---|
| Pot 9 | 2 Hot, 2 Cold, 4 Hot, 4 Cold |
| Pot 11 | 2 Cold, 3 Hot, 4 Hot, 4 Cold |
| Pot 7E | 1 Hot, 3 Cold, 4 Hot, 4 Cold |

All other rings displayed some movement around the tube.

TABLE C-6

Chemistry Specifications

| | |
|---|---|
| pH | 8.2-9.2 |
| specific conductivity | < 7 μmhos/cm |
| Cl | < 0.1 ppm |
| $N_2H_4$ utilized for pH + $O_2$ control | |

Chemical Analyses

| | |
|---|---|
| 3X weekly: | pH, specific conductivity, Cl, (pots 11 and 7E - Na, $PO_4$) |
| weekly | $O_2$, $NH_3$ |

Duration approximately 30 days

Figure C-13

POT 9 - WATER SOAK

PHASE III CHEMISTRY DATA

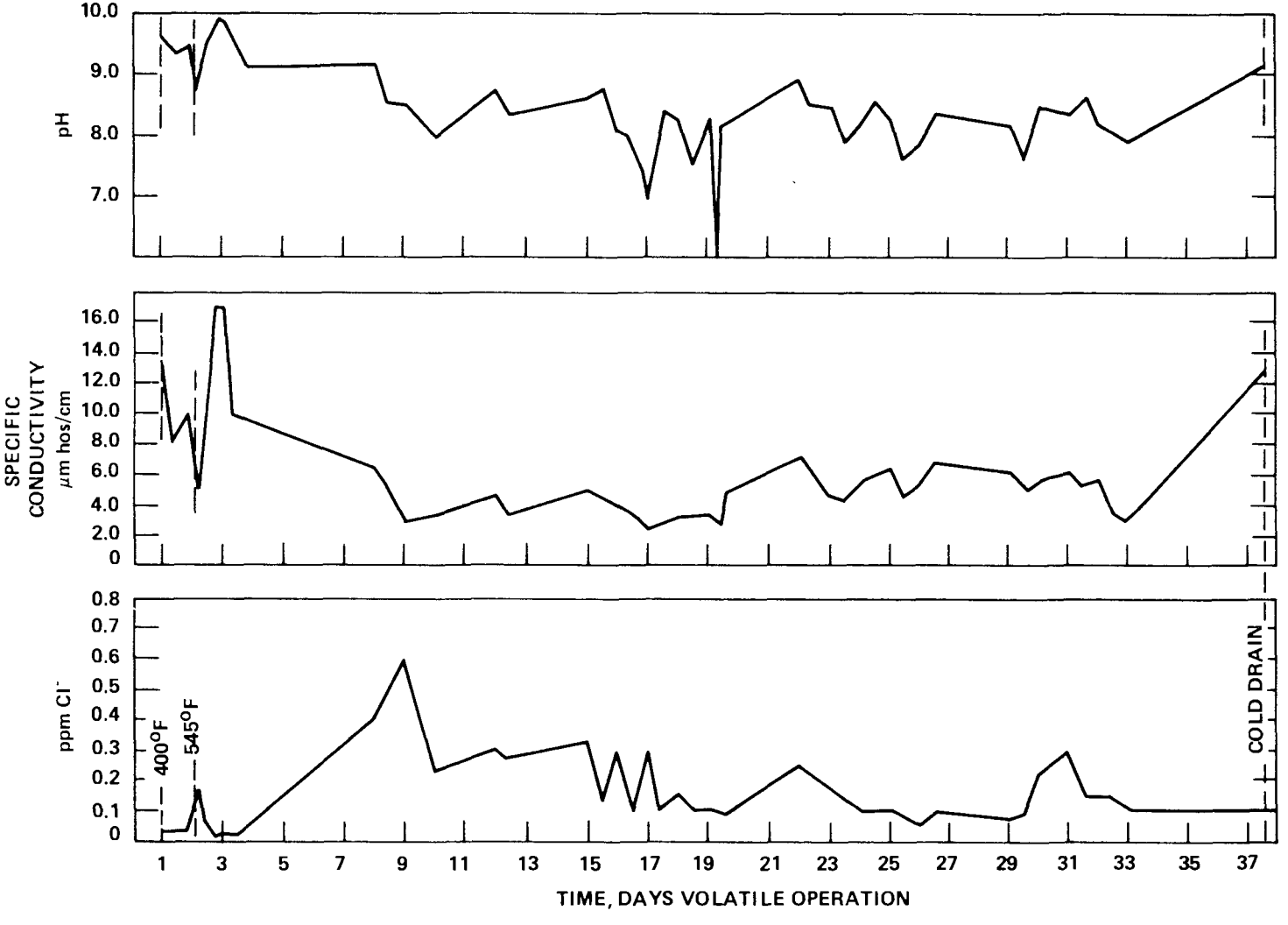

Figure C-14
POT 11 - 1000 ppm PHOSPHATE SOAK,
PHASE III CHEMISTRY DATA

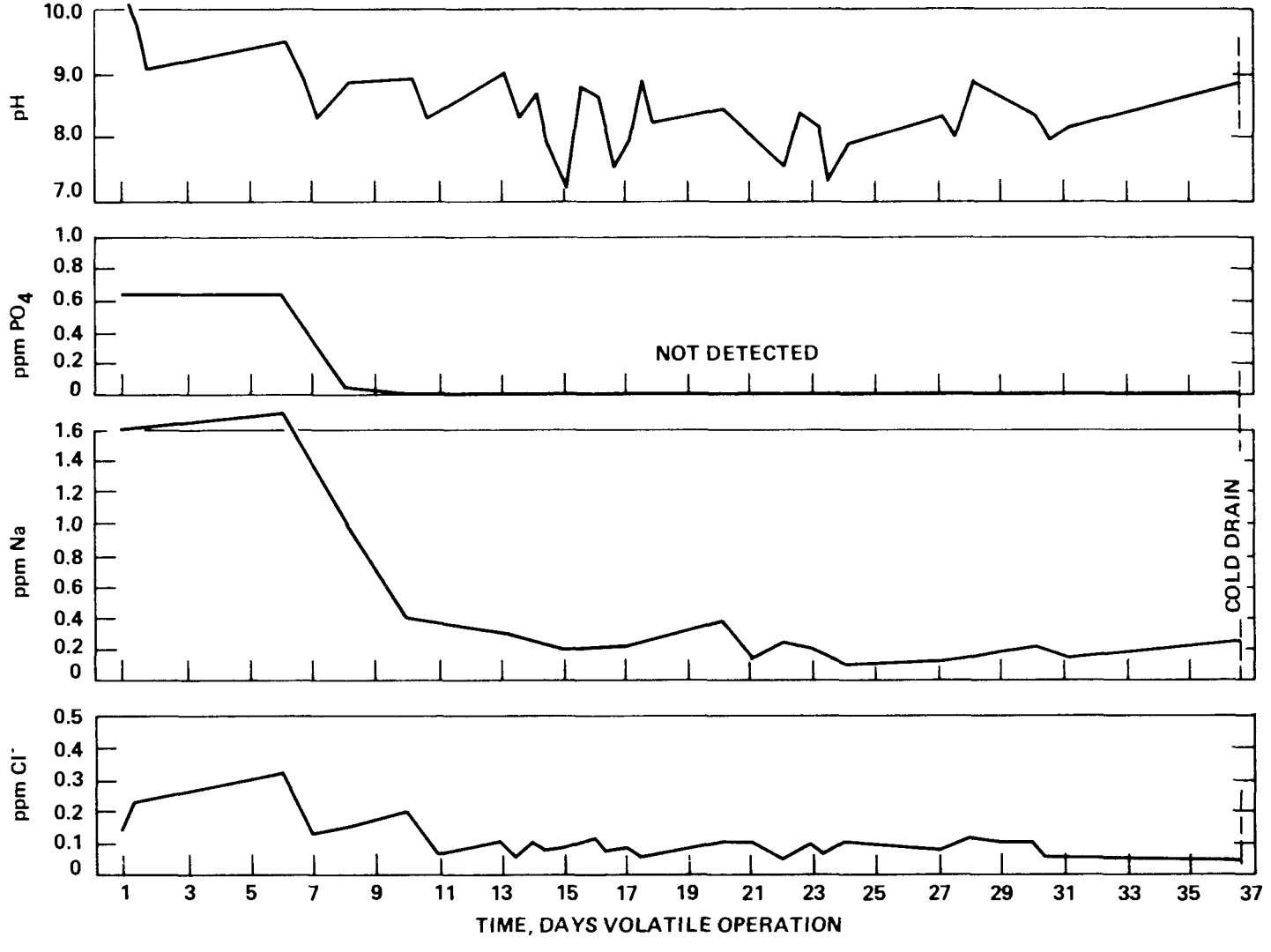

Figure C-15
POT 7E - 3000 ppm PHOSPHATE SOAK,
PHASE III CHEMISTRY DATA

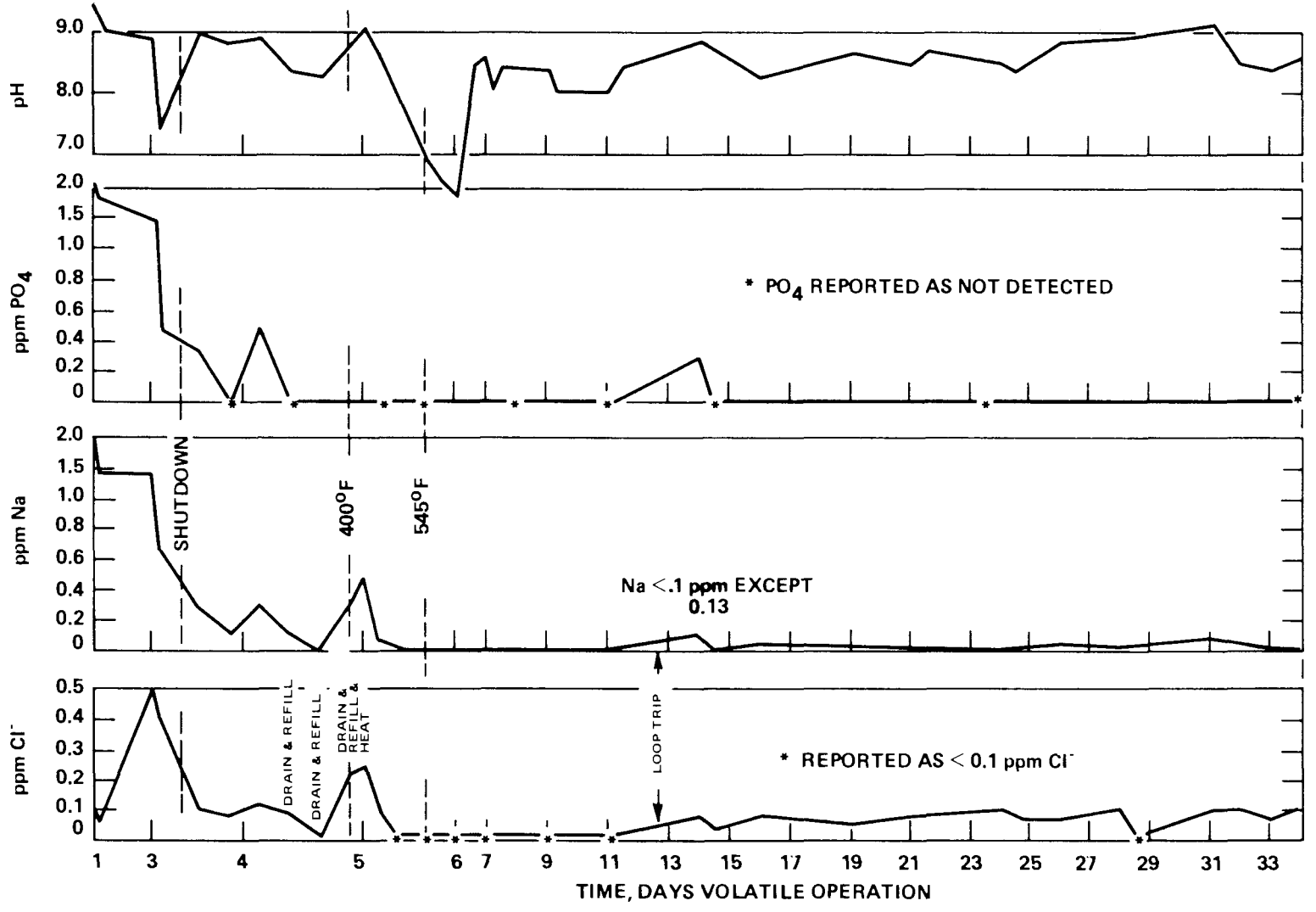

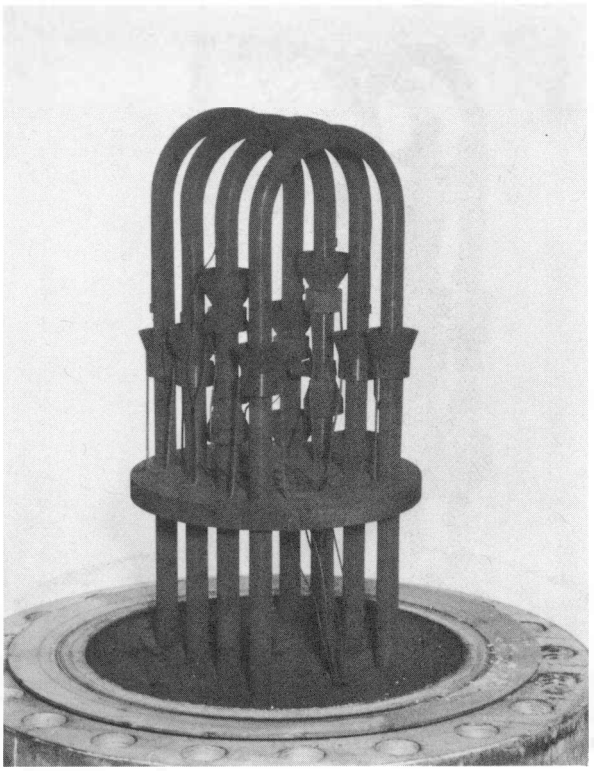

Figure C-16. Pot 9
Water Soak Tube Bundle
Post-Phase III

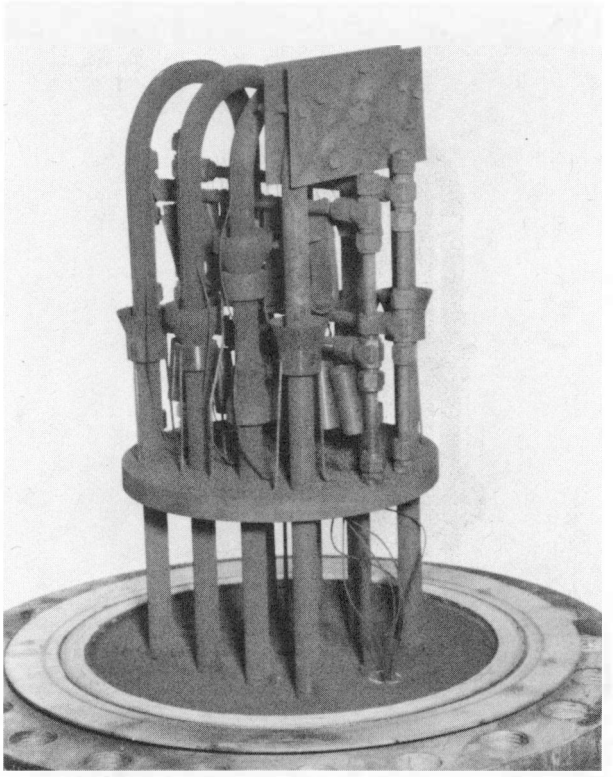

Figure C-17. Pot 11 - 1000 ppm $PO_4$ Soak
Tube Bundle
Final Examination

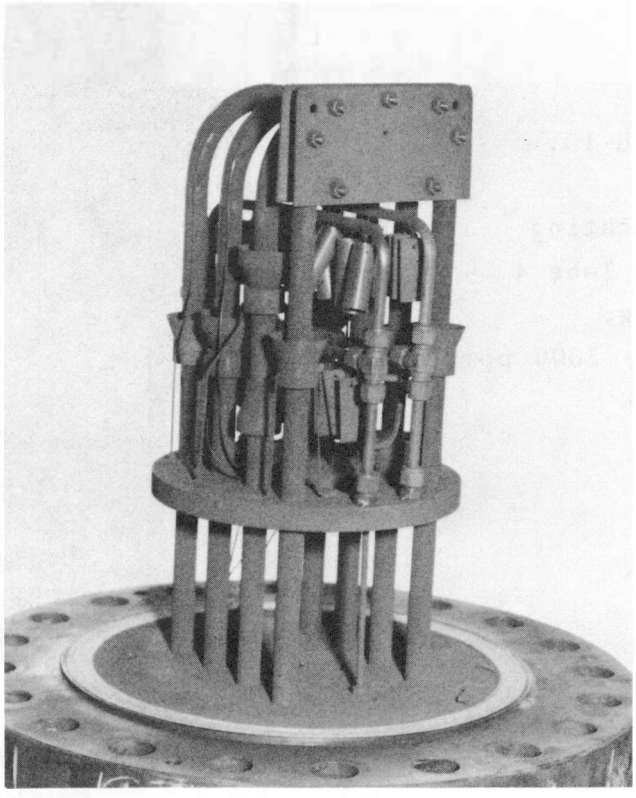

Figure C-18. Pot 7E - 3000 ppm $PO_4$ Soak
Tube Bundle
Final Examination

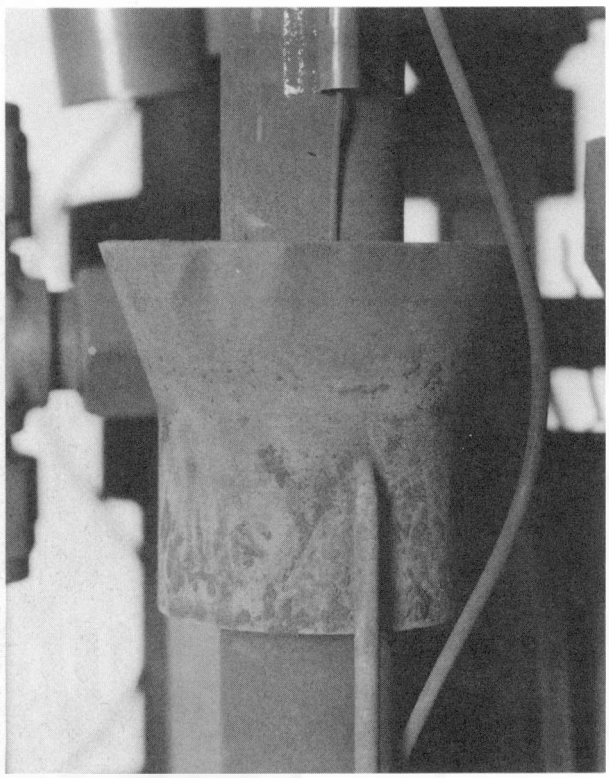

Figure C-19.

Concentrating
Ring on Tube 4
Cold Leg,
Pot 7E - 3000 ppm
$PO_4$ Soak

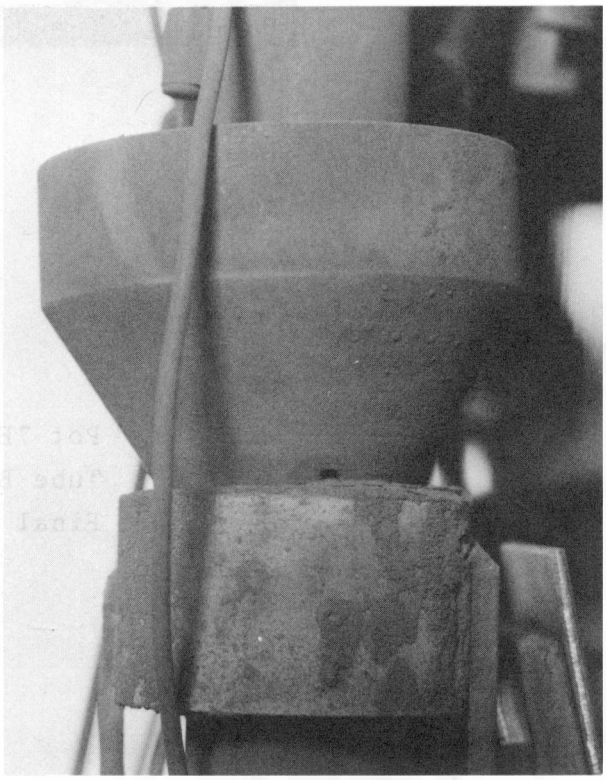

Figure C-20.

Distorted Ring
on Tube 4 Hot Leg
Pot 7E - 3000 ppm
$PO_4$ Soak

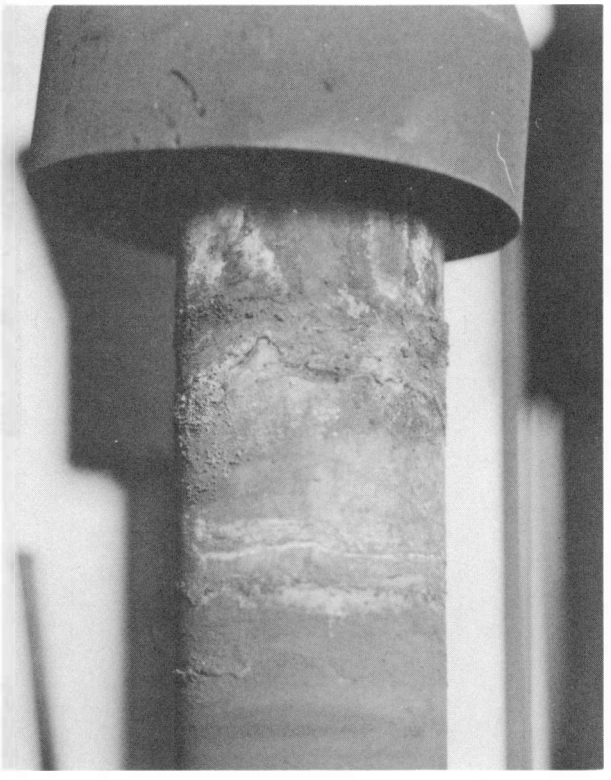

Figure C-21.

Steam Blanket
Deposit Formation
at Umbrella
Concentrating Area
Pot 7E - 3000 ppm
$PO_4$ Soak

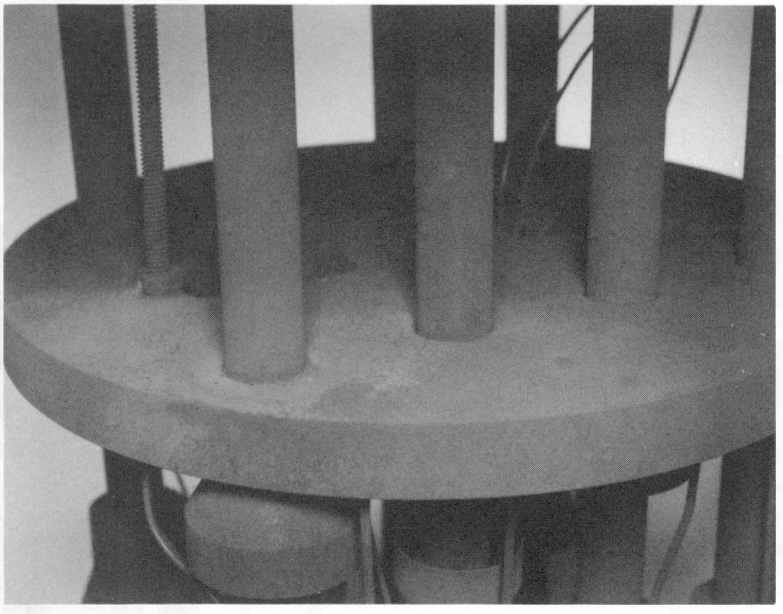

Figure C-22.

Copper Spiral
Pattern at
Tube 4 Support
Plate Area
Pot 9 - Water Soak

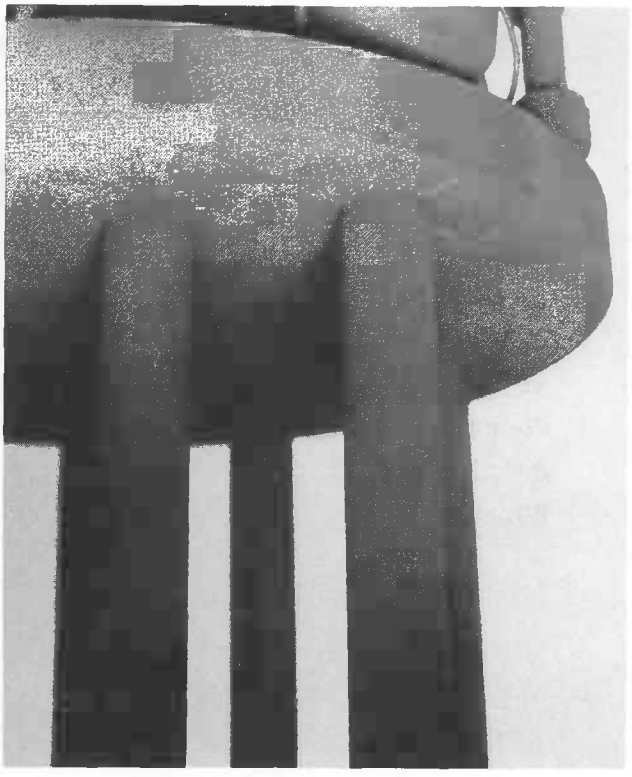

Figure C-23.

Pot 11 Support
Plate Area

Figure C-24.

Copper Spiral
on Pot 7E
Tube 4 Support
Plate Area

Appendix D

# POT BOILER CORROSION COUPON ANALYSIS

## EXPERIMENTAL

Corrosion coupons (nine each) of five different materials (1010CS, A-508, A-533-A, 409SS, and Alloy 600) were present during the Neutralization and Post-Soak Operation phases of the two phosphate soak tests. Three double U-bends with Alloy 600 inner and 1010 CS outer members were also included. All specimens were secured with stainless steel wire to a supporting rack such that they were immersed in the bulk water. Neither the coupons nor the supporting rack were insulated from the rest of the pot boiler.

Corrosion coupon and double U-bend specimens were cleaned, descaled, and weighed to measure weight loss. The U-bend specimens were examined visually at magnifications up to 60X for crack-like indications. Specimens were then sectioned, polished, etched, and examined under higher magnification for indications of intergranular cracking.

## RESULTS

Weight change results of the coupons are presented in Tables D-1 and D-2 for pots 11 (1000 ppm $PO_4$) and 7E (3000 ppm $PO_4$), respectively, and the data are summarized in Table D-3. The observed corrosion rates of the various materials ranked relatively as expected. The carbon steel, which has no real alloying additives, and the low alloy grades A508 and A533, exhibited the highest corrosion rate. The corrosion rate for 409SS, a 12 percent chromium grade, was significantly lower, while the rate in Alloy 600, the most highly alloyed material tested, was negligible. None of the specimens

tested exhibited pitting, scaling, or other forms of corrosion. In terms of practical engineering applications, there were no differences in corrosion rates for the various materials between the two pot boilers.

Visual and metallographic examinations of the double U-bend specimens showed no indications of cracking in any of the specimens. Pitting of less than 2 mils on the OD surface of the carbon steel members was noted. No crevice corrosion was detected on the Alloy 600 or carbon steel.

In summary, for the materials tested, no significant adverse effects on corrosion rates were noted, which could be related to exposure to phosphates. Double U-bend specimens also showed no serious corrosion.

TABLE D-1
CORROSION RATES FROM POT 11
1000 PPM $PO_4$ SOAK

| Material | Specimen Number | Corrosion Rate, MPY (1) | Weight Loss MDD (2) |
|---|---|---|---|
| C-Steel | 25C | 0.569 | 3.114 |
| | 27C | 0.595 | 3.263 |
| | 29C | 0.502 | 2.747 |
| | 32C | 0.595 | 3.260 |
| | 41C | 0.572 | 3.137 |
| | 48C | 0.584 | 3.195 |
| | 49C | 0.556 | 3.004 |
| | 51C | 0.572 | 3.131 |
| | 60C | 0.679 | 3.715 |
| A-508 | 33T | 0.351 | 1.925 |
| | 37T | 0.390 | 2.141 |
| | 46T | 0.362 | 1.984 |
| | 47T | 6.604* | 36.157* |
| | 50T | 0.398 | 2.183 |
| | 52T | 0.412 | 2.264 |
| | 54T | 0.376 | 2.059 |
| | 57T | 0.398 | 2.180 |
| | 59T | 0.401 | 2.191 |
| A-533-A | 7X | 0.592 | 3.246 |
| | 14X | 0.578 | 3.159 |
| | 15X | 0.564 | 3.086 |
| | 16X | 0.527 | 2.892 |
| | 27X | 0.570 | 3.122 |
| | 29X | 0.564 | 3.089 |
| | 30X | 0.570 | 3.117 |
| | 32X | 0.550 | 3.013 |
| | 42X | 0.541 | 2.963 |
| 409 SS | 7E | 0.146 | 0.791 |
| | 12E | 0.157 | 0.850 |
| | 17E | 0.194 | 1.044 |
| | 21E | 0.177 | 0.959 |
| | 23E | 0.157 | 0.847 |
| | 32E | 0.151 | 0.819 |
| | 36E | 0.157 | 0.844 |
| | 41E | 0.171 | 0.920 |
| | 43E | 0.157 | 0.861 |
| Alloy 600 | 23I | 0.024 | 0.138 |
| | 31I | 0.023 | 0.133 |
| | 35I | 0.023 | 0.137 |
| | 37I | 0.025 | 0.144 |
| | 38I | 0.019 | 0.111 |
| | 42I | 0.017 | 0.100 |
| | 46I | 0.013 | 0.077 |
| | 47I | 0.019 | 0.109 |
| | 54I | 0.027 | 0.156 |

(1) Mils per year
(2) Milligrams per square decimeter per day
* Results inconsistent with other data and not included in data analysis.

TABLE D-2
CORROSION RATES FROM POT 7E
3000 PPM $PO_4$ SOAK

| Material | Specimen Number | Corrosion Rate, MPY (1) | Weight Loss MDD (2) |
|---|---|---|---|
| C-Steel | C-56 | 0.542 | 2.972 |
| | C-61 | 0.509 | 2.793 |
| | C-63 | 0.497 | 2.717 |
| | C-65 | 0.521 | 2.854 |
| | C-70 | 0.497 | 2.714 |
| | C-90 | 0.488 | 2.669 |
| | C-94 | 0.479 | 2.627 |
| | C-95 | 0.563 | 3.090 |
| | C-96 | 0.612 | 3.356 |
| A-508 | A-149 | 0.460 | 2.530 |
| | A-150 | 0.409 | 2.239 |
| | A-151 | 0.412 | 2.263 |
| | A-152 | 0.421 | 2.314 |
| | A-153 | 0.464 | 2.544 |
| | A-154 | 0.418 | 2.284 |
| | A-155 | 0.448 | 2.448 |
| | A-158 | 0.430 | 2.351 |
| | A-159 | 0.421 | 2.296 |
| A-533-A | B-118 | 0.430 | 2.351 |
| | B-119 | 0.439 | 2.402 |
| | B-120 | 0.460 | 2.527 |
| | B-121 | 0.482 | 2.645 |
| | B-122 | 0.433 | 2.369 |
| | B-123 | 0.464 | 2.539 |
| | B-124 | 0.445 | 2.436 |
| | B-126 | 0.482 | 2.633 |
| | B127 | 0.548 | 2.993 |
| 409 SS | S-71 | 0.142 | 0.776 |
| | S-72 | 0.136 | 0.745 |
| | S-75 | 0.133 | 0.712 |
| | S-82 | 0.112 | 0.606 |
| | S-84 | 0.118 | 0.639 |
| | S-85 | 0.130 | 0.706 |
| | S-88 | 0.130 | 0.703 |
| | S-90 | 0.136 | 0.739 |
| | S-92 | 0.164 | 0.876 |
| Alloy 600 | I-124 | 0.028 | 0.165 |
| | I-128 | 0.027 | 0.159 |
| | I-138 | 0.028 | 0.166 |
| | I-139 | 0.025 | 0.149 |
| | I-148 | 0.028 | 0.167 |
| | I-150 | 0.022 | 0.128 |
| | I-158 | 0.027 | 0.159 |
| | I-159 | 0.031 | 0.182 |
| | I-162 | 0.027 | 0.160 |

(1) Mils per year
(2) Milligrams per square decimeter per day

TABLE D-3

AVERAGE CORROSION RATES
FROM POT BOILER TESTS

| Material | Pot | PPM of $PO_4$ | Average Corrosion Rate, MPY (1) | S(3) | Average Corrosion Rate MDD (2) | $\bar{S}$(3) |
|---|---|---|---|---|---|---|
| C-Steel | 11 | 1000 | 0.58 | 0.05 | 3.2 | 0.3 |
| | 7E | 3000 | 0.52 | 0.04 | 2.9 | 0.2 |
| A-508 | 11 | 1000 | 0.39 | 0.02 | 2.1 | 0.1 |
| | 7E | 3000 | 0.43 | 0.02 | 2.4 | 0.1 |
| A-533-A | 11 | 1000 | 0.56 | 0.02 | 3.1 | 0.1 |
| | 7E | 3000 | 0.46 | 0.04 | 2.5 | 0.2 |
| 409 SS | 11 | 1000 | 0.16 | 0.01 | 0.88 | 0.08 |
| | 7E | 3000 | 0.13 | 0.01 | 0.72 | 0.08 |
| Alloy 600 | 11 | 1000 | 0.021 | 0.004 | 0.12 | 0.03 |
| | 7E | 3000 | 0.027 | 0.002 | 0.16 | 0.01 |

Notes: (1) Mils Per Year
(2) Milligrams per Square Decimeter per Day
(3) Standard Deviation

# Appendix E

## POT BOILER DENT METALLOGRAPHY

### EXPERIMENTAL

Pots 11 (1000 ppm $PO_4$) and 7E (3000 ppm $PO_4$) were examined. Dents on tube 4 at both carbon steel concentrating rings and at the hot leg support plate were sectioned for optical and scanning electron microscopy (SEM). Figure E-1 shows the location of these dents on the tube and Figure E-2 is a sketch of a typical dent after sectioning for examination. Specimen identification numbers (given on Figure E-1) indicate the tube leg (hot or cold), the pot bundle number, the tube number, and the specimen code letter (K-support plate; D,I - concentrating rings).

For all specimens, the morphology of the oxide in the crevice region was examined in detail by optical microscopy. Comparisons were made of the oxide formations at different locations within the same specimen and between different specimens.

The concentrating ring dents were further examined by scanning electron mecroscopy (SEM) supplemented by energy dispersive spectrometry (EDS) analysis to identify elements present. Areas for SEM/EDS examination were identified from the light microscopy studies. At each area, a low magnification (39-50X) SEM was obtained which was then used to select four to six areas for examination at higher magnification (2100X). A qualitative search of the magnetite in each area was conducted via EDS to identify chemical species present. The support plate sections were also examined by SEM. Additionally, the magnetite was examined with the electron microprobe (EMP) supplemented with wave length dispersive spectrometry (WDS), which provided a sensitive X-ray mapping

of the elemental distribution. This technique allows areas of local concentration of specific elements (chloride phosphorus) to be associated with specific structures of the magnetite morphology.

## RESULTS

### Light Microscopy

Photo micrographs of the oxide structures observed in the specimens are shown in Figure E-3 through E-14. The top of each photograph corresponds to the top of the specimen as found in the pot boiler. The oxide of all locations was voluminous and completely filled the crevice. The oxide thickness shown in the micrographs varied from about 0.020 inch in Figure E-3 to about 0.066 inch in Figure E-14. This thickness included the original crevice (size approximately 0.010 inch), the additional crevice area caused by the denting, plus the depth of attack in the carbon steel.

The corrosion was relatively uniform at different locations in the same specimen and did not vary greatly between different specimens. The oxide generally consisted of successive regions of relatively fine magnetite and relatively coarse magnetite. The laminations were not as evident in some of the photomicrographs as they were during visual examination. The magnetite also exhibited a significant amount of cracking and some porosity (see, for example, Figure E-4), but the amounts varied between different locations. Some plated copper was also observed in a few localized areas near the magnetite/Alloy 600 interfaces. An example of this is shown in Figure E-3 where the intermittent white granular area (not the white strips) near the oxide/Alloy 600 interface were identified as copper by EDS.

The above observations are typical of oxides grown on carbon steel in acid chloride environments.

## Scanning Electron Microscopy (SEM)

Concentrating Ring Sections. Seven regions were selected from the ring specimens for SEM examination. These regions are shown in Figure E-15, E-21, E-26, E-32, E-38 and E-44 and E-49. Each figure is followed by a series of higher magnification SEM's taken of 4-6 areas within each region, together with the Energy Dispersive Spectrometry (EDS) output identifying the elements present in each area. All specimens were sputtered with gold prior to examination. This accounts for the gold X-ray in all EDS plots. Table E-1 summarizes the SEM observations and the EDS analyses.

The most significant observation is that in none of the EDS analyses was phosphorus identified as one of the elements present in the oxide. The sensitivity of the typical EDS is approximately one percent, with poorer sensitivity for elements with low atomic numbers. Therefore if present, phosphorus (Atomic Number 15) did not exceed a maximum of one percent of the oxide in the areas analyzed.

In both specimens from pot 11 (1000 ppm $PO_4$), chlorine was identified in a band roughly 15 mils wide beginning about 5 mils from the carbon steel surface. However, chloride was found in only one specimen from pot 7 (3000 ppm $PO_4$), at the center section of the tube #4 cold leg carbon steel ring. As in the previous specimens, chlorine was found in a band 5 mils wide beginning about 5 mils from the carbon steel surface. In addition, however, chlorine was also found adjacent to the I600 interface. The only other elements observed in the vicinity of the carbon steel-magnetite interface were iron and occasionally Silicon. Silicon was observed intermittently throughout the various areas of magnetite. In all likelihood

it came from the polishing material trapped in the oxide; however, since carbon steel is deoxidized by the addition of Silicon, it possibly could have come from the steel itself. Another possible though unlikely source is the seawater with which the pots were faulted. The concentration of silicon in seawater is less than 1 ppm as $SiO_2$.

In general the areas nearest the I600 showed the greatest variety of elements. These included Cu, Ni, Ca, Mg, Mn and S. Copper and nickel probably originated from the mixture of $Fe_3O_4$, Cu, CuO, and NiO used to prepack the crevice regions. Titanium was also found in one sample near the I600 tubing. This was probably from the I600 tubing which has a known Ti content. In general copper and sulfur were found in the same area of the magnetite.

The high magnification SEMS showed that the morphology of the magnetite varied significantly, from very smooth textured surfaces that were essentially featureless to very coarse textured surfaces with many large and small pits, pores, cracks, granules and indentations. A review of Table E-1 suggests that the course textured magnetite harbored a greater variety of elements, probably because the large surface area provided locations at which these elements could absorb or precipitate. In general, the various structures observed were similar to structures usually observed in magnetite on carbon steel exposed to acid chloride environments.

Support Plate Specimens. These sections were examined by Electron Microprobe (EMP) to determine the distribution of chlorine and phosphorus across the oxide layer. Table E-2 and Figures E-56 through E-63 present the results of the EMP analyses. Table E-2 also summarizes the low magnification SEM, EDS, and X-ray mapping results obtained as part of the EMP analyses.

Phosphorus was detected via X-ray mapping at two locations - near the top and bottom of specimen H-7E-4-K from the 3000 ppm $PO_4$ test. In both cases, the phosphorus was in the vicinity of the I600/magnetite interface (Figure E-60 and E-61). Although the oxide was scanned in detail, EDS analysis showed Phosphorus present only at the bottom of the specimen. This discrepancy is probably the result of the different sensitivities of the two methods. X-ray mapping, which is performed by wavelength dispersive spectrometry (WDS) is more sensitive to low concentrations.

Phosphorus was not uniformly dispersed through the magnetite, but was concentrated in localized regions. Comparison of the X-ray maps with the SEM results indicated that Phosphorus was confined primarily to the areas of the oxide near the Inconel-600 characterized by porosity, cracks, and other discontinuities. From the EDS results, the concentration of phosphorus was estimated to be 2 percent by weight. As with all semi-quantitative EDS work the error ranges from a factor of 1/2 to 2. Hence the range is 1-4 percent by weight.

Chloride was identified and mapped at the center location of each of the support plate specimens. There were indications by X-ray mapping that some Chloride was present near the Alloy 600/magnetite interface, but by far the greatest quantity was near the carbon steel interface (Figures E-56 and E-58). Chloride content was estimated at 8 percent and 5 percent at two locations in specimen H-11-4-K, (1000 ppm $PO_4$ test) and 6 percent at one location in specimen H-7E-4-K (3000 ppm $PO_4$ test). Again the error band is 1/2 to 2.

Other elements identified by EDS are included in Table E-2 and can be attributed to sea salts (Mg, Ca, Mn, S), the prepacking material (Cu, Ni), polishing operation, or the base metals.

The morphology of the oxide itself as observed by SEM was essentially identical to that found in the concentrating ring specimens.

TABLE E-1

RESULTS OF SEM AND EDS ANALYSIS OF RING SPECIMENS

| Specimen | Position | Location | SEM Observations | Elements Identified | Figure No. |
|---|---|---|---|---|---|
| H-11-4-I | Top | 1 | Fairly Smooth Texture, Numerous Pits or Pores | Si, Cl | E-16 |
| | | 2 | Very Smooth Texture, No Pits or Pores | Cl | E-17 |
| | | 3 | Generally Smooth Texture, Some Pits or Pores and Darker Areas | Cl | E-18 |
| | | 4 | Generally Coarse Texture, Numerous Pits, Pores (Some Fairly Large), Numerous Small Cracks | Si, Cl, Mn, Cu | E-19 |
| | | 5 | Coarse Structure, Pits and Pores | S, Ca | E-20 |
| | Center | 1 | Smooth to Slightly Coarse Texture, Some Small Pits | Si, Cl | E-22 |
| | | 2 | Very Smooth Texture, No Pits or Pores | Si, Cl | E-23 |
| | | 3 | Smooth Texture, Pits Pores, Some Cracks | Si, Ni, Cu | E-24 |

TABLE E-1 (continued)

RESULTS OF SEM AND EDS ANALYSIS OF RING SPECIMENS

| Specimen | Position | Location | SEM Observations | Elements Identified | Figure No. |
|---|---|---|---|---|---|
| | | 4 | Coarse Texture, Numerous Pits, Pores, or Other Indentations of Surface | Si, Ca, Ni, Cu | E-25 |
| C-11-4-D | Center | 1 | Coarse Texture, Many Small Pits or Pores, Some Darker Areas | Si, Cl | E-27 |
| | | 2 | Coarse Texture, Many Small Pits or Pores, Mix of Light and Dark Areas | Cl | E-28 |
| | | 3 | Smooth, Texture, Some Large and Deep Pits, Some Small and Shallow Pits | -- | E-29 |
| | | 4 | Coarse Texture, Numerous Large and Deep Pits or Pores | -- | E-30 |
| | | 5 | Smooth Texture, Many Parallel Polishing Marks, Light Particles on Surface, a few Pits or Pores | Si, Cr, Ni | E-31 |
| H-7E-4-I | Top | 1 | Coarse Textures, Elongated and Large Pits | Si | E-33 |
| | | 2 | Coarse Texture, Numerous Pits or Pores | Si | E-34 |
| | | 3 | Coarse Texture, Some Deep Pits or Pores, Shallow Identations | Si, S, Ca, Cu | E-35 |

TABLE E-1 (continued)

RESULTS OF SEM AND EDS ANALYSIS OF RING SPECIMENS

| Specimen | Position | Location | SEM Observations | Elements Identified | Figure No. |
|---|---|---|---|---|---|
| | | 4 | Coarse, Granular Texture With Many Pits or Pores | Si, S, Ca, Cu | E-36 |
| | | 5 | Coarse, Granular Texture; Many Granules on Surface; Some Pits or Pores | Si, S, Ca, Cu | E-37 |
| H-7E-4-1 | Center | 1 | Coarse Texture; Some Pits or Pores | -- | E-39 |
| | | 2 | Coarse Texture; Many Pits or Pores | Si | E-40 |
| | | 3 | Coarse Texture, Many Pits or Pores; Some Large Porosity | Si, S, Cu | E-41 |
| | | 4 | Coarse Granular Texture; One Large Crack | Mg, Si, S, Ca | E-42 |
| | | 5 | Coarse Granular Texture; Some Pits or Pores; Granules on Surface | Si, S, Ca, Ni | E-43 |
| C-7E-4D | Top | 1 | Coarse Texture; A few Pits or Pores; Large Shallow Indentations Near Top | -- | E-45 |
| | | 2 | Very Coarse Texture | -- | E-46 |
| | | 3 | Coarse Texture; Many Pits or Pores | -- | E-47 |
| | | 4 | Coarse Texture; Many Large and Small Pits and Pores | S, Cu | E-48 |

TABLE E-1 (continued)

RESULTS OF SEM AND EDS ANALYSIS OF RING SPECIMENS

| Specimen | Position | Location | SEM Observations | Elements Identified | Figure No. |
|---|---|---|---|---|---|
| C-7E-4-D | Center | 1 | Coarse Texture; Many Large and Small Pits; Several Raised Areas | Si, Cl | E-50 |
| | | 2 | Coarse Texture; Some Large, Shallow Pits | Cl | E-51 |
| | | 3 | Coarse Texture; Many Large and Small Pits, Pores and Indentations | Si | E-52 |
| | | 4 | Coarse Texture, Granules on Surface; Many Pits and Pores; One Large Crack | Si | E-53 |
| | | 5 | Coarse Texture; Granules in Localized Areas; Pits or Pores | Si, S, Ca | E-54 |
| | | 6 | Coarse Texture; Many Large and Small Pits, Pores, and Indentations | Mg, Si, S, Cl, Ca, Ti, Ni | E-55 |

TABLE E-2

SUMMARY OF OBSERVATIONS ON SUPPORT PLATE SECTIONS

| Specimen | Position | Location | SEM Observations | Elements Identified | Figure No. |
|---|---|---|---|---|---|
| H-11-4-K | Center | 1 | Fairly Smooth Texture; Some Pits or Pores, Small Crack | Al, S, Ni | E-56, E-57 |
| | | 2 | Coarse Texture; Numerous Pits and Pores; One Large Crack | Mg, Cl, Ni | E-56, E-57 |
| | | 3 | Smooth Texture; Some Pits and Pores; Some Granules on Surface | Cl, Ni | E-56, E-57 |
| H-7E-4-K | Top | 1 | Coarse Texture; Numerous Pits, Pores, Large Voids; Cracks | Mg, Si, P, Ca, Ti, Mn Ni, Cu | E-61, E-62 |
| | Bottom | 1 | Coarse Texture; Numerous Pits, Pores, Voids; Small Cracks | Mg, Si, P, S, Ca, Ti, Cr, Mn, Ni, Cu | E-60, E-63 |
| | Center | 1 | Coarse Texture; Many Pits, Pores, Voids; Several Cracks | Si, Ni | E-58, E-59 |
| | | 2 | Coarse Texture; Many Pits, Pores, Etc. | Si, Ni | E-58, E-59 |
| | | 3 | Coarse Texture; Many Pits, Pores, Etc. | Si, Cl, Mn, Ni | E-58, E-59 |

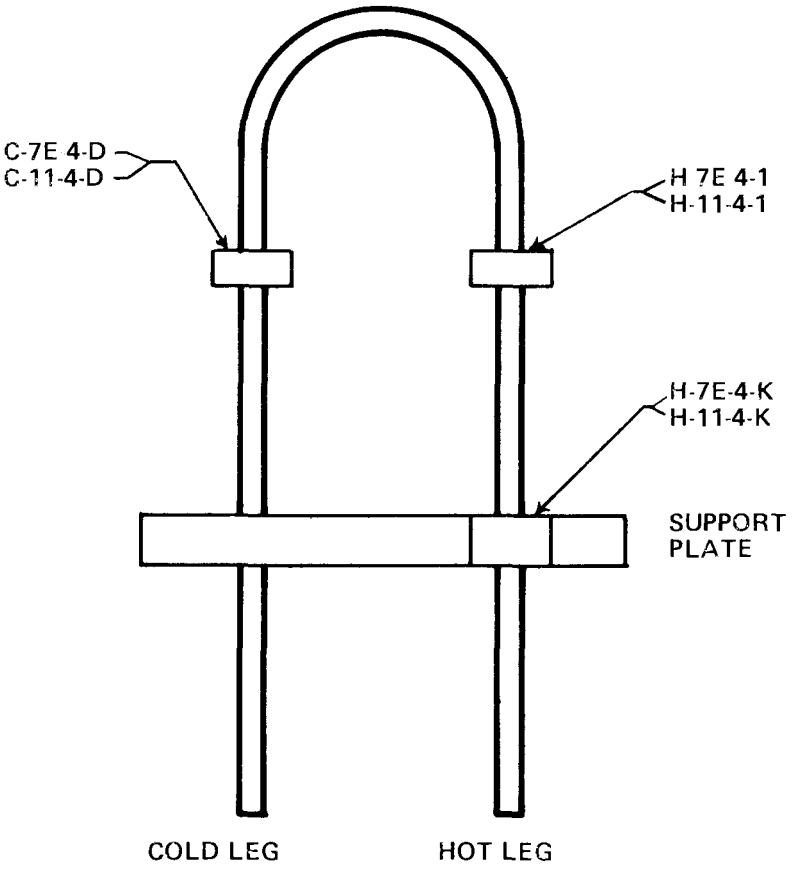


Figure E-1
LOCATION OF SPECIMENS REMOVED FROM TUBE 4
OF POT BOILERS 7E AND 11

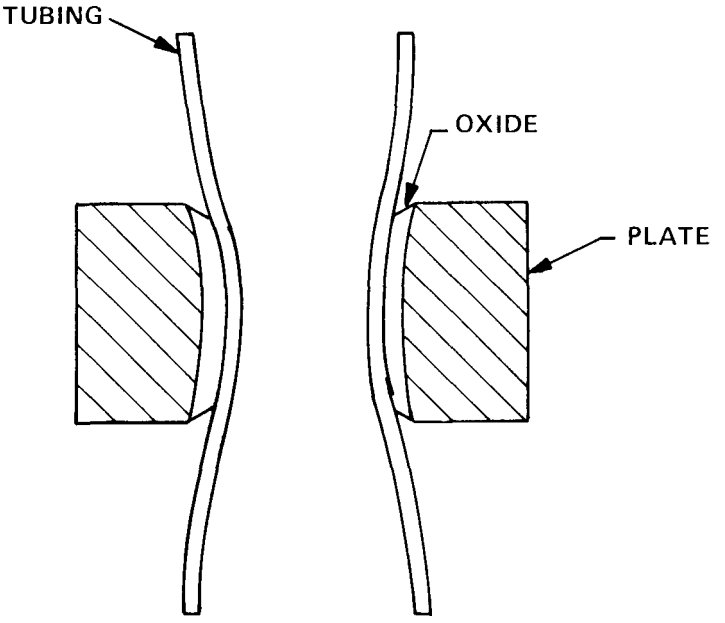


Figure E-2
SCHEMATIC OF TYPICAL SPECIMEN
AFTER SECTIONING FOR EXAMINATION

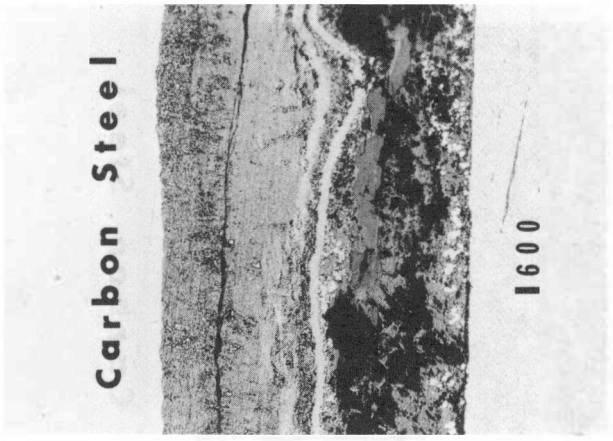


Figure E-3. Photomicrograph of the Oxide Near the Top of Specimen H-11-4-I (as-polished, 90X)*


Figure E-4. Photomicrograph of the Oxide Near the Center of Specimen H-11-4-I (as-polished, 90X)*

*Please note that the illustrations on this page have been reduced 10% in printing.

1000 ppm Phosphate Soak

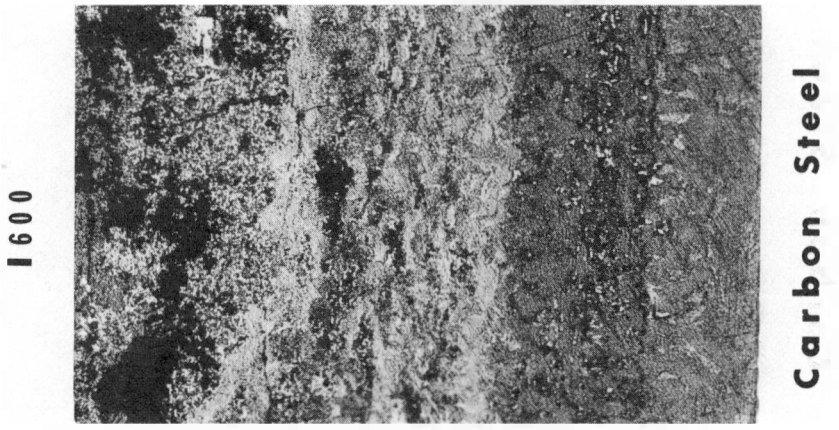


Figure E-5. Photomicrograph of the Oxide Near the Center of Specimen C-11-4-D (as-polished, 90X)*

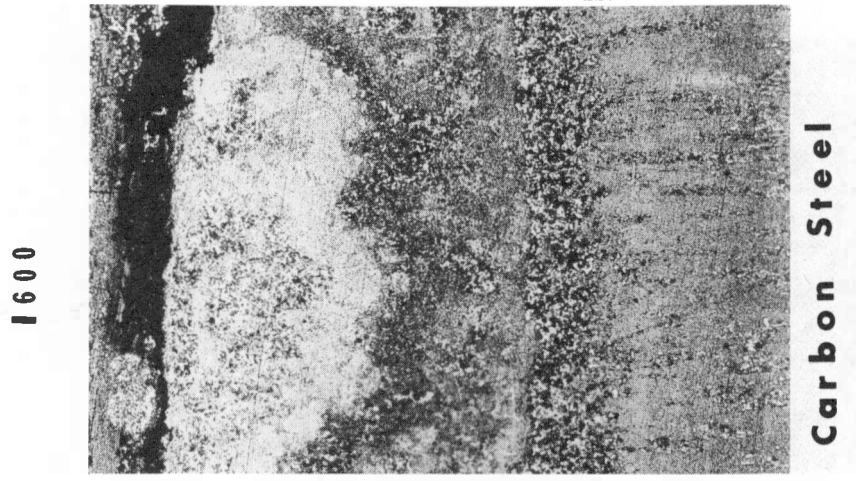


Figure E-6. Photomicrograph of the Oxide Near the Center of Specimen H-11-4-K (Support Plate Specimen, 90X)*

*Please note that the illustrations on this page have been reduced 10% in printing.

3000 ppm Phosphate Soak

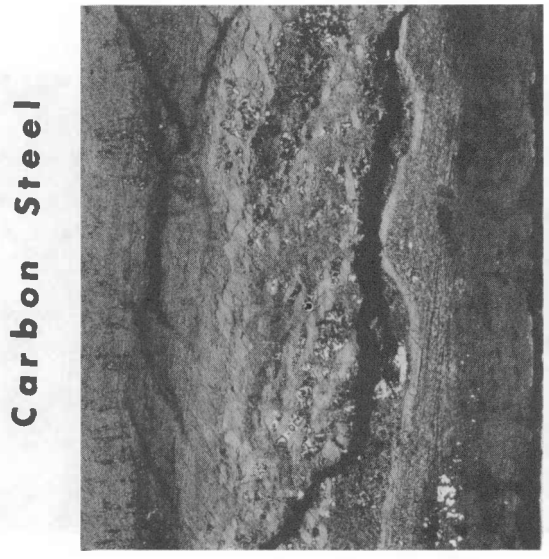


Figure E-7. Photomicrograph of the Oxide Near the Top of Specimen H-7E-4-I (as-polished, 90X)*

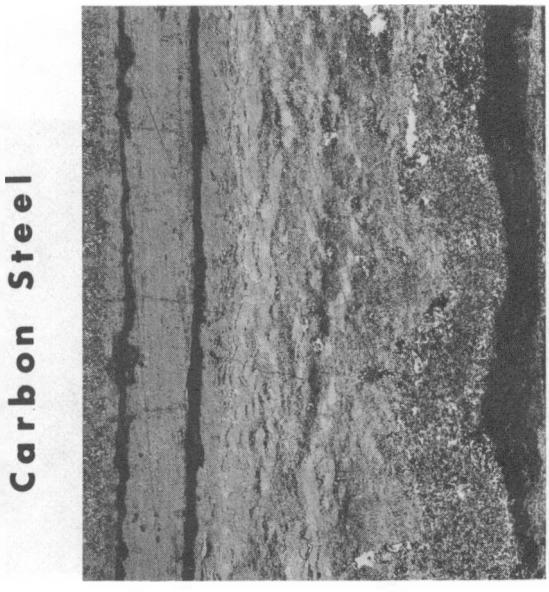


Figure E-8. Photomicrograph of the Oxide Near the Center of Specimen H-7E-4-I (as-polished, 90X)*

*Please note that the illustrations on this page have been reduced 10% in printing.

3000 ppm Phosphate Soak

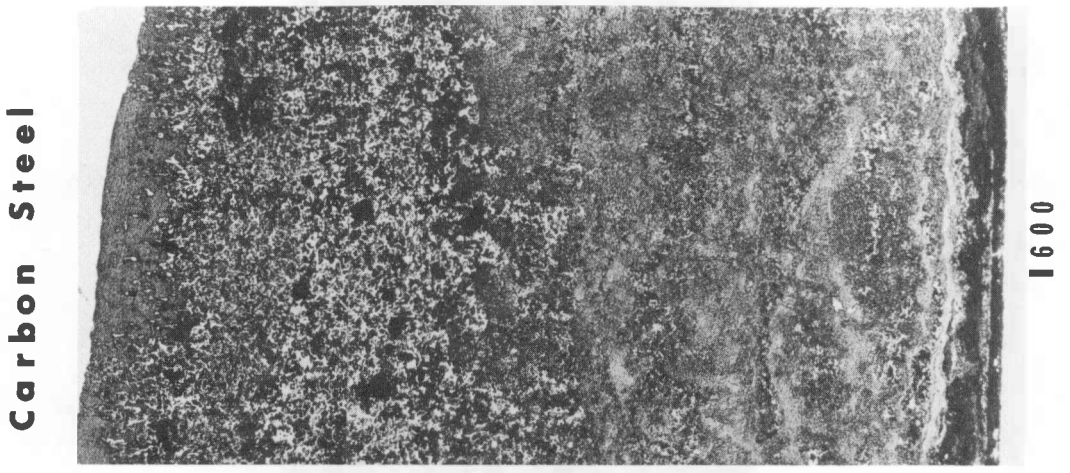


Figure E-9. Photomicrograph of the Oxide Near the Top of Specimen H-7E-4-K (Support Plate Specimen) (as-polished, 90X)*

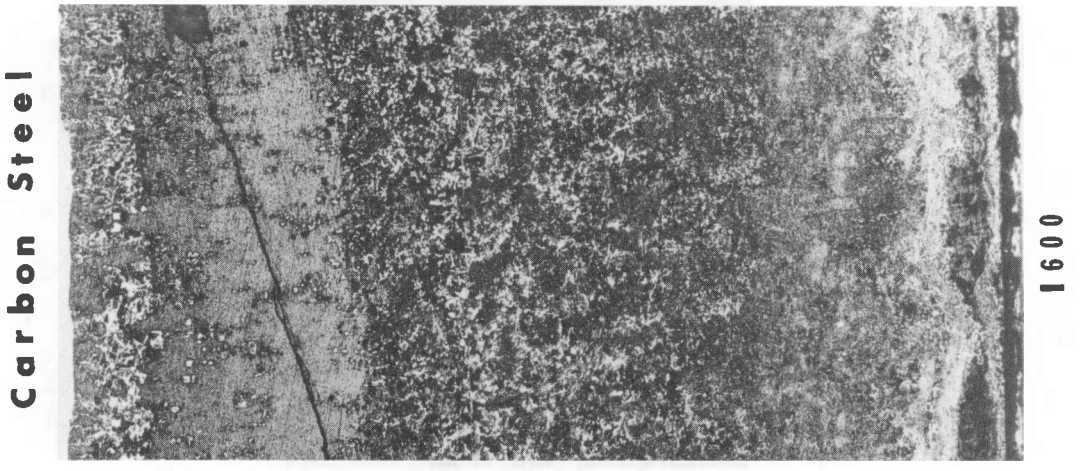


Figure E-10. Photomicrograph of the Oxide Near the Center of Specimen H-7E-4-K (as-polished,90X)*

*Please note that the illustrations on this page have been reduced 10% in printing.

3000 ppm Phosphate Soak

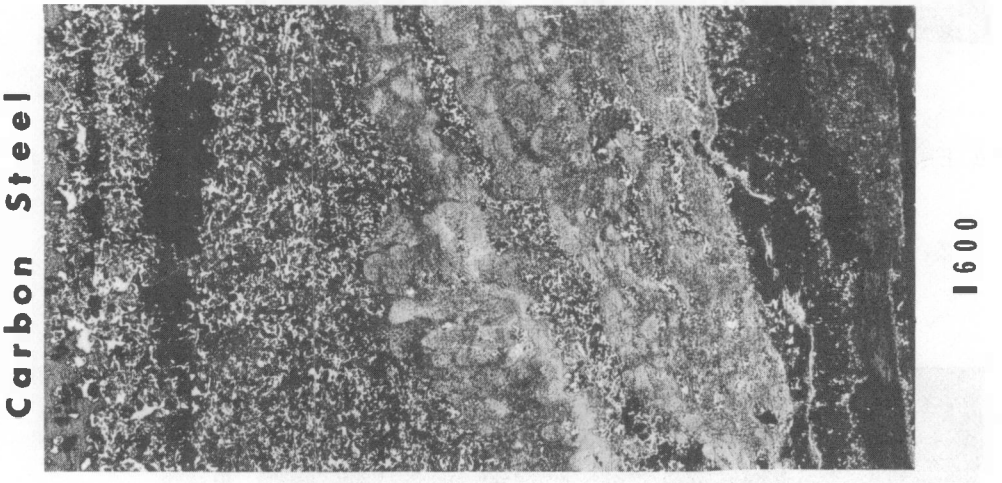


Figure E-11. Photomicrograph of the Oxide Near the Bottom of Specimen H-7E-4-K (as-polished, 90X)*

*Please note that the illustrations on this page have been reduced 10% in printing.

3000 ppm Phosphate Soak


Figure E-12. Photomicrograph of the Oxide Near the Top of Specimen C-7E-4-D (as-polished, 90X)*


Figure E-13. Photomicrograph of the Oxide Near the Center of Specimen C-7E-4-D (as-polished, 90X)*

*Please note that the illustrations on this page have been reduced 10% in printing.

3000 ppm Phosphate Soak

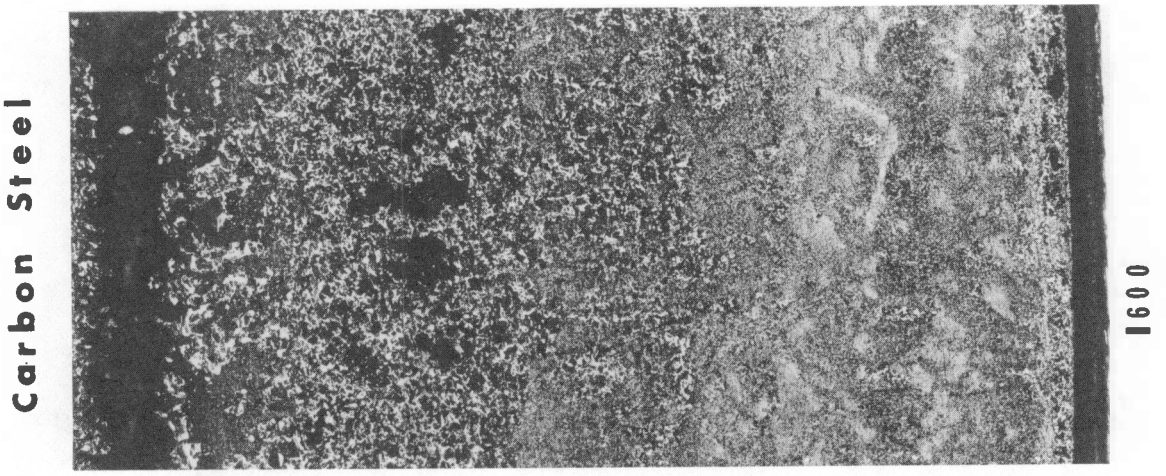


Figure E-14. Photomicrograph of the Oxide Near the Center of Specimen C-7E-4-B (as-polished, 90X)*

*Please note that the illustrations on this page have been reduced 10% in printing.

1000 ppm Phosphate Soak


Figure E-15. Scanning Electron Micrograph of the Crevice Region Near the Top of Specimen H-11-4-I Showing the Five Locations at which Higher Magnification SEMS and EDS Analyses were Obtained (30X)*

*Please note that the illustrations on this page have been reduced 10% in printing.

1000 ppm Phosphate Soak

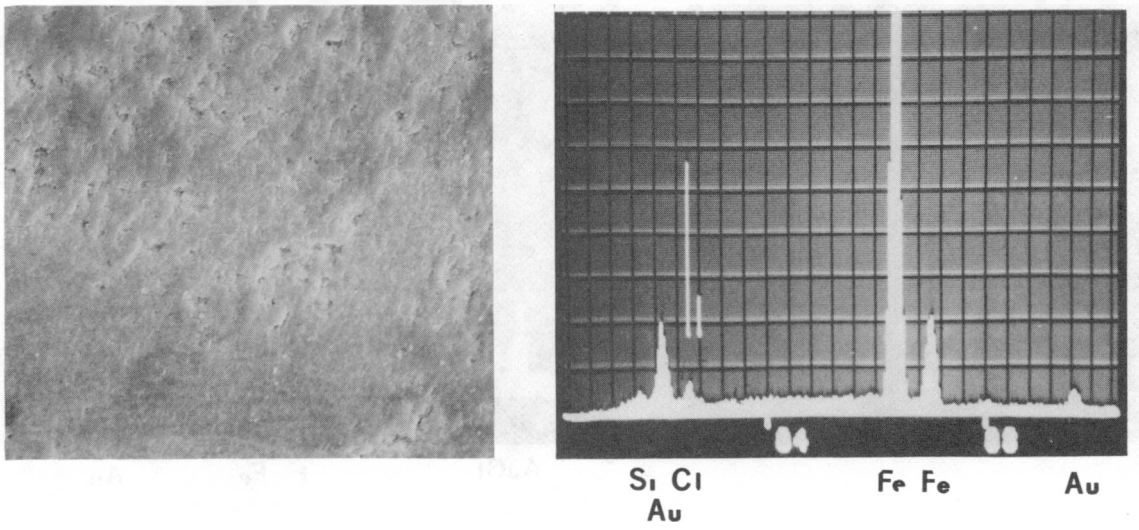


Figure E-16. SEM and EDS Analysis of Area 1 of Figure E-15 (1200X)*

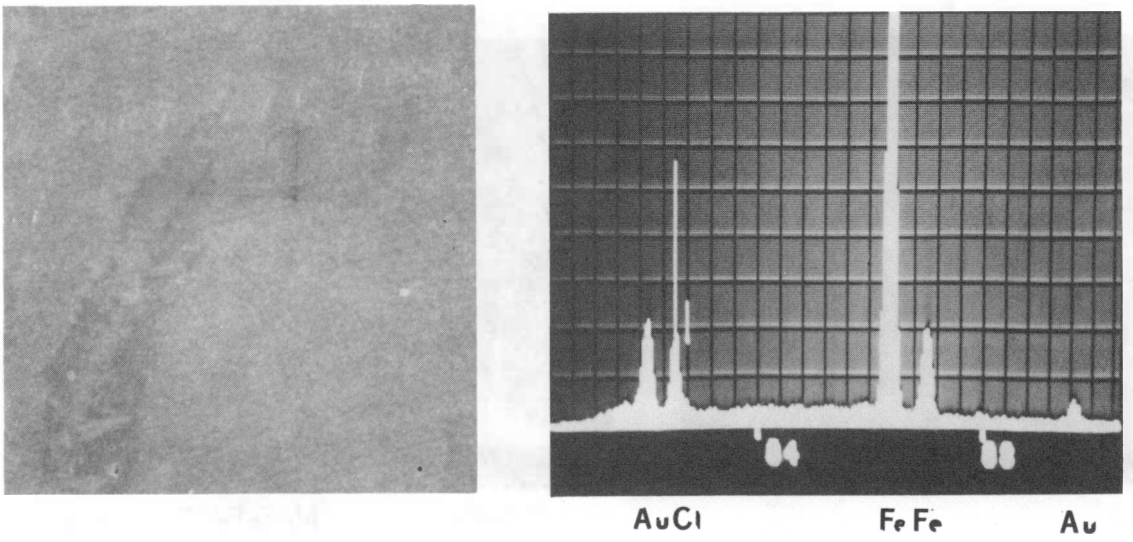


Figure E-17. SEM and EDS Analysis of Area 2 of Figure E-15 (1200X)*

*Please note that the illustrations on this page have been reduced 10% in printing.

1000 ppm Phosphate Soak

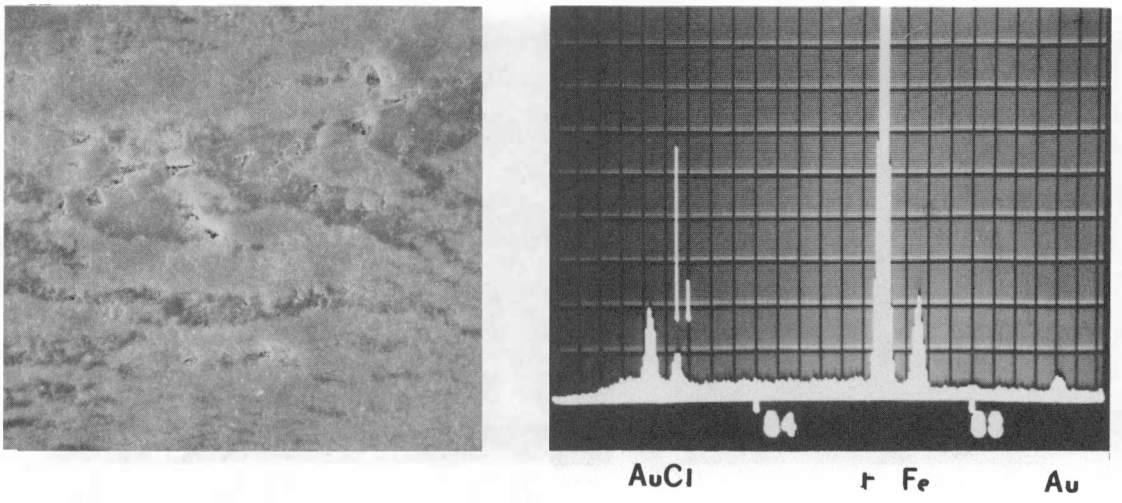


Figure E-18. SEM and EDS Analysis Results from Area 3 of Figure 15 (1200X)*

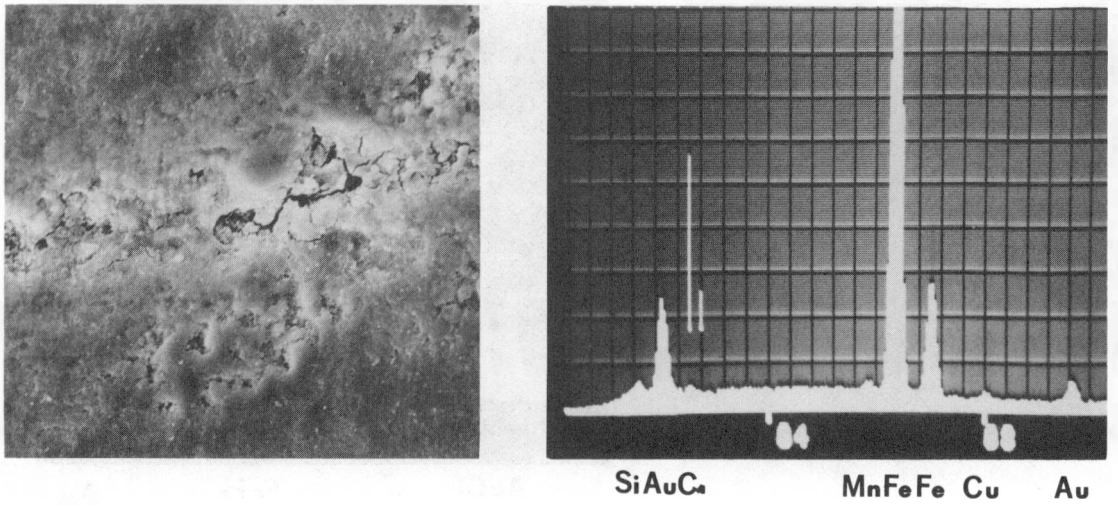


Figure E-19. SEM and EDS Analysis Results from Area 4 of Figure 15 (1200X)*

*Please note that the illustrations on this page have been reduced 10% in printing.

1000 ppm Phosphate Soak

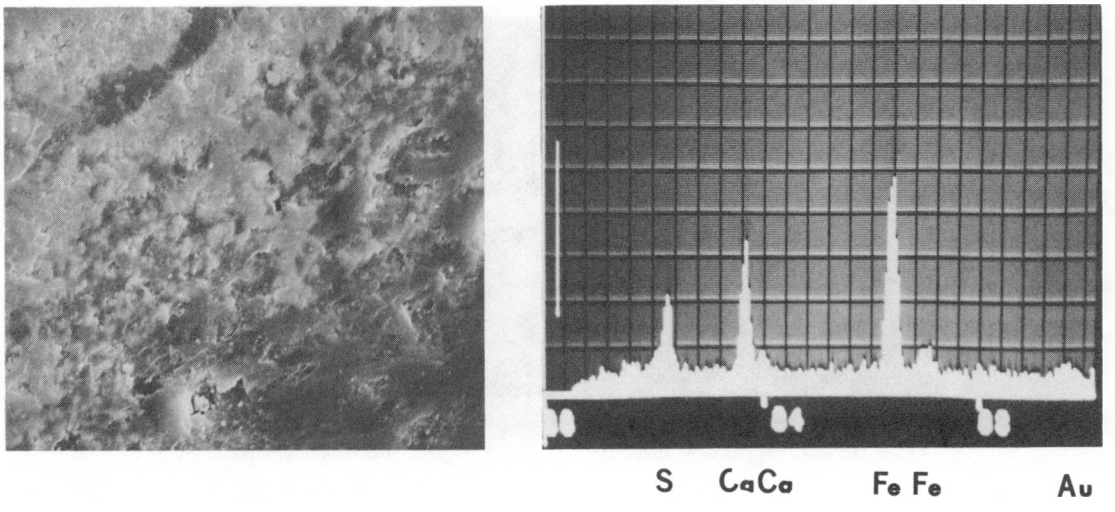


Figure E-20. SEM and EDS Analysis Results from Area 5 of Figure 15 (1200X)*

*Please note that the illustrations on this page have been reduced 10% in printing.

1000 ppm Phosphate Soak

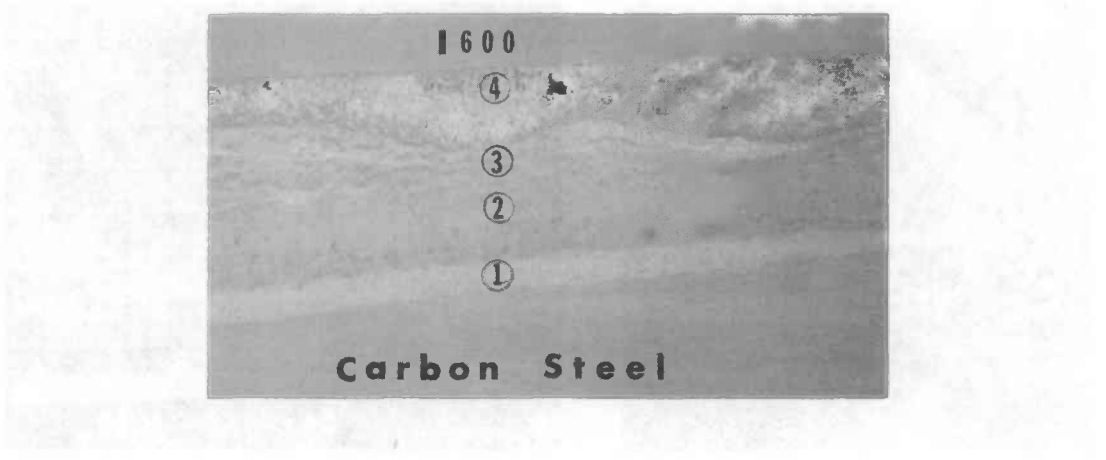


Figure E-21. Scanning Electron Micrograph of the Crevice Region Near the Center of Specimen H-11-4-I Showing the Four Locations at which Higher Magnification SEM and EDS Analyses were Obtained (39X)*

*Please note that the illustrations on this page have been reduced 10% in printing.

1000 ppm Phosphate Soak

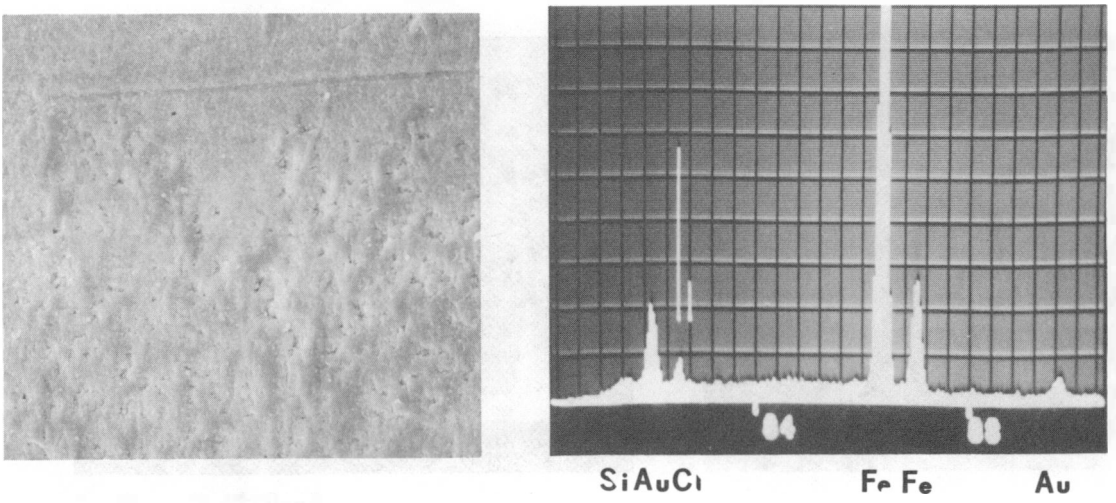


Figure E-22. SEM and EDS Analyses of Area 1 of Figure E-21 (1200X)*

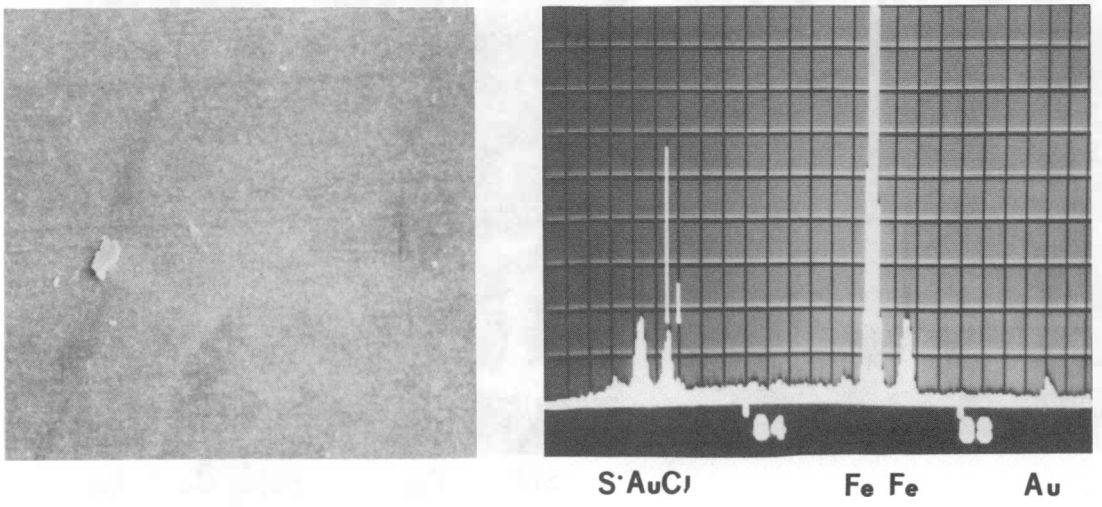


Figure E-23. SEM and EDS Analyses of Area 2 of Figure E-21 (1200X)*

*Please note that the illustrations on this page have been reduced 10% in printing.

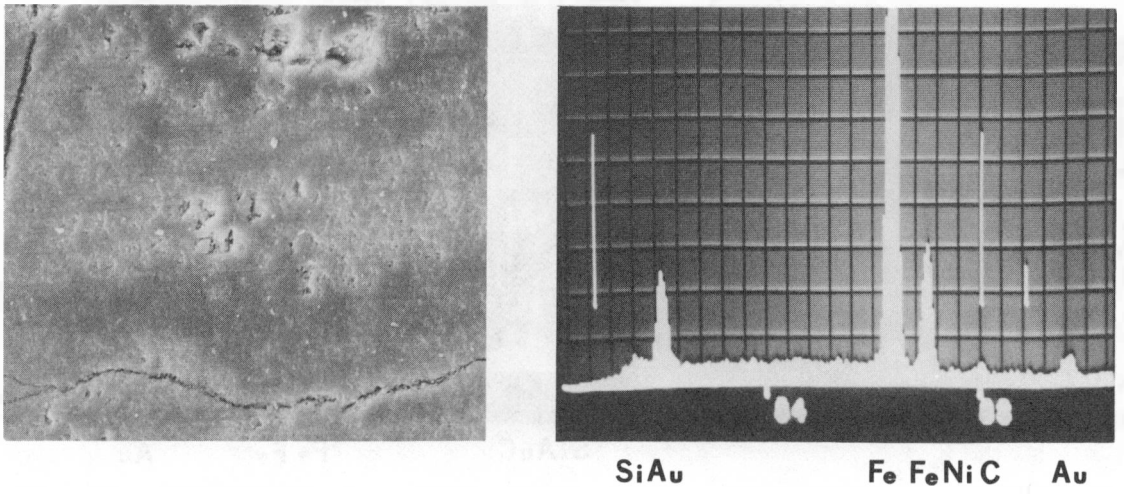


Figure E-24. SEM and EDS Analyses of Area 3 of Figure E-21 (1200X)*

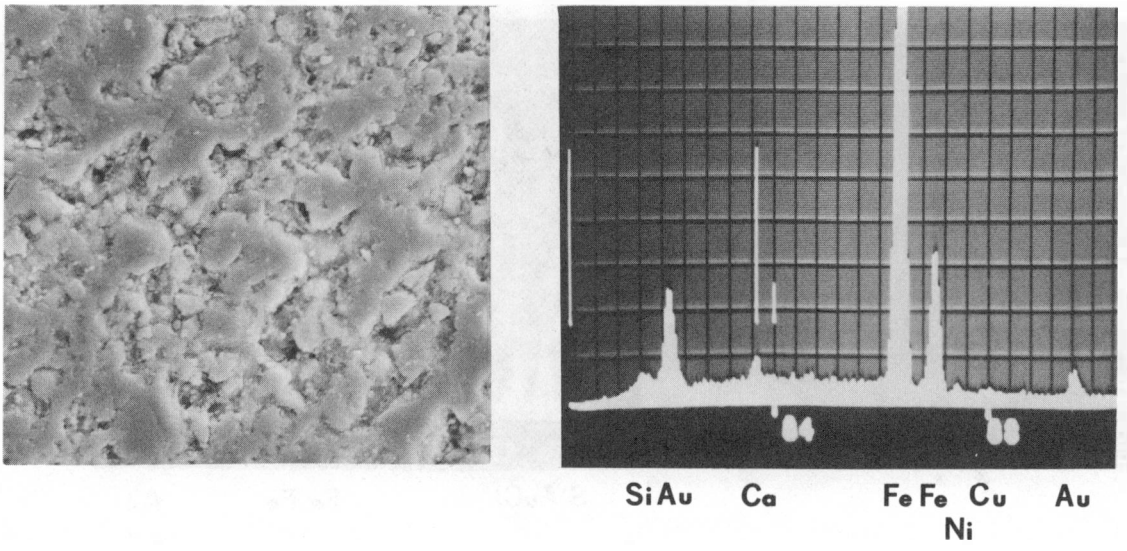


Figure E-25. SEM and EDS Analyses of Area 4 of Figure E-21 (1200X)*

*Please note that the illustrations on this page have been reduced 10% in printing.

1000 ppm Phosphate Soak

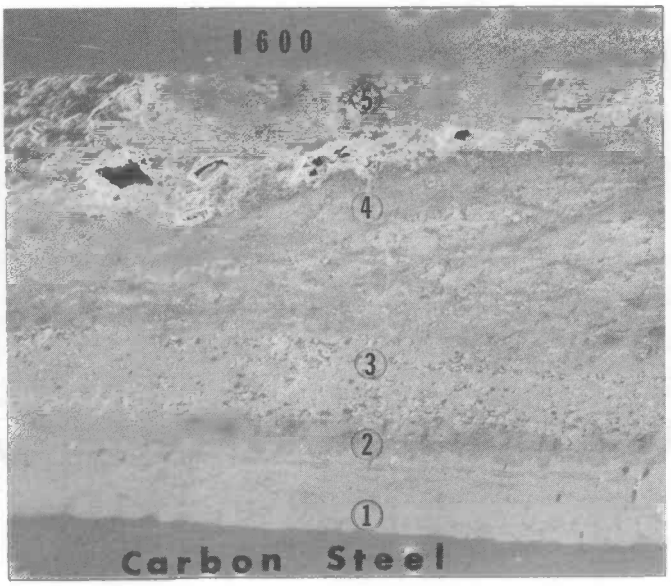


Figure E-26. Scanning Electron Micrograph of the Crevice Region Near the Center of Specimen C-11-4-D Showing the Five Locations at which Higher Magnification SEM and EDS Analyses were Obtained (39X)*

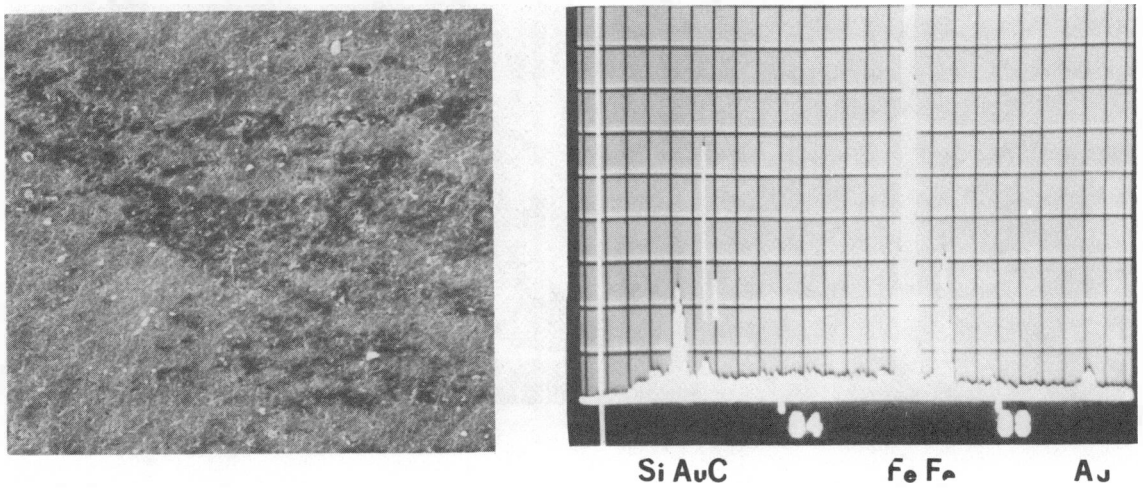


Figure E-27. SEM and EDS Analyses of Area 1 of Figure E-26 (1200X)*

*Please note that the illustrations on this page have been reduced 10% in printing.

1000 ppm Phosphate Soak

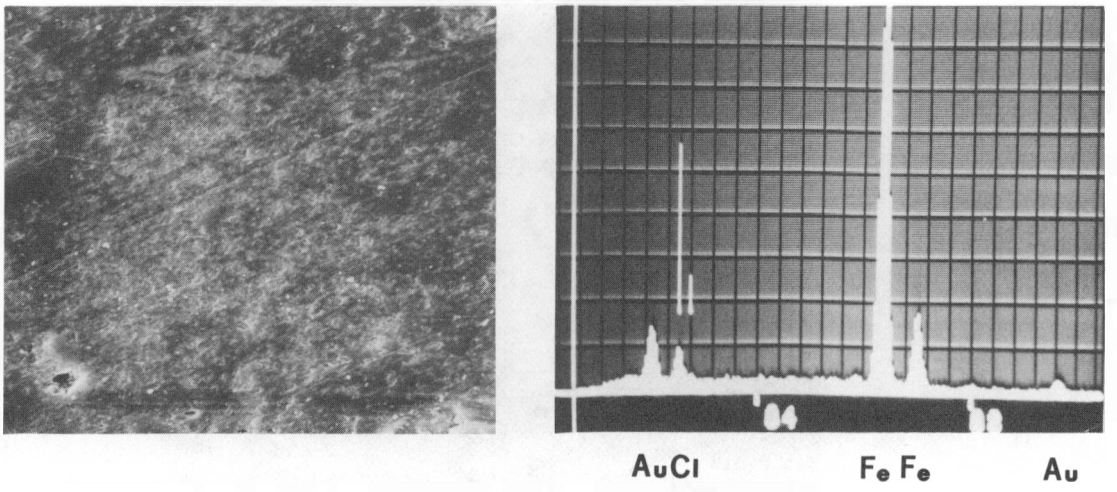


Figure E-28. SEM and EDS Analyses of Area 2 of Figure E-26 (1200X)*

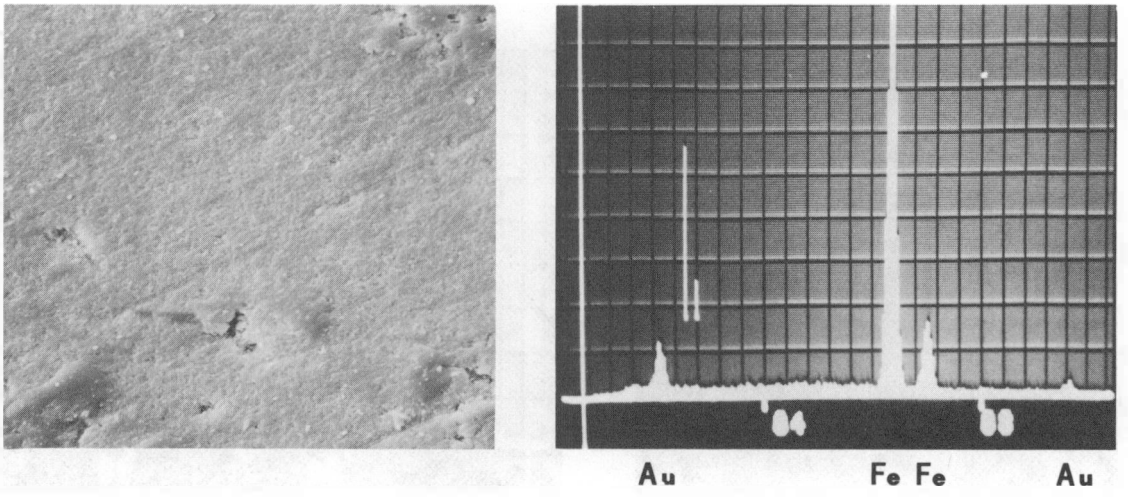


Figure E-29. SEM and EDS Analyses of Area 3 of Figure E-26 (1200X)*

*Please note that the illustrations on this page have been reduced 10% in printing.

1000 ppm Phosphate Soak

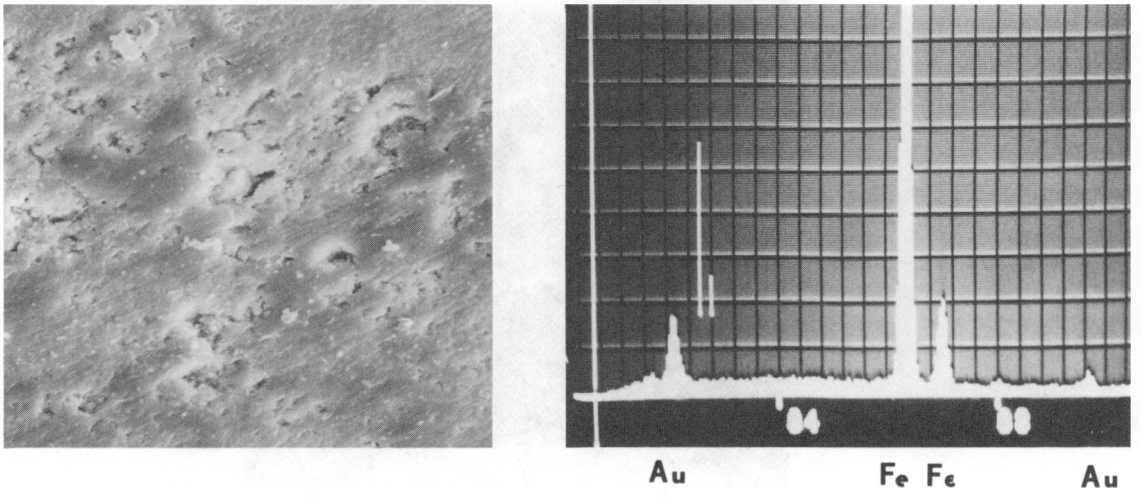


Figure E-30. SEM and EDS Analyses of Area 4 of Figure E-26 (1200X)*

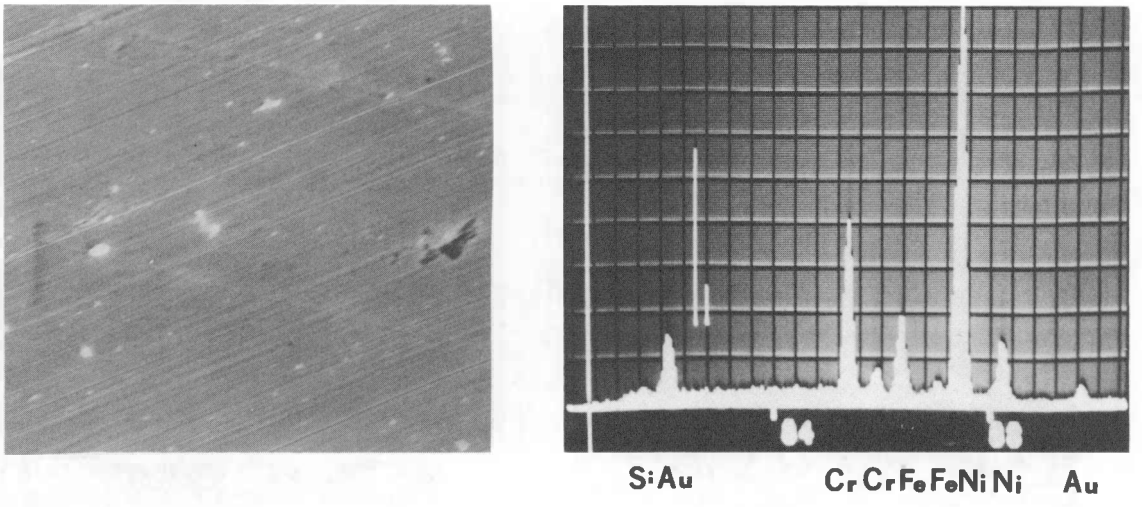


Figure E-31. SEM and EDS Analyses of Area 5 of Figure E-26 (1200X)*

*Please note that the illustrations on this page have been reduced 10% in printing.

3000 ppm Phosphate Soak

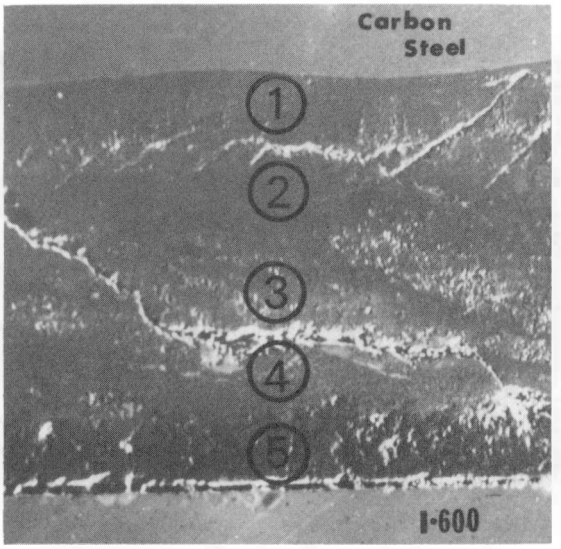


Figure E-32. Scanning Electron Micrograph of the Crevice Region Near the Top of Specimen H-7E-4-I Showing the Five Locations at which Higher Magnification SEM and EDS Analyses were Obtained (50X)*

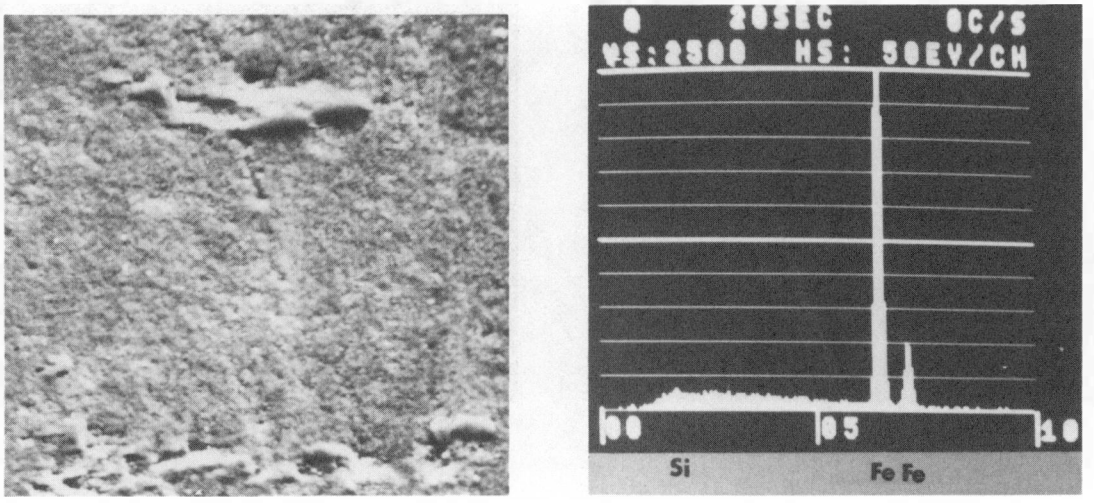


Figure E-33. SEM and EDS Analysis Results from Area 1 of Figure E-32 (1200X)*

*Please note that the illustrations on this page have been reduced 10% in printing.

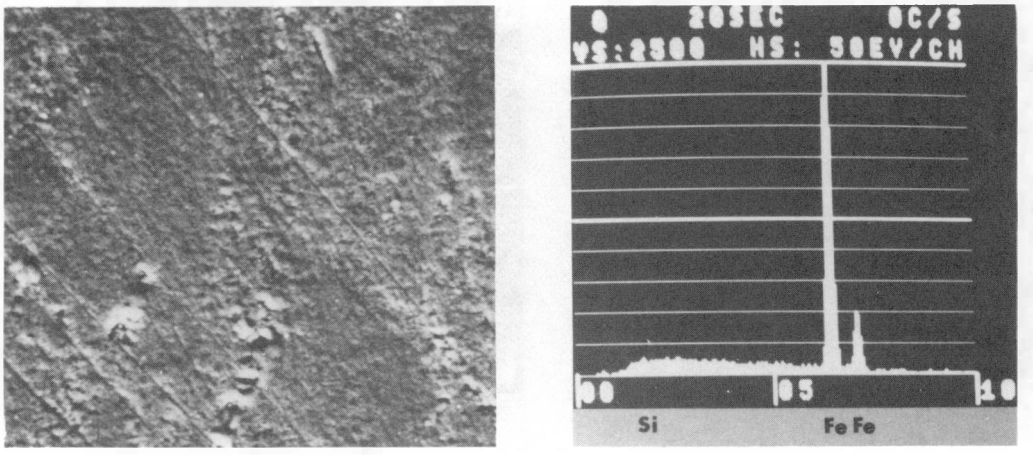


Figure E-34. SEM and EDS Analysis Results from Area 2 of Figure E-32 (1200X)*

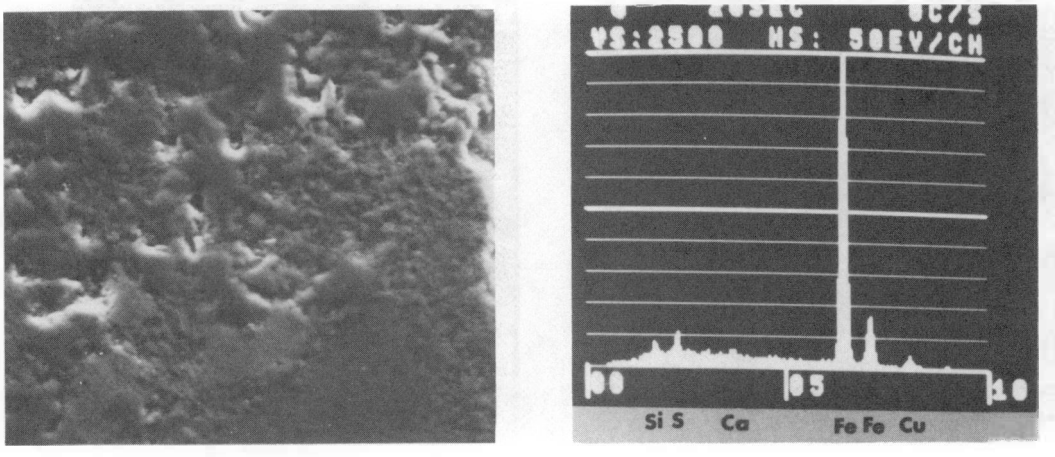


Figure E-35. SEM and EDS Analysis Results from Area 3 of Figure E-32 (1200X)*

*Please note that the illustrations on this page have been reduced 10% in printing.

3000 ppm Phosphate Soak

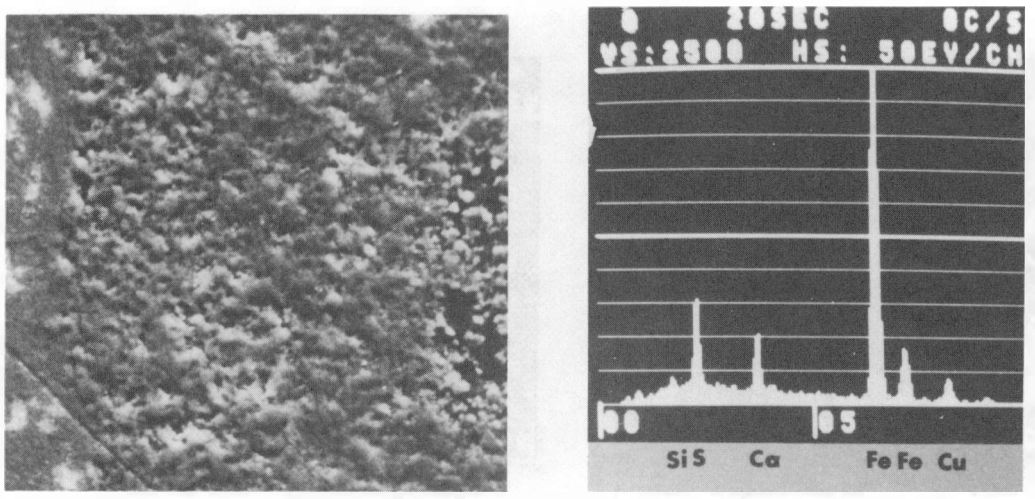


Figure E-36. SEM and EDS Analysis Results from Area 4 of Figure E-32 (1200X)*

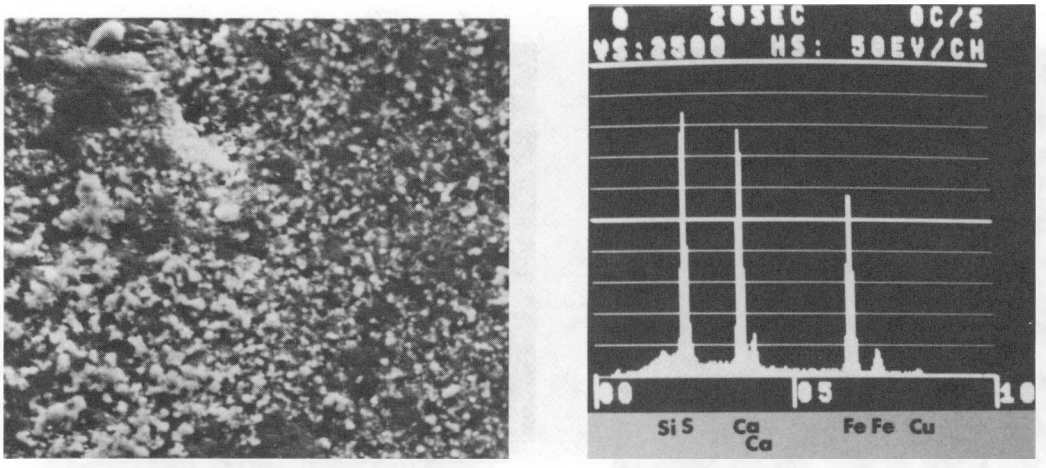


Figure E-37. SEM and EDS Analysis Results from Area 5 of Figure E-32 (1200X)*

*Please note that the illustrations on this page have been reduced 10% in printing.

3000 ppm Phosphate Soak

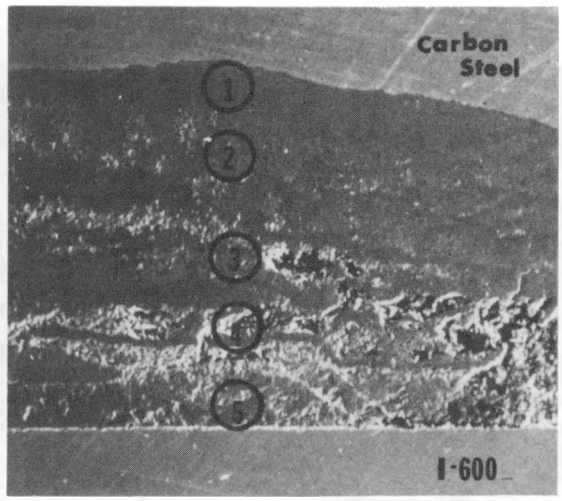


Figure E-38. Scanning Electron Micrograph of the Crevice Region Near the Center of Specimen H-7E-4-I Showing the Five Locations at which Higher Magnification SEM and EDS Analyses were Obtained. (50X)*

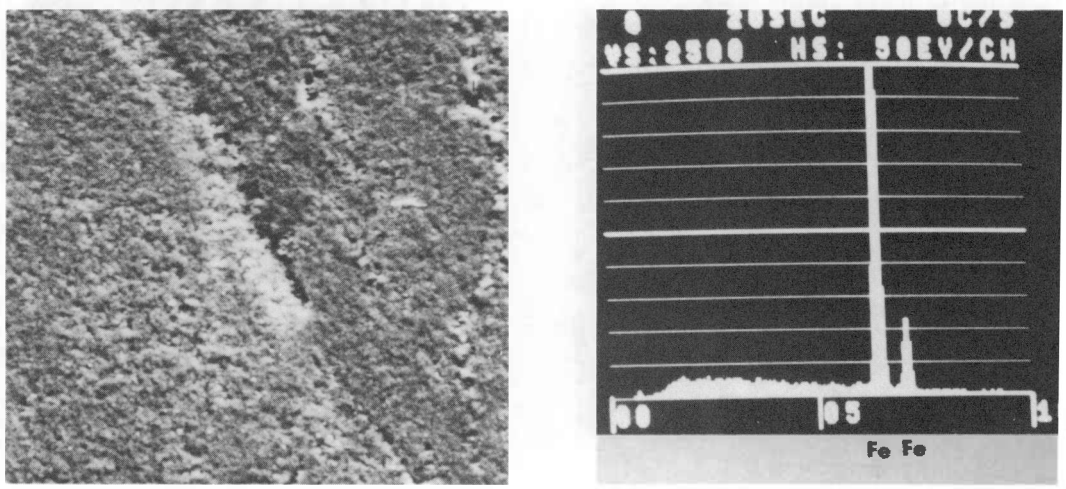


Figure E-39. SEM and EDS Analysis Results from Area 1 of Figure E-38 (1200X)*

*Please note that the illustrations on this page have been reduced 10% in printing.

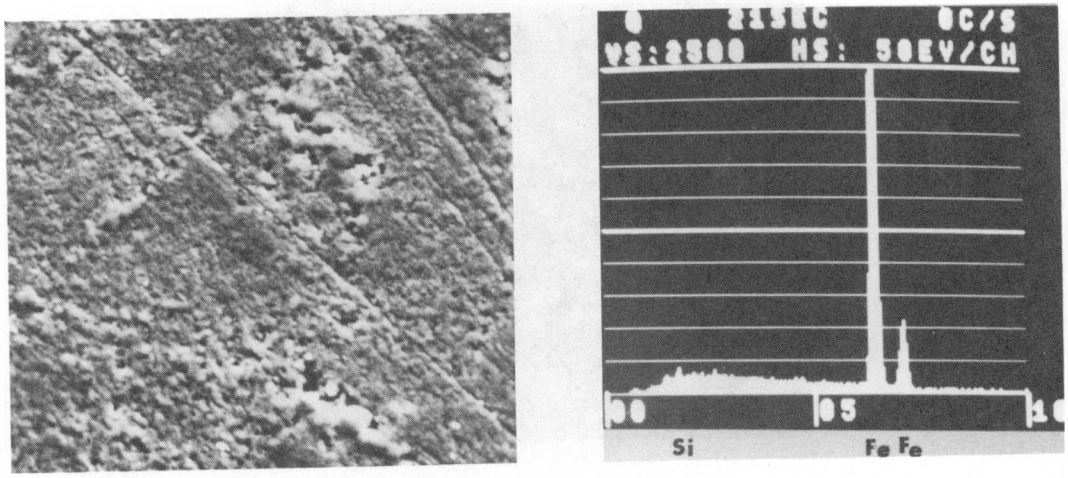


Figure E-40. SEM and EDS Analysis Results from Area 2 of Figure E-38 (1200X)*

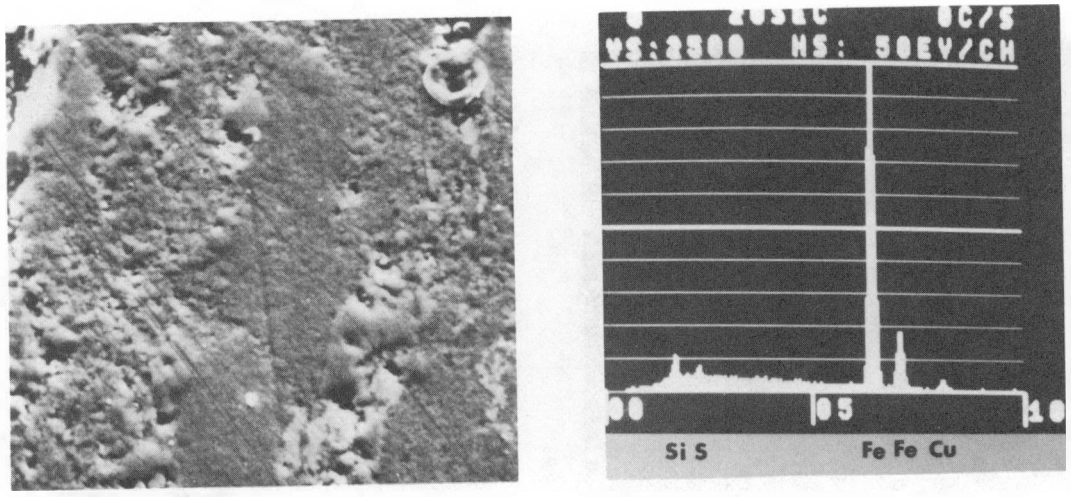


Figure E-41. SEM and EDS Analysis Results from Area 3 of Figure E-38 (1200X)*

*Please note that the illustrations on this page have been reduced 10% in printing.

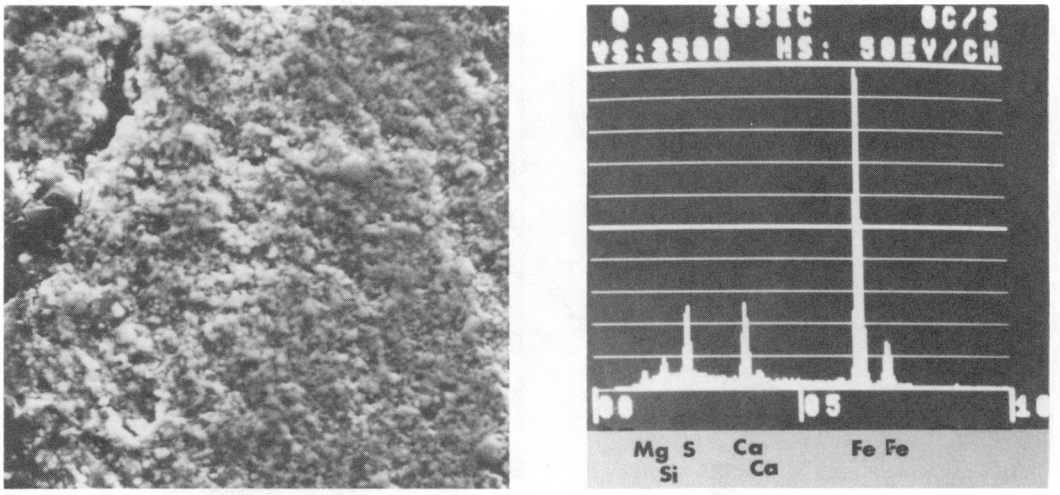


Figure E-42. SEM and EDS Analysis Results from Area 4 of Figure E-38 (1200X)*

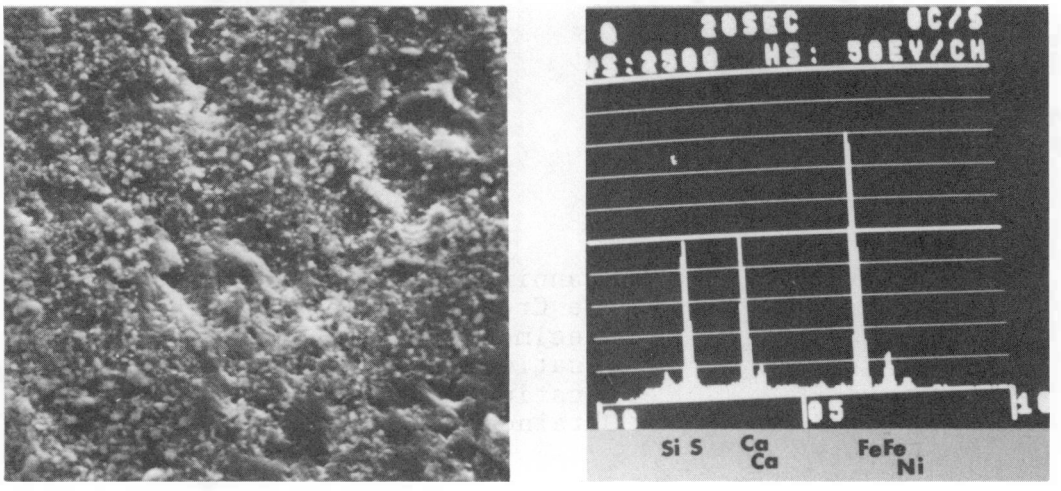


Figure E-43. SEM and EDS Analysis Results from Area 5 of Figure E-38 (1200X)*

*Please note that the illustrations on this page have been reduced 10% in printing.

3000 ppm Phosphate Soak

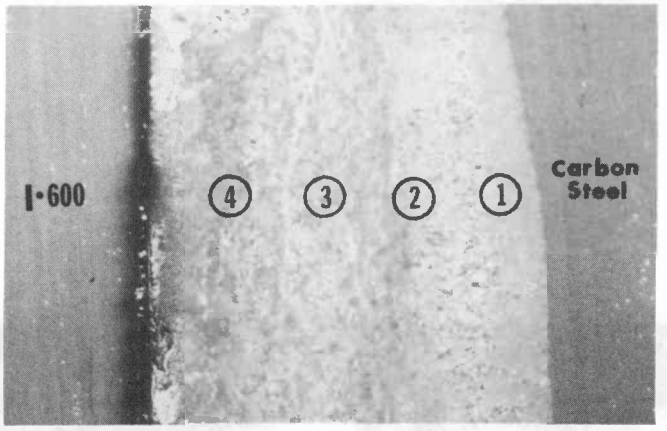


Figure E-44. Scanning Electron Micrograph of the Crevice Region Near the Top of Specimen C-7E-4-D Showing the Four Locations at which Higher Magnification SEM and EDS Analyses were Obtained (39X)*

*Please note that the illustrations on this page have been reduced 10% in printing.

3000 ppm Phosphate Soak

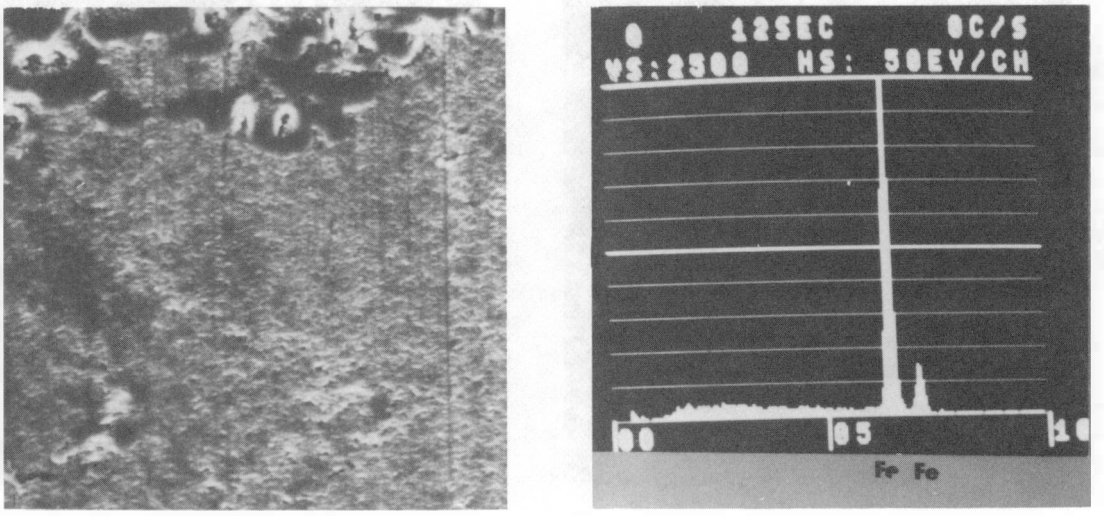


Figure E-45. SEM and EDS Analysis of Area 1 of Figure E-44 (1200X)*

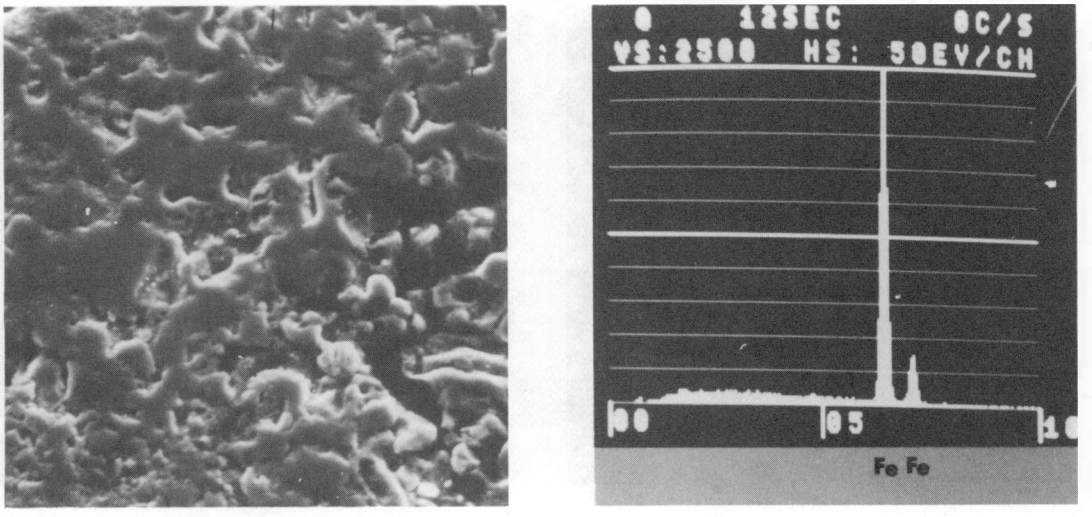


Figure E-46. SEM and EDS Analysis of Area 2 of Figure E-44 (1200X)*

*Please note that the illustrations on this page have been reduced 10% in printing.

3000 ppm Phosphate Soak

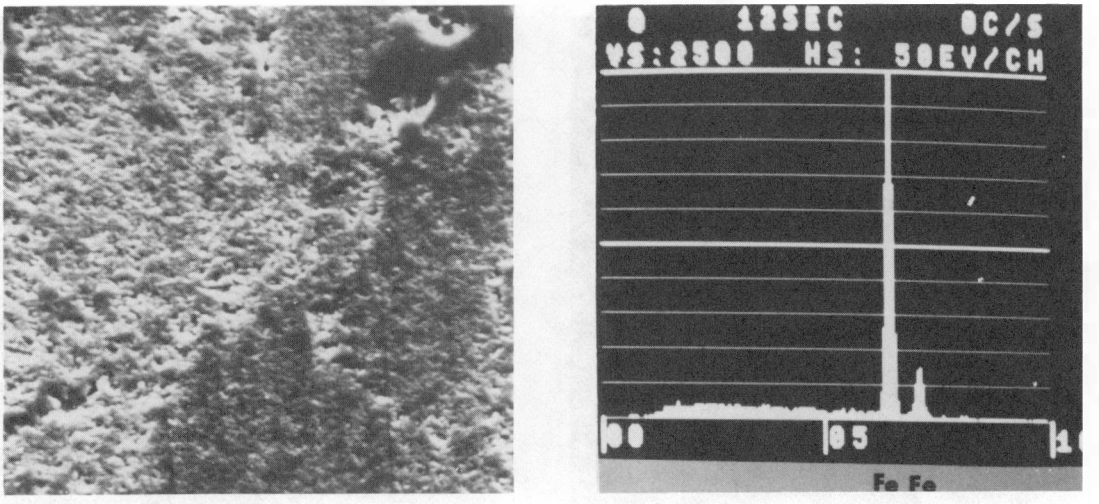


Figure E-47. SEM and EDS Analysis of Area 3 of Figure E-44 (1200X)*

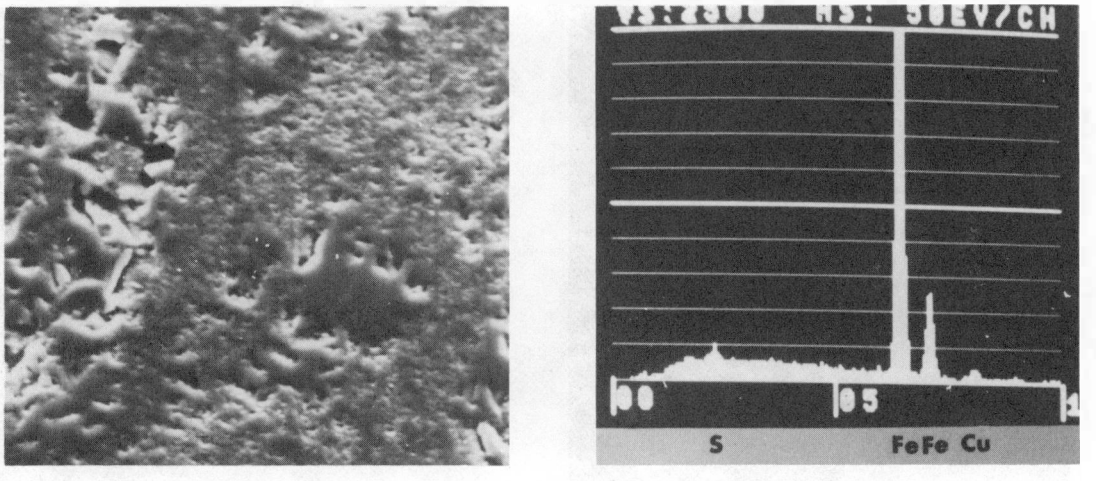


Figure E-48. SEM and EDS Analysis of Area 4 of Figure E-44 (1200X)*

*Please note that the illustrations on this page have been reduced 10% in printing.

3000 ppm Phosphate Soak

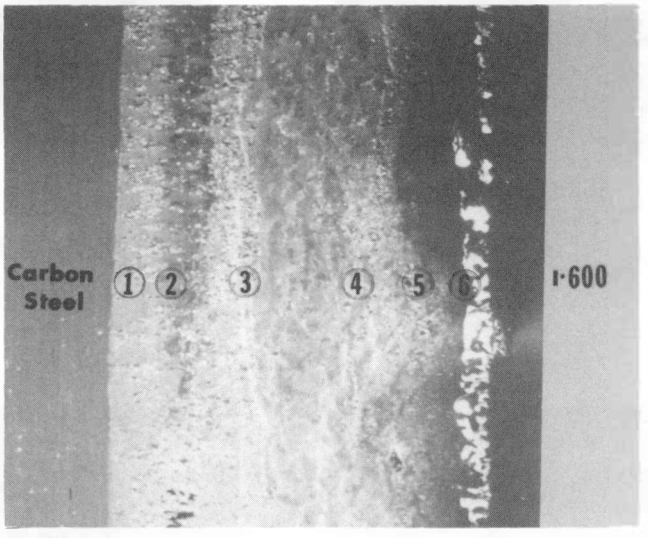


Figure E-49. Scanning Electron Micrograph of the Crevice Region Near the Center of Specimen C-7E-4-D Showing the Six Locations at which Higher Magnification SEM and EDS Analyses were Obtained (55X)*

*Please note that the illustrations on this page have been reduced 10% in printing.

3000 ppm Phosphate Soak

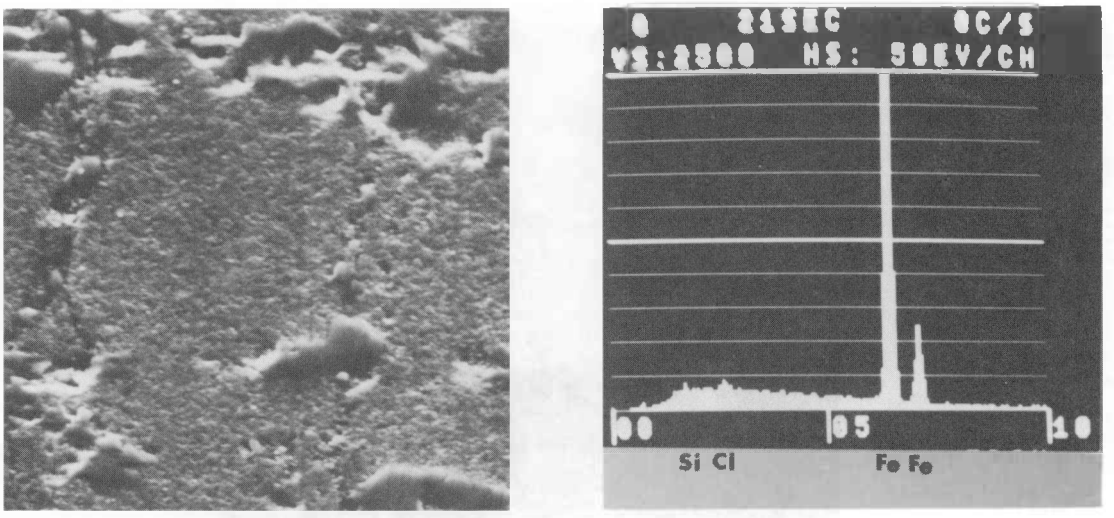


Figure E-50. SEM and EDS Analysis of Area 1 of Figure E-49 (1200X)*

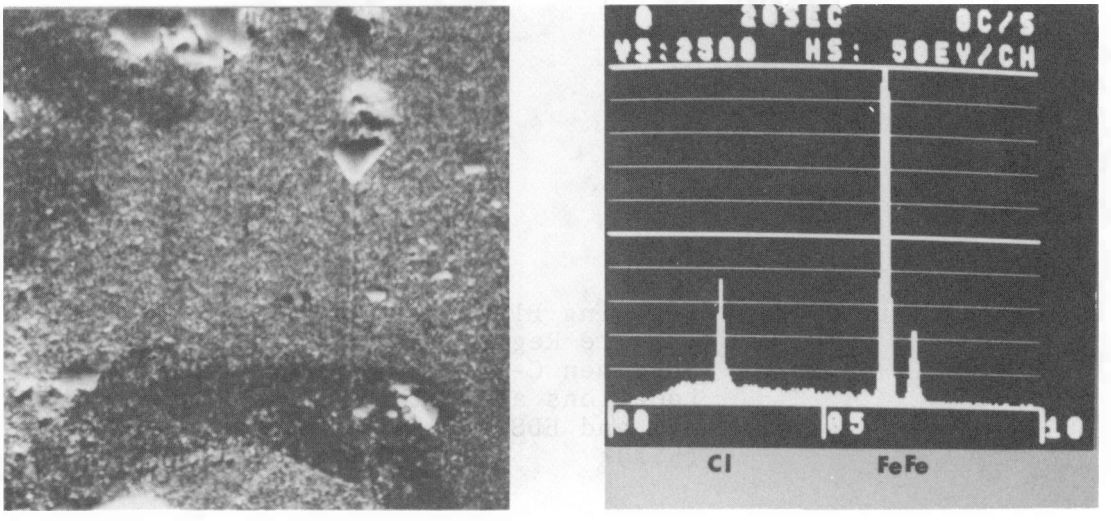


Figure E-51. SEM and EDS Analysis of Area 2 of Figure E-49 (1200X)*

*Please note that the illustrations on this page have been reduced 10% in printing.

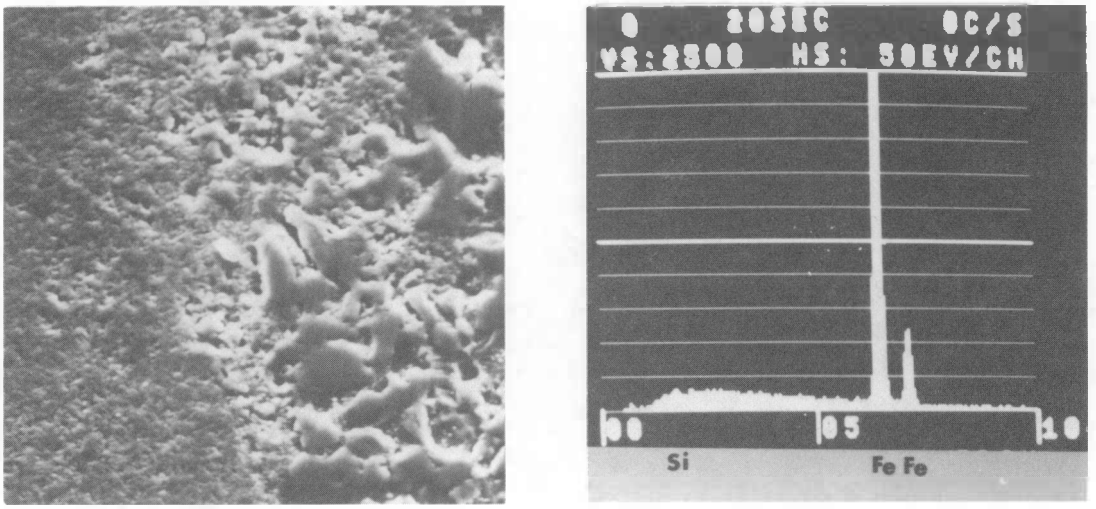


Figure E-52. SEM and EDS Analysis of Area 3 of Figure E-49 (1200X)*

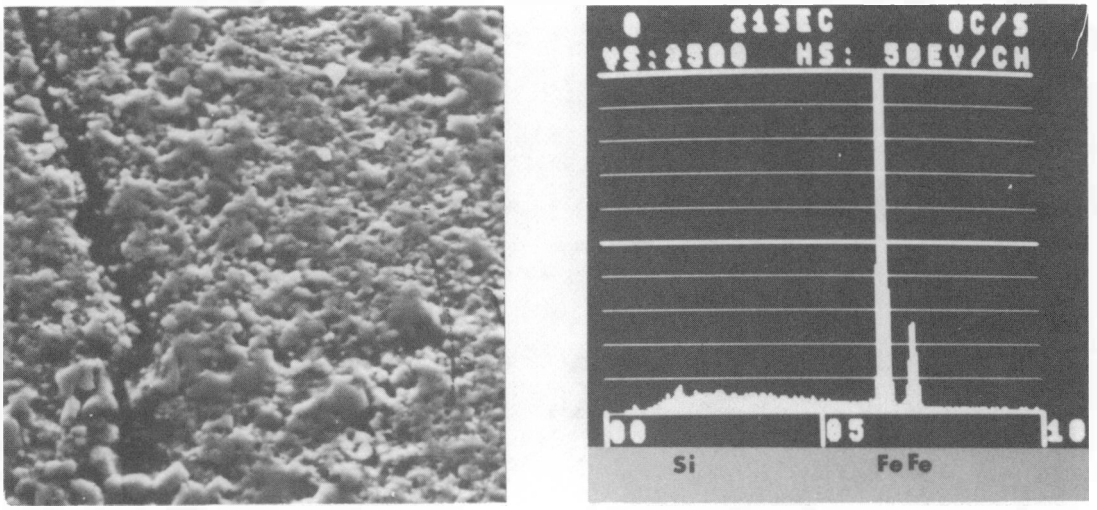


Figure E-53. SEM and EDS Analysis of Area 4 of Figure E-49 (1200X)*

*Please note that the illustrations on this page have been reduced 10% in printing.

3000 ppm Phosphate Soak

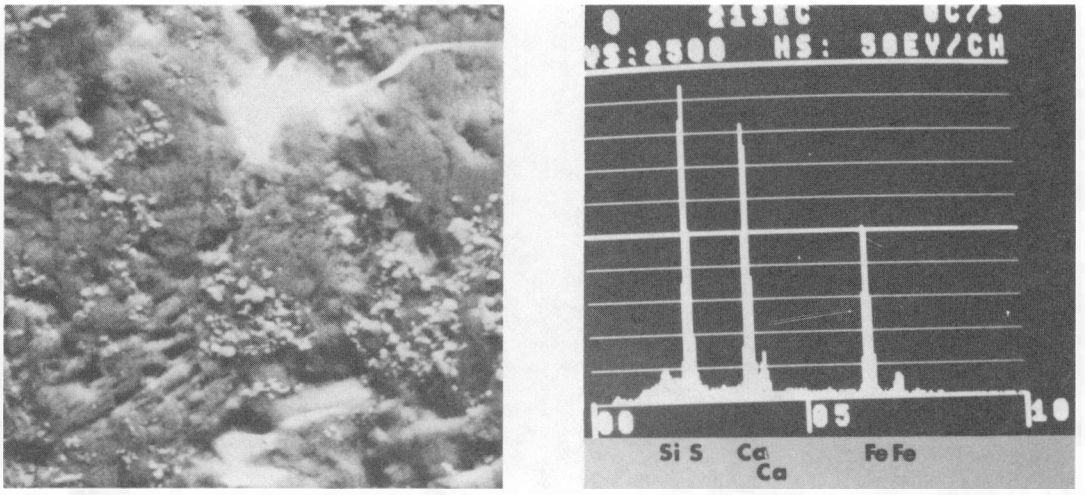


Figure E-54. SEM and EDS Analysis of Area 5 of Figure E-49 (1200X)*

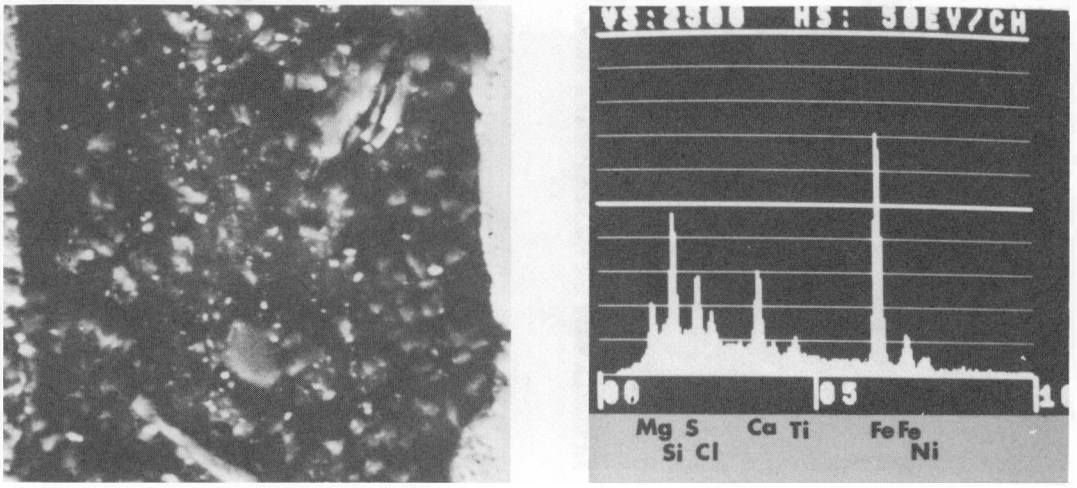


Figure E-55. SEM and EDS Analysis of Area 6 of Figure E-49 (1200X)*

*Please note that the illustrations on this page have been reduced 10% in printing.

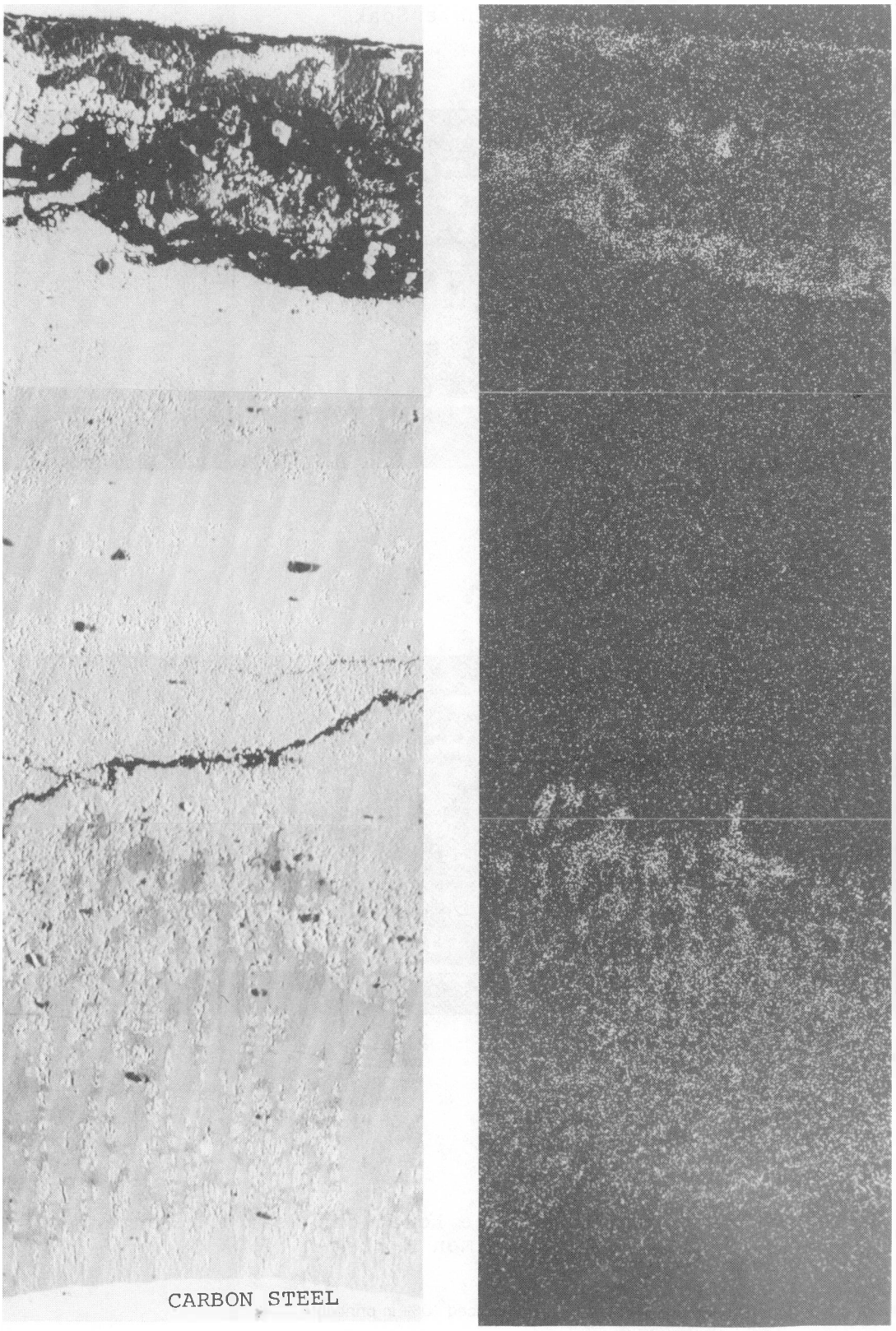


Figure E-56. SEM and Cl X-Ray Map from the Center of Support Plate Specimen H-11-4-K (150X)*

*Please note that the illustrations on this page have been reduced 10% in printing.

1000 ppm Phosphate Soak

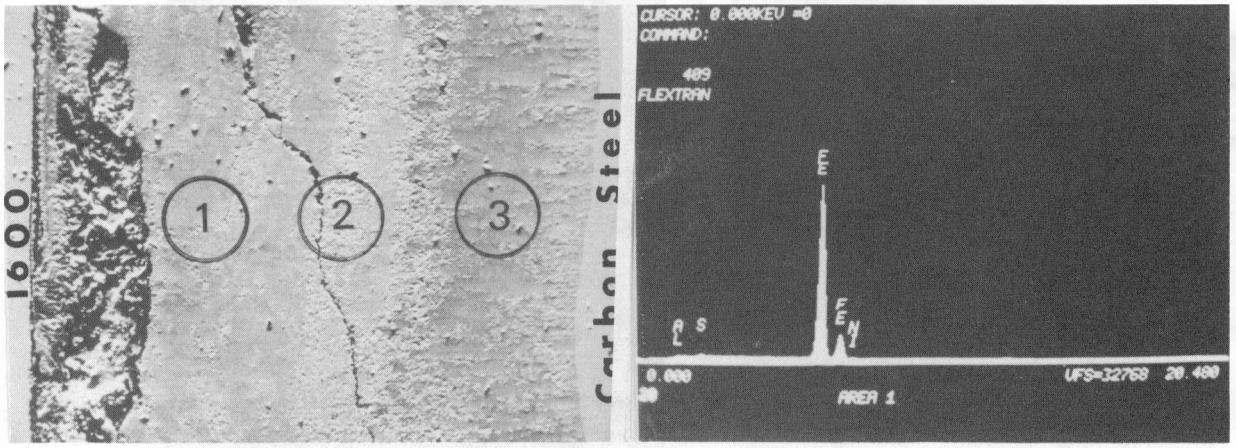


1

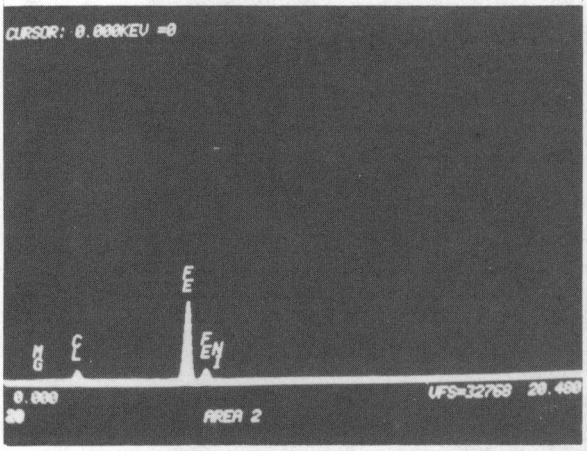


2

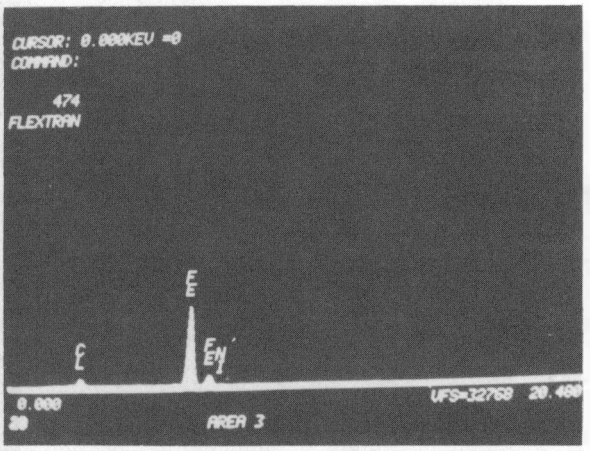


3

Figure E-57. EDS Analyses from Three Locations Near the Center of Support Plate Specimen H-11-4-K (150X)*

*Please note that the illustrations on this page have been reduced 10% in printing.


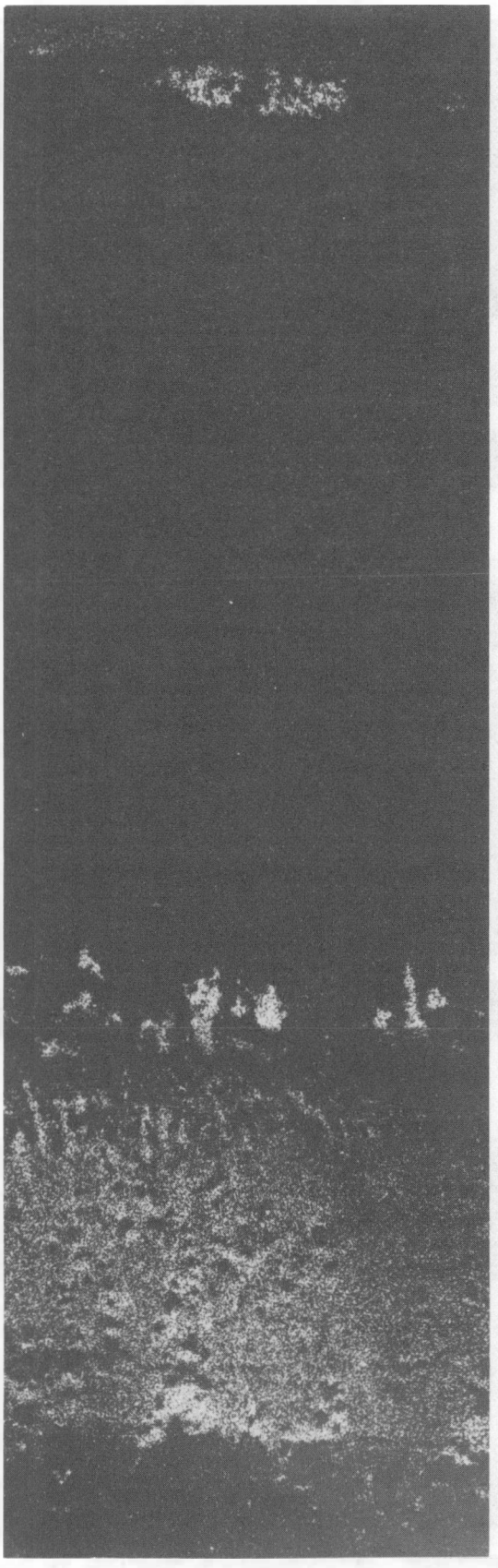

Figure E-58. SEM and Cl X-Ray Map from the Top of Support Plate Specimen H-7E-4-K (150X)*

*Please note that the illustrations on this page have been reduced 10% in printing.

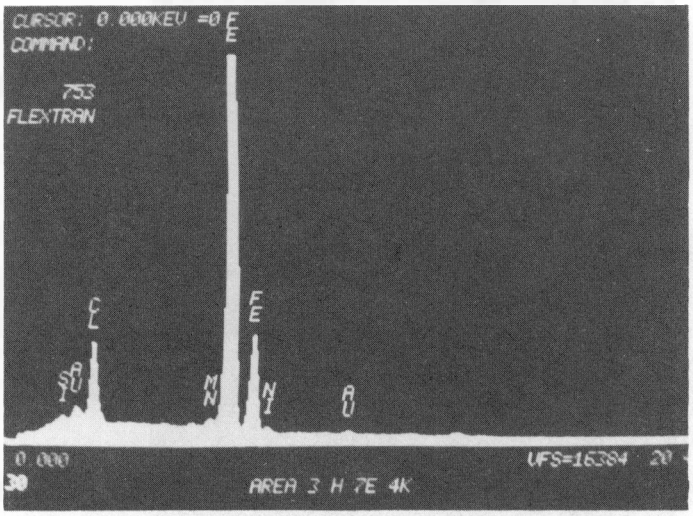


A

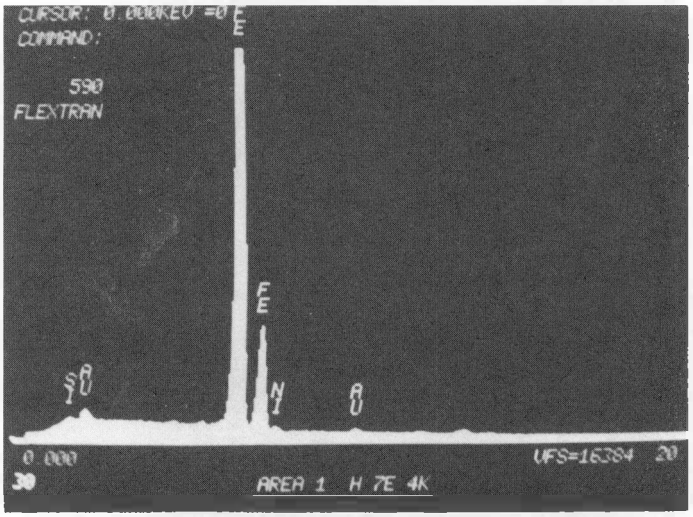


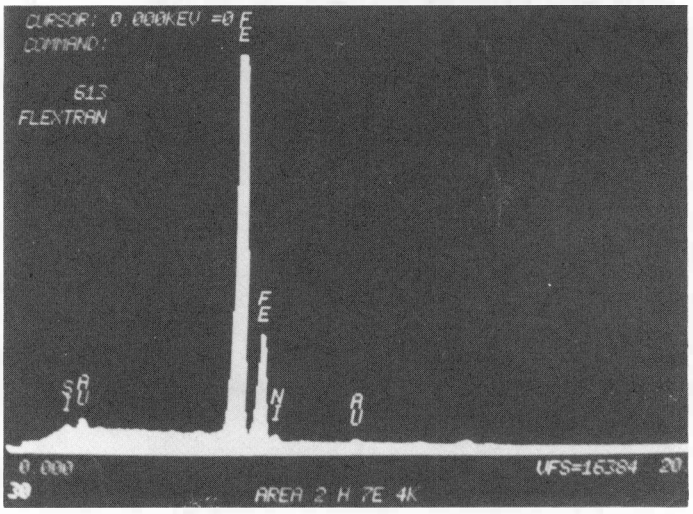


C

3000 ppm Phosphate Soak

Figure E-59.

EDS Analyses from Three Locations Near the Center of Support Plate Specimen H-7E-4-K

(a) Carbon Steel/ Oxide Interface

(b) Center of Crevice

(c) Alloy 600/Oxide Interface

3000 ppm Phosphate Soak

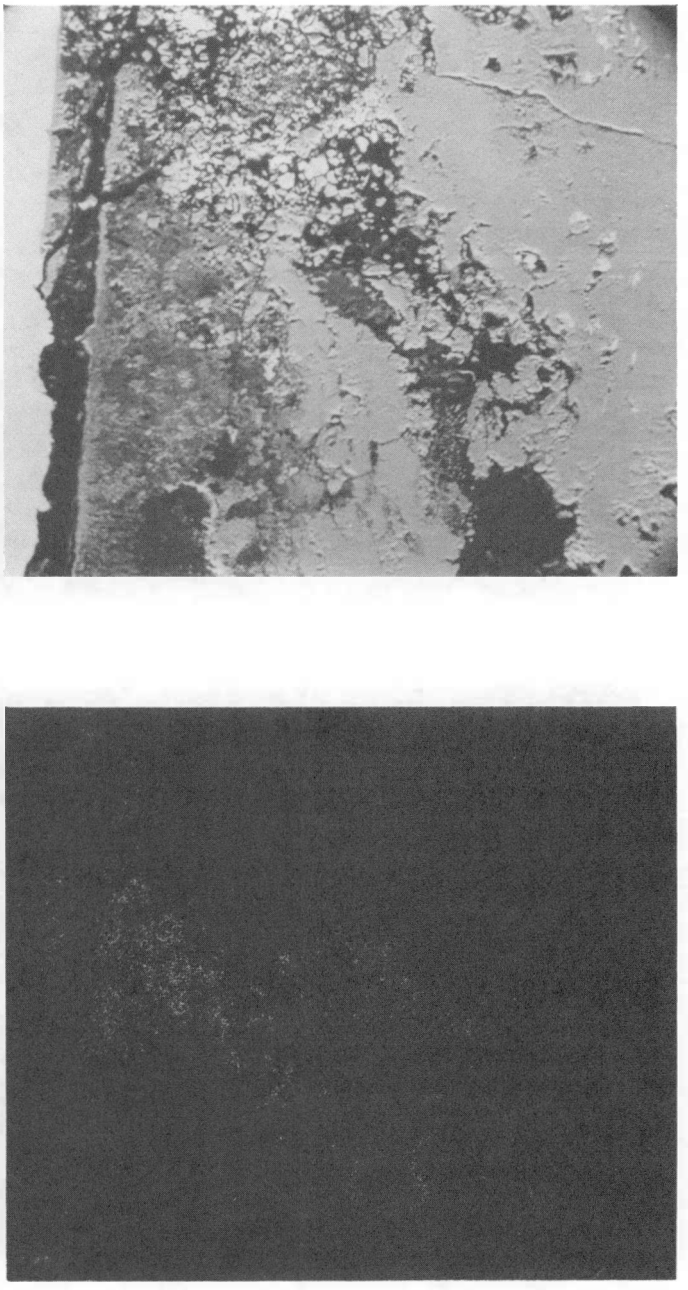

Figure E-60. SEM and P X-Ray Map of the Area Near the Alloy 600/Oxide Interface Near the Bottom of Support Plate Specimen H-7E-4-K (150X)*

*Please note that the illustrations on this page have been reduced 10% in printing.

3000 ppm Phosphate Soak

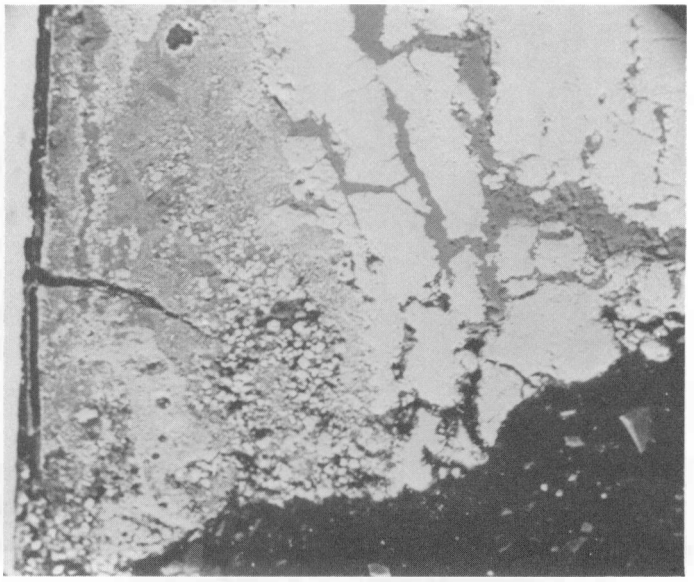

Figure E-61. SEM and P X-Ray Map of the Area Near the Alloy 600/Oxide Interface Near the Top of Support Plate Specimen H-7E-4-K (150X)*

*Please note that the illustrations on this page have been reduced 10% in printing.

3000 ppm Phosphate Soak

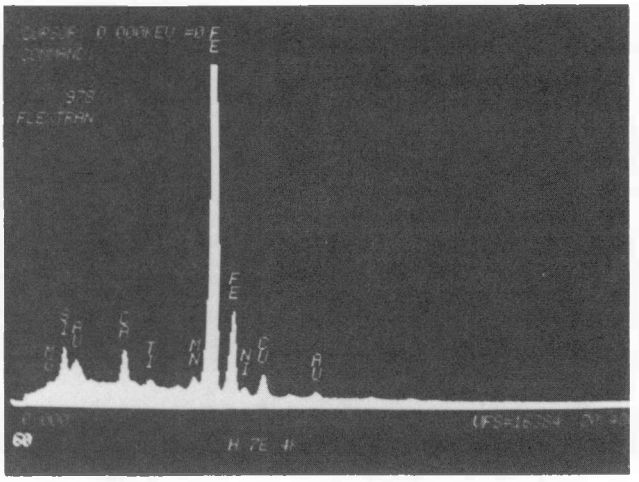

Figure E-62. EDS Analysis of the Area Shown in Figure E-61

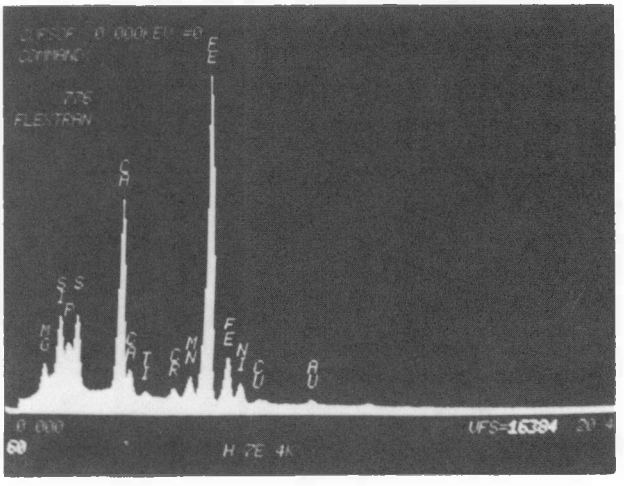

Figure E-63. EDS Analysis of the Area Shown in Figure E-60